UNIVERSITY OF NEWCASTLE UPON TYNE
DEPARTMENT OF CIVIL ENGINEERING

SEDIMENT TRANSPORT OVER DEPOSITED BEDS IN SEWERS

by

ABDEL KAHER S. M. EL-ZAEMEY

BSc, MSc

Thesis submitted in fulfillment of the requirements for the Degree of Doctor of Philosophy in Civil Engineering.

September 1991

To My Country, YEMEN, My Roots
To My Parents, My Past
To My Wife, My Present
To My Children, My Future

ABSTRACT

In sewer networks deposition of solids can occur from time to time, due to the intermittent nature of flow. The longer the deposits remain in sewer systems the more likely it is that the sediment properties will change. Eventually these depositions can become cemented (consolidated) especially during dry weather flow (DWF) when the boundary shear stress values are lower than the critical values and the velocity is not enough to carry the sediment along the sewers.

The main objective of the present study was to highlight and cover the shortage of methods and approaches in understanding the nature of sediment transport problems in sewers with a build up of permanent deposits.
Extensive experiments were carried out in a circular cross section channel (D=305 mm) with various fixed bed thicknesses namely 47 mm, 77 mm and 120 mm, and three different bed roughnesses ($0.0 < k_{s\,(mm)} < 1.40$).

In the first part of the study, the characteristics of flow in a circular cross section channel with flat bed was studied, the object being to investigate how the deposited bed affects velocity and bed shear stress distributions in the channel. The measurements showed a very strong dependency on the bed thickness, flow depth and bed roughness. The turbulence characteristics of such a channel were also investigated with a Laser Doppler Anemometer (LDA).

An empirical method of determining the flow friction factor (Darcy-Weisbach's factor) for circular cross section channels with sediment beds was developed and compared with previous methods.

It has been shown (Ackers, 1984, May, 1989) that the presence of stable deposits in the invert of sewers increases the sediment capacity of the channels and consequently, reduces the required gradient along which the channel will be laid.

Due to incomplete information concerning the behaviour and the mechanism of sediment transport in circular channels with flat beds, the second part of this study was devoted to a comprehensive investigation of:

(a) The incipient motion of grouped touching particles resting on the channel bed. The investigation led to the proposition of predictive equations for the critical values of shear stress and velocity at threshold of particle motion. The results were compared with past research results.

(b) Bed load transport of non-cohesive sediments without deposition. Six different sizes of particles were used ranging from $0.53 < d_{50}\,(mm) < 8.4$. Equations were developed to predict the sediment transport in circular cross section channels with different flat bed thicknesses. These equations can be used for designing deposit free sewers with flat beds and for identifying sewers suffering from a build up of deposits in the existing system.

ACKNOWLEDGEMENTS

I am very grateful to my supervisor Dr. Chandra Nalluri for his guidance, encouragement, and personal concern for me during the research leading to this thesis.

I also like to thank Professor P. Novak for his generous contribution to this study.

I also like to express my appreciation for the technical support provided by the staff of the Hydraulics Laboratory of the Civil Engineering Department.

I am also indebted to the British Council for providing the grant that made possible for me to come to Newcastle to conduct this research.

Special acknowledgments are due to the University of Sana'a of Yemen for their unconditional support by granting a leave of absence, during all these years. I specially wish to express my gratitude to Dr. M. Al-Iryani, deputy minister of High Education and Scientific Research for his encouragement and support.

Finally, I would like to extend my deepest gratitude and acknowledge the unwavering support of my parents for their moral support, and my wife umm Mohammed for her patience and understanding during the period of this study. To my loved children Somia, Mohammed and Fares, who remain in a continuous source of joy and comfort to me.

LIST OF SYMBOLS

A cross sectional area of the flow

b sediment bed width

d particle size

d_{50} median diameter of particles in a mixture

C Chezy roughness coefficient

C_D drag coefficient

C_L lift force coefficient

C_v sediment concentration by dry volume

D internal diameter of pipe channel

D_{gr} dimensionless particle number $\left\{\left[(S_s-1)g/\upsilon^2\right]^{1/3} d_{50}\right\}$

F_d Froude number of particle $(=V/\sqrt{(S_s-1)gd})$

F_{gr} mobility parameter in Ackers' equation

Fr flow Froude number $= \dfrac{V}{\sqrt{gy_o}}$

g gravitational constant

G_{gr} General transport parameter in Ackers' equation

h location of maximum velocity in channel section

k_s overall Nikuradse's equivalent sand roughness

k_{ss} overall Nikuradse's equivalent sand roughness with sediment

k_{sb} Nikuradse's equivalent sand roughness of bed

m empirical parameter in Ackers' equation

n overall Manning roughness coefficient

P wetted perimeter of the flow

q_s bed load in volume per unit time per unit width

Q flow rate

Q_s absolute volume rate of sand

R overall hydraulic radius (A/P)

R_b bed hydraulic radius

R_w wall hydraulic radius

S longitudinal bed slope of channel

S_s relative density of sediment (ρ_s/ρ)

t_s sediment bed thickness

u local velocity

u_{max} maximum local velocity

u' turbulent velocity fluc tuation

u_* shear velocity

u_b bottom velocity

u_{*b} bed shear velocity

V mean velocity

V_c mean velocity for incipient motion

y_o depth of uniform flow

y_t total depth of ($y_o + t_s$)

W_o settling velocity of particle

W_e effective width in Ackers' equation

W_s sediment width in clean pipe

γ specific weight of water

γ_s specific weight of sediment

θ_w half angle subtended by the water-line at the centre of pipe channel

θ_o half angle subtended by the sediment bed surface at the centre of pipe channel.

λ overall friction factor (clear water)

λ_b bed friction factor (clear water)

λ_s overall friction factor with sediment transport

λ_{sb} bed friction factor with sediment transport

μ dynamic viscosity of water

υ kinematic viscosity of water ($=\mu/\rho$)

ρ density of water

ρ_s density of sediment

τ_o mean shear stress ($=\rho gRS$)

τ_{oc} critical mean shear stress

$\bar{\tau}_b$ computed mean bed shear stress (ρgR_bS)

τ_{bm} measured bed shear stress

ϕ non- dimensionless transport parameter ($=C_v\ VR/\sqrt{gd^3(S_s-1)}$)

ψ non-dimensional shear stress ($=\tau_o/\ (\rho_s-\rho)gd_{50}$)

CONTENTS

LIST OF FIGURES

LIST OF PLATES

LIST OF TABLES

CHAPTER 1

INTRODUCTION

1.1 General

As man has been forced to cope with the processes of sediment transportation and deposition to protect himself and utilize the processes to his advantage, many engineers and scientists have studied extensively the transport of sediment by rivers (alluvial channels) for more than a century.

The transport of sediment particles by a flow of water can be in the form of bed-load and suspended-load, depending on the flow conditions and the size of the bed material particles. The suspended load may also contain some wash load, which is generally defined as the portion of the suspended load which is governed by the upstream supply rate and not by the composition and properties of the bed material.

Sediment transport in lined channels and drainage systems is not strictly related to loose or alluvial boundary hydraulics, since the boundaries are usually fixed. Theories dealing with sediment in fixed bed channels and drainage systems aim to solve the problem of sediment at the bottom of the system. However in the past sediment transport in fixed bed channels has not attracted much attention and the information available is inadequate.

Some of the main problems which are caused by sediment within drainage systems or lined irrigation channels are listed

below.

1. The presence of sediment in the form of a deposit reduces the hydraulic capacity of the channel by reducing the available cross sectional area of flow and increasing the channel wall roughness. This reduction in hydraulic capacity can result in those parts of the system upstream of the deposits becoming surcharged, which results in lower velocities due to backwater effects, thereby allowing more sediment deposition to take place.
2. Sediment in drainage systems may cause blockages.
3. The presence of sediment deposits in irrigation channels or in sewerage and drainage systems limits the levels to which flows can be drawn down.

In sewer systems there has been an investigation by CIRIA, (1987). They reported that the presence of sediment deposits which occur in many older combined sewer and surface drains is very great. It is suggested that up to 25,000 km of sewers and drains in U.K. may be affected. Therefore, CIRIA (1987) has emphasized the need to re-examine the current state of knowledge of the processes of sediment movement in sewers and of design methods.

1.2 Objective Of This Research

A well established research programme to develop sufficient knowledge of the characteristic of sediment movement over fixed bed channels has been recognised as the main subject of research at the University of Newcastle Upon Tyne. The present study is a continuation of this programme which aims

to assess the effect of permanent deposits on the invert of channels of circular cross section.

The self cleansing velocity, which can be briefly defined as the velocity that prevents any deposition on the invert of pipes, is an important factor in the design of sewer systems. This velocity determines the minimum gradients at which pipes need to be laid. There has been encouraging work carried out by a number of researchers in producing the right self-cleansing velocity. However all of these studies have major drawbacks.

Firstly, the area of agreement between them is very limited. This may be attributed to two main reasons. In developing theoretical analysis, some researchers made certain assumptions to simplify as well as to justify their analysis. Another reason is the extrapolation of experimental results to conditions found in sewers. May (1982) has pointed out that this type of approach is unreliable for a problem as complicated as sediment transport. In view of this disagreement between the researchers, further research is needed to explain the differences.

Secondly, most of the experiments have been conducted in full circular channels, despite the fact that in sewer networks the deposition of solids occurs spasmodically, due to the intermittent nature of flow. The longer the deposits remain in the sewer systems the more likely it is that the sediment properties will change. Eventually these deposits, due to their weight, can become consolidated or cemented especially during dry weather flow (DWF) when the boundary shear stress values are lower than the critical values and the velocity is

not enough to carry the sediment along the sewers. Permanent deposits in pipe inverts do have an effect on the sediment carrying capacity and hydraulic resistance of sewers. Very few researchers have paid attention to studying the sediment transport over deposited flat beds in circular channels. Most of the current design criteria (May, 1982, Novak & Nalluri 1984, Mayerele, 1988) which incorporate the non-cohesive sediment transport theories may be inappropriate for real sewer sediment deposits. Such existing methods take no account of the nature of in-pipe deposits.

More recently May et al (1989) extended their experimental programme to study the movement of sediment over a very small thickness (t_s=1%D) of loose deposited bed in circular channel and they added a new parameter to their previous model. This model was designed to take into consideration the effect of the deposited bed thickness on the carrying capacity of the circular channel.

Kuhil (1989) developed a theory to predict the sediment transport in sewers with and without sediment standing on the invert, but the theory was only tested on data from full-flow experiments with beds of loose deposits.

Alvarez (1990) studied the influence of cohesion on sediment movement in channels of circular cross sections and he tried to develop a model to predict the non-cohesive sediment in circular channels with rigid flat beds. As is clear from the aim of his research, Alvarez (1990) did not attach great importance to the problem of non-cohesive sediment and as a

result, only a few experiments were conducted to develop the model.

It can be concluded that there is a serious lack of comprehensive rational approaches for analysis and design of sewers whilst the existing deposition is permanent. Extensive research is still necessary to advance knowledge on sediment transport over deposited beds in sewers.

A comprehensive assessment of sewer systems should take into account the following major aspects in order to achieve a satisfactory analysis:

a) the hydraulic characteristics of the flow, taking into account flow resistance, velocity and bed shear stress distributions and turbulence intensity,

b) initiation of sediment motion, and

c) bed load transport.

All this information should be considered in developing design models. Rational approaches require the establishment of formulae based on an understanding of the fundamental principles of sediment movement in sewers. Unfortunately, the majority of the existing models are not developed with these in view.

Therefore the present research will cover the shortage of methods in solving some of the sediment transport problems in sewers, and it has been decided to:

(1) investigate the hydraulic characteristics of the flow in circular cross section channels with different sediment bed

thicknesses and

(2) study the effect of the deposited bed thicknesses and roughnesses on sediment transport capacity.

In order to achieve these aims an experimental programme with uniform flow conditions was planned which was carried in a circular channel (D=305 mm) with flat rigid beds. Three different bed thicknesses ranging from 15% to 39% of the pipe diameter were employed in this study. Three different bed roughnesses were tested for each bed.

The strategy followed in this work was to attempt to set up models based on fundamental considerations and basic mechanisms of sediment motion in sewers. Where this was not possible, the findings were presented, discussed and highlighted. It is not expected that such a thesis can reveal all the problems connected with sewers and a lot of research is still needed to reach universal, unifying and rational design models. This work should be seen as an important contribution towards the achievement of this goal.

1.3 Outline Of The Thesis:

The thesis consists of eight chapters and nine appendices.

Following the introductory chapter, Chapter 2 provides a general survey of literature on sediment movement. The first part of this chapter describes different theories and formulae dealing with sediment transport in loose boundaries. An extensive survey is then carried out into the different

investigations concerning sediment transport in rigid boundary channels.

Chapter 3 is devoted to the theories and design methods of storm sewers and describes sediment movement in sewerage and drainage systems. The effect of the cross section shapes that may influence the sediment yields has been introduced.

Chapter 4 describes the experimental equipment employed and the procedures adopted in preliminary experiments and sediment transport investigations.

Chapter 5 explains the results of the hydraulic characteristic investigations which include the study of flow resistance, and velocity, bed shear stresses and turbulence distributions.

Chapter 6 analyses the data of the study of initiation of motion and develops new equations for describing the physical movement of grouped touching particles resting on the bed of the channel. A comparison with the available equations is also presented.

Chapter 7 analyses the data of the sediment transport experiments. Then comprehensive comparisons are made between the present results and the available bed load theories and formulae and the bed load transport equations are developed.

Chapter 8 summarises the conclusions obtained from the

present investigations followed by some valuable recommendations for further work.

CHAPTER 2

LITERATURE REVIEW

2.1 Introduction

Open-channel flow over a movable boundary behaves differently from rigid boundary open-channel flows. In alluvial channels, rigid boundary relations apply only if there is no movement of bed and bank material. Once the general movement of the bed material has started, the flow and boundary interact in a complex manner. Salient features that differentiate between flow over movable and rigid boundaries are:-

1. In alluvial channels, the flow and boundary shape are interrelated. After general movement of the bed (as bed load) has started, the alluvial bed is distorted, giving rise to bed forms. The shape, size and rate of movement of these bed forms vary with flow conditions.
2. The magnitude of the roughness elements, as represented by the bed forms, can be of the same order of magnitude as the depth of flow. Relative roughness of this magnitude is generally not encountered in rigid boundary systems.
3. The alluvial boundary moves at both the grain and bed forms scales. Grains rolling at the boundary may introduce additional shear by their rotation and their wakes may change the turbulence level close to the boundary. In addition the movement of bed forms creates unsteadiness of flow in the vertical plane due to the changing bed elevation.
4. At an advanced stage of sediment movement some of the bed material is carried by the current and is referred to as

suspended load. The presence of particles in suspension affects the turbulence characteristics and the specific weight and the apparent viscosity of the fluid.

5. As the bed forms achieve dimensions comparable to the depth, the flow is no longer uniform and the depth and velocity change along and across the channel.

2.2 Sediment Transport In Movable Boundary Channels

2.2.1 Initiation Of Motion

a) General

Water flowing over a bed of sediment exerts forces on the grains that tend to carry them along. The forces that resist the entraining action of the flowing water differ according to the grain size and grain size distribution of the sediment. For coarse sediment, e.g., sands and gravels, the forces resisting motion are caused by the weight of the particles. Finer sediment that contain appreciable fractions of silt or clay, or both, tend to be cohesive and resist entrainment mainly by cohesion rather than by the weight of individual grains. The forces acting on a sediment particle are the particle weight, lift force and drag force. When the drag force is less than a certain critical value the channel bed material remains motionless. Then the bed can be considered as rigid. But when the shear stress over the bed attains or exceeds its critical value, particle motion begins. In general, the observation of particle movement is difficult in nature. The most dependable data available have resulted from laboratory experiments. Also the beginning of

motion is difficult to define. This difficulty is a consequence of a phenomenon which is random in time and space.

b) Critical Shear Stress

Most data on critical shear stress for non-cohesive sediments have been observed in flume experiments. Such experiments show that the motion of sediment grains at the bed of a stream is highly unsteady and nonuniformly distributed over the bed area. In near critical conditions the motion of grains in any small area of bed occurs in gusts, the incidence of which increases as the shear stress increases. Observation of a large area of a sediment bed when the shear stress is near critical value will show that the incidence of gusts of sediment motion appears to be random in both time and space. In general it is possible to state that the threshold condition for the beginning of particle motion depends on the parameters b, y, d, g, ρ_s, ρ, ν, u_{*c} which yield through dimensional analysis:

$$\frac{\tau_c}{\rho(S_s-1)gd} = \frac{u_{*c}^2}{(S_s-1)gd} = f\left[\frac{d}{b}, \frac{d}{y_o}, \frac{\rho_s}{\rho}, \frac{u_{*c}\,d}{\upsilon}\right] \tag{2.1}$$

where b the width of the channel, y_o the uniform depth of flow, d the diameter of particle, g the gravitational acceleration, ρ_s the density of the particle, ρ the density of the water, υ the kinematic viscosity of fluid, S_s the relative density of sediment (ρ_s/ρ) particle, τ_c being the critical (at threshold) shear stress and $u_{*c}(=\sqrt{\tau_c/\rho})$ the shear velocity at the threshold.

Practically speaking, for fine particles the influence of $\frac{d}{b}$ and $\frac{d}{y_o}$ on particle equilibrium can be ignored. Also, if ρ_s is constant, the influence of $(\frac{\rho_s}{\rho})$ can be included in a coefficient in the final equation. Then the relation takes the form:

$$\frac{\tau_c}{\rho(S_s-1)gd} = f\left[\frac{u_{*c}\, d}{\upsilon}\right] \qquad (2.2)$$

Shields (1936), conducted experiments to develop an explicit solution of Eq.2.2 using a graphical presentation called Shields diagram (Fig 2.1) which is widely accepted, and $[\tau_c/\rho(S_s-1)gd]$ is often referred to as the entrainment parameter $(1/\psi)$, and $(u_{*c}d/\upsilon)$ is called the Reynolds' number of the particle (R_{e*}).

At $\frac{u_{*c}\, d}{\upsilon} > 400$, the boundary is completely rough and $(1/\psi)$ is independent of Reynolds' number (R_{e*}) and is equal to:

$$1/\psi = \frac{\tau_c}{\rho\,(S_s-1)gd} = 0.056 \qquad (2.3)$$

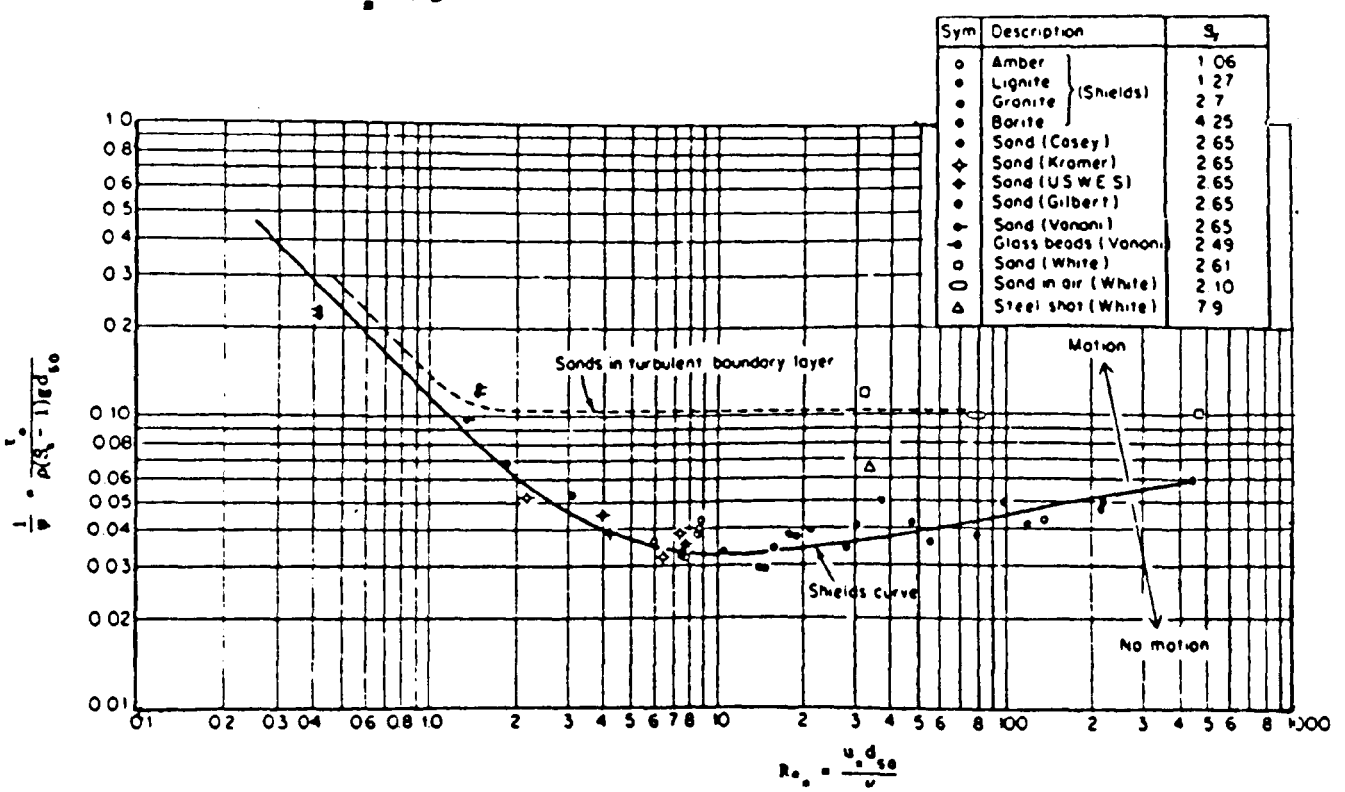

FIGURE 2.1 SHIELDS DIAGRAM: DIMENSIONLESS CRITICAL SHEAR STRESS Vanoni (1964)

Grass (1970) showed that for any area of flat bed there will be a random distribution of critical shear stresses. Some bed particles are more exposed and easily detached than others. For a given flow there will be a random distribution of shear stresses (turbulent nature of the flow) acting on the bed. Thus, there are two independent distributions of shear stress and when they start to overlap the weakest grains will begin to move.

Grass (1970) defined quantitatively critical movement in terms of the overlap (see Fig 2.2) of the two distributions as the multiple "n_p" of the sum of the standard deviation of the distributions that separate the two mean values.

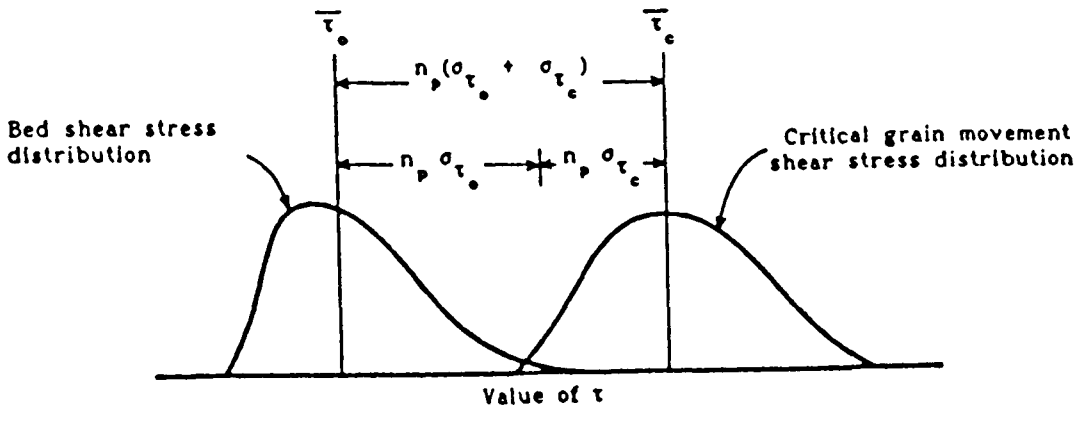

FIGURE 2.2 OVERLAP OF THE SHEAR STRESS DISTRIBUTIONS (after Grass, 1970)

Alvarez (1990), conducted initiation of erosion experiments with non-cohesive sediments in channels of circular cross section (D=154 mm) with loose flat beds. A wide range of uniform sand sizes ($0.5 < d_{50}(mm) < 4.1$) was used with a relative density of $2.48 \leq S_s \leq 2.61$, and sediment bed

thickness ratio of $t_s/D \cong 0.12$.

In every experiment a uniform size sand constituted the flat sediment bed (modeling deposited sewer sediment bed). Initiation of erosion was achieved by small increments of the shear stress. He determined critical shear stress by extrapolation to nearly zero bed load ($C_v=10^{-8}$) from the C_v (sediment volumetric concentration) vs. τ_o (shear stress) curves. A summary of Alvarez (1990) results are shown in Fig. 2.3. The entrainment function was found to be best described by ($r^2=0.788$):

$$\frac{\tau_{bc}}{\rho(S_s-1)gd} = 0.77 \left[\frac{y_o}{P}\right]^{0.17} (\lambda_b)^{0.9} \left[\frac{y_o + t_s}{D}\right]^{0.38} \qquad (2.4)$$

where τ_{bc} is the computed bed shear stress (in a laboratory where a narrow flume with glass walls and sand bed having a varying roughness over the perimeter, the hydraulic radius of the bed, R_b, instead of R is commonly used to eliminate the side wall effects), ρ is the density of water, S_s is the relative density of sediments, g is the acceleration due to gravity, d is the particle size, y_o is the normal flow depth, P is the wetted perimeter, λ_b is the computed bed friction factor, t_s is the sediment bed thickness.

c) Critical Velocity

The earliest observations of critical or threshold conditions for the initiation of sediment motion were reported in terms of critical velocity.

For loose sediment bed Manning's n can be calculated from

$$n = 0.04\, d^{1/6} \qquad \text{(Strickler's)} \qquad (2.5)$$

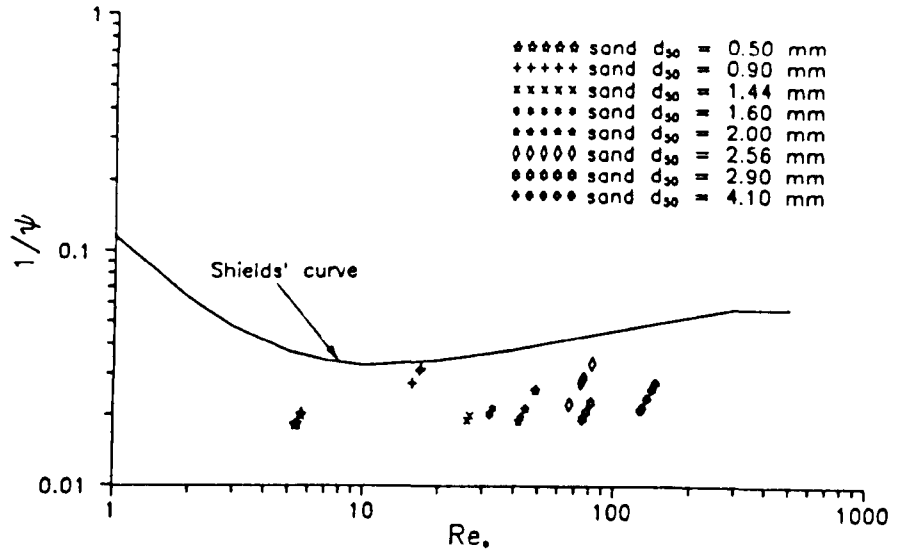

a) Mean Shear Stress Values

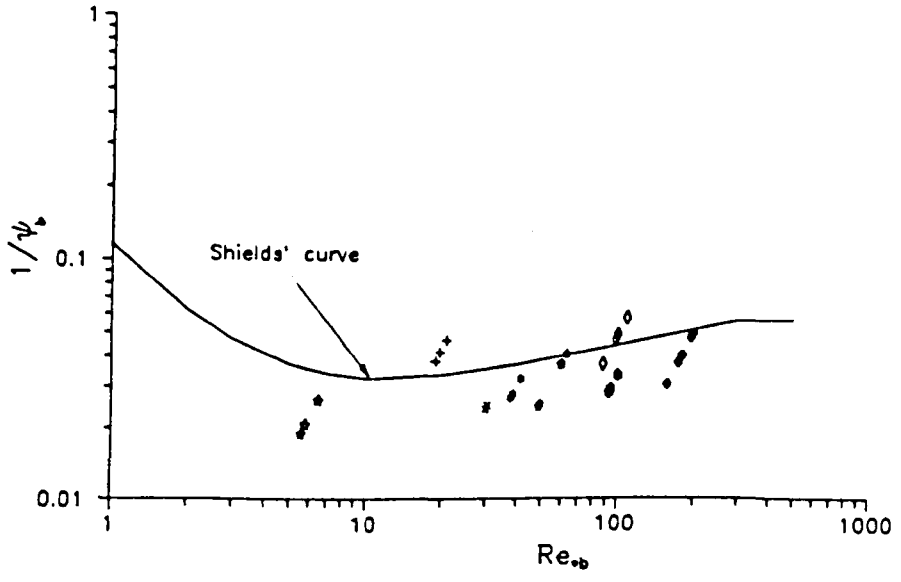

b) Bed Shear Stress Values

FIGURE 2.3 SHIELDS DIAGRAM FOR INITIATION OF MOTION OF NON-COHESIVE SEDIMENTS IN CIRCULAR CROSS SECTION WITH LOOSE BED CHANNELS (Alvarez 1990)

where d is the particle size in m.

Combining Equations 2.3 and 2.5 with Manning's equation yields:

$$\frac{V_c}{\sqrt{gd(S_s-1)}} = 1.96 \left[\frac{d}{R}\right]^{-1/6} \qquad (2.6)$$

Bogardi (1968) suggested, for critical conditions, the following relationship:

$$\frac{V_c}{\sqrt{gy_o(S_s-1)}} = 1.7 \left[\frac{d}{R}\right]^{-0.405} \qquad (2.7)$$

where y_o is the flow depth.

2.2.2 Bed Load Transport

When the flow over the movable boundaries of a channel has hydraulic conditions exceeding the critical condition for motion of the bed material, sediment transport will start. If the motion of entrained particles is one of rolling, sliding, and sometimes jumping in the bed layers, this kind of sediment transport is commonly referred to as bed-load transport.

Kalinske (1947) took into consideration turbulent fluctuations of the velocity at the bed, which were assumed to be normally distributed, and presented the following equation for the computation of bed load:

$$\frac{q_s}{u_* d} = 10 \ (1/\psi)^2 \qquad (2.8)$$

where q_s is the volume rate of sediment transport per unit width, u_* the shear velocity, and d the sediment size.

Einstein (1942, 1950) found that the beginning and cessation of sediment motion could be expressed by the concept of probability. He argued that in turbulent flow the fluid forces acting on the particle vary with respect to both time and space, and therefore the movement of any particle depends upon the probability that at a particular time and place the applied forces exceed the resisting forces. For equilibrium the number of particles eroded must equal the number deposited. The Einstein equation is given as:

$$\phi = f(\psi) \qquad (2.9)$$

with $$\phi = \frac{C_v \ V \ R}{\sqrt{g \ d^3 \ (S_s-1)}}$$

known as the transport parameter and

$$\psi = \frac{(S_s-1) \ d}{S \ R}$$

as the flow intensity parameter where C_v is sediment volumetric concentration and V is the mean flow velocity. Figure 2.4 shows ϕ versus ψ for experimental and field data.

Brown (1950) reformulated the Einstein formula to fit his data, (0.315 mm $< d_{50} <$ 28.6 mm and 1.25 $< S_s <$ 4.2).
The formula becomes:

$$\phi = 40 \ (1/\psi)^3 \qquad (2.10)$$

which is valid for ϕ less than 0.4. The lower part of the plot (see Fig 2.5) curves away from the asymptote $\frac{1}{\psi}$ = 0.056, which represents the threshold condition of Shields' data (Eq. 2.3).

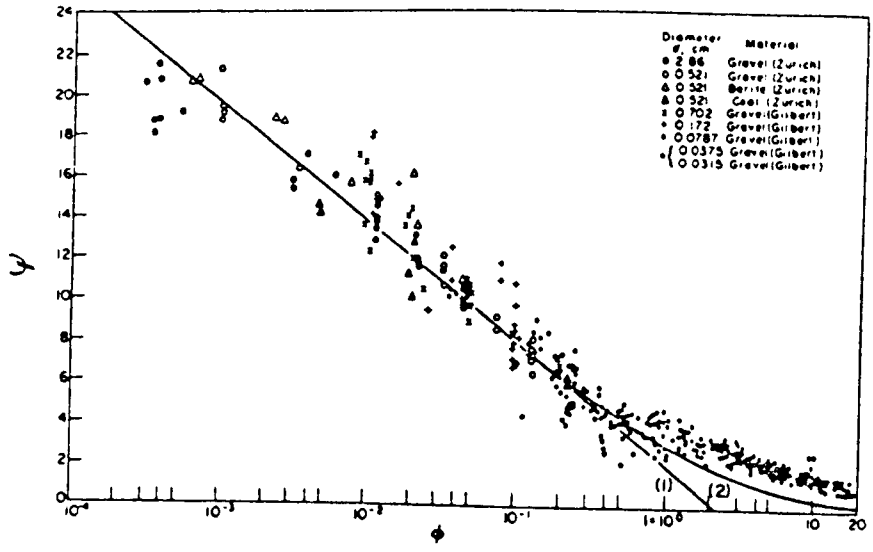

FIGURE 2.4 EINSTEIN'S BED LOAD EQUATIONS

(after Einstein, 1942)

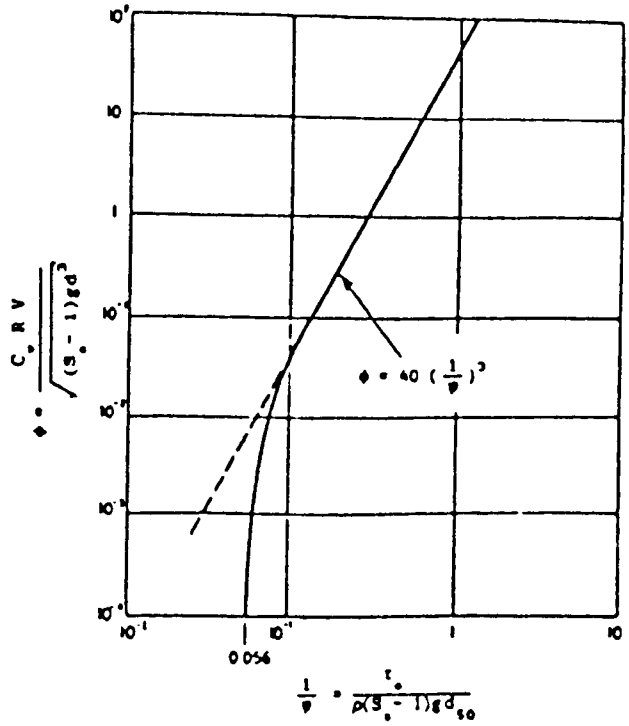

FIGURE 2.5 BROWN'S CURVE

Meyer-Peter and Muller in 1948 presented the following formula

$$\frac{\gamma R (n'/n)^{3/2} S}{d} - 0.047(\gamma_s - \gamma) = 0.25 \sqrt[3]{\frac{\rho}{g}} \frac{(q_b')^{2/3}}{d} \qquad (2.11)$$

which is widely used for sand mixtures. Equation 2.11 was obtained as the best fit of experimental data with sand ranges $0.4 \text{ mm} < d_{50} < 28.6 \text{ mm}$ and $1.25 < S_s < 4.2$, and wide channels, where γ_s is the specific weight of the sediment, n and n′ are Manning's total roughness coefficient and grain roughness coefficient respectively, q_b' is the bed load rate in weight per unit time per unit width.

In Eq. 2.11 the term $(n'/n)^{3/2} S = S'$ represents the energy loss due to grain resistance, which is responsible for sediment transport.

In 1954 Chein showed that equation 2.11 gives results comparable to those of Einstein (see Fig. 2.6) and that it can be written as:

$$\phi = \left(\frac{4}{\psi} - 0.188 \right)^{3/2} \qquad (2.12)$$

Graf and Acaroglu (1968) analysed several laboratory (open and closed conduits) and field data and obtained the following relation

$$\phi = 10.39 \left(\frac{1}{\psi} \right)^{2.52} \qquad (2.13)$$

Eq. 2.13 is valid for $10^{-2} < \phi < 10^{-3}$, $0.09 < d(mm) < 2.78$ and $2.65 < S_s < 2.69$.

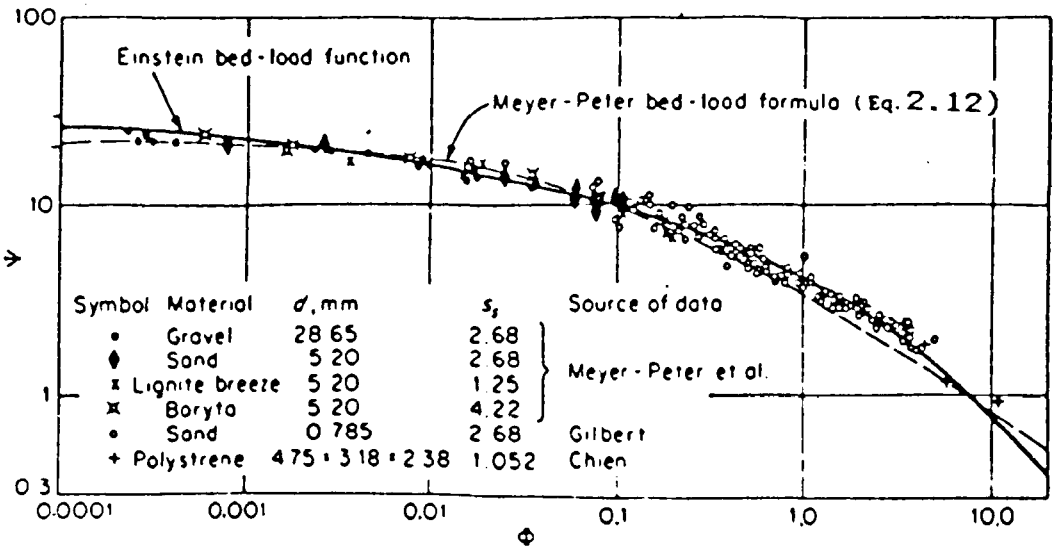

FIGURE 2.6 COMPARISON OF THE BED LOAD EQUATION OF EINSTEIN AND MEYER-PETER ET AL. (Chein 1954)

2.2.3 Suspended Load Transport

Only at relatively small values of excess shear stress, $\tau_o - \tau_c$, is the transport confined to bed loads only. Increase in bed shear stress soon leads to suspension and to transport as bed and suspended load. Since suspension is transported at approximately the velocity of flow the quantity of sediment transported as suspended load is usually very much greater than that of bed load which moves much more slowly. The sediment is maintained in suspension, against the gravitational fall velocity, by the diffusion of turbulence from the bed. For this the RMS (root mean square) values of

the vertical turbulence components ($\sqrt{\overline{v'^2}}$) need to be equal or greater than the fall velocity W_o .

Boundary layer flow studies indicate that $\sqrt{\overline{v'^2}}$ is of the same order as the shear velocity u_* (Raudkivi 1990). Thus for initiation of suspension $\frac{u_*}{W_o} \geq 1.0$.

Based on his experimental data for the initiation of suspension Van Rijn (1984) proposed the following relationships:

$$\frac{u_{*c}}{W_o} = \frac{4}{D_{gr}} \qquad (2.14)$$

for $1.0 < D_{gr} \leq 10$

$$\frac{u_{*c}}{W_o} = 0.04 \qquad (2.15)$$

for $D_{gr} > 10$

where $D_{gr} = \left\{ \left[\frac{(S_s - 1) g}{\upsilon^2} \right]^{1/3} d \right\}$

Rouse (1937) proposed the following equation for the distribution of suspended sediment concentration:

$$\frac{C_v}{C_a} = \left[\frac{a\ (y_o - y)}{y\ (y_o - a)} \right]^{\left(\frac{W_o}{\kappa\ u_*} \right)} \qquad (2.16)$$

where C_v is the sediment volumetric concentration at a height y, a is a reference level where the concentration is C_a , y_o is the flow depth and κ is the Von-Karman constant.

2.3 Sediment Transport In Fixed Bed Channels

2.3.1 Initiation of Motion

The determination of incipient motion is important not only to the study of sediment transport but also to the design of hydraulic structures. Most engineers use either critical shear stress or critical average velocity as a criterion for incipient motion.

Craven (1953) studied the condition for the beginning of movement of particles in pipes flowing full. The experiments were conducted in two pipes, one of 152.4 mm diameter and one of 50.8 mm diameter of proportionate length. Three grades of uniform quartz sand (0.25,0.58 and 1.62 mm) were used. For each run the pipe was filled with sand to a predetermined level, then the flow rate was measured until movement was observed. He concluded that for no permanent deposition in the pipe, the following formula should be applied.

$$\frac{Q}{D^2\sqrt{(S_s-1)gd}} \geq 2.5 \qquad (2.17)$$

in which Q is the flow rate and D is the pipe diameter. Considering that there is no permanent deposit in a pipe, and replace Q by $V\frac{\pi D^2}{4}$, equation 2.17 can be rearranged as:

$$\frac{V_c}{\sqrt{gd\ (S_s-1)}} \geq 3.18 \qquad (2.18)$$

V_c being the velocity that eliminates sediment deposit in pipe-full flow condition.

Ambrose (1953) carried out further investigations for pipes flowing part-full. He conducted experiments to identify the necessary slopes of the pipes which eliminates sediment resting on the bottom of the pipe, employing essentially the same equipment as Carven did. Only the results in which no inert bed was present in the pipe are shown below. Under this condition the movement of particles occurs over a relatively smooth fixed surface. Fig. 2.7 shows the relation between water depth ratio and the transport function.

$$\frac{Q}{g^{2/5}\, D^2\, Q_s^{1/5} (S_s - 1)^{2/5}} = f\left(\frac{Y_o}{D}\right) \qquad (2.19)$$

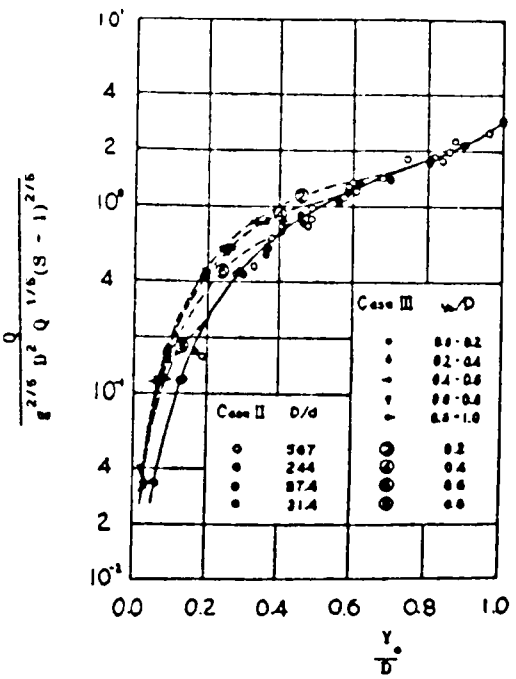

FIGURE 2.7 DISCHARGE FUNCTION FOR IMPENDING DEPOSITION (Ambrose 1953)

Ippen and Verma (1953) investigated the motion of discrete particles along a fixed bed coated with uniform sand.

Experiments were conducted in a rectangular flume 611 mm wide and 4.6 m long having the bottom roughened with sand particles, resulting in equivalent roughnesses of 0.75 mm and 1.8 mm. The particles used as sediment were plastic (2.0 mm and 3.0 mm diameter, S_s= 1.28) and glass spheres (3.2mm and 4.0 mm in diameter, S_s=2.38). Figure 2.8 was suggested to identify the incipient motion considering the effect of all variables involved in the phenomenon. In this figure, k_s is Nikuradse's equivalent sand roughness, and d is the sediment sphere diameter. To bring all points on their plot approximately to Shields line, they suggested the following empirical relation:

$$\frac{1.5\,\tau_o}{\rho g\,(S_s-1)^{1/2}\,k_s} = \frac{11.6\,d}{\delta'} = f\,(R_{*})\qquad(2.20)$$

where (δ') is the sublayer thickness, τ_o is the mean shear stress and R_{*} is particle Reynolds' number.

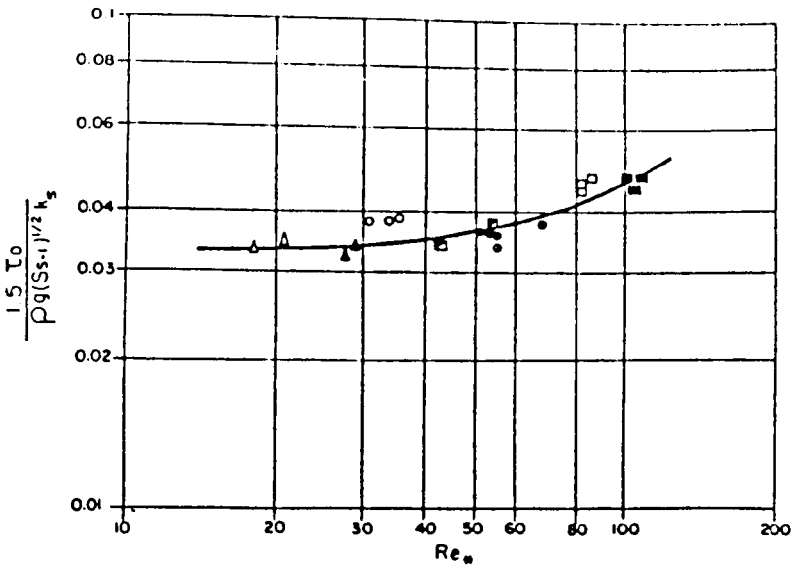

Bed load material		Bed roughness - Sand grain diameter ks	
d (mm)		1.80 mm	0.75 mm
Plastic Ss = 1.28	2.0	○	△
	3.2	●	▲
Glass Ss = 2.38	3.2	□	▣
	4.0	■	●

FIGURE 2.8 ENTERTAINMENT FUNCTION (Ippen and Verma 1953)

Bonapace (1981) analysed theoretically the lift force acting on individual particles at the threshold of movement, by incorporating the Colebrook-White resistance equation and correlating with published data. The following equation was obtained for the energy gradient (S) of the flow needed to produce movement of particles in the pipe flowing full:

$$S \log \left[\frac{15\, d_m}{k_s + 6.5\, V(gDS)^{-0.5}} \right] = 0.0488\, (S_s - 1)\, \frac{d_m}{d} \qquad (2.21)$$

where d_m is the maximum particle size, D is the pipe diameter, d is the mean particle size and V is the flow velocity.

Novak and Nalluri (1975) investigated the incipient motion of discrete particles on smooth fixed beds of open channels in both rectangular and circular tilting flumes. They identified incipient motion by a slight sliding and/or tossing of the particles and an occasional bigger movement of one or two particles. The particles were placed along the centre line of the channel in such a way that there is no interference amongst them. Their study covered a range of particle diameters varying from 0.6 to 50 mm of natural river materials with average relative density of S_s=2.56.

A general equation for the threshold condition was given as:

$$\frac{V_c}{\sqrt{gd(S_s - 1)}} = 0.61\, (d/R)^{-0.27} \qquad (2.22)$$

where V_c is the critical velocity for incipient motion, d is the particle size and R is the hydraulic radius.

Novak and Nalluri (1984) reanalysed the data of Ojo (1978) collected from experiments in a 15 m long and 300 mm diameter circular section flume and in two 15 m and 6 m long 300 mm wide rectangular glass-walled tilting flumes; the latter were also used for all the rough bed experiments. The range of particles size d (equivalent diameter) used in the experiments was from 0.6 to 50 mm with an average relative density of 2.56. The bed of the rectangular section flume was artificially roughened ($0.30 < k_s\,(mm) < 4.2$) giving an experimental range of $0.008 < (d/R) < 1.0$, and $3.5 < (d/k_s) < \infty$, R being the hydraulic radius of the entire cross section. The critical velocities for incipient motion was expressed by the functional relationship:

$$\frac{V_c}{\sqrt{gd\,(S_s-1)}} = a\,(d/R)^b \qquad (2.23)$$

where a and b are constants and functions of bed conditions and single/touching particles involved, as summarized in Table 2.1.

TABLE 2.1: COEFFICIENTS a AND b IN THE ABOVE FUNCTIONAL RELATIONSHIP (2.23) (Novak-Nalluri 1984)

bed condition	channel shape	single/ touching particles	k_s (mm)	d/R	d/k_s	a	b	Eq.
smooth bed	pipe and rectangular	single	0.0	0.008-1.0	∞	0.61	-0.27	2.23.1
rough bed	rectangular	single	0.3-4.42	0.01-0.03	3.5-80	0.54	-0.38	2.23.2
smooth and rough beds	rectangular	touching	0.0-4.2	0.01-0.3	3.5-∞	0.5	-0.40	2.23.3

2.3.2 Bed Load Transport

a) Rectangular Channels

Perdoli (1963) carried out experiments in two rectangular channels (300 mm wide, 6 m long and 600 mm wide, 44m long) five different sediment sizes ranging from 2.6 mm to 11.1 mm; a range of sediment volumetric concentrations from 0.0014 to 0.0049 were used in 600 mm wide flume and two sediment sizes, 2.6 mm and 5.2 mm, in 300 mm wide channel, the volumetric concentration was in the range from 0.000022 to 0.01. Perdoli studied the bed-load transport in rectangular channels with fixed smooth beds.

Mayerle's et al (1991) re-evaluated Perdoli's results in terms of ϕ and ψ for each flume as follows:

$$\phi = 16.56\ \psi^{-1.60} \qquad (2.24.1)$$

for 300 mm wide flume.

$$\phi = 44.21\ \psi^{-2.03} \qquad (2.24.2)$$

for 600 mm wide flume

It has to be mentioned here that Eqs. 2.24.1 and 2.24.2 are not carefully represented the data as it was found that different equations (with better correlations) can be developed for each sediment size.

Ojo (1980) studied sediment transport as bed-load in two rectangular flumes, 6.0 m long and 12.0 m long, both 300 mm wide. The bed load transport was defined as the maximum possible rate of transportation along the channel without the

tendency for the sediment to deposit. Five uniform particle sizes of sand having an average relative density equal to 2.68 and d_{50} varying from 0.48 mm to 1.80 mm were used, covering a range of sediment volumetric concentration from 1.72×10^{-5} to 1.62×10^{-4}. His results were expressed in terms of (ϕ) and (ψ) using the hydraulic radius of the entire cross section as follows:

$$\phi = 6.30 \ (\psi)^{-1.8} \qquad (2.25)$$

Novak and Nalluri (1975, 1984) studied sediment transport as bed-load over rigid smooth beds with bed load defined as the maximum possible rate of transport along the channel without the tendency for the sediment to deposit. The experiments were carried out in three flumes; a 152 mm diameter, 10 m long PVC pipe, a 305 mm diameter, 8 m long perspex pipe, and a 305 mm wide, 15 m long glass walled rectangular flume. Sediment particles ranging from 0.15 mm to 2.0 mm, and average relative density S_s=2.56 were used, covering the range of sediment concentration by volume from 6.6×10^{-5} to 2.4×10^{-3} in the 152 mm diameter pipe channel, 1.7×10^{-5} to 1.17×10^{-4} in the 305 mm diameter pipe channel and 2.6×10^{-4} to 3.8×10^{-4} in the 305 mm wide rectangular channel. From the results, considering the hydraulic radius of the entire cross section, they derived the following equation for the non-deposition condition:

$$\phi = 11.6 \ (\psi)^{-2.04} \qquad (2.26)$$

Replacing channel slope S by Darcy-Weisbach's equation for head loss,

$$S = \frac{\lambda V^2}{8gR} \qquad (2.27)$$

Eq. 2.26 can be written as:

$$\frac{V_L}{\sqrt{8gR\ (S_s-1)}} = 0.632\ (d/R)^{0.175}\ C_v^{0.325}\ \lambda_o^{-0.662} \qquad (2.28)$$

in which λ_o is the Darcy-Weisbach's friction coefficient without sediment, V_L the limit deposition velocity, S_s the relative density of the sediment, R the hydraulic radius, d the particle size, and C_v the volumetric sediment concentration.

Mayerle (1988) studied sediment transport as bed load in rigid smooth and rough beds. Experiments were conducted on the transport of non-cohesive sediments without deposition in rectangular channels (widths 311.5 and 462.3 mm with rigid smooth and rough beds and in a smooth circular cross section channel 152 mm diameter). Uniform materials having relative density $2.49<S_s<2.69$, and d varying from 0.5 mm to 8.74 mm were used; the beds were artificially roughened by two different techniques, namely by glueing water proof sand paper to the bed (k_s=0.5 mm) and by glueing rubber mat (k_s=0.75 mm). The bed load transport was defined as the maximum possible rate along the channels without any tendency for the sediment to deposit, i.e, the sediment at the limit of non-deposition. Using the dimensionless analysis approach, Mayerle combined the parameters that influenced the sediment transport process.

By using the regression analysis method, the following equations were finally selected to calculate the average flow velocity for limit-deposition in rectangular cross section channels:

$$\frac{V_L}{\sqrt{gd(S_s-1)}} = 11.59\ C_v^{0.15}\ D_{gr}^{-0.14}\ (R_b/d)^{0.43}\ \lambda_{bs}^{0.18} \qquad (2.29)$$

with $r^2 = 0.93$,

$$\frac{1}{\sqrt{\lambda_{bs}}} = -2.0 \log \left[\frac{k_{ssb}}{11.54\ R_b} + \frac{2.51}{R_{eb}\sqrt{\lambda_{sb}}} \right] \qquad (2.30)$$

with $r^2 = 0.38$

$$\frac{k_{ssb} - k_{bs}}{R_b} = 0.0245 \left[D_{gr} \right]^{0.40} C_v^{0.44} \qquad (2.31)$$

where R_b the bed hydraulic radius, V_L the mean velocity of flow, λ_{bs} the bed friction coefficient with sediment, d is the equivalent particle size ($\cong d_{50}$) and k_{sb} and k_{ssb} are the equivalent bed roughnesses with clear water and with sediment respectively.

Kithsiri (1990), using the same experimental facilities as Mayerle (1988), extended the range of relative roughness ($0.73 < k_s(mm) < 5.61$). He conducted limit deposition experiments using the rectangular flume 311.5 mm wide. He used uniformly graded sands (d_{50}) ranging from 1.0 to 8.4 mm in size with relative density varying between 2.61 and 2.63. The volumetric sediment concentrations ranged between 1.0×10^{-5} and 4.3×10^{-3}.

Using his own data and Mayerle's data Kithsiri proposed a method based on determining the minimum shear stress required for non-deposition condition. The method is based on the following best fit equations:

$$\frac{\tau_b}{\rho(S_s-1)gd} = 12.93 \left[D_{gr}\right]^{-0.21} \left[\frac{d}{R_b}\right]^{-0.98} C_v^{0.29} \lambda_{bs}^{1.5} \qquad (2.32)$$

with $r^2 = 0.918$, and

$$\lambda_{bs} = 0.851 \lambda^{0.86} C_v^{0.04} D_{gr}^{0.03} \qquad (2.33)$$

with $r^2 = 0.964$.

Eq. 2.32 can be re-written (using Darcy's equation 2.27) as:

$$\frac{V_L}{\sqrt{gd(S_s - 1)}} = 10.17 \left[D_{gr}\right]^{-0.11} \left[\frac{d}{R_b}\right]^{-0.49} C_v^{0.15} \lambda_{bs}^{0.25} \qquad (2.34)$$

Eq. 2.34 is similar to Eq. 2.29 developed by Mayerle (1988). The slight differences in the exponents are attributed to the difference in the level of bed roughnesses.

b) Channels Of Other Cross Sections

Craven (1953), studied the sediment transport in smooth pipe flowing full, using essentially the same equipment as that used in the incipient motion studies. Fluid and sediment discharges were established at predetermined rates and so maintained until equilibrium was reached. He derived an expression for the maintenance of the sediment in motion at

all times which reads:

$$\frac{Q}{D^{2.5}\ C_v^{1/3}\ (S_s-1)^{1/2}} \geq 5.0 \qquad (2.35)$$

and can be rearranged as follows:

$$\frac{V}{\sqrt{gd(S_s-1)}} \geq 6.37\ C_v^{1/3}\ (d/D)^{-0.50} \qquad (2.36)$$

Equation 2.35 enables either the computation of the necessary velocity for the maintenance of sediment-free pipes or the maximum amount of sediment that the flow can carry without getting deposited.

Ambrose (1953) extended Craven's investigation to pipes under free surface conditions, using essentially the same equipment. For the range $10^{-4}<C_v<0.06$ his data fits the following equation

$$\frac{Q}{g^{2/5}\ D^2\ \ Q_s^{1/5}(S_s-1)^{2/5}} = 3.61\ (y_o/D)^{1.50} \qquad (2.37)$$

for any degree of filling y_o/D, Q_s being the sediment discharge. For half-full depth condition, equation (2.37) can be rearranged as:

$$\frac{V}{\sqrt{2g\ (S_s-1)\ D}} = 2.45\ \ C_v^{1/4} \qquad (2.38)$$

Laursen (1956) reported the results of an experimental programme carried out using three types of closely-graded sand and two types of mixed sand with d_{50} sizes ranging from 0.25mm to 1.6mm and $1.8\text{x}10^{-4} < C_v < 3.0\text{x}10^{-1}$. Measurements were made with part-full and full flow pipes. May (1975) showed that Laursen's results for the limit of deposition in pipes (51 and 152 mm diameters) flowing full and part-full can be expressed quite well by:

$$\frac{V}{\sqrt{2g\ (S_s-1)\ y_o}} = 7.0\ \ C_v^{1/3} \qquad (2.39)$$

Eq. 2.39 is valid only for flow depths between $0.1<(y_o/D)<1.0$, with y_o being placed by D in full pipe flow conditions.

Robinson and Graf (1972) carried out transport experiments in two smooth pipes (102 and 152 mm diameters) flowing full. They used two sediment sizes, 0.45 and 0.88 mm. The volumetric sediment concentration (C_v) varied between 10^{-3} and $7\text{X}10^{-2}$. A relation for the limit of deposition criterion was obtained:

$$\frac{V}{\sqrt{2g\ (S_s-1)D}} = \frac{0.928\ C_v^{0.105}\ \ d^{0.056}}{1\ -\tan(\Theta)} \qquad (2.40)$$

where d is the sediment size in mm, $\tan(\Theta)$ the slope of the

pipe and V is velocity at limit deposition.

May (1982) conducted experiments using smooth pipes of 158 mm diameter and 21 m long and 77 mm diameter and 20 m long flowing full and part full. Three types of sediment were used: a medium sand with a d_{50} size of about 0.6mm, a fine rounded gravel with a d_{50} size of about 5.8 mm and a similar but somewhat larger gravel with a d_{50} size of about 7.9 mm. The three types of sediment all had average relative density of 2.65, covering the range of sediment volumetric concentration $4.7\text{x}10^{-6} < C_v < 2.1\text{x}10^{-3}$, and flow velocities in the range of 0.45 and 1.2 m/s were used.

A conceptual model was proposed which described the motion of sediment in flume traction up to the limit of deposition. It has been suggested that the relation between the concentration and flow velocity be obtained for little or no-deposition:

$$C_v = 0.0205\ (D^2/A)\ (d/R)^{0.6}\left[\frac{V_L^2}{g(S_s-1)D}\right]^{3/2}\left[1-\frac{V_c}{V_L}\right]^4 \qquad (2.41)$$

where V_L is the self cleansing velocity, limit deposition, and V_c is the effective threshold velocity predicted by Novak and Nalluri's equation for rigid smooth channels (Eq.2.23.1) May made use of Colebrook-White's equation to find the friction factor for clear water flow in smooth pipe. Provided there is no deposition, he assumed that the hydraulic roughness caused by sediment would not exceed 10% and it should be added as a simple addition to the friction

factor for clear water flow.

In 1989, May et al revised equation 2.41 in order to provide a better description of the effects of part-full flow on the limit of deposition. Eq. 2.41 rearranged gives:

$$C_v = 2.11 \times 10^{-2} \, (y_o / D)^{0.36} (A/D^2)^{-1} (d/R)^{0.6} \left[1 - \frac{V_c}{V_L}\right]^4 \left[\frac{V_L^2}{g(S_s - 1)D}\right]^{3/2} \qquad (2.42)$$

Ackers (1984), introduced an approach combining the Ackers-White's sediment transport formulae (1973) with the Colebrook-White's resistance equation, to cover channels of any shape of cross section. The Ackers-White's, (A-W), equations were developed primarily for wide open channels with sediment bed. Introducing the concept of an effective width (W_e) over which the sediments were spread during the motion, Ackers concluded that an effective bed width of about ten times the sediment diameter would fit the method, reasonably well, for clean pipe transport calculations.

The general definition of the non-dimensional transport equation is given below: (see Appendix I)

$$G_{gr} = C_v \, (R/d) \quad (A/W_e R)^{1-n} \, (u_* / V)^n \qquad (2.43)$$

where G_{gr} is the transport parameter in A-W equation, (1973) and n the transition exponent dependent on sediment size. The model was calibrated using May's (1982) experimental data

for limit deposition condition. It was found that W_s=10d for non-deposition and W_s=D for some deposition conditions.

Loveless (1986) presented new ideas on the condition of the limit deposition which followed, in part, the treatment of May (1982) and also attempted to clarify the question of the effective width for sediment transport at the limit of flume traction raised by Ackers (1984).

By equating the drag, friction and lift forces on sediment particles lying on a fixed bed, he developed a general equation for flume traction (sediment movement in rigid beds), given as:

$$\frac{(\beta V - u)^2}{g(S_s - 1)d} = \left[\frac{2\,\alpha_2}{\alpha_1}\right]\left[\frac{(\tan\phi\cos\alpha - \sin\alpha)}{C_D + \tan\phi\ C_L}\right] \qquad (2.44)$$

where u is the velocity of the grain, α the gradient of the conduit, α_1 and α_2 are shape coefficients ($\alpha_1 = A_p/d^2$, $\alpha_2 = W/\rho g d^3$, where A_p is the projected area and W is the weight of the particle; $(\alpha_2/\alpha_1)=2/3$ and $\alpha_2 = 0.524$ for spherical particles); ϕ is the friction angle between the surface and the grain, C_L is the lift coefficient for the grain and β, a non-dimensional parameter introduced by May (1982), is the ratio of the flow velocity in the vicinity of the particle to the average flow velocity.

Loveless then argued that the coefficient of drag, (C_D), acting on each sediment particle will depend on the particles spacing. Employing Ackers' effective bed width, W_s, he

proposed a relationship for the particle spacing coefficient, η, given below as:

$$\eta = \frac{Q_s}{u\, d\, W_s\, \alpha_2} \qquad (2.45)$$

where Q_s is the sediment rate.

At the limit of deposition a value of 0.5 was suggested for η. The theory presented was tested on three different conduit shapes; rectangular, oval, and circular cross sections. The sediments used were non-cohesive fine and coarse sand (although only the fine sand results were reported in his paper). Both sands were nearly uniform in size having d_{50} of 0.45 mm and 1.5 mm respectively.

Suki (1987) studied sediment transport on rigid smooth and rough pipes flowing full. Experiments were conducted in two rigid smooth pipes: 164 mm and 253 mm diameter, and 18 m. long and in four pipes with rigid rough bed ($0.83<k_s(mm)<2.70$): 155 mm, 159 mm, 162 mm and 249 mm diameters and 18 m long. Sediment sizes ranging from 1.3 mm to 8.0 mm, with an average relative density of $S_s = 2.63$, were employed in the smooth pipe experiments, covering a range of sediment volumetric concentrations from 2.5×10^{-5} to 4.79×10^{-4}. In the rigid rough type experiments, sediment sizes ranging from 1.30 mm to 8.0 mm were used, covering a range of sediment volumetric concentrations from 1.9×10^{-5} to 1.02×10^{-3}.

Two equations were produced from the analysis.

$$\frac{V}{\sqrt{gd(S_s-1)}}=2.86\left\{\frac{k_s}{d+k_s}\right\}^{0.22}\left\{\frac{\log(43.13(1+d/k_s))}{\log(4.8D/k_s)}-\frac{2.01\ D(d/k_s)C_v}{d\ k_s}\right\}^{-1}$$

(2.46)

for smooth pipes and

$$\frac{V}{\sqrt{gd(S_s-1)}}=2.73\left\{\frac{k_s}{d+k_s}\right\}^{0.3}\left\{\frac{\log(43.13(1+d/k_s))}{\log(4.8\ D/k_s)}-\frac{6.28\ D(d+k_s)C_v}{d\ k_s}\right\}^{-1}$$

(2.47)

for rough pipes ($0.83<k_s(mm)<2.7$).

Eq. 2.46 which was developed for smooth pipes is highly dependent on k_s. Therefore, this equation will give indeterminate estimate of velocity when it is applied to new smooth pipes where k_s is less than or equal to zero.

Mayerle (1988), studied the sediment transport as bed load in smooth pipe channel, 152 mm in diameter and proposed the equation describing the average velocity for non-deposition in circular cross section channels as:

$$\frac{V}{\sqrt{gd(S_s-1)}} = 14.43\ \ C_v^{0.18}\ \ D_{gr}^{-0.14}\ (R/d)^{0.56}\ \ \lambda_s^{0.18}$$

(2.48)

where λ_s is the channel friction factor with sediment, which can be calculated from Colebrook-White's equation.

2.3.3 Suspended Load Transport

Macke (1982) introduced a new computational method which permits partly filled pipelines to be designed in such a way that sediment free flow conditions are produced. For this purpose, Macke defined the critical transport condition as the condition which only just prevents permanent sedimentation on the bottom.

A computational method which expresses the total transport load Q_s as a function of the mean shear stress τ_o and the actual settling velocity W_o was proposed by the equation :

$$Q_s^* = Q_s \ (S_s-1) \ \rho g \ W_o^{1.5} = C_1 \ \tau_o^n \qquad (2.49)$$

where Q_s^* is the sediment parameter $\left[\frac{N}{s} \ (\frac{m}{s})^{3/2}\right]$ and the coefficient C_1 as well as the exponent n are subject to the respective transport conditions and the flume geometry. To define the above relationship, Macke conducted experiments in pipes having the nominal diameters 192 mm, 290 mm and 445 mm. Two sand sizes where used, 0.16mm and 0.37mm, and flow range $0.1<y_o/D<0.9$. For $Q_s^* \geq 2.0x10^{-4}$, the sediment transport is defined by the approximate expression:

$$Q_s \ (\rho_s-\rho) \ g \ W_o^{1.5} = 0.000164 \ \tau_o^3 \qquad (2.50)$$

CIRIA (1987) expressed Macke's method using SI units and assuming the fluid is water in the form:

$$V = 1.98 \ \lambda_o^{-0.6} \ W_o^{0.30} \left[(S_s-1) \ A. \ C_v\right]^{0.2} \qquad (2.51)$$

where λ_o is the Darcy-Weisbach's friction factor of the flow. Eq. 2.51 is not applicable for $C_v\ Q\ g\ (S_s-1)W_o^{1.5} \leq 2.0\times10^{-4}$. At these lower rates Macke proposed that τ_o should be greater than 1.0 N/m^2.

The fall velocity W_o (m/s), in equation (2.49) can be obtained using the following equation:

$$W_o = \sqrt{\frac{4}{3}\frac{gd\,(S_s-1)}{C_D}} \qquad (2.52)$$

in which C_D is the drag coefficient. Macke proposed for $R_{*d}\left[-W_o\ d/\upsilon\right] \geq 0.1$, the following equation for C_D:

$$C_D = \frac{24}{R_{*d}} + \frac{5.06}{\sqrt{R_{*d}}} + 0.25 \qquad (2.53)$$

For $R_{*d} < 0.1$,

$$C_D = 24/R_{*d} \qquad (2.54)$$

Arora et al (1984) attempted to identify the criteria for the total (bed and suspended) load to occur without any deposition along rigid smooth and rough conveyances. Experiments were conducted in a rectangular channel 400 mm wide, 16 m. long with rigid smooth and rough beds, in a trapezoidal channel (bottom width 200 mm, side slope 1:1) and in a semicircular channel (diameter 400 mm) with both rigid and smooth beds. Three uniform sands of relative density 2.65 and sizes of 0.147 mm, 0.106 mm and 0.082 mm and uniform coal (S_s=2.04) particle of size 0.164 mm,

covering a range of sediment volumetric concentration from 3.5×10^{-5} to 6.56×10^{-3} were used.

The main conclusions arrived at are:

1) the limiting concentration of transported material, (C_v), in rigid boundary channels increases with an increase in the value of D_h/y_o (where D_h is the hydraulic depth = area/ surface width, B,), and

2) the C_v in rigid boundary channels of various shapes is a unique function of the parameter (see Fig. 2.9):

$$C_v = f\left\{\frac{q\left\{S/(S_s-1)\right\}^{2.5}}{\upsilon\,\lambda_b^2\,(W_o d/\upsilon)^{0.6}}\left\{\frac{D_h}{y_o}\right\}^{2.0}\right\} \qquad (2.55)$$

in which q is the unit water discharge and λ_b is the bed friction factor.

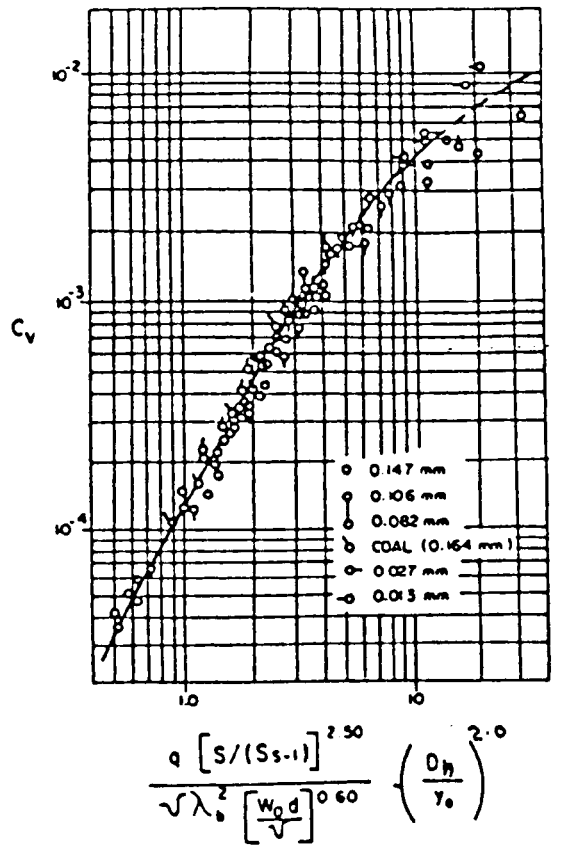

FIGURE. 2.9 ARORA ET AL'S (1984) CRITERIA FOR THE TOTAL LOAD WITHOUT DEPOSITION

Nalluri (1986) reanalysed Arora et al's data for no deposition in the rectangular channel with rigid smooth bed, and presented the results in terms of flow intensity (ψ) and transport (ϕ) parameters using the bed hydraulic radius as follows:

$$\phi = 100 \quad \psi^{-4.5} \tag{2.56}$$

This equation is applicable in the range $10^{-1} < \phi < 10^{1}$.

Westrich and Juraschek (1985), using the energy balance concept (i.e the non-deposition suspended sediment transport is characterized by the fact that no bed load transport is occurring and therefore, no energy consuming interaction between bed forms and the flow can take place) conducted experiments using a fixed bed rectangular flume (700 mm wide for smooth boundary conditions and 1000 mm for rough boundary conditions), and very fine quartz powder (S_s = 2.65) with medium particle sizes of 0.026 mm, 0.038 mm, 0.050 mm and 0.110 mm. The experimental data show a reasonable correlation between the transportable sediment concentration, C_{vs}, and the energy parameter $\left\{\frac{\tau_b \quad V}{(\rho_s-\rho)\, g y_o \bar{W}_o}\right\}$.
In the rough wall experiments the channel boundary was hydraulically rough. However the roughness it-self does not obviously affect the transport capacity. The experimental relationship shows that the limiting suspended sediment concentration (C_{vs}) in rigid boundary channels is described by the correlation:

$$C_{vs} = 0.0018 \frac{\tau_b \; V}{(\rho_s - \rho) \; g \; Y_o \; W_o} \qquad (2.57)$$

Equation 2.57 was compared with the published experimental data, (Fig. 2.10). This comparison using Arora et al's (1984) data, showed a large discrepancy in the sediment concentrations.

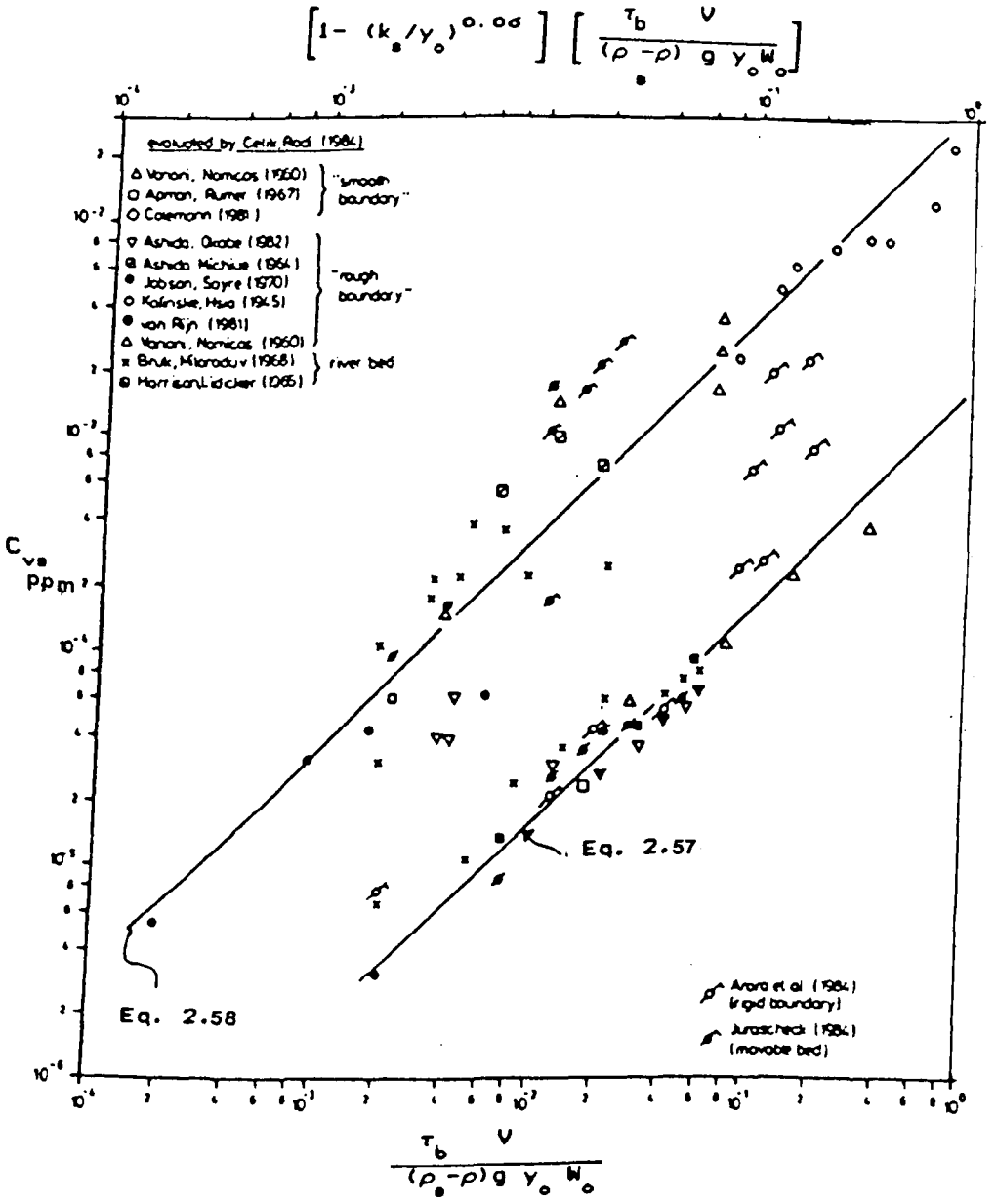

FIGURE 2.10 SEDIMENT TRANSPORT CAPACITY PREDICTED BY EQS. 2.57 and 2.58 WITH LITERATURE DATA.

Celik and Rodi (1984, 1985) from an evaluation of special laboratory and field measurements with smooth and rough rigid boundary and loose flat bed channels suggested the correlation:

$$C_{vs} = 0.034 \left[1-(k_s/y_o)^{0.06}\right] \left[\frac{\tau_b V}{(\rho_s-\rho) g\ y_o\ W_o}\right] \qquad (2.58)$$

where k_s/y_o is the relative roughness, τ_b the bed shear stress, y_o the flow depth, and W_o is the fall velocity of the particle.

CHAPTER 3

SEDIMENTS IN SEWERS WITH DEPOSITED BEDS

3.1 General

Sub-surface masonry storm drains were constructed at least as early as 3000 years ago. Extending well into the nineteenth century, sewers and drains in Europe were intended primarily for storm water conveyance. There were no sanitary sewers; human and other wastes were deposited on courtyards and on streets. The discharge of faecal matter and other human wastes into storm sewers and drains was generally prohibited. With the realization that infectious diseases were water borne, the planning and construction of combined sewer systems began in large European and U.S. cities in the mid-nineteenth century. The construction of combined sewer systems subsequently slowed down early this century, primarily because of surface water pollution attributed to combined sewer overflows (Metcalf & Eddy, 1972). Sedimentation problems were recognised to be common in most of the existing systems.

In arid zones where rainstorms are infrequent but intense with rainfalls approaching 100 to 150 mm/hour for periods of up to 15 minutes, separate sewers were recommended for several reasons, including the following:-

(1) Combined sewers would be disproportionately large. For example, service for a densely populated 20 hectares (300 people per hectare) would require a pipe designed for 6000 to 7000 l/s. The dry weather sewage flow would be only about 10

l/s. The practical effect of this would be deposition of sewage solids during the dry seasons with the flushing out of solids, if erodable, to the wadis during rain storms.

(2) If combined sewers were too small, sewage/storm water would back up through house connections causing health hazards.

(3) The sediment carried by the storm water would clog combined sewers if sediment traps were not placed up-stream of the entry place.

The sediment in storm sewers is broadly similar in characteristics to those found in combined sewers i.e one that conveys both storm and foul water, as the prime source of the surface wash-off is common to both types of drainage system. However, the two types of system differ markedly with regard to the behaviour of sediments within the system. As flow in a storm sewer is intermittent which is not usually the case in a combined system, sediment transport will consist of a pulsed series of inputs from the surface and a series of cycles of transport, deposition and erosion within the sewer. While in many respects this parallels the behaviour of surface derived inorganic sediments in a combined sewer, storm sewer sediment will not receive additional inputs of settled pollutants from the flowing sewage during dry weather flow (DWF), when the flow is minimal.

3.2. Nature Of Sediment In Storm Sewers

There have been only a few investigations that looked into

the nature and amount of sediment found in storm sewers. One of these is Sarter et al (1974) who found that the major constituent of pollution from roads was inorganic matters, similar to common sand and silt, and the average loading intensity of solid material was 400 Kg/Km of kerb and that 57% of the solid material was larger than 0.25 mm in diameter.

Ellis (1976) investigated the sediment and water of urban storm sewers in the Silk Stream catchment in north London, the composition of the urban sediment comprised 45% - 70% of inorganic material by weight.

Brocker (1984) stated that the estimated volume of sewer depositions range between 20% and 45% of the in-line storage capacity and he reported that the contribution from surfaces to pipe deposits is very small compared to the contribution from dry weather flows.

Water Research Centre (1984) report indicated that the sediment sampling carried out in various sewer sites suggested that d_{65} will typically be in the range of 0.5 to 5.0mm.

Suki (1987), in his study stated that the types of sediment in a storm sewer are mainly sand and gravel having a specific gravity of 2.65. The nature of flow in a storm sewer is intermittent and this sand and gravel, due to its weight, usually forms a deposit at the end of each storm.

Crabtree (1988), reported that predominantly coarse granular mineral material was found in the invert of pipes, and a

sample taken from a storm sewer during the survey revealed that almost 98% of the sediment found were gravel and sand.

Verbank (1990) collected data from Brussels combined sewer lines which are mainly composed of egg-shaped sewers; he noticed the accumulation of deposits on sewer inverts over several months (Fig. 3.1), and found that the sediments deposited are primarily composed of coarse sand material, which will be moved only during exceptionally intense summer storms.

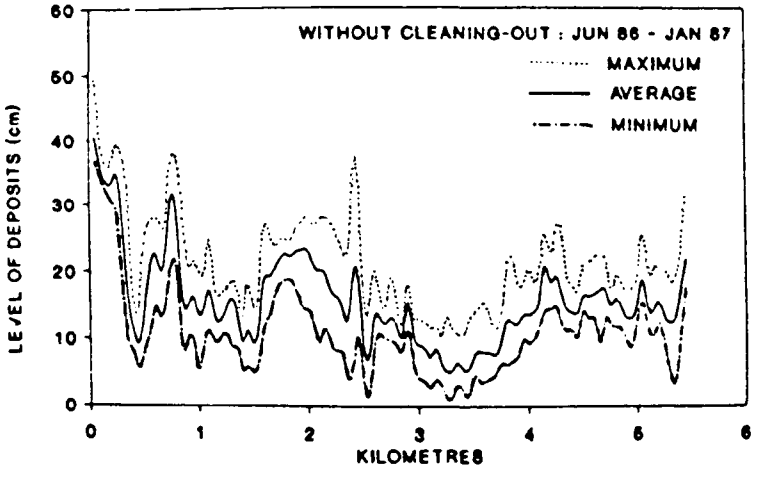

FIGURE 3.1 IN-SEWER DEPOSITION OF BRUSSELS MAIN TRUNK SEWER, (after Verbank, 1990)

It is known that the main factors that may influence the sediment yields are:-

1- Geographical location

2- Sewer system type (storm or combined)

3- Land use (rural, residential, commercial or industrial)

4- Time of year

5- Preceding dry period

6- Gritting

7- Rainfall characteristics, and

8- Condition of the invert (i.e no bed, loose bed, rigid cemented bed)

3.3 Sewer Design Standards

a) Design Flow

In general, storm sewers must be able to discharge the peak flow without any overloading. However, the profile will usually not be sized only up to the peak flow. Some reserves of capacity are normally allowed, since the peak flow is only a stationary mean value which can be surpassed on occasions. But this is not the only reason for designing the sewer larger than for the peak flow. Full flowing sewers favour the generation of sulphides. To avoid this, sufficient ventilation is of great importance.
Therefore a maximum flow of two-third full is advised in most sewer systems.

b) Flow Calculations

Traditionally, without any consideration of the sedimentation problem, sewer slope is calculated by the general relationship derived by Darcy-Weisbach's equation (Eq. 2.27).

The friction factor may be calculated by the Colebrook-White formula, which is assumed to be applicable to all kinds of fluids and flow conditions:

$$\frac{1}{\sqrt{\lambda_o}} = -\ 2\ \mathrm{Log}\left(\frac{2.51}{R_e\sqrt{\lambda_o}} + \frac{k_s}{3.71\ D}\right) \qquad (3.1)$$

The design of the sewer system must satisfy the major criterion which is the so called "Self-Cleansing" velocity; this varies, according to different standards, from 0.5 to 1.5 m/s according to the size and shape of the sewer; this velocity, in theory should be able to keep in motion grit of 2-3 mm in size.

A minimum size of sewer of 200mm is recommended generally to avoid clogging even if deposition occurs temporarily.

3.4. Fixed Deposited Beds In Sewers

Where the sewer system is laid with mild slopes or where the flow velocity is below the threshold velocity for sediment transport, a continuous sedimentation will form a flat bed. In Dry Weather Flow (DWF), especially in arid areas where the dry season lasts for quite a long time the deposited bed will become permanent and less erodable.

In the normal sense of gravitational settling, no deposition is possible around the upper half of the perimeter of a circular sewer simply because of the downward orientation of this part of the perimeter. Therefore, the region of the boundary of a circular sewer susceptible to deposition is limited to the lower portion of the sewer with a possible maximum bed thickness of 0.5D.

The non-mobile sediment at the bottom of the pipe affects the velocity field because the cross section adopts different shapes depending on bed thickness and flow depths; also the sediment bed has a roughness which is different from that of the side walls (usually larger). The total effect is a higher resistance to flow, i.e, a decrease in flow capacity and increase in the head loss due to friction between flow and the sediment bed.

The shape of the channel flow-section varies considerably with sediment bed thickness and flow depth. For flow up to half-full depth the channel assumes trapezoidal-like section with sides having a single curvature, while for flow above half-full depth the channel sides have two curvatures opposing each other which in turn may considerably influence the hydraulic characteristics of the channel.

Laplace et al (1990) have studied the transport of solids in sewer networks. In a comprehensive survey carried out in a trunk sewer in Marseille (France), they noted that the volume of sediment increases substantially during the first rains and much less during subsequent ones; they confirmed that the volume deposited in the sewer seems to become stable after several months.

With the fact that in sewers where the sediment bed has become consolidated or cemented to some extent making it impossible to be eroded even under full flow conditions, rehabilitating existing sewer systems and retaining as much as possible of them is more economical. In light of this it

is crucial to be able to assess the hydraulic and sediment movement performance of a sewer with flat deposited beds.

3.5 Self-Cleansing Conditions For Sewers

Current practice for the design of self-cleansing sewers is to ensure that either the flow velocity or the shear stress produced by the flow exceeds a certain limiting value. Such limits are usually linked with a requirement that they be achieved at a given depth (e.g with the pipe half-full) or with a given frequency (e.g. once a day on average for a combined sewer). These conditions lead to values of minimum gradient below which gravity sewers should not be laid if they are intended to be self-cleansing.

British Standards code of practice 2005 and BS 8005 recommend velocities of 0.76 m/s for part-full and 1.0 m/s for full-bore flow conditions respectively.

According to Yao (1974) a minimum velocity of 0.6 m/s when flowing full is considered adequate for sanitary sewers. The corresponding minimum velocity for storm sewers is 0.9 m/s. For combined sewers a full flow minimum velocity of 1.5 m/s is desirable.

Most of the recommended design methods for self-cleansing sewers by various authors are based on minimum flow velocity. However, there is a trend towards abandoning the critical velocity concept in favour of the critical shear stress. Support of this approach is provided by Shields (1936) who demonstrated the relationship between shear stress and the movement of particles over a plane bed of similar particles.

Yao (1974), studied the use of minimum shear stress in the design of self-cleansing sewers and for practical applications he suggested a critical shear stress of 1.0 N/m^2 to 2.0 N/m^2 for sanitary sewers and of 2.9 N/m^2 to 3.9 N/m^2 for storm sewers. The minimum shear stresses and minimum velocities which have been recommended for the design of self-cleansing sewers by various researchers are presented in Tables 3.1 and 3.2. But for both the above described criteria, the effect of sediment concentration or the sediment size was not taken into account.

It must be mentioned here that the experiments carried out during recent years on this subject suggest that the self-cleansing velocity is not constant but depends on a number of factors such as type, size and the concentration of sediments, size, shape and surface roughness of the conveyance and flow rate. Novak and Nalluri (1984) concluded that, for deposit-free conditions, much higher velocities (hence gradients) are needed in large pipes (D≥ 300 mm) than previous engineering recommendations envisaged.

TABLE 3.1 Recommendations For Sewer Design In Terms Of a Minimum Shear stress (CIRIA 1987)

Reference	Country	Sewer Type	Minimum Shear N/m^2	Conditions
Lysne (1969)	Norway		2.0 - 3.0	
Yao (1974)			1.0 - 2.0	
Lindholm (1978	Norway	Foul Combined	2.0 3.0 - 4.0	
Scandiacunsult	Sweden Oslo		1.0 - 1.5 4.0	1/4 full
Bischof (1976)	FRG		2.5	

TABLE 3.2: RECOMMENDATION FOR SEWER DESIGN IN TERMS OF MINIMUM VELOCITY (CIRIA 1987)

Reference	Country	Sewer Type	Min. Veloc. (m/s)	Conditions
ASCE (1970)	USA	Foul Storm	0.6 0.9	full or half-full
Los Angeles (1973)	USA	Storm	1.52	half-full
ATV (1969)	FRG		0.5	any depth
Bielecki (1982)	FRG		1.5	pipe full
Imhoff (1956)	FRG		0.5	half-full
Bartlett (1976)	UK	Storm	0.75-1.0	pipe-full D>900 mm
BSI (1986)	UK	storm foul combined	0.75 1.0	pipe-full pipe-full

3.6 Effect of Shape of Channel Cross Section on Transportation of Sediments

This section summarises results of studies made to determine the effect of pipe shapes on sediment transportation. Zenz and Othmer (1960) considered the possibility of increasing the carrying capacity of pipelines by altering the shape of the conduit cross section. They investigated two elliptical pipes (with the major axis of the ellipse either vertical or horizontal) and two divided circular pipes (with a dividing plate placed either vertically or horizontally). They found that the limit deposit velocities within all these shapes were greater than that within the round tube. Thus, they concluded that rounded pipes were the optimum shape to carry suspended load.

Fröhlich (1985) (see Raudkivi1990), studied the sediment transport characteristics of a circular pipe at partial flow depths. The study showed that a pipe with a flat bed at 0.1 diameter depth is more efficient in deposit free sediment transport than the circular cross section. Writing the sediment transport load Q_s proportional to $\eta\rho QS$, i.e stream power approach, where ρ is density of water, Q is water discharge, S is slope, and η is the transport efficiency, and evaluating η yields:

circular cross section	$\eta = 31.58\ S^{1.17}$	(3.2.1)
flat bed at depth 0.1 D	$\eta = 64.69\ S^{1.07}$	(3.2.2)
V-groove bed	$\eta = 54.03\ S^{1.5}$	(3.2.3)

The sediment transport efficiency with 0.1 D flat bed depth and full-pipe flow is seen to increase about four times compared to a circular cross section. The 0.1 D flat bed depth reduces the water discharge to about 7.5% or requires a 3% larger diameter for the same flow at the same slope. Figure 3.2. shows that the sediment load (Q_{sp}) and concentration (C_p) for a circular pipe flowing at partial flow depth have been normalised by the values of the pipe flowing full (Q_s, C_v). The relative sediment concentration distribution for the 0.1 D flat bed depth cross section (C_{pf}/C_f) is shown by a dotted line where C_{pf} refers to sediment concentration in a circular channel with flat bed depth of 0.1 D at part-full flow, and C_f is the sediment concentration in a pipe-full flow with flat bed where y_o=0.9 D (y_o is flow depth).

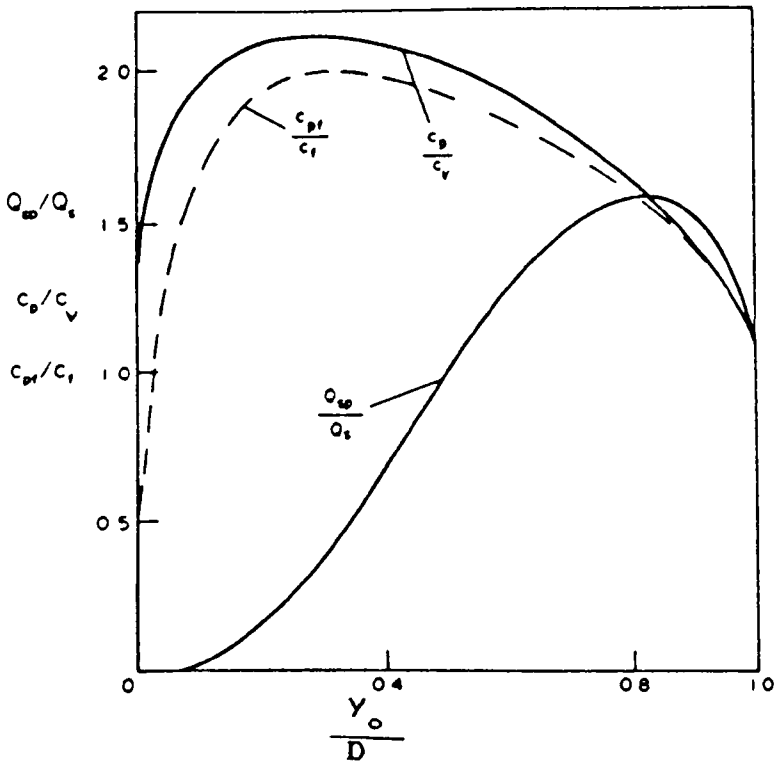

FIGURE 3.2 SEDIMENT TRANSPORT CHARACTERISTICS OF CIRCULAR CHANNEL WITH AND WITHOUT FLAT BED (after Frohlich, 1985)

Loveless (1986) conducted non-cohesive sediment transport experiments in three different conduit shapes, (see Fig.3.3); rectangular, oval, and circular cross sections. The most interesting findings of his theory are:

1- that the effective width (W_e) for sediment transport is a key determinant of the critical velocity necessary to achieve non-deposit conditions. For example the maximum value of the critical non-deposit velocity (V_c), is less than 0.5 m/s for the rectangular conduit placed with its longer side horizontal. For the circular pipe, however, the maximum velocity was 0.63 m/s and for the oval pipe it was 0.71 m/s.

2- the most efficient conduit shape for the conveyance of

high concentrations of non-cohesive sediment was found to be a rectangular conduit with its longer axis horizontal- the shape of a typical box culvert.

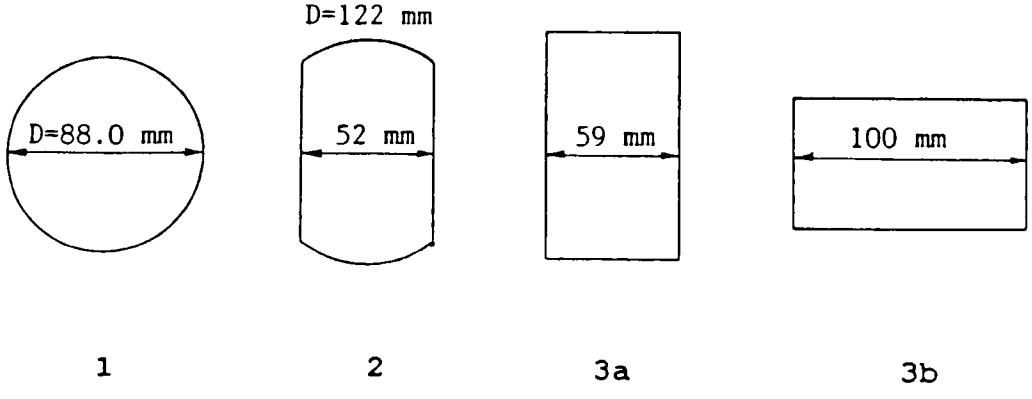

FIGURE. 3.3 CONDUIT SECTIONS
(adopted by Loveless, 1986)

Dhillon et al (1988) examined the effect of conveyance shape on sediment transport in rigid boundary channels and concluded that the rectangular section with its width longer than its depth is the most efficient for transportation of sediment and is followed by a trapezoidal section.

Paul and Sakhuja (1990), investigated the causes responsible for sediment deposition in lined channels with different cross sections as shown in Fig. 3.4. These channels were put into operation in India in order to minimise maintenance costs and improve efficiency. They concluded that the shape of conveyance is the major factor responsible for sediment deposition in rigid boundary channels; the most efficient

conveyance shape for sediment transport is the rectangular section with its longer side horizontal, while the cup-shaped section is the least efficient for sediment transport.

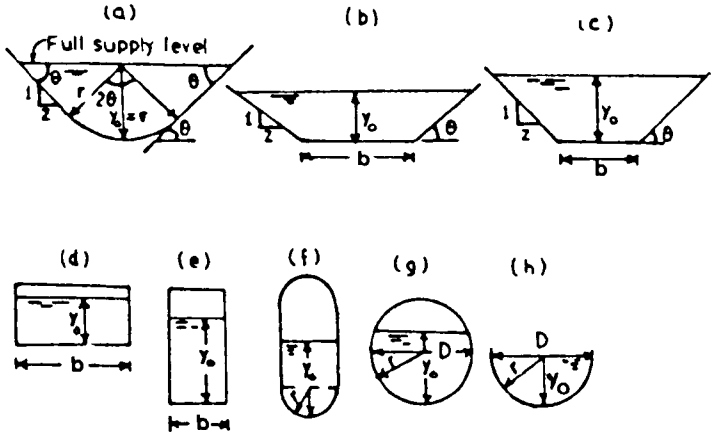

FIGURE 3.4 DIAGRAMS OF CROSS SECTIONS (after Paul and Sakhuja, 1990)

Al-Saqri (1990) reanalysed the results of the Mayerle (1988) study for rectangular and circular channels. The effect of shape on the determination of the minimum velocity required for the sediment to be transported without any deposition was investigated. He concluded that at higher values of C_v and D_{gr} and for any given value of d/R, the sediment particles may be coarse enough to move as a bed load either over a narrow band width along the invert of the circular channel or along the whole width of the rectangular channel. As a result of this difference of movement, the sediment transport for a circular channel is always less than that of the rectangular ones. As the values of C_v and D_{gr} decrease, the sediment particles become fine enough to move in suspension rather than near the bed. In this case the movement of

particles in rectangular cross sections will be influenced by the effect of secondary currents which will increase the mixing of particles from the zones of higher and lower velocities and also increase the energy losses and the corresponding friction factor which in turn will increase the required minimum velocity in rectangular cross section channels.

Recently, Alvarez (1990) studied the influence of sediment bed thickness on sediment transport. He concluded that for similar levels of shear stress the transport rate (weight per unit time per unit width) increases with bed thickness i.e. with increase in bed width.

3.7 Theories of Sediment Transport Over Deposited Beds

a) Loose Sediment Beds

In sewers, the sediment concentration is established by upstream supply. The question is whether the potential transport capacity of the flow is greater or less than the supply rate, which in turn determines whether depositions or scouring of any bed deposits will occur.

The first investigation in this area was performed by Laursen (1956) and concluded that the sediment transporting capacity of a pipe flowing part full decreases once deposition begins. If the sediment and water discharges are kept constant, the depth of the deposits will continue to increase until the pipe flows full and surcharges. He investigated equilibrium conditions for deposited beds only in the case of

pipe full flow. A graphical relationship was established between the proportional depth t_s/D of the sediment deposit (where t_s is the sediment deposit depth) and the parameter: (as shown in Figure 3.5)

$$L = \frac{Q}{\sqrt{g\ (S_s-1)\ D^5\ C_v^{1/3}}} \qquad (3.3)$$

It is convenient to express the relationship by means of a formula, and a reasonable fit is given by:

$$t_s/D = 2\ (L+1)^{-1/3} - 1 \qquad (3.4)$$

It is stressed that this equation does not have any particular theoretical basis, but simply describes the shape of the mean experimental curve presented by Laursen.

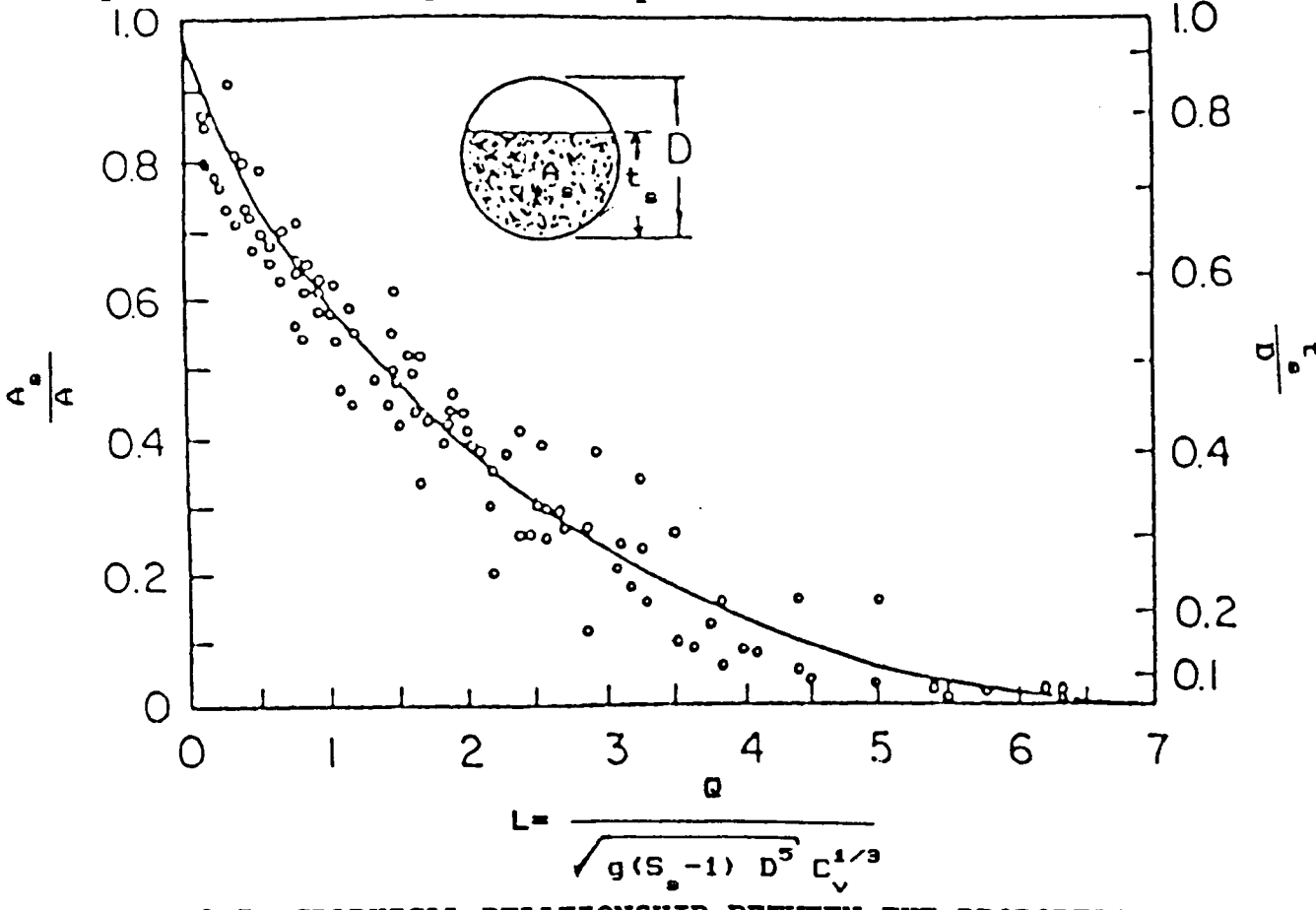

FIGURE 3.5 GRAPHICAL RELATIONSHIP BETWEEN THE PROPORTIONAL DEPTH (t_s/D) AND THE PARAMETER L. (after Laursen 1956)

Graf and Acaroglu (1968) developed a theory for analysis and design of sewers with deposited bed, which can be used in predicting rates of sediment transport in alluvial channels and pipes with bed deposits. Dimensional analysis led to the definition of a transport parameter and a shear intensity parameter. A relationship between these two quantities was established using published data for pipes and flumes with deposited beds. The resulting equation can be expressed in the form:

$$\frac{V}{\sqrt{8g(S_s-1)R}} = 0.732\ \lambda_s^{-0.624}\ C_v^{0.248}\ (d/R)^{0.252} \qquad (3.5)$$

where R is the hydraulic radius of the free flow area, λ_s is the overall friction factor which takes account of the deposited bed, d is the sediment size, and V is the mean flow velocity.

Eq. 3.5 indicates that the required mean velocity decreases as friction factor increases. This is contrary to expectations because as the friction factor increases, the flow resistance should increase, thus demanding a higher velocity to overcome the increased resistance.

In 1978 Ackers adopted the Ackers-White sediment transport equation to describe the movement of sediment in pipes. For the case of a loose deposited bed, it was initially assumed that the effective width of sediment transport was equal either to the diameter of the pipe or to the width of the water surface, if the pipe was flowing less than half-full.

Other choices however, can be made and CIRIA (1987) suggested that the effective width be taken as equal to the channel width of the deposited bed (see Appendix I).
A detailed evaluation of Ackers' equation for the case of deposited beds in sewers has not yet been made due to the lack of experimental data.

In 1989 May et al, stated that the transition from flume traction to movement with a loose deposited bed does not significantly decrease the sediment transporting capacity of the flow. They found that beyond the limit of deposition, the transport rate increases as the mean sediment depth (t_s) increases, using a 300 mm diameter concrete pipe and mean deposited depth t_s/D = 1% . Tests were carried out with 0.72 mm sand and using flow velocities between 0.5 m/s and 1.5 m/s, proportional depths of flow between $\frac{3}{8}$ full and pipe full and volumetric sediment concentrations between $3x10^{-7}$ and $4.4x10^{-4}$. The following equation was suggested:

$$C_v=0.04\left[D^2/A\right]\left[y_o/D\right]^{0.36}\left[d/R\right]^{0.6}\left[1-(V_c/V_m)\right]^{4}\left[\frac{V_m^2}{g(S_s-1)D}\right]^{3/2} \qquad (3.6)$$

where V_m is minimum flow velocity corresponding to specified depth of sediment deposit, y_o is the depth of flow, and V_c is the threshold velocity predicted by Novak and Nalluri's equation for smooth and rough beds (Eq.2.23.3).

Kuhil (1989), studied the non-cohesive sediment transport in sewers with and without loose sediment bed on the invert.

Two separate pipes (164mm and 353mm) were employed for smooth and rough pipes flowing full. The experiments were carried out in the range of $1.3<d_{50}(mm)<8.0mm$, with different roughnesses ranging $0.0<k_{s(mm)}<2.7$. He developed a conceptual model which incorporates the effect of pipe overall roughness and the effect of bed depth. It is valid for smooth and rough pipe with and without loose deposition and suggested the following equations:

$$TP_1 = 0.0447385 \quad SP^{2.336} \tag{3.7}$$

for deposited loose bed;

$$TP_2 = 0.0152039 \quad SP^{1.42} \tag{3.8}$$

for non-deposited bed (clean pipe).

where:

$$TP = \frac{C_v \, R^{4/3} \, (S_s - 1)^{1/2}}{V \, k_{ss}^{1/3} \, (g \, d_{50})^{1/2}} = \text{Transport Parameter}$$

$$SP = \frac{u_*^2}{\left[(S_s - 1) \, g \, d_{50}\right]} = \text{Shear Parameter}$$

$$k_{ss} = \frac{k_s P_w + d_{50} P_b}{P_w + P_b} = \text{Overall pipe roughness Parameter}$$

(for deposition and no-deposition regimes)

where u_* is the shear velocity, P_w the wall wetted perimeter, P_b the bed wetted perimeter, V the flow velocity, S the slope, and k_s is pipe roughness.

b) Fixed Sediment Beds

The only available work that deals with sediment transport in circular cross section channels with fixed sediment beds is that of Alvarez (1990), who conducted a very limited number of non-cohesive transport experiments with non-deposition criterion in a circular channel (D=154mm) with smooth and rough fixed flat beds ($t_s/D=0.26$). He used uniformly graded sands ranging from 0.9 to 5.7 mm. Using a multi-regression analysis, he developed the following equation at limit deposition:

$$\frac{\tau_o}{\rho(S_s-1)gd_{50}} = 3.42\ C_v^{0.66}\left[\frac{d_{50}}{R}\right]^{-1.32}(\lambda_s)^{0.78} \qquad (3.9)$$

with a correlation coefficient $r^2=0.978$.
Using the separated values (computed bed shear stress), to eliminate the effect of smooth side walls, the equation representing the phenomena becomes:

$$\frac{\tau_b}{\rho(S_s-1)gd_{50}} = 1.60\ C_v^{0.64}\left[\frac{d_{50}}{R}\right]^{-1.27}(\lambda_{sb})^{0.62} \qquad (3.10)$$

with a correlation coefficient $r^2=0.977$. In order to consider the effects of channel shape the parameter (y_o/P) is incorporated in the analysis and equations 3.9 and 3.10 thus become:

$$\frac{\tau_o}{\rho(S_s-1)gd_{50}} = 1.01\ C_v^{0.65}\left[\frac{d_{50}}{R}\right]^{-1.34}(\lambda_s)^{0.58}\left[\frac{y_o}{P}\right]^{-0.18} \qquad (3.11)$$

with a correlation coefficient $r^2=0.979$, and

$$\frac{\tau_b}{\rho(S_s-1)gd_{50}} = 0.26\, C_v^{0.63} \left[\frac{d_{50}}{R}\right]^{-1.32} (\lambda_{sb})^{0.35} \left[\frac{y_o}{P}\right]^{-0.4} \tag{3.12}$$

with a correlation coefficient r^2-0.983.

As a conclusion, it is obvious that there is a serious lack of information available for analysis and design of sewers in which permanent deposition occurs and the following study is planned to take into account the following points:

1) A method which will take into consideration all the important hydraulic parameters which may play significant roles in the mechanism of sediment transport over fixed deposited beds. This method has to be sufficiently simple for its engineering applications.

2) The influence of deposited bed thickness and its roughness on the hydraulic and sediment transport capacities.

CHAPTER 4

EQUIPMENT AND EXPERIMENTAL PROCEDURES

4.1 The Test Rig

4.1.1 General

Experiments were carried out in a 305 mm diameter tilting flume with an overall length of 12.75 m. Three different flat false beds made of uPVC sheets were used with bed thicknesses that could easily be changed. The thicknesses (t_s) of these beds were 47mm, 77mm and 120mm. Details of a circular cross section channel with flat bed is shown in Fig. 4.1 a. (see Appendix B for more details on geometry of circular cross section channels with flat beds).

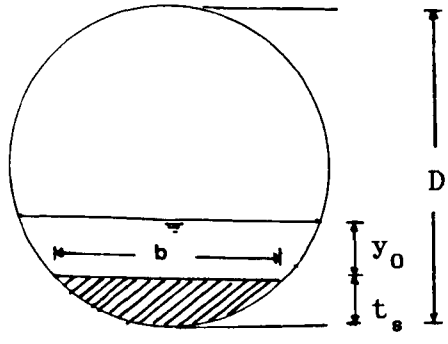

FIGURE 4.1a CHANNEL OF A CIRCULAR CROSS SECTION WITH FLAT BED

The flume was constructed from uPVC with a 2.75 m long central perspex section. The channel was mounted on a stiff steel structure, supported by five steel supports along its longitudinal axis. On the upper portion of the pipe, window openings were made all along its length.

Longitudinal alignment of the flume was carried out using a surveying theodolite and the necessary adjustments of the

pipe and rail were made. The leveling was then within ± 1.0 mm of the straight line, which was considered acceptable. There was no noticeable vertical deflection when leveling the flume with water, as the supporting framework was solid and very rigid (see Fig. 4.1b and Plate 4.1).

The channel slope was varied by a jack, which displaced the flume's wheeled supports (resting on steel wedges). The slope was computed from the difference in water level of two vertical cylinders fixed at each end of the flume (11.223 m apart) interconnected by plastic tubing.

4.1.2 Flume Inlet

It was found that the inlet condition could be improved by the use of one or several honeycomb screens. Presumably the screen has the effect of damping out some of the large scale turbulence generated in the inlet tank and making a more uniform inlet velocity distribution. At lower discharges the screens were not used, but for high and medium discharges two screens were used which resulted in adequate uniform flow for all conditions.

4.1.3 Flume Outlet

A tail gate at the end of the channel was found helpful in achieving uniform flow conditions very quickly and enabled the adjustment of the flow depths whenever necessary. The gate was designed in such a way that the water flowing in the channel and sediment travelling along the channel bed could pass through with no noticeable backwater effects.

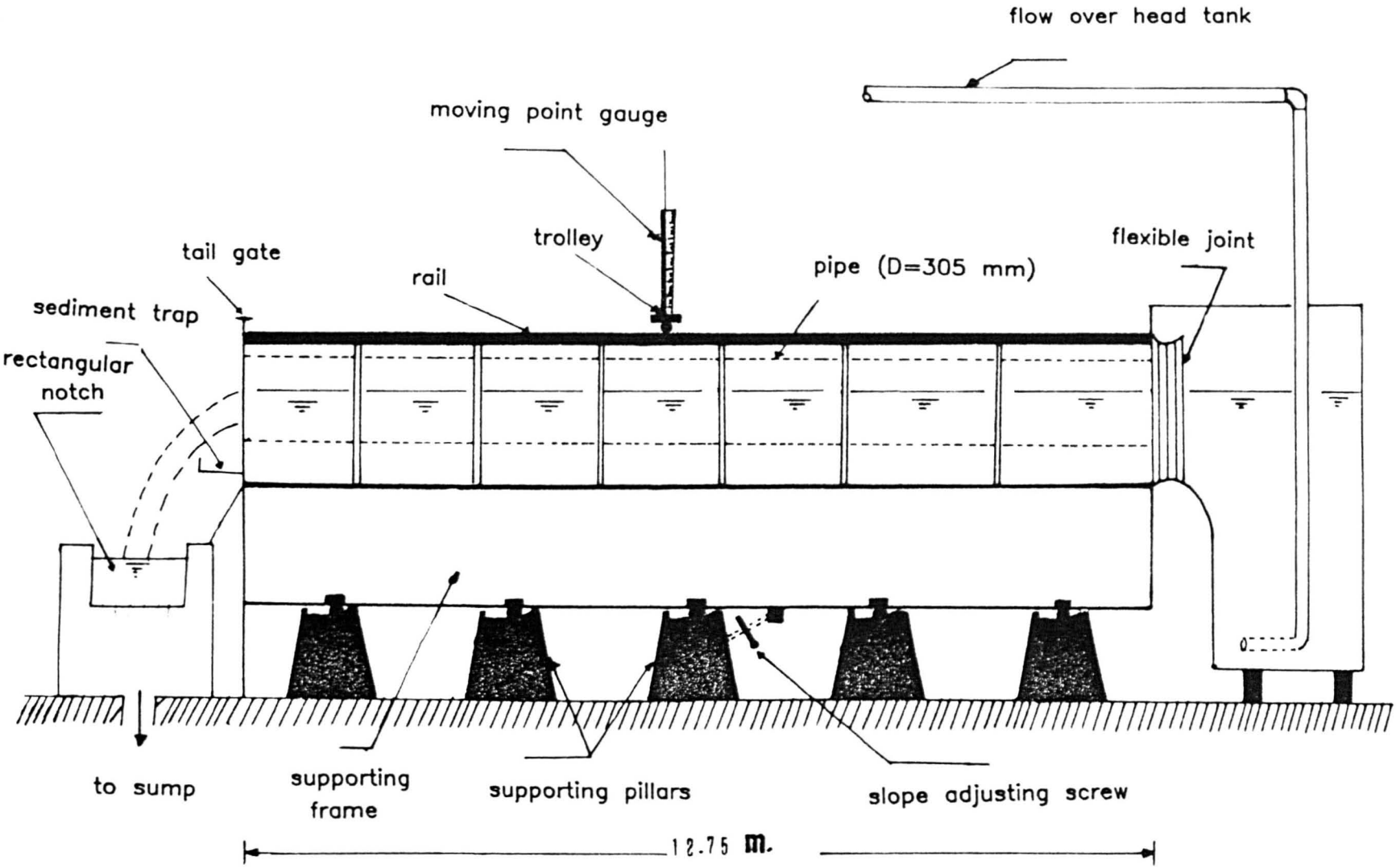

FIGURE 4.1b GENERAL LAYOUT OF THE 305 mm DIAMETER FLUME

PLATE 4.1 GENERAL VIEW OF TEST RIG

4.1.4 Water Supply

Two 100 mm diameter pipes supplied water to the flume through a stilling tank (inlet tank) (see Fig. 4.1b). The rate of flow was controlled by two valves positioned along the supply line and very close to the stilling tank.

4.2 Experimental Measurements

4.2.1 Measurement Of Water Depths

The flume was fitted with a rail along its top, along which point gauges mounted on an instrument carriage ran, enabling the water depth to be measured at any position. The gauge could measure water depths to an accuracy of 0.1 mm.

4.2.2 Discharge Measurements

Water discharge rates were measured with a rectangular notch weir (with side contraction) mounted on the collecting tank downstream of the flume using the following equation (Rehbock):

$$Q = \left\{1.777 + 0.245\left(\frac{h + 0.0012}{0.443}\right)\right\} 0.4495(h + 0.0012)^{3/2} \qquad (4.1)$$

where Q is the flow rate in (m^3/s), and h is the water head above the crest of the weir in (m). The discharge was computed with a maximum error of ± 1.5% (BS 3680). Orifice plates located in each of the two 100 mm diameter supply pipelines were used for checking the weir discharge measurements. The discharges obtained using both techniques

were very similar.

4.2.3 Temperature Measurements

Temperature measurements were made with a thermometer, from which the kinematic viscosity of water, υ, was calculated using the following equation:

$$\upsilon = \frac{1.79 \times 10^{-6}}{1 + 0.03368\ T + 0.000221\ T^2} \quad (m^2/s) \qquad (4.2)$$

where T is the temperature in degrees Centigrade.

4.3. Establishment Of Uniform Flow

4.3.1 General

The establishment of uniform flow was achieved through a graphical method. With the bed slope set to a certain value as desired, a constant discharge was supplied to the flume. The tail gate at the down stream end was adjusted to a certain position, so that the flow was nearly uniform. The gate position was marked so that it could be reset to exactly the same position, when necessary. Then the bed slope was reduced a little and flow depths along the centre line were measured at every metre from the outlet, using the point gauge. While keeping the flow rate and the gate position unchanged, depths along the flume (surface profiles) were measured for five different bed slopes. The best fit straight line was obtained for each surface profile, using least squares regression. For each bed slope, flow depths at equal distances upstream and downstream (h_u and h_d

respectively) of the centre of the flume were obtained from the regression lines. Then (h_u-h_d) versus bed slope and h_u versus bed slope graphs were plotted as shown in Figure 4.2.

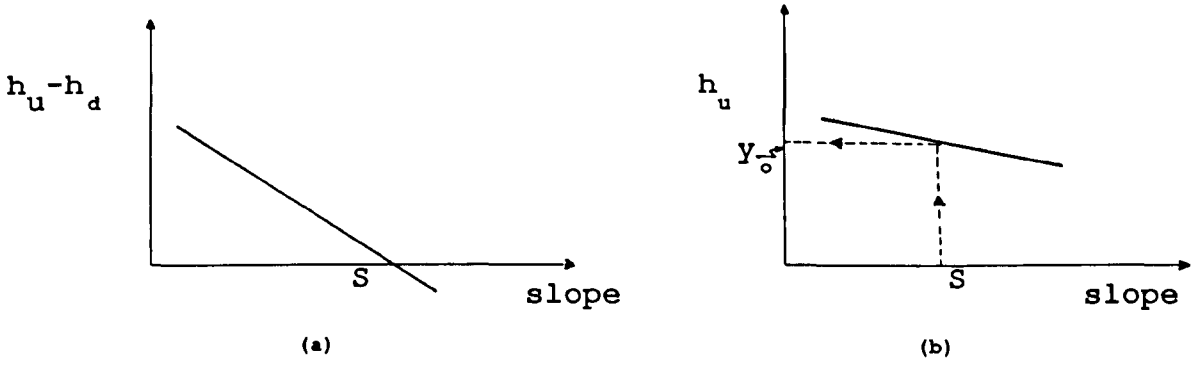

FIGURE 4.2 GRAPHICAL METHOD TO ESTABLISH UNIFORM FLOW

The slope corresponding to $(h_u-h_d)=0.0$ was obtained from Figure 4.2a as the uniform flow slope S for that particular discharge and gate position. Uniform flow depth y_o was read from Figure 4.2b, corresponding to the slope S. Then the bed slope of the flume was adjusted to S and flow depth measurements were taken to check whether the flow was uniform. In all cases, flows were found to be nearly uniform (changes in flow depths were less than 2 mm). When the upstream and downstream depths were not equal, a correction was introduced for non-uniformity of flows in the analysis (see section 4.3.2).

To determine whether the flow was fully developed over the required flow depth range, vertical velocity profiles were

taken at intervals along the channel centre line for a series of discharges. The velocity profiles were found to be identical through-out the channel test length of the flume which confirmed that the flows were fully developed.

4.3.2 Correction For Non-Uniformity Of Flow

If flow in an open channel is perfectly uniform, the channel bed slope S_b will be equal to the water surface slope S_w and the energy gradient S_f (friction slope). In most cases it was found that S_w was slightly different from S_b. Therefore, the energy gradient S_f was computed by applying a correction to the bed slope based on the gradually varied flow equation,

$$\frac{dy}{dx} = \frac{(S_b - S_f)}{1 - Fr^2} \qquad (4.3)$$

where Fr is the Froude number of the flow and $\frac{dy}{dx}$ the water surface slope (S_w). For uniform flow conditions the three slopes should be equal $(S_b = S_w = S_f)$. Assuming the flow is nearly uniform the effective slope (S) can be expressed as:

$$S = S_b - (S_b - S_w)(1 - Fr^2) \qquad (4.4)$$

It is apparent from Eq. 4.4 that as the flow approaches uniform conditions the correction $(S_b - S_w)(1-Fr^2)$ becomes smaller as the effective slope converges to the channel bed slope (S_b).

4.4 Equipment For Velocity and Turbulence Measurements

Velocity profiles were measured at various sections of the flume to check the uniformity of the flows. These measurements were also used for the determination of the shear stresses exerted on the bed by the flowing water. The velocity profiles were obtained using a Pitot Tube, several 10 mm Propeller current meters, and a Laser Doppler Velocimeter (LDV).

4.4.1 Pitot Tube

A pre-calibrated Pitot tube connected to a high precision pressure difference reading device (± 0.1 mm water column) was employed. The internal and external diameters of the Pitot Tube were 0.8 and 2.3 mm respectively. The velocity was given by:

$$u = 14 \sqrt{\Delta h} \qquad (4.5)$$

where u is the local velocity in (cm/s) and Δh is the manometer deflection in (m) of water.

4.4.2 Propeller Current Meter

Several Propeller Current Meters (Nixon Ltd. and HR Ltd.) were used. The propeller diameter was 10 mm and the lowest position at which velocity was measured was 7.5 mm from the bed. The probes were factory pre-calibrated by means of a towing tank rig, and were regularly cross-checked with the Pitot tube. The range of velocities varied from 0.0 to 1.5 m/s (0.0 to 300 HZ) with a maximum absolute error of 0.015

m/s. The readings were taken from a digital counter that was set to give 10 seconds average. For each position 10 readings were averaged (i.e 100 seconds) to obtain the local mean velocity.

4.4.3 Laser Doppler Anemometer

The use of the Laser Doppler Anemometer (LDA) to measure velocity and turbulence has become very common recently. In contrast to hot-wire instruments and some other conventional techniques, laser anemometers are non-contact optical instruments which enable the fluid flow structure in liquids to be investigated without disturbance. (see Appendix C for full details of LDA).

The LDA measurement method has four main features; these are:

1- The creation of a "measuring volume", consisting of the crossing point of two monochromatic laser beams which create a local fringe system, which is precisely located within the flow without disturbing the flow.

2- The method is absolute and require no calibration.

3- The detection, by a photo multiplier, of the variation of light intensity caused by the scattering point as they pass through the fringe system of the scattering volume.

4- The processing and interpretation of light intensity signals in terms of time-mean velocities and fluctuation velocities.

The Laser Doppler system used in this study (TSI equipment) operates in a one component Forward Scattered Differential

Doppler mode with frequency shifting. This comprises a 20 mW Helium-Neon Laser which is recommended for a forward scattered mode only with a light wave length of 633 nm (=0.633 μm). The power supply to the laser was provided by a laser exciter (spectra-physics Model 216-2). In the beam splitter optical unit (TSI Model 915) the laser beam was directed into a prism that split the beam into two parallel beams, each displayed 25 mm from the original beam and in the same plane as the original beam. Connected to the beam splitter is the brag cell (TSI Model 9182). Turbulence measurement procedures are shown in Appendix C.

4.5 Bed Roughnesses

Three bed roughnesses were used in this investigation. Firstly, the experiments were conducted in the smooth circular channel having three different bed thicknesses namely 47mm, 77mm and 120mm. Then the beds were artificially roughened by coating them with uniform size sand grains of 0.53mm and 1.0mm.

The roughness was prepared by sticking carefully graded sand on one side of double sided adhesive tape sheets, the other side of which was pasted to the channel bed. Care was taken to avoid any part of the tape sheet bulging as this would cause disturbance to flow. A generous coat of Poly Varnish paint was applied over the tape sheets to increase the grip on the sand particles. The uniformly graded sand particles were then spread carefully on the wet paint as evenly as possible and the bed was then left to dry. Excess loose sand

on the bed was then removed by introducing a large discharge into the flume.

The rough bed so formed was found to:

(1) consist of one layer of sand grains;

(2) have the grains well packed on the bed, and

(3) remain in water without change of roughness concentration of the bed throughout the period of test.

Plates 4.2a and 4.2b show respectively the two different roughness elements used.

4.6 Determination of Equivalent Sand Roughness of Beds

The Colebrook-White equation (Eq. 3.1) is the most appropriate for dealing with flow resistance in pipes, because it has a sound theoretical basis and can be applied over a wide range of flow and roughness conditions.

For open channel flow incorporating the equivalent diameter (D), in Eq. 3.1, expressed in terms of the hydraulic radius R (D=4 R; Ackers, 1958) would give the sand roughness as:

$$k_s = 14.8\ R \left[10^{-1/(2\sqrt{\lambda_c})} - \frac{2.51}{R_* \sqrt{\lambda_c}} \right] \qquad (4.6)$$

where λ_c is the Darcy-Weisbach friction factor.

Eq. 4.6 gives Nikurades' equivalent sand roughness of a representative hypothetical circular pipe (running full) that has the same energy gradient at the same discharge as the open channel in question. The values of effective roughness k_s for each test conducted in each bed are given in Appendix D.

For a particular channel bed thickness the effective roughness was quite consistent. Hence an average was taken for each

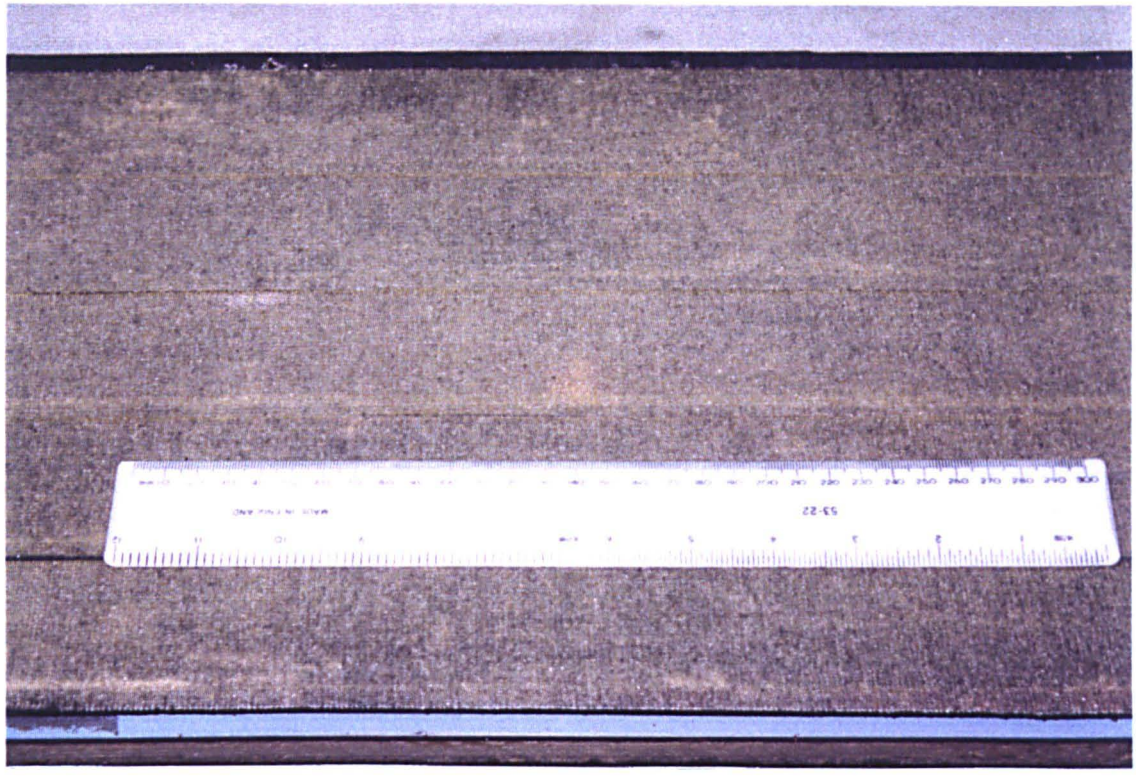

FIGURE 4.2 RIGID BED ROUGHNESS I
(a) sand size d_{50}=0.53mm

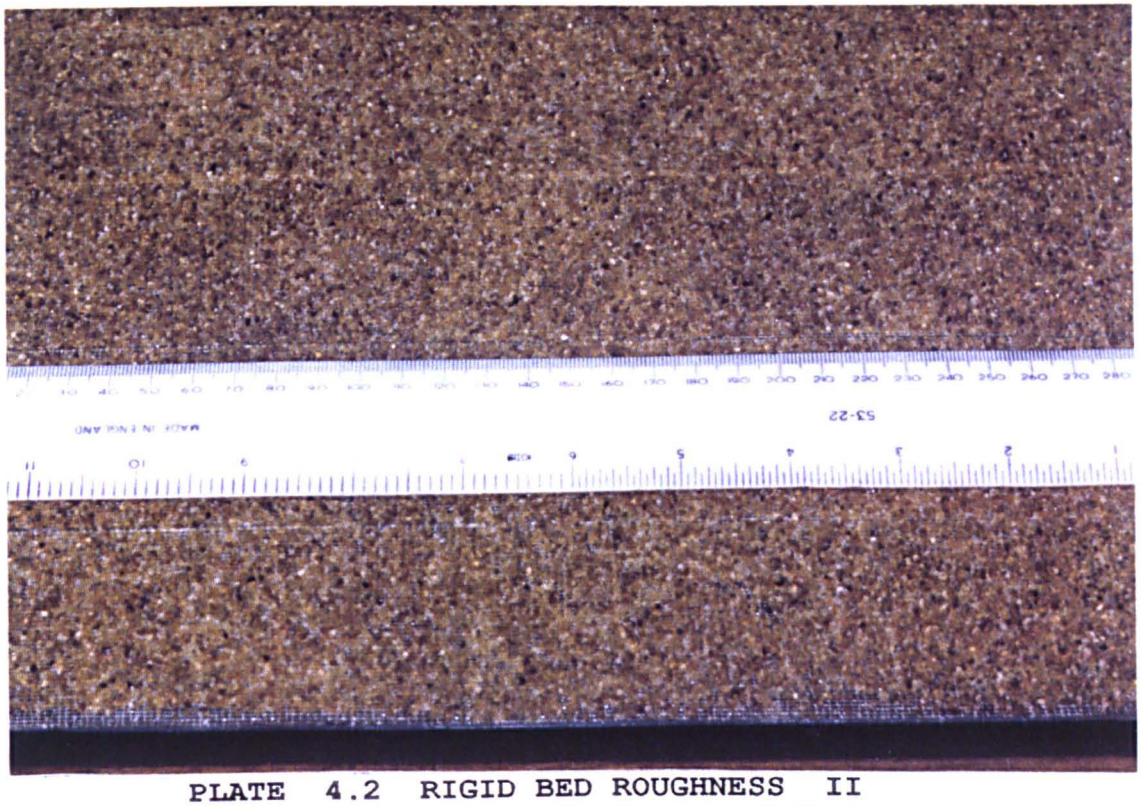

PLATE 4.2 RIGID BED ROUGHNESS II
(b) Sand size d_{50}=1.0 mm

bed thickness and the corresponding results are tabulated in Table 4.1a.

Although the same sand grain sizes were used in beds 1, 2 and 3 for roughnesses I and II, the difference in the value of k_s between the three beds is mainly due to minor losses such as the degree of concentration of grains forming the roughness.

TABLE 4.1a AVERAGE k_s FOR DIFFERENT BED THICKNESSES

Bed depth (mm)	Bed condition	Sand diameter d_{50} (mm)	Average k_s (mm)	Average Manning's n
47	smooth	0.00	-0.1	0.0090
47	rough (I)	0.53	0.94	0.0118
47	rough (II)	1.00	1.32	0.0125
77	smooth	0.00	0.05	0.0094
77	rough (I)	0.53	0.71	0.0115
77	rough (II)	1.00	1.36	0.0127
120	smooth	0.00	0.10	0.0097
120	rough (I)	0.53	0.73	0.0112
120	rough (II)	1.00	1.46	0.0127

It may be observed from the two sets of roughnesses that the effective roughness exceeds the actual sand grain diameter (d_{50}) by almost 50% as shown in Table 4.1a. It is necessary to mention that k_s value does not give the roughness height but rather reflects and describes the surface character (roughness or smoothness). Henderson (1984), based on field investigation reported that, where the sediment forms a plane bed in sewers, the appropriate k_s value is 50% higher than

the size (d_{65}) of deposit sands.

The values of k_s were found to be sensitive to changes in depth of flow; the greatest roughness is generally associated with a lower depth of flow. This finding is confirmed by Ackers et al (1964).

The average value of each roughness for the three different bed thicknesses are tabulated in Table 4.1b.

TABLE 4.1b AVERAGE VALUES OF k_s

Bed condition	Sand diameter d_{50} (mm)	Average k_s (mm)
Smooth	0.00	0.00
Roughness I	0.53	0.80
Roughness II	1.00	1.40

For each systematic test the clean water hydraulic parameters were initially measured in order to analyse their changes in the presence of sediments. These results were used for the characterization of the bed roughness. The ranges of flow conditions studied in the experiments are summarised in Table 4.2 (detailed calculations of A, P, R of the channel geometry are shown in appendix D).

TABLE 4.2 RANGES OF FLOW CONDITIONS INVESTIGATED; D=305 mm

SETTING		b/y_o	y_t/D	R (m)	V (m/s)
SMOOTH BEDS	Bed 1 220 mm wide	1.1-3.8	0.34-0.82	0.042-0.086	0.40-0.87
	bed 2 265 mm wide	1.9-6.7	0.38-0.70	0.031-0.073	0.36-0.88
	Bed 3 298 mm wide	2.4-7.4	0.50-0.79	0.032-0.064	0.46-0.83
ROUGH. I	bed 1 220 mm wide	1.4-3.6	0.35-0.67	0.044-0.081	0.47-0.79
	bed 2 265 mm wide	2.0-4.5	0.45-0.68	0.044-0.072	0.45-0.73
	bed 3 298 mm wide	2.4-6.7	0.54-0.80	0.035-0.065	0.47-0.81
ROUGH. II	bed 1 220 mm wide	1.3-3.6	0.35-0.70	0.044-0.082	0.47-0.80
	bed 2 265 mm wide	2.1-4.3	0.46-0.67	0.045-0.071	0.54-0.83
	bed 3 298 mm wide	3.6-3.9	0.64-0.69	0.051-0.056	0.56-0.73

TABLE 4.2 CONT.

SETTING		R_*	Fr
SMOOTH BEDS	Bed 1 220 mm wide	74919.3 - 221062.0	0.30-1.10
	bed 2 265 mm wide	55477.9 - 257400.9	0.52 - 1.16
	Bed 3 298 mm wide	55116.7 - 172573.5	0.47 - 0.87
ROUGH. I	bed 1 220 mm wide	79474.7 - 240437.6	0.39 - 0.82
	bed 2 265 mm wide	66150.9 - 191107.8	0.52 - 0.85
	bed 3 298 mm wide	55382.7 - 164939.6	0.43 - 0.85
ROUGH. II	bed 1 220 mm wide	81889.4 - 235555.5	0.49 - 0.83
	bed 2 265 mm wide	91354.8 - 216308.2	0.64 - 0.79
	bed 3 298 mm wide	102967.1 - 138395.4	0.59 - 0.83

4.7 Sediment Supply, Discharge and Collection

4.7.1 Sieve Analysis

Uniformly graded sands received from the supplier were mechanically separated using BS sieves in order to improve their uniformity. For each sediment size, three sets of sieve analyses were done. The resultant particle size distribution curves are shown in Fig 4.3.

For the analysis of experimental data, the size of the 50% finer (i.e. d_{50}) was considered as the sediment diameter.

Six different sizes of particles were employed in the sediment transport experiments as shown in Table 4.3.

TABLE 4.3 UNIFORM SAND CHARACTERISTICS

	d_{50} mm	sieve size min (mm)	sieve size max (mm)
A	0.53	0.356	0.71
B	1.0	1.18	0.80
C	2.0	2.36	1.70
D	2.9	3.35	2.36
E	5.6	6.30	5.0
F	8.4	10.0	7.10

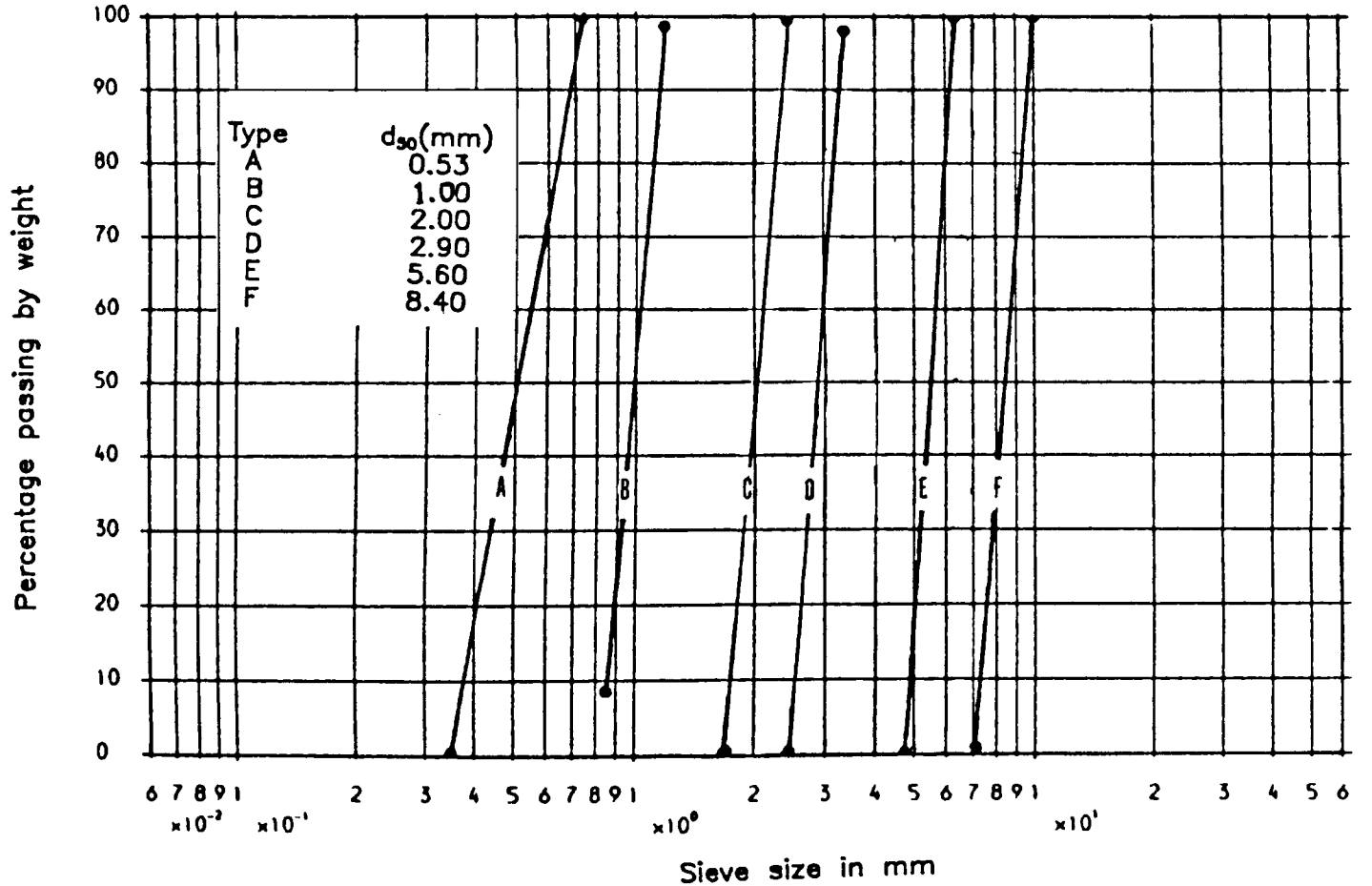

FIGURE 4.3 GRADING CURVES FOR SEDIMENTS

4.7.2 Sediment Density

The density of sediment particles was assessed by a water displacement method. For each sediment size, five samples were tested and the average value was adopted. Table 4.4 shows the values of particle size d_{50}, sediment density ρ_s and relative density S_s of sand samples used in the experiments.

TABLE 4.4 DENSITY OF SAND PARTICLES

	d_{50} mm	Density (kg/m^3) ρ_s	Relative Density S_s
A	0.53	2590	2.59
B	1.0	2560	2.56
C	2.0	2590	2.59
D	2.9	2600	2.60
E	5.7	2560	2.56
F	8.4	2610	2.61

4.7.3 Sediment Feeder

A vibratory sediment feeder made by Glen Creston Ltd, England, was placed above the rail at the upstream side of the channel (see Fig. 4.4).

The funnel was filled with dry sediment and the feeder was then switched on to make the chute operate continuously. The period of operation was controlled using the timer dial which caused the chute to stop automatically once the period had elapsed.

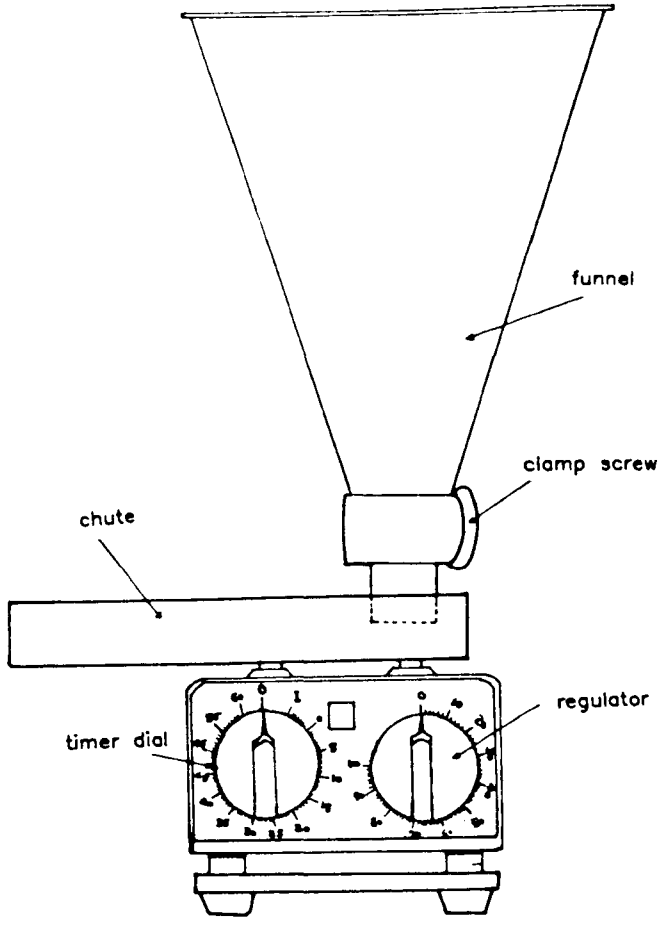

FIGURE 4.4 VIBRATORY FEEDER

4.7.4 Sediment Transport Experimental Procedure

Once the uniform flow conditions were achieved, sediment was supplied using the vibrating feeder, with a very low rate. The rate of supply was increased gradually until the limit of deposition was observed. This was achieved when the sediment particles moved closely to each other and had a temporary deposition before they continued their movement.

At high flow velocities with small sediment sizes, this was

taken to be the point when particles tend to form a dune but could still be moved directly by the flow. It was noticed that any increase in the sediment feed rate above the limit led to permanent deposition of the lower layers of the particles while the upper particles still moved.

Since the bed load transport was defined as the maximum possible rate of transport along the channel without any tendency for the sediments to form a permanent deposition, special attention was paid not to allow any permanent deposition on the bed. While sediments were transported by the flow, its uniformity was checked by measuring flow depths at several points. If the uniformity of the flow was changed due to the introduction of sediments, the tail gate was adjusted to re-set the uniform flow conditions again. The sediment supply rate was checked by increasing or decreasing it slightly, to see whether it had reached the limit of deposition condition.

Once it was decided that the transport was at the limit of deposition, the water depths were measured again and the slope was adjusted to restore uniform flow conditions as necessary. A constant rate of sediment feed just under this limiting condition was then maintained for at least 20 minutes to obtain a constant rate of transport over the entire length of the flume. The sediment discharge was then measured before the material entered the flow, by weighing a certain amount of material collected during a fixed time. This measurement was carried out several times during each test and the average value adopted. Plate 4.3 shows the

sediment being collected for evaluation of the transport rate.

At the outlet, the flume was provided with a sand trap to collect the conveyed material which was then dried in an oven for re-use.

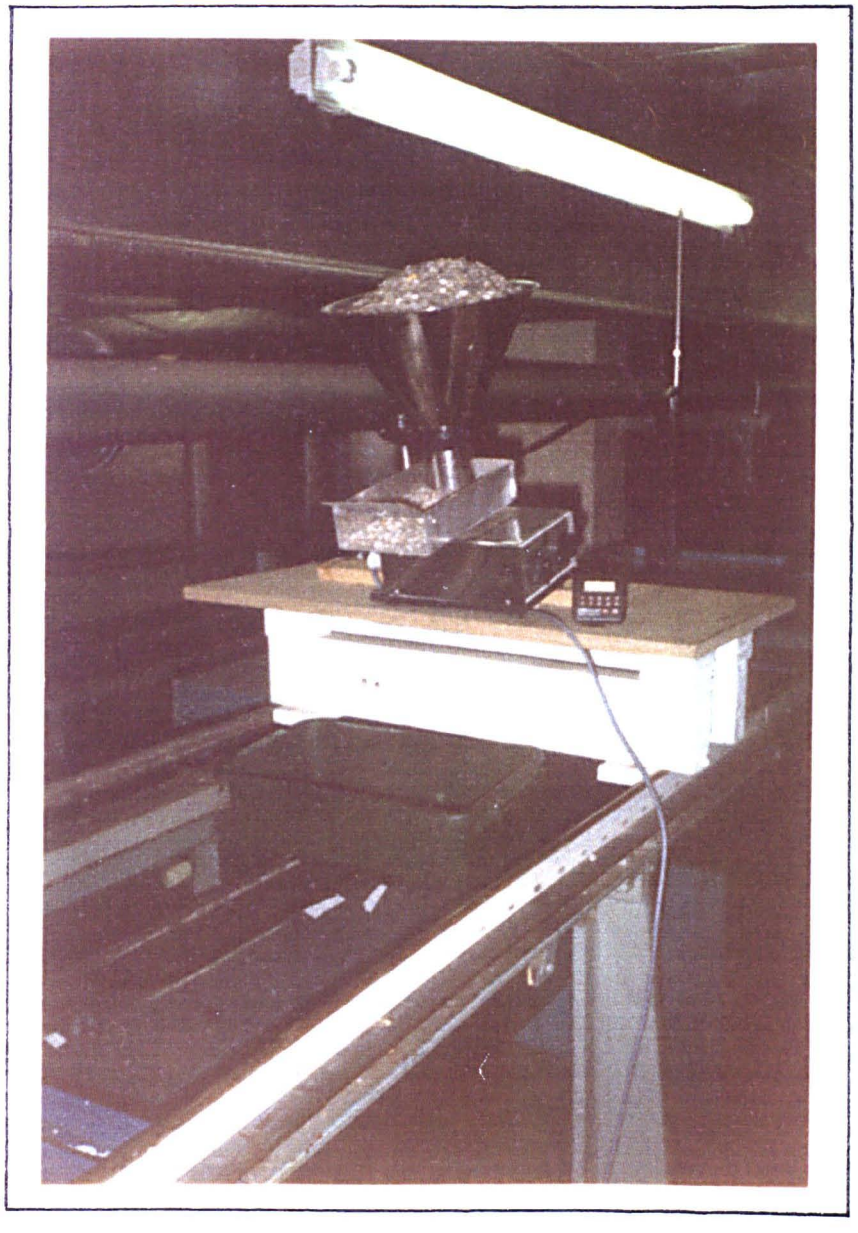

PLATE 4.3 SEDIMENT BEING COLLECTED

CHAPTER FIVE

HYDRAULIC CHARACTERISTICS OF CHANNELS OF CIRCULAR CROSS SECTION WITH FLAT BEDS

5.1 INTRODUCTION

Tractive force distribution in an open channel flow is a function of the velocity distribution in the channel. Tractive force distribution is an involved part of a very complex flow phenomenon including turbulence and secondary currents. The boundary shear (or tractive force) distribution strongly influences the transport of sediment and sediment deposition along the channel. If channels are to remain reasonably stable and self-cleansing when in use, a full understanding of the velocity, shear stress and turbulence distributions is essential prior to their design.

The cross sectional shape of the circular channel varies considerably with sediment bed thickness and flow depth, and the velocity and shear stress distributions are influenced by these associated shape effects. Therefore, in this study, measurements of velocity and turbulence were made in the 305 mm diameter pipe channel rig (see Fig. 4.1) with different flat bed (smooth and rough) thicknesses flowing partly full, y_t/D ranging between 0.33 and 0.81. Bed shear stress distributions were obtained indirectly from inner-law velocity data.

5.2 FLOW RESISTANCE

In fluid flow, energy is continuously dissipated as the fluid has to do work against resisting forces arising from fluid viscosity. Due to dissipation of energy, there is an energy loss often thought of as "head loss" in the direction of flow. The resistance mechanism is the shear stress by which the slow moving layer of fluid near the boundary exerts a retarding force on the adjacent layer of fast moving fluid. The resistance depends upon the boundary conditions (turbulent, shear stresses).

In the last few decades, a great deal of research has been devoted to studying the resistance to flow in pipes and open channels; but no attention has been paid to the flow over circular channels with flat beds such as sewers with fixed deposited beds.

In order to establish some recognisable connection between the three different flat bed thicknesses in this study, a series of clear water experiments were made on each bed during the investigation. The friction factor was determined in the standard manner from the slope of the energy gradient, obtained after the establishment of uniform flow as described in section 4.3.

5.2.1 THEORETICAL BACKGROUND

a) Flow Resistance in Pipes

In the 1930's the flow resistance in pipes was formulated by

the use of two dimensionless parameters, Reynolds' number (the ratio of inertial to viscous forces)

$$R_e = \frac{V D}{\upsilon} \tag{5.1}$$

and Darcy-Weisbach's friction factor (Eq. 2.27).

In a fully developed turbulent boundary layer passing a hydraulically smooth surface a thin viscous sub-layer exists over the boundary surface, the depth (δ') of which may be obtained from Von-Karman's experimental relationship:

$$\delta' = \frac{11.6\ \upsilon}{u_*} \tag{5.2}$$

where u_* is the shear velocity ($=\sqrt{gRS}$). Substitutions of u_* into the Darcy-Weisbach equation and by using the shear stress equation $\tau_o=\rho gRS$, with subsequent arrangement gives:

$$u_* = \sqrt{\lambda/8}\ V \tag{5.3}$$

For Reynolds' number < 25000 the smooth pipe curve is given by the empirical (Blasius') equation:

$$\lambda = \frac{0.223}{R_e^{0.25}} \tag{5.4}$$

At higher Reynolds' numbers the smooth pipe curve follows a general logarithmic relationship. Prandtl (1933) defined the equation for the velocity in a two dimensional pipe flow as:

$$\frac{1}{\sqrt{\lambda}_o} = 2 \log \left(R_e \sqrt{\lambda} \right) - 0.8 \qquad (5.5)$$

which is referred to as the smooth pipe flow law.

In rough turbulent flow the friction factors can be obtained from the following equation:

$$\frac{1}{\sqrt{\lambda}_o} = 2 \log \left[\frac{3.7\ D}{k_s} \right] \qquad (5.6.1)$$

and for channels of smooth walls and rough beds, separated values of friction factors (bed only) are used. Eq. 5.6.1 becomes:

$$\frac{1}{\sqrt{\lambda}_b} = 2 \log \left[\frac{3.7\ D}{k_{sb}} \right] \qquad (5.6.2)$$

At the transition between smooth and fully rough turbulent flow, Colebrook-White equation (Eq. 3.1) (HRS 1981) is now widely accepted as the most reliable and accurate formula available to describe the frictional effects in pipe flow problems under a wide range of conditions.

b) Flow Resistance In Open Channels

Keulegan (1938) showed that the resistance coefficient relationship for a two dimensional open channel flow, having smooth boundaries should be expressed as follows:

$$\frac{1}{\sqrt{\lambda}_c} = A' \text{ Log } R_e \sqrt{\lambda_c} - B' \qquad (5.7)$$

where A′ and B′ are experimental coefficients having values of 2.03 and 1.08 respectively.

Many researchers have found different values for A′ (2 - 2.17) and B′ (1.06-2.07). These include Reinus (1961), Shih and Grigg (1967), Tracy and Lester (1961), Rao (1967), Mayers (1982), Kazemipour and Apelt (1979, 1982) and Mayers and Brennan (1990). The variations in the values A′ and B′ are attributable to differences in cross sectional shapes.

In the transition turbulent open channel flow, the hydraulic radius is often introduced into equation (3.1) in place of the pipe diameter (that is, D=4R), to account for depths of flow below pipe-full. Experimental evidence tends to support this procedure (Ackers, 1958). The Colebrook-White equation can thus be written for non-circular channels as:

$$\frac{1}{\sqrt{\lambda_c}} = -2 \log \left[\frac{k_s}{14.8R} + \frac{2.51}{R_e \sqrt{\lambda_c}} \right] \qquad (5.8)$$

Equation 5.8 gives Nikurade's equivalent sand roughness (k_s) of a representative hypothetical circular pipe, running full, that has the same energy gradient at the same discharge as the open channel flow in the equation.

5.2.2 Analysis of Experimental Data

The experimental work was carried out in a 12.75 m long, 305 mm diameter tilting flume. Three different smooth and rough fixed bed thicknesses were employed in experiments; these thicknesses were 47 mm (bed1), 77 mm (bed 2), and 120 mm (bed

3). Details of the data collected are tabulated in Appendix D.

Channel friction factors, λ_c, were calculated for each run using the Darcy-Weisbach equation. Figure 5.1 shows the variation of friction factors with Reynolds number, $R_e (=4RV/\upsilon)$, for the three flat smooth beds. For comparison the friction factors calculated by the Karman-Prandtl equation (5.5) for smooth pipe flow (R_e taken as $4RV/\upsilon$) are also shown in the figure. The values are seen to fall around the Karman-Prandtl smooth pipe curve. However, there is appreciable scatter as the substitution of D by 4R in Darcy's equation for head loss yields friction factors for the hypothetical equivalent pipe of a circular cross section.

Figs. 5.2 and 5.3 show the variation of Darcy-Weisbach friction coefficients (for beds only, λ_b) with Reynolds' number for rough beds ($R_{eb}=4R_bV/\upsilon$).
The experiments were carried out with clear water for various flume bed configurations (different bed thickness and bed roughness). Since the flume had smooth walls and a fixed rough bed, that caused the overall friction factors to decrease as the water depth increased.
Equation 5.6.2 (for rough turbulent flow) was also shown in the figures.

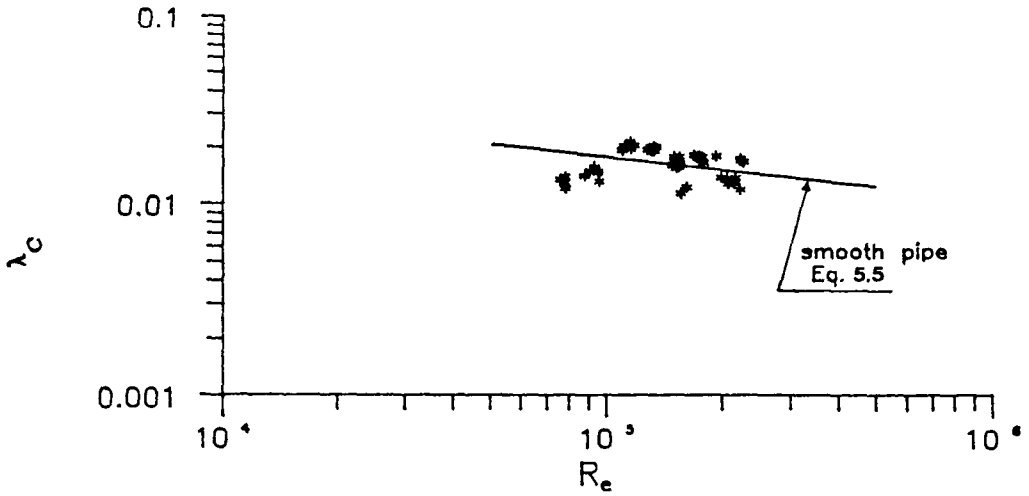

I) SMOOTH BED 1 (t_s=47 mm)

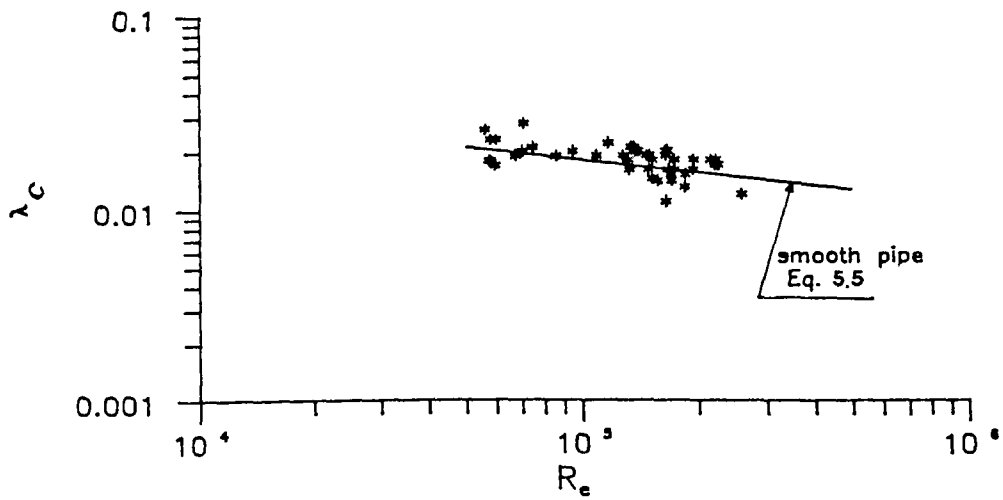

II) SMOOTH BED 2 (t_s=77 mm)

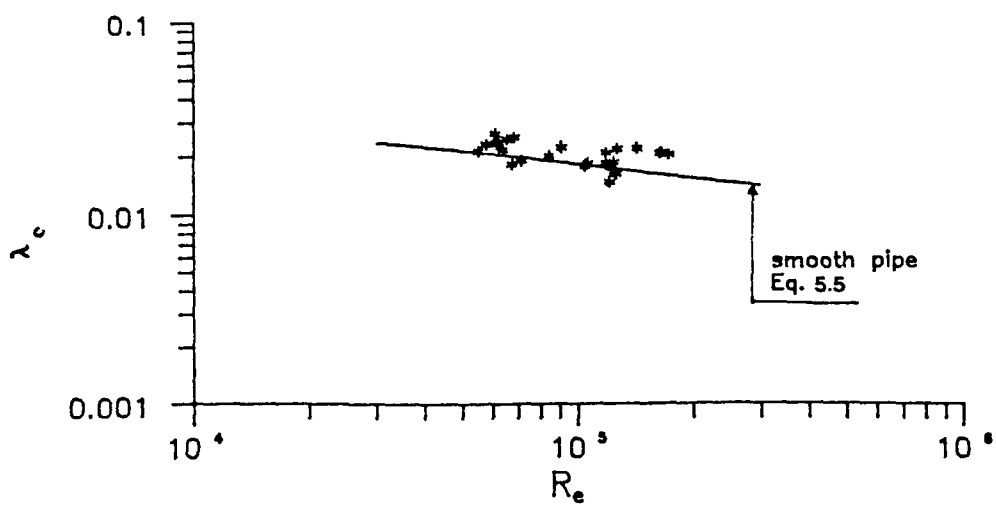

III) SMOOTH BED 3(t_s=120mm)

FIGURE 5.1 REYNOLDS NUMBERS (R_e) AGAINST FRICTION FACTOR (λ_c) (smooth beds)

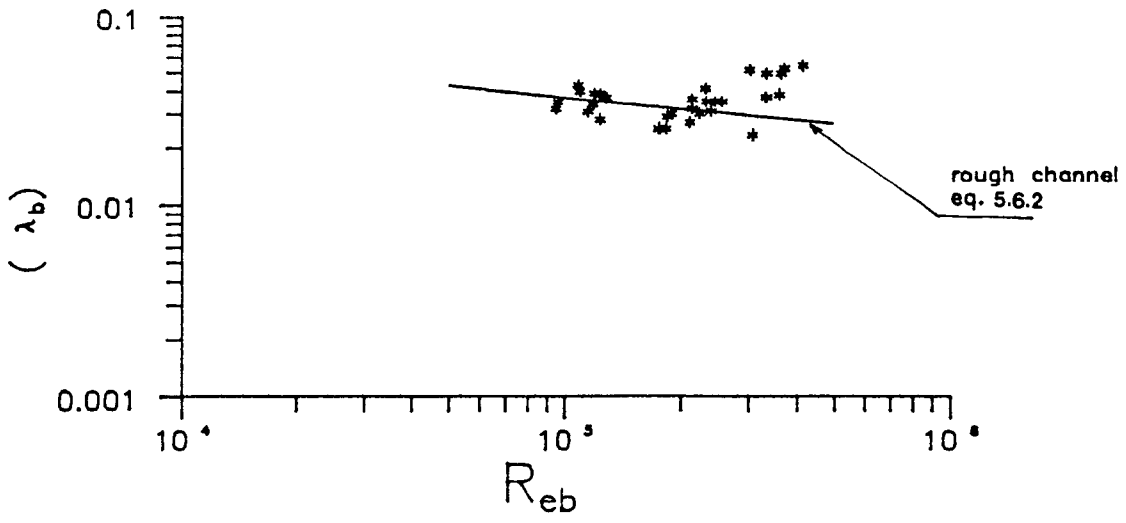

I) BED 1(t_s=47mm)

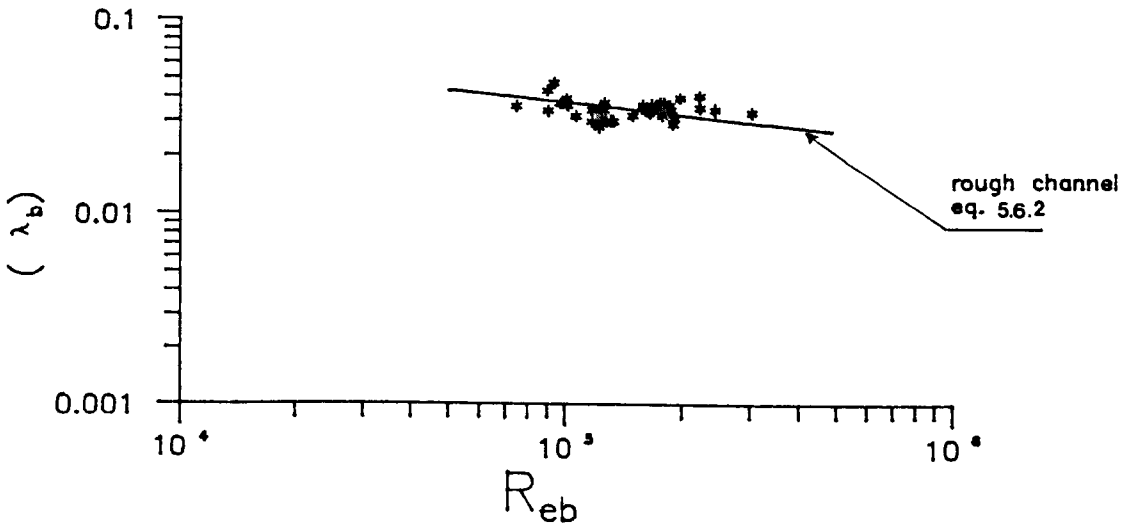

II) BED 2 (t_s=77mm)

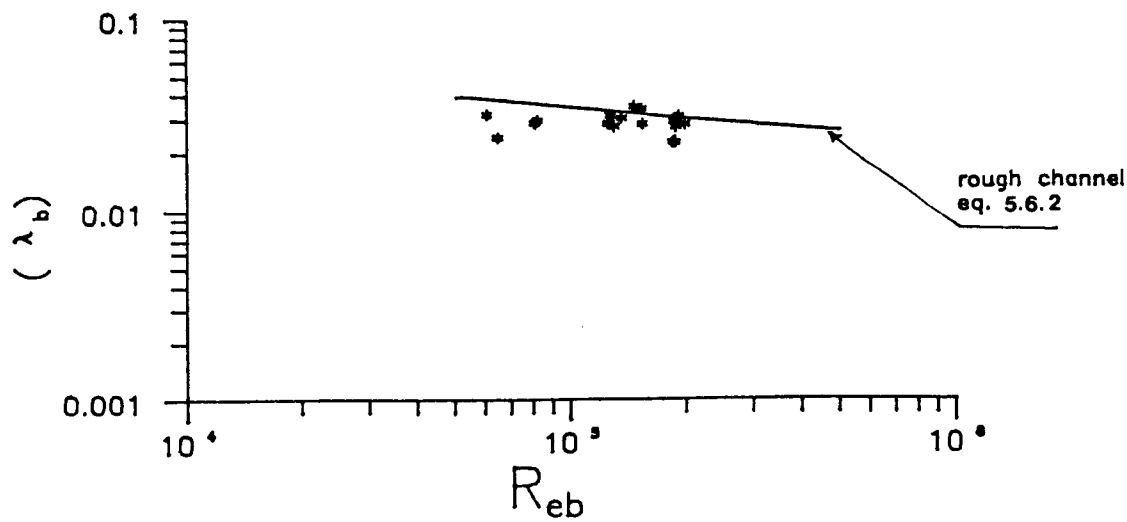

III) Bed 3 (t_s=120 mm)

FIGURE 5.2 REYNOLDS NUMBERS (R_{eb}) AGAINST FRICTION FACTOR (λ_b)

(roughness I; k_s=0.8 mm)

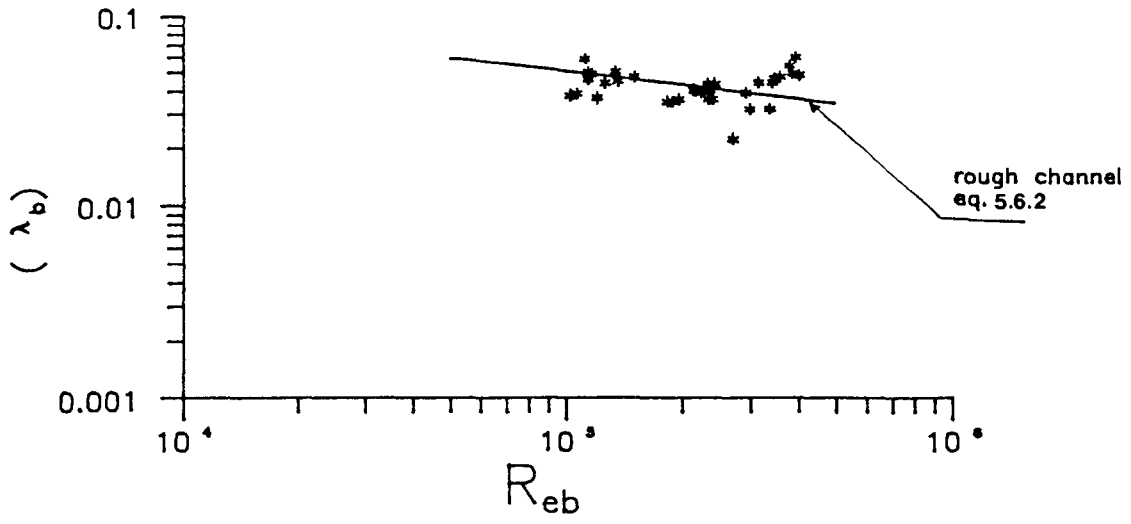

I) BED 1(t_s=47mm)

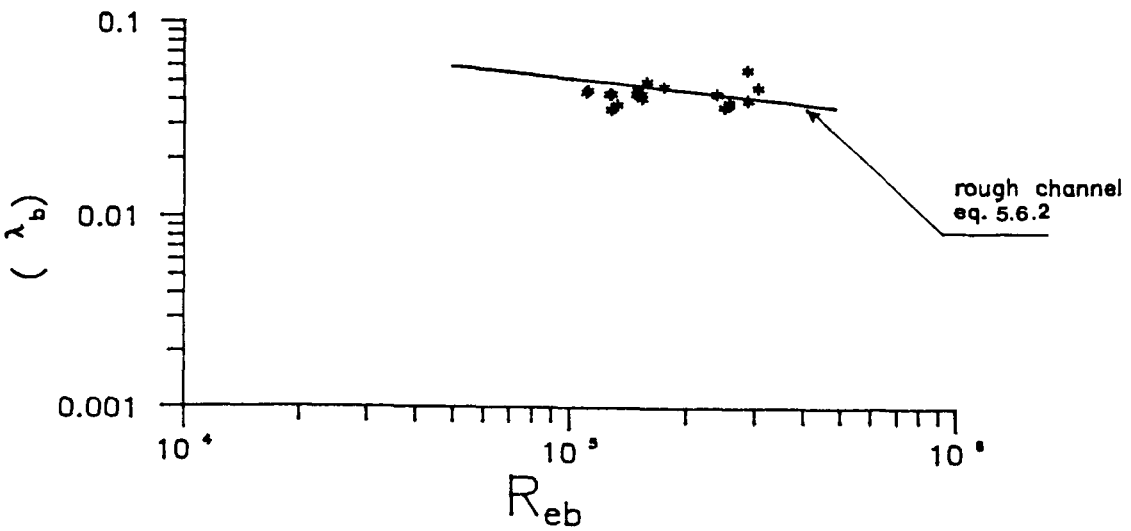

II) Bed 2 (t_s=77mm)

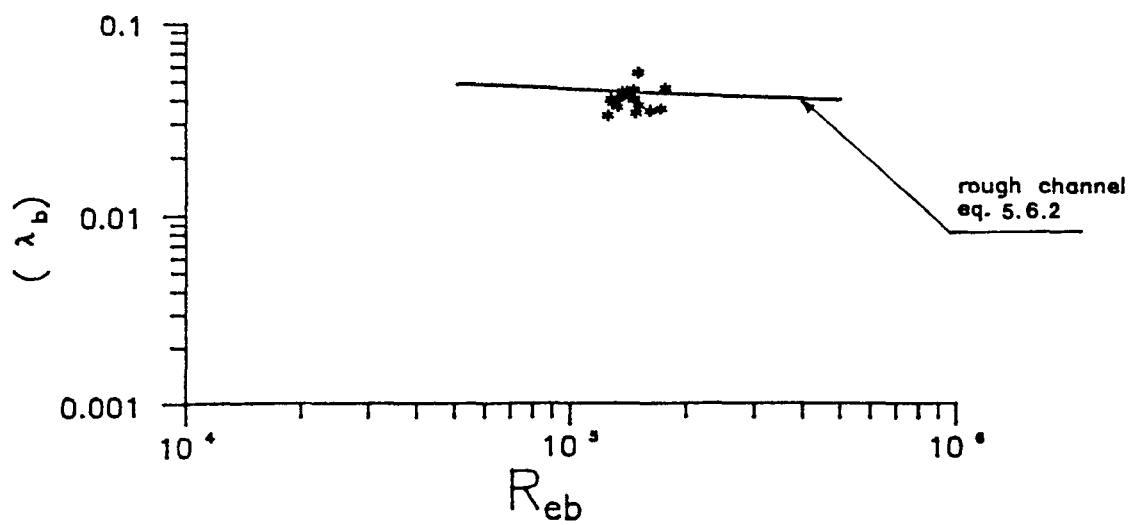

III) Bed 3 (t_s=120 mm)

FIGURE 5.3 REYNOLDS NUMBERS (R_{eb}) AGAINST FRICTION FACTOR (λ_b) (roughness II; k_s=1.40 mm)

5.2.3 The Effects Of Shape on The Resistance Of Channel Flows

The shape of the channel flow-section varies considerably with sediment bed thickness and flow depth, and the friction factors, velocity and shear stress distributions are influenced by the associated shape effects.
The shape effect makes itself known in a much more unpredictable way in an open channel flow because of the existence of the free surface and the modification of the secondary current patterns resulting from changes in depth.

Measurements of velocity and turbulence intensities by Nalluri and Novak (1973) in a circular conduit clearly showed a pronounced change in the distribution of velocity as the depth of flow increased and as the flow pattern changed from two-dimensional (low depths) through three-dimensional (medium depths) back to almost two-dimensional (large depths) pipe flow.

Recent studies have attempted to consider the shape effect by introducing some additional dimensionless parameters. Jayaraman (1970), introduced two non-dimensional parameters, B/P and y_o/P where B is the water surface width, P is the wetted perimeter and y_o is the normal flow depth, which he expected would represent the shape effects. Kazemipour and Apelt (1979) proposed that the friction factor in open channel flow, λ_c, can be obtained from the equivalent pipe friction factor λ_o (Eq. 5.5) and the following expression:

$$\lambda_c = \sigma \lambda_o \qquad (5.9)$$

in which σ depends on two geometric ratios, the ratio of wetted perimeter to free surface width P/B, and the ratio of free surface width to the average flow depth B/y_o. They derived a functional relationship for σ from data collected in smooth rectangular channels. Kazemipour and Apelt (1980) also carried out experimental work in semi-circular channels and attempted to formulate the data to obtain a shape factor as suggested in equation (5.9); the shape factor in this case was in terms of A/D^2 and P/D in which A is the cross sectional area of flow, P is the wetted perimeter, and D is the conduit diameter. More recently, Kazemipour and Apelt (1982) have confirmed their proposal for σ with additional data from smooth rectangular channels.

a) Channels With Smooth boundaries

Nalluri and Adepoju (1985) conducted experiments in smooth channels of circular cross section over the flow depth range of $0<y_o<D$. They found that the measured friction factors were greater than those predicted from full pipe relationships (e.g. Prandtl, Blasius). They proposed a new relation to predict the friction factors in smooth circular conduits flowing partly full. Two dimensionless parameters, the flow Reynolds number (R_{ey}) defined by Vy_o/υ and Shear Reynolds number (R_{e*}) defined by u_*P/υ, were correlated according to the following functional relationship

$$R_{e*} = f\ (R_{ey}) \qquad (5.10)$$

For part-full flow the equation becomes (Nalluri and Adepoju

1985):

$$R_{e*} = 0.836\ (R_{ey})^{0.865} \qquad (5.11)$$

and for full pipe flow, using Blasius' equation, the functional relationship becomes:

$$R_{e*} = 0.624\ (R_{e})^{0.875} \qquad (5.12)$$

It was necessary to investigate the influence of the channel cross sectional shape adopted at each flow depth on the general relationship given in Eq. 5.10.

Figs. 5.4a, 5.4b and 5.4c show the plot of R_{e*} versus R_{ey} for all the present data from the smooth beds (bed 1, bed 2 and bed 3) at depths approximately one third-full, half-full and two thirds-full.

Also shown in the same figure is the Nalluri-Adepoju equation for part-full circular cross section channel flow. It can be seen from Fig. 5.4 that the data fitted three different lines corresponding to the flow depths and the present investigation shows that Eq. 5.11 (Nalluri and Adepoju 1985) is less successful in predicting the shear Reynolds number.

An alternative comparison (Fig. 5.5) was made between the present data (for all smooth beds) at flows up to half-full depths and more than half-full depths with full pipe equation (Eq. 5.12) and part-full pipe equation (Eq. 5.11). It can be seen that the measured shear Reynolds numbers are higher than those predicted by Eqs. 5.11 and 5.12.

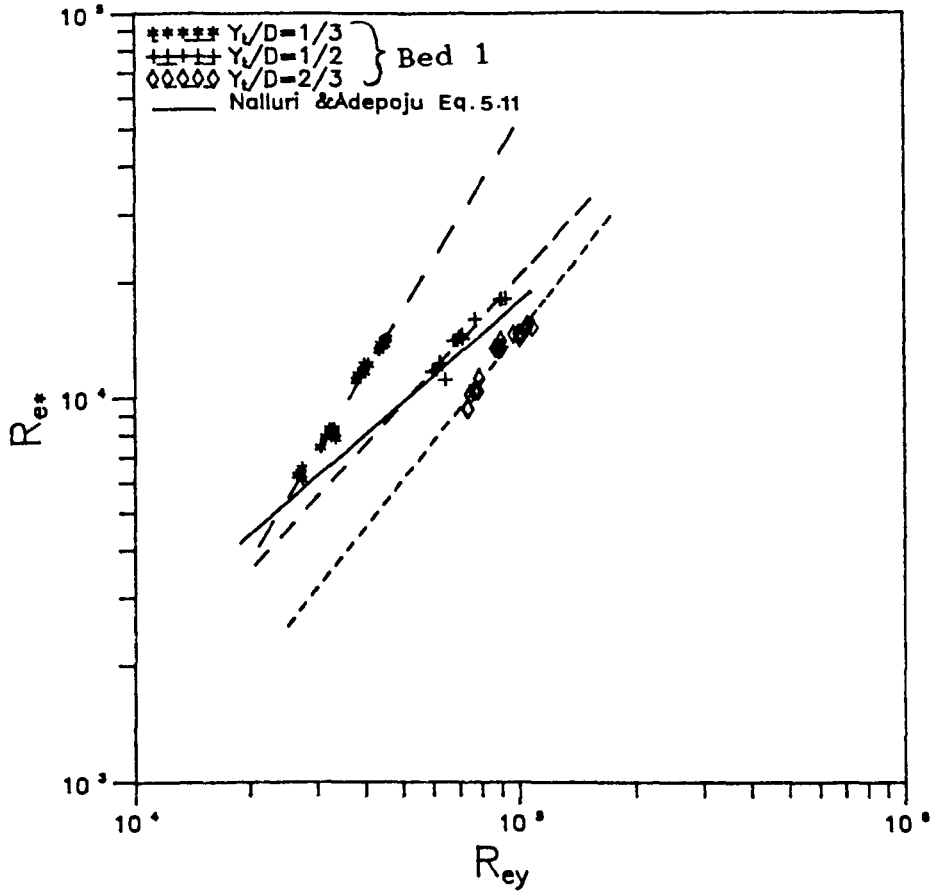

FIGURE 5.4a R_{e*} **VERSUS** R_{ey} **(bed 1)**

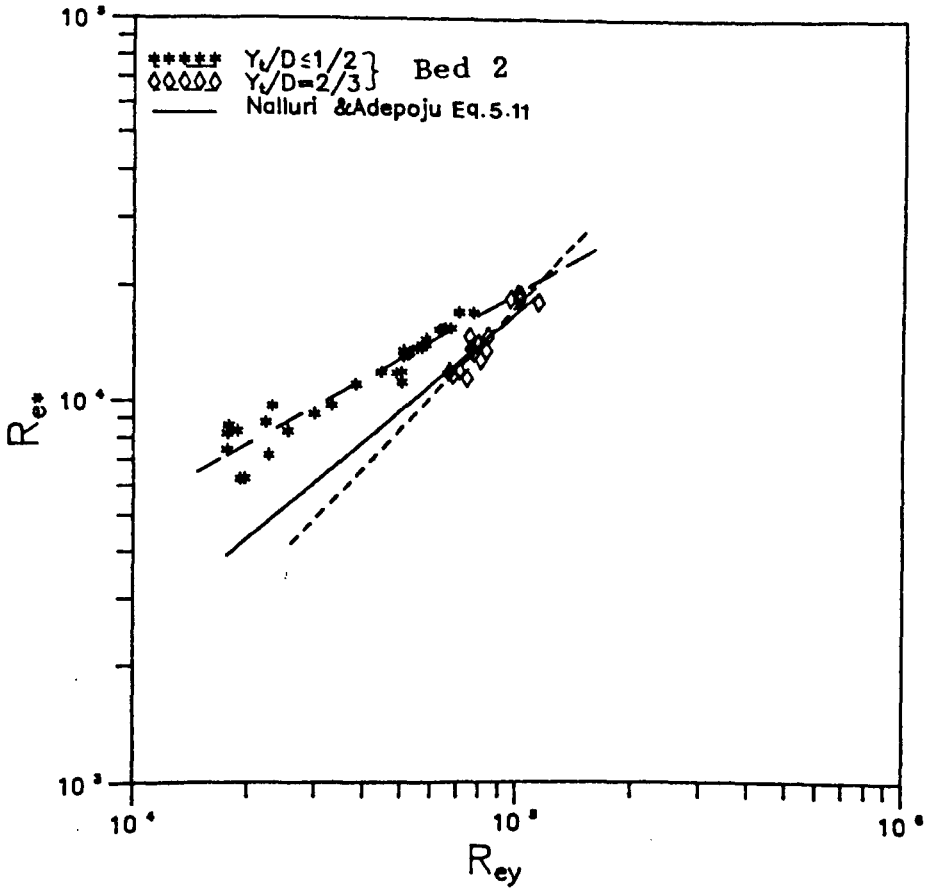

FIGURE 5.4b R_{e*} **VERSUS** R_{ey} **(bed 2)**

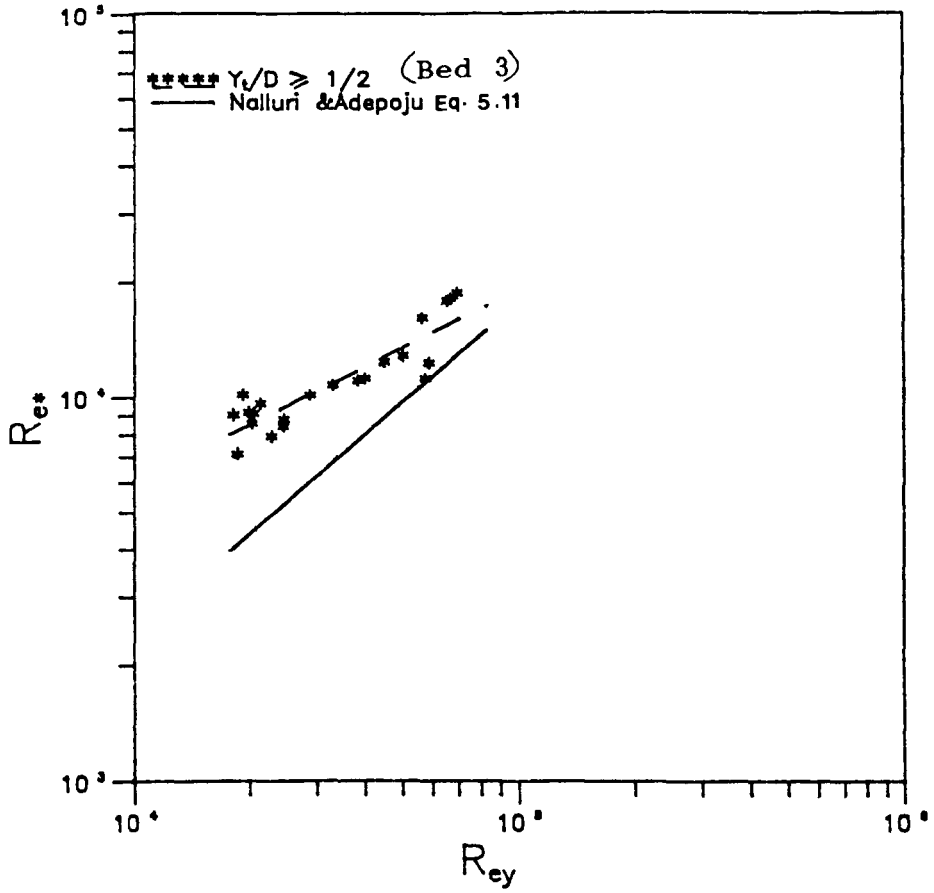

FIGURE 5.4c R_{e*} VERSUS R_{ey} (bed 3)

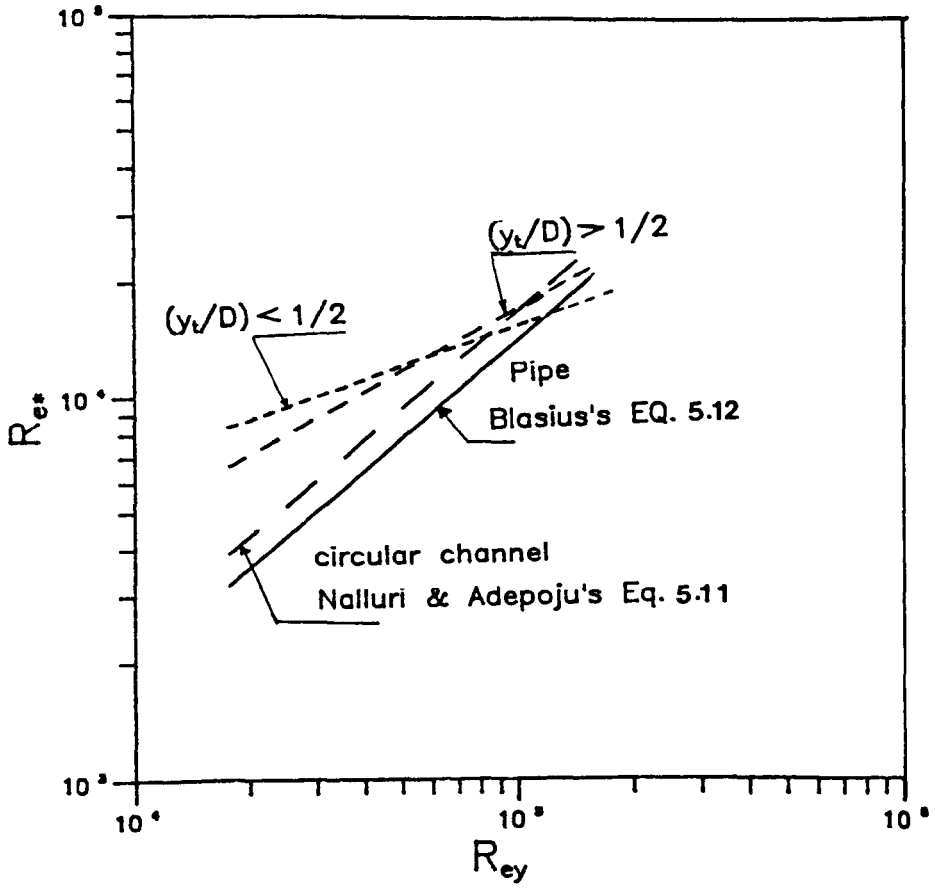

FIGURE 5.5 R_{e*} VERSUS R_{ey} (all smooth beds)

Predicting the flow resistance (friction factor) over flat beds in circular cross section channels is crucial for their design so that the resulting hydraulic variables of the flow will convey the imposed quantities of water and bed load materials while maintaining a stable channel.

The changes in flow resistance in fixed bed channels with steady flow are considered to be due to changes in flow depths and with changes in the shape of channel cross section (see Fig. 4.1a).

An attempt has been made to develop a universal equation to describe the flow resistance in circular cross section channels with smooth boundaries by utilizing the functional relationship given by Eq. 5.10. The best fit equation was found to be as follows (see Fig. 5.6):

$$R_{e*} = 82\ (R_{ey})^{0.46} \qquad (5.13)$$

with r= 0.84

Sturm and King (1988), carried out experiments in horse-shoe shaped conduits, and concluded that the friction factor in horse-shoe conduits can be formulated as a fraction of the pipe value (obtained from Moody diagram) with the friction factor varying with y_o/D, the relative depth. Similar findings were obtained by Alvarez (1990), who concluded that the friction factor of the bed (λ_b) is dependent on bed roughness, bed thickness or bed width (b) and on flow depth (y_o). Therefore the parameter y_o/b can be incorporated in

the functional relationship (Eq. 5.10) to take into consideration the shape effect of the channel at different flow depths and bed thicknesses. Thus Eq. 5.10 becomes:

$$R_{e*} = f\ (R_{ey},\ y_o/b\ ) \qquad (5.14.1)$$

In Fig. 5.7 the relative flow depth $(\frac{y_t}{D})$ is plotted against $\frac{y_o}{b}$ for the three flat bed thicknesses. It can be seen that the parameter y_o/b depends on the flow depth and on flat bed thickness. Three different relationships for the three flat bed thicknesses (47, 77 and 120 mm) as shown in Fig. 5.7.

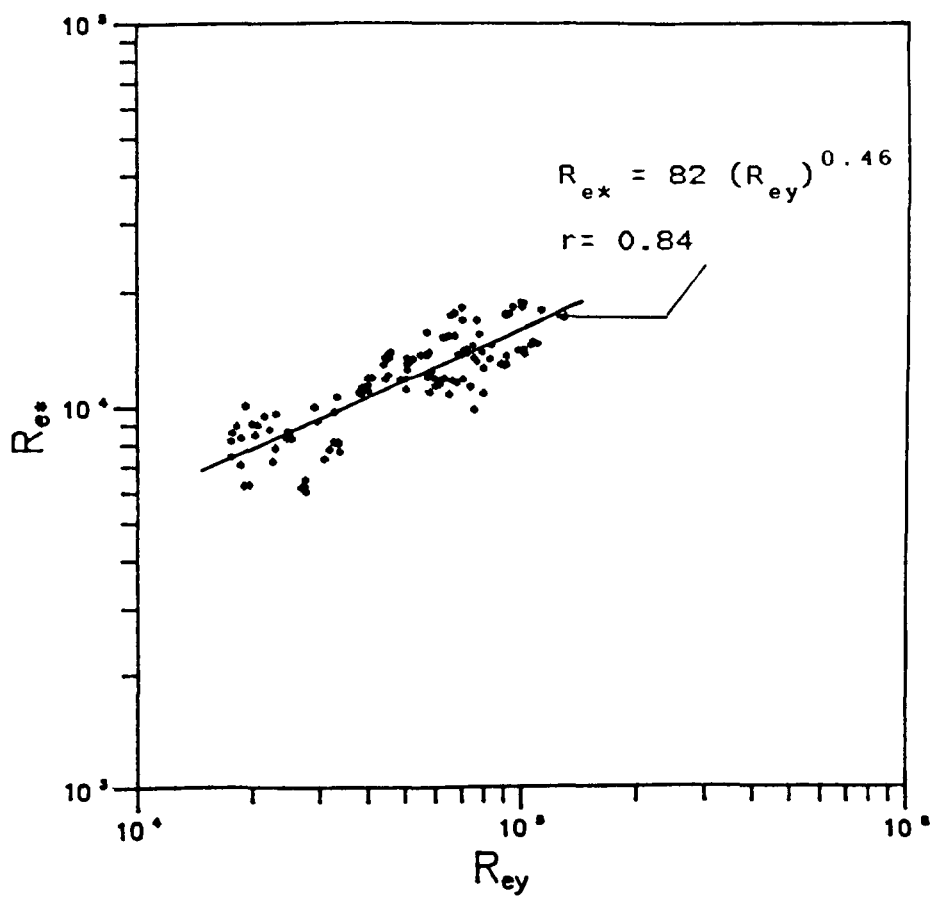

FIGURE 5.6 R_{e*} AGAINST R_{ey}

(for all flow ranges in smooth beds)

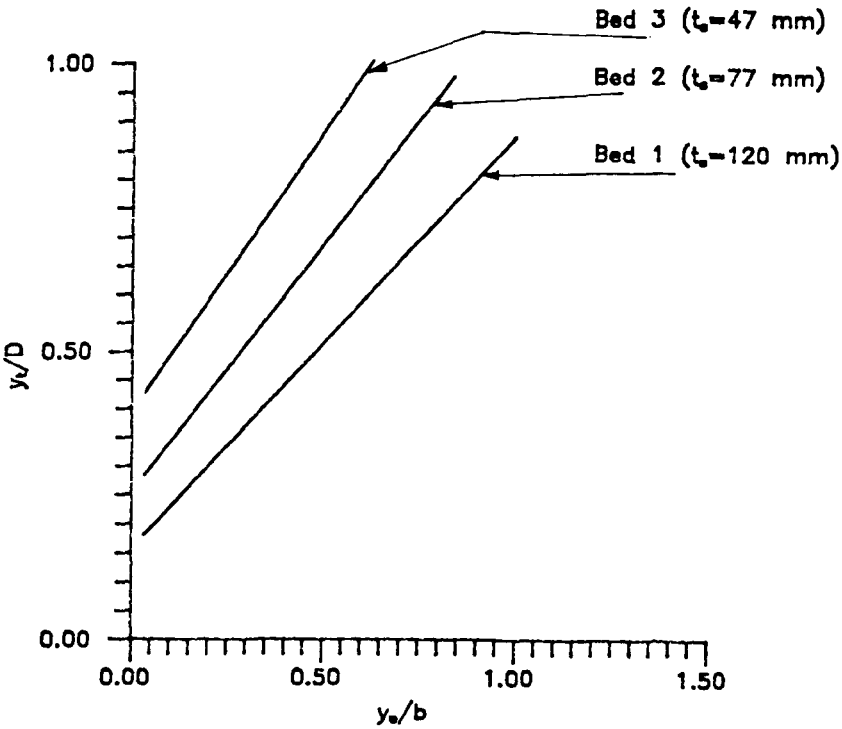

FIGURE 5.7 $\frac{y_t}{D}$ AGAINST $\frac{y_o}{b}$

The width of flat bed is important in determining the hydraulic radius (R) for a given area of flow. For any particular flow depth, the wetted perimeter of a narrow bed is less than that of a wider bed. Due to the effect of curvature in the upper part of the circular channel, a slight increase in the bed depth leads to a much larger increase in the bed width which in turn increases the wetted perimeter and reduces the hydraulic radius. Therefore, the parameter $\frac{y_0}{b}$ is considered in this study to represent the possible shape effects.

A multiple regression analysis was performed with the data and the shear Reynolds number was found to be best described by (see Fig. 5.8a):

$$R_{*} = 0.14 \ (y_o/b)^{-0.68} \ (R_{*y})^{0.98} \qquad (5.14.2)$$

(r=0.96).

where R_{e*} is the shear Reynolds number ($=u_* P/\upsilon$), y_o is the flow depth, b is the channel bed width and R_{ey} is the flow Reynolds number ($=Vy_o/\upsilon$).

From Eq.5.14.2, the channel friction factor (λ_c) can be given by the equation

$$\lambda_c = 0.16\ R_{ep}^{-2}\ R_{ey}^{1.96}\ (y_o/b)^{-1.4} \qquad (5.14.3)$$

where R_{ep} is Reynolds number with respect to wetted perimeter ($=VP/\upsilon$) and R_{ey} is the flow Reynolds number (Vy_o/υ).

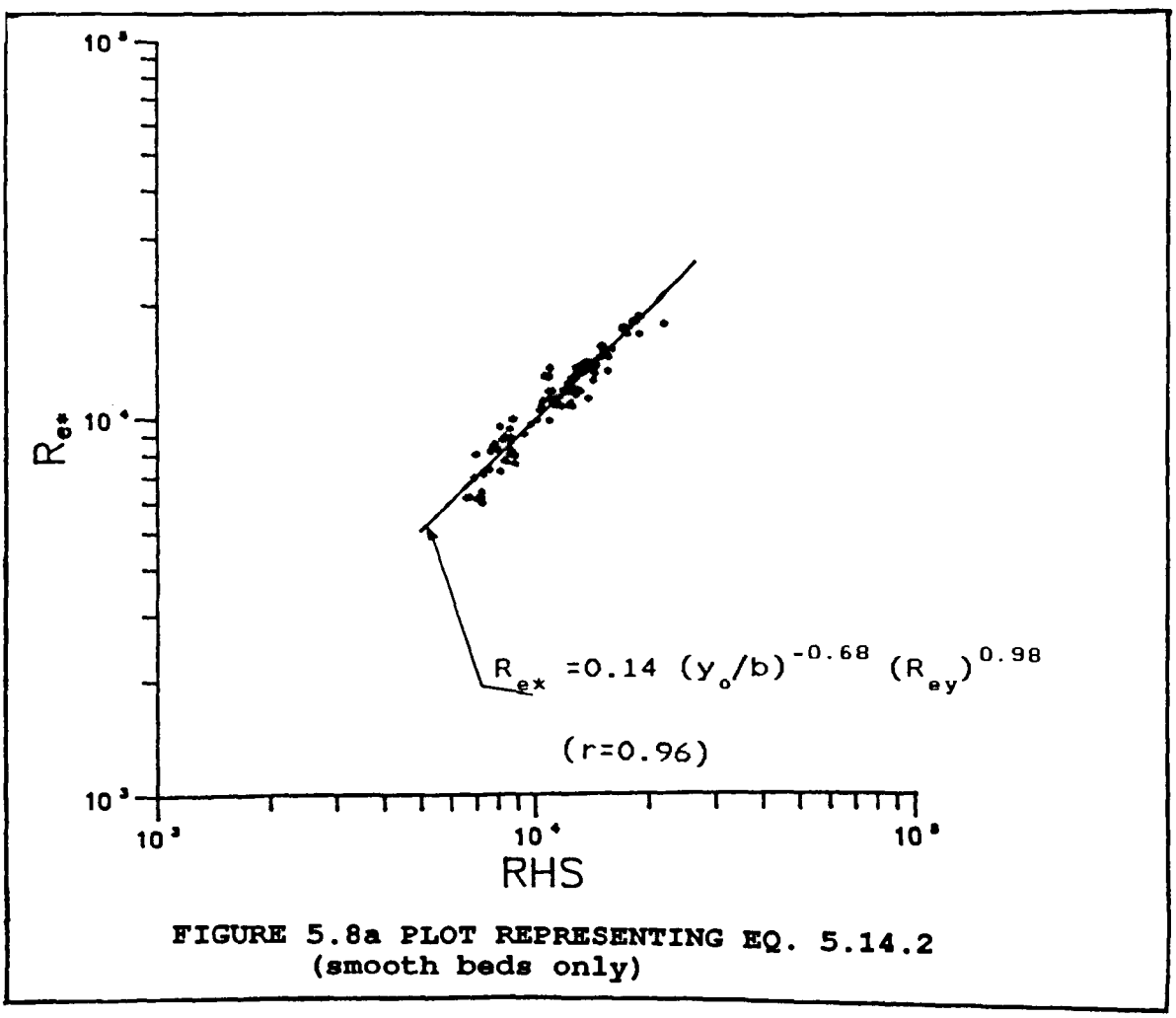

FIGURE 5.8a PLOT REPRESENTING EQ. 5.14.2 (smooth beds only)

Fig. 5.8b presents a comparison between the measured friction factors of smooth beds and the predicted values of Eq. 5.14.3. Despite some scattering the plot indicates that Eq. 5.14.3 provides a good estimate of the channel friction factors.

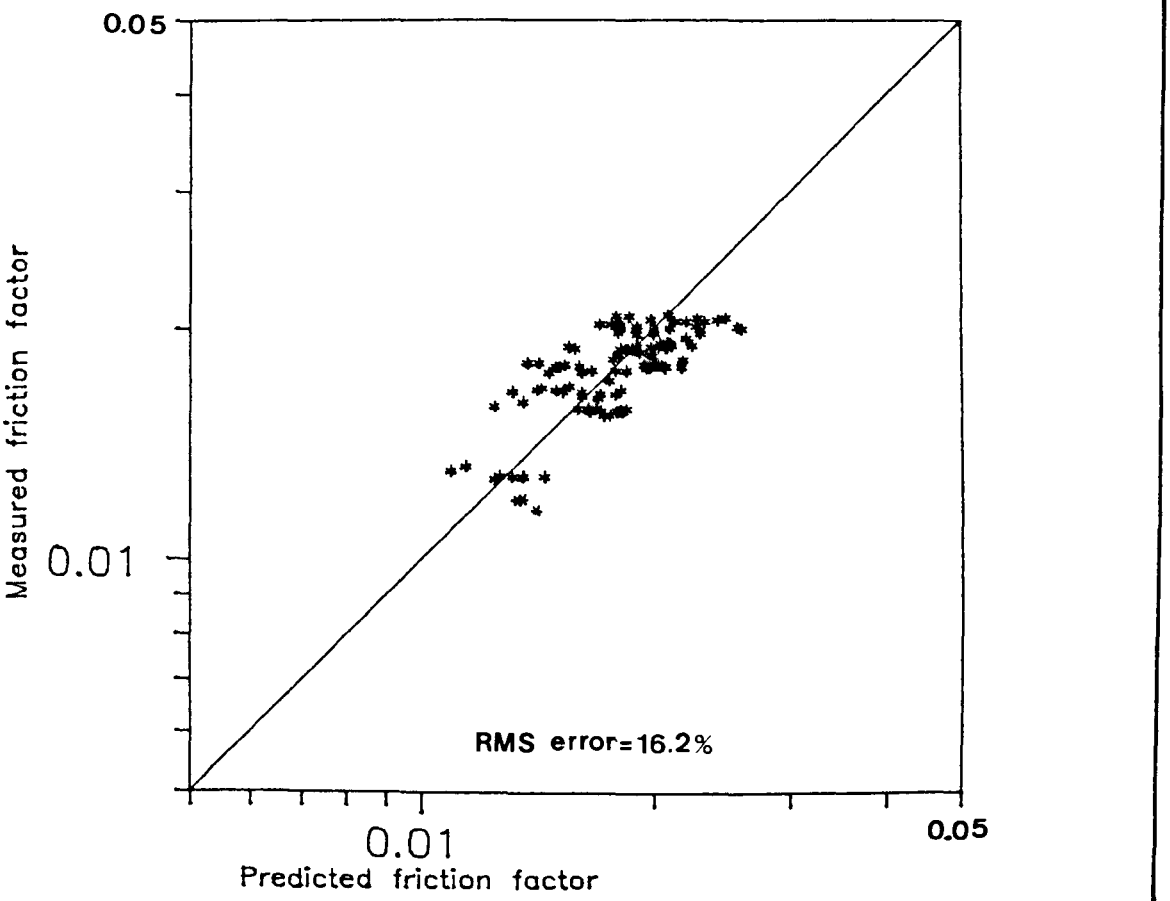

FIGURE 5.8b MEASURED FRICTION FACTORS AGAINST PREDICTED VALUES (by Eq. 5.14.3) FOR SMOOTH BEDS

b) Channels With Rough Beds

To obtain the friction factor of the channel with rough beds accurate channel roughness must be known. The friction factors for circular channels with rough beds may be satisfactorily expressed in terms of flow (y_o, P) and roughness (k_s) elements.

A representative k_s for channels with rough beds are shown in Table 4.1b.

Following the development of the relationship 5.10, a new parameter (y_t/k_s) which reflects the channel roughness was incorporated into Eq. 5.10. Therefore Eq. 5.1o becomes:

$$R_{e*} = f\ (R_{ey},\ y_t/k_s) \qquad (5.15.1)$$

A linear regression analysis was performed, and relationship 5.15.1 found to be best described by (see Fig. 5.9 a):

$$R_{e*} = 43.07\ \ (R_{ey})^{0.529}\ \ (y_t/k_s)^{-0.084} \qquad (5.15.2)$$

with r= 0.923.

where y_t is the total depth (flow depth + bed thickness) and k_s is the overall equivalent sand roughness of the channel.

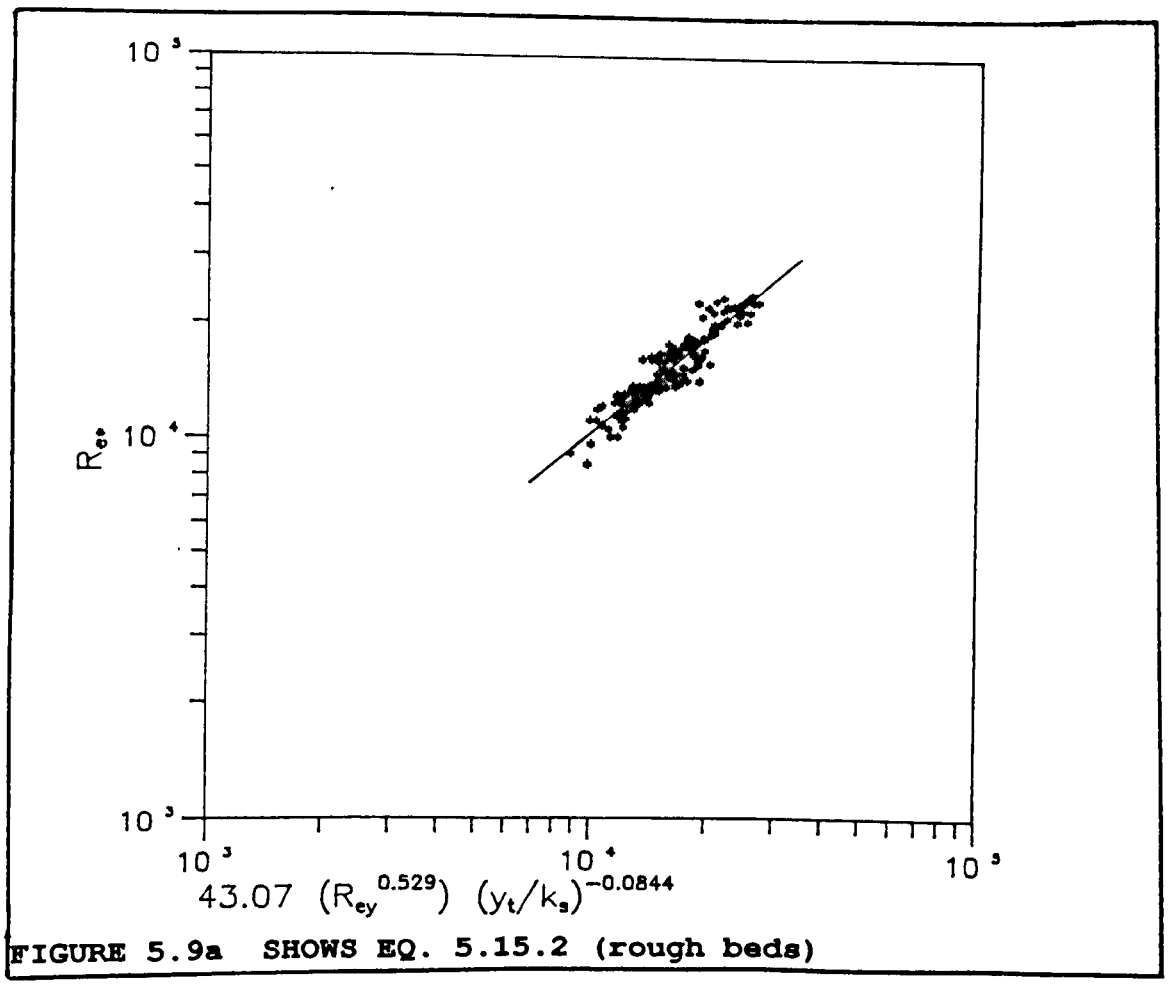

FIGURE 5.9a SHOWS EQ. 5.15.2 (rough beds)

Using Darcy-Weisbach's equation (Eq. 2.27), Eq. 5.15.2 was rearranged as:

$$\lambda_c = 14.84 \times 10^3 \ (R_{ep})^{-2} \ (R_{ey})^{1.06} \ (y_t/k_s)^{-0.17} \qquad (5.15.3)$$

Fig. 5.9b presents the comparison between measured friction factors of channels with rough beds plotted against predicted values by Eq. 5.15.3. The graph shows that the equation (5.15.3) provides a reasonable estimate of the channel friction factors with an error of not more than ±20%. It is important to mention that this type of computation is very sensitive and data scattering is inevitable.

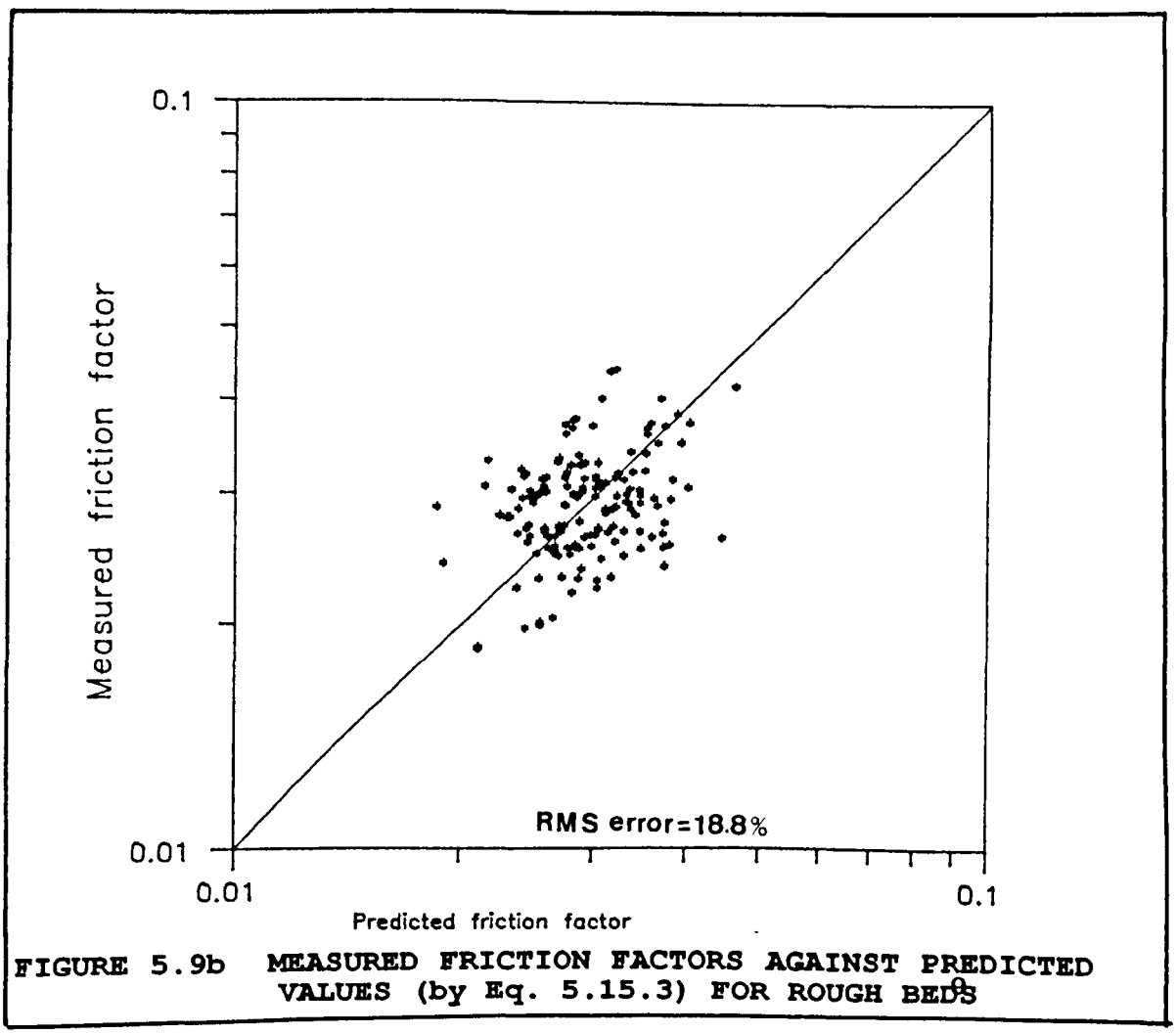

FIGURE 5.9b MEASURED FRICTION FACTORS AGAINST PREDICTED VALUES (by Eq. 5.15.3) FOR ROUGH BEDS

5.3. Velocity Distributions

The velocity profiles were measured for different flow conditions in all three beds. A pitot tube, a propeller current meter and a Laser Doppler Velocimeter (LDA) were used for this purpose. Complete velocity distribution mappings (isovels) were made for each of the three depths (1/3, 1/2 and 2/3 full) for all three beds. A Listing of velocity data is given in appendix E. Detailed experimental data for each test are tabulated in table 5.1.

The results show that at shallow flow depths the velocity distribution revealed a different pattern dependent on bed roughness.

It was found that in smooth beds the flow is two-dimensional (2D) (see Figs. 5.10 and 5.11) which can be attributed to the reduction of direct side-wall effects. For rough bed channels it was found that the flow becomes three-dimensional (see Figs. 5.12 and 5.13) due to an increase in secondary currents and the creation of a bottom vortex in addition to a free surface vortex. Secondary currents are generated and modified as a result of the anisotropy of turbulence, which is caused by the boundary conditions of the bed, the side wall and the free surface, as well as the aspect ratio of the channel geometry. Secondary currents affect the primary mean flow, producing three-dimensional structures. Three dimensional flows have been observed in smooth trapezoidal and rough bed rectangular channels by Tominaga et al (1989).

TABLE 5.1 Details of Velocity Measurements Tests

Bed 1 (t_s=47 mm)								
Run No.	y_o mm	Q m^3/s	S	V m/s	τ_o (ρgRS) N/m^2	R_e	F_r	k_s mm
V1	57.15	0.0068	0.0015	0.458	0.597	73746.9	0.645	smooth
V2	55.7	0.009	0.0027	0.62	1.08	97854.9	0.884	smooth
V3	107.5	0.0181	0.0013	0.604	0.842	156004	0.615	smooth
V4	155.1	0.0271	0.00097	0.613	0.756	199715.7	0.50	smooth
V5	71.25	0.012	0.00284	0.634	1.15	126537	0.8	smooth
V6	67.17	0.0087	0.0008	0.49	0.39	85052.07	0.64	smooth
V7	157.6	0.0304	0.0009	0.67	0.726	220017.6	0.54	smooth
V8	59.5	0.0067	0.00153	0.43	0.653	73397.15	0.59	0.80
V9	60.5	0.0064	0.00128	0.40	0.554	64947.7	0.54	0.80
V10	104.7	0.0173	0.0016	0.592	1.014	151020.3	0.61	0.80

Bed 2 (t_s = 77 mm)								
Run No.	y_o mm	Q m^3/s	S	V m/s	τ_o (ρgRS) N/m^2	R_e	F_r	k_s mm
V11	32.13	0.0042	0.0024	0.464	0.64	50317.4	0.707	smooth
V12	124.4	0.0219	0.001	0.598	0.692	147750.2	0.535	smooth
V13	82.1	0.0174	0.0023	0.72	1.24	145469.9	0.822	smooth
V14	124.7	0.0222	0.0012	0.603	0.826	167038.0	0.54	smooth
V15	78.95	0.0186	0.0028	0.807	1.488	170789.4	0.936	smooth

Table 5.1 Cont.

Run No.	y_o mm	Q m^3/s	S	V m/s	τ_o N/m^2	R_e	F_r	k_s mm
V16	82.02	0.0012	0.00149	0.486	0.809	96593.8	0.55	0.80
V17	116.5	0.0219	0.00169	0.637	1.129	160475.6	0.595	0.80
V18	53.88	0.0078	0.00286	0.501	1.15	73256.12	0.703	1.40
V19	60.84	0.0080	0.0023	0.455	1.001	76802.9	0.603	1.40

Bed 3 (t_s=120 mm)								
Run No.	y_o mm	Q m^3/s	S	V m/s	τ_o N/m^2	R_e	F_r	k_s mm
V20	55.94	0.0076	0.0011	0.446	0.445	67436.6	0.6	smooth
V21	119.1	0.0191	0.0011	0.551	0.696	123997.4	0.47	smooth
V22	83.24	0.0147	0.0021	0.586	1.08	111978.4	0.63	0.80
V23	125.7	0.0188	0.0014	0.515	0.912	11584.4	0.46	0.80
V24	45.84	0.0065	0.0026	0.468	0.899	58439.99	0.698	0.80
V25	105.9	0.0198	0.0027	0.631	1.575	126059	0.59	1.40
V26	61.5	0.0103	0.0032	0.554	1.39	83581.4	0.71	1.40
V27	66.7	0.0097	0.0011	0.50	0.46	75744.4	0.59	smooth
V28	104.4	0.0183	0.0011	0.66	0.54	117676	0.66	smootn

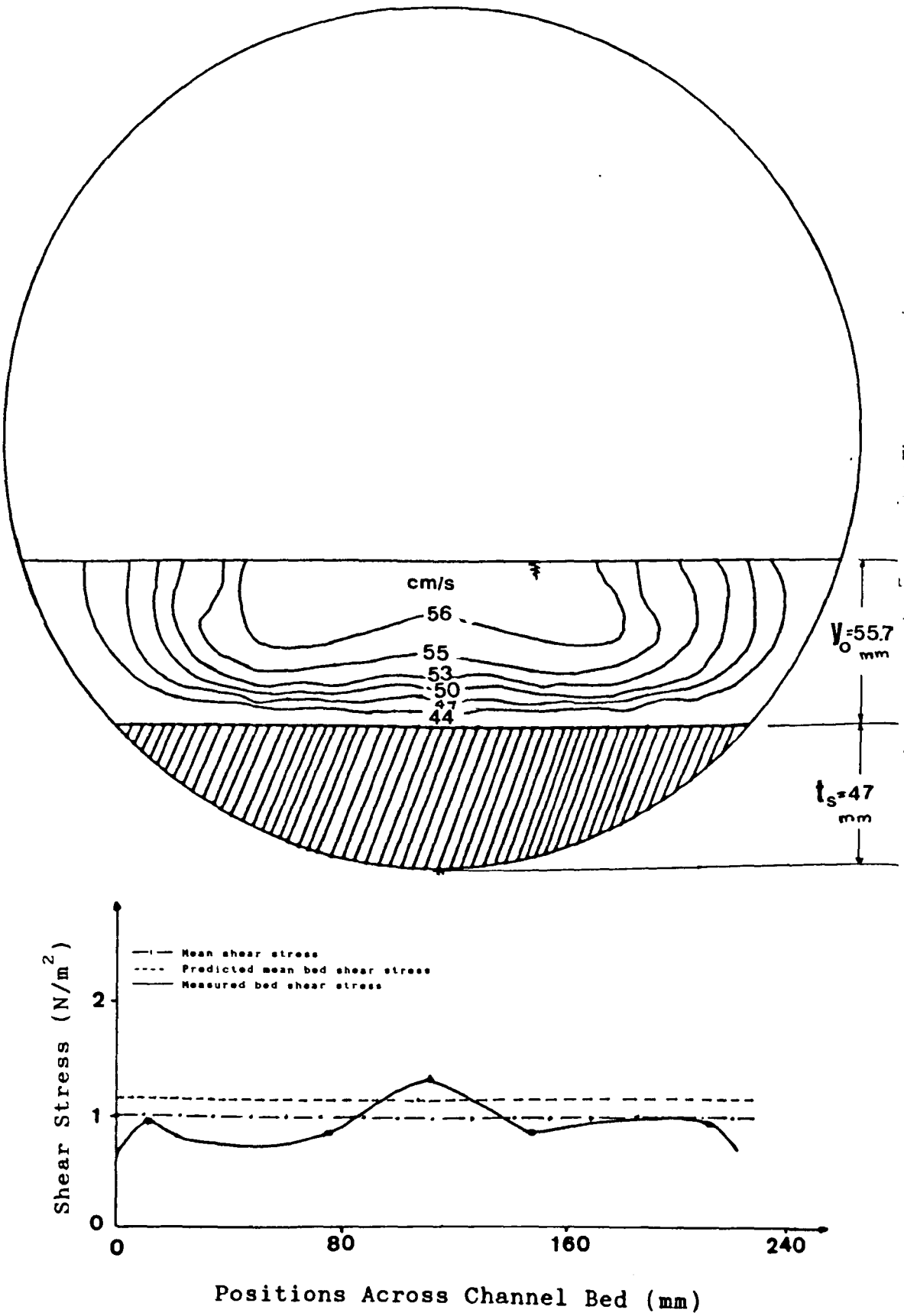

FIGURE 5.10 VELOCITY AND SHEAR DISTRIBUTION CURVES (y_o=55.7mm, S=0.0027, k_s=0.00)

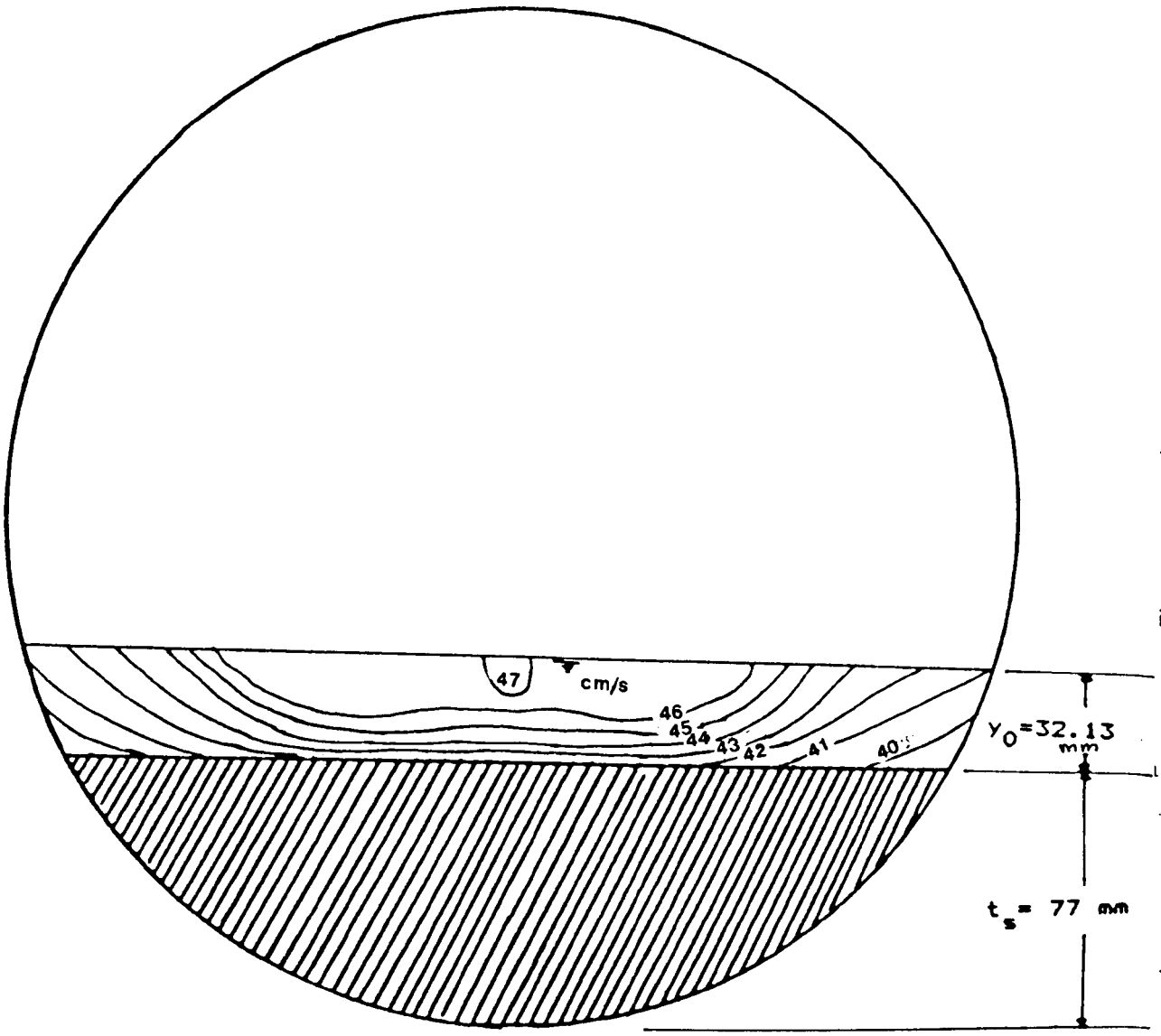

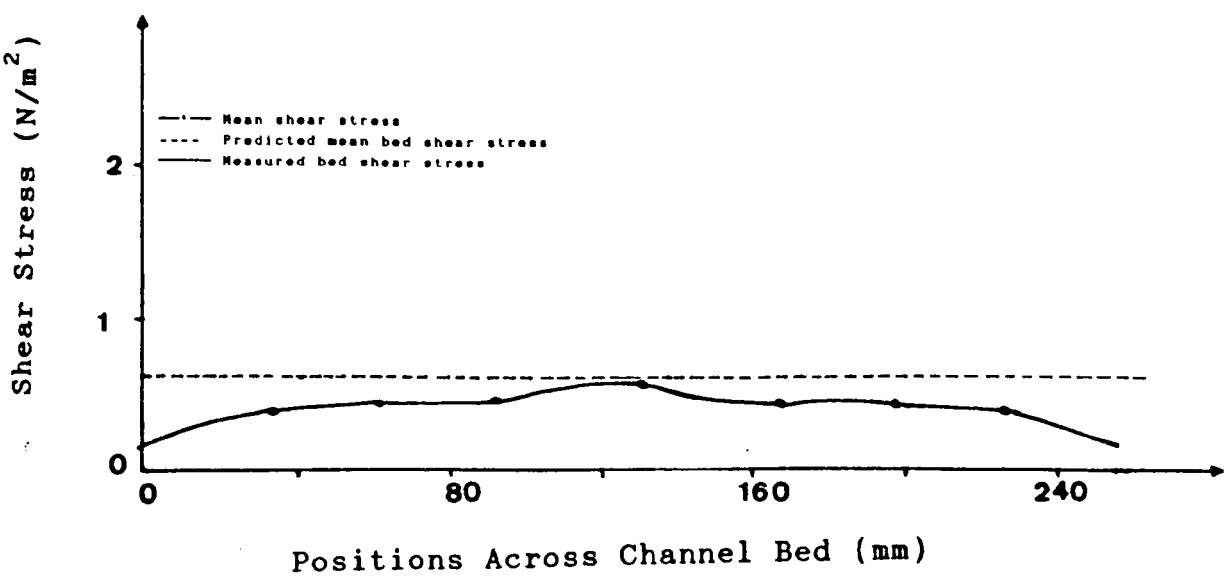

FIGURE 5.11 VELOCITY AND SHEAR DISTRIBUTION CURVES (y_o=32.13mm, S=0.0024, k_s=0.00)

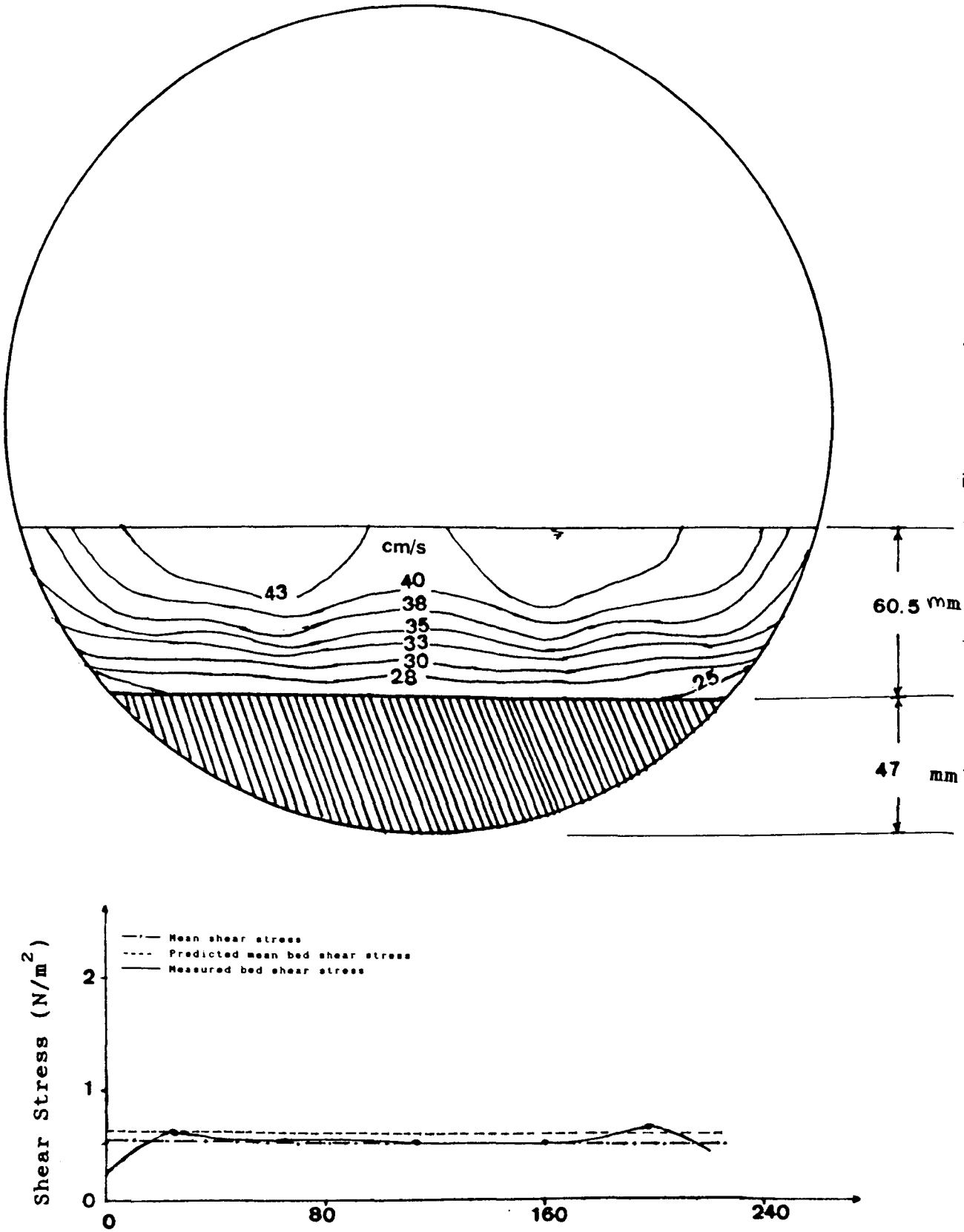

FIGURE 5.12 VELOCITY AND SHEAR DISTRIBUTION CURVES
(y_o=60.5mm, S=0.00128, k_s=0.80)

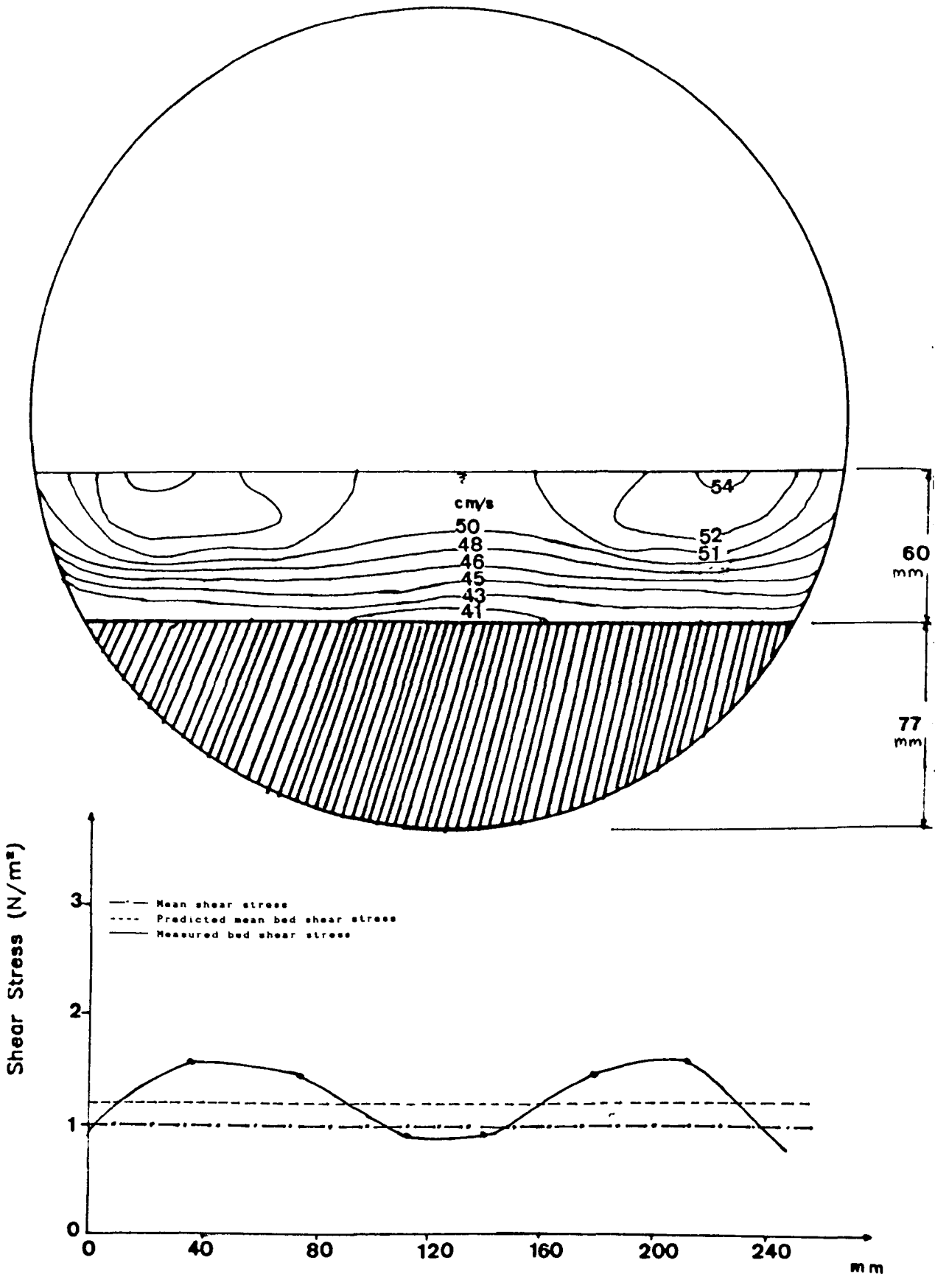

FIGURE 5.13 VELOCITY AND SHEAR DISTRIBUTION CURVES
(y_o=60.8mm, S=0.00229, k_s=1.40)

At flows up to half-full depths (see Figs. 5.14 t0 5.17), only one maximum velocity appears below the free surface (analogous to wide open channels). The flow section at this depth does not have a trapezoidal-like shape, as that at one third-full depth, but approaches the shape of a rectangular channel due to the introduction of wall curvature at the perimetric level of the circular channel. Thus the velocity distribution at half-full depths appears to be similar, to some extent, to that in rectangular channels (Knight and Macdonald, 1979, Nezu and Rodi, 1985 and Tominaga et al 1989) The most accurate explanation of the depressed point of maximum velocity, though difficult to formulate, is the mechanism of secondary currents.

At higher flow depths ($\frac{y_o + t_s}{D}$ >0.60), the velocity distributions change from that with one position of maximum velocity, as in the case of medium depth, to two maxima close to the water surface. The influence of side wall curvature has become very pronounced and a vortex can be generated between the free surface and the side wall. Consequently a three-dimensional flow structure is developed (see Figs. 5.18 to 5.20). It has to be mentioned here that the velocity distributions in circular cross section channels at large flow depths (open channel flow) is almost three-dimensional flow as stated by Novak and Nalluri (1973). Therefore, one can say that the velocity distributions over the flat beds of circular cross section are strongly influenced by flow depths and bed roughness. These findings agree with previous work (Alvarez 1990).

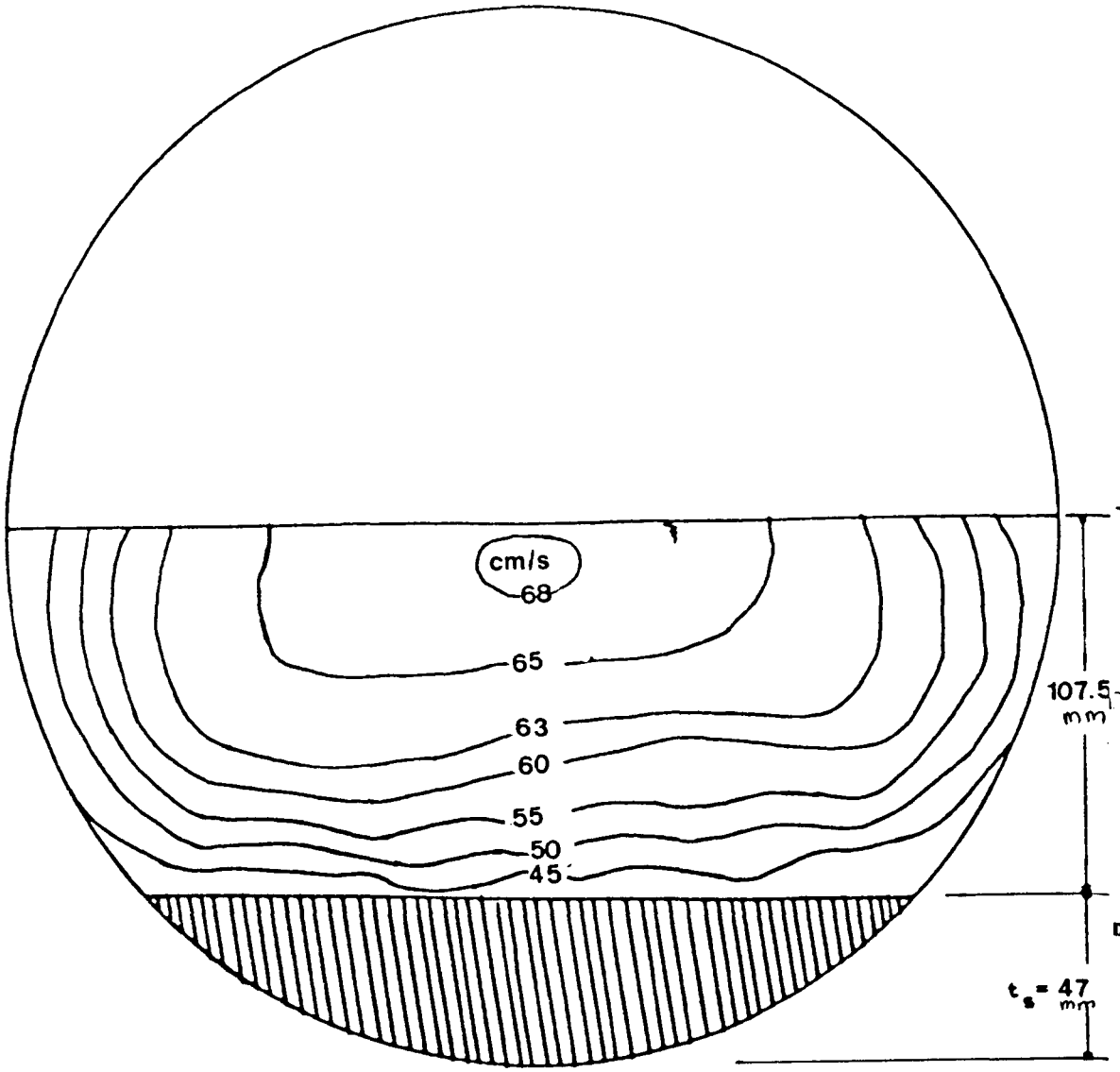

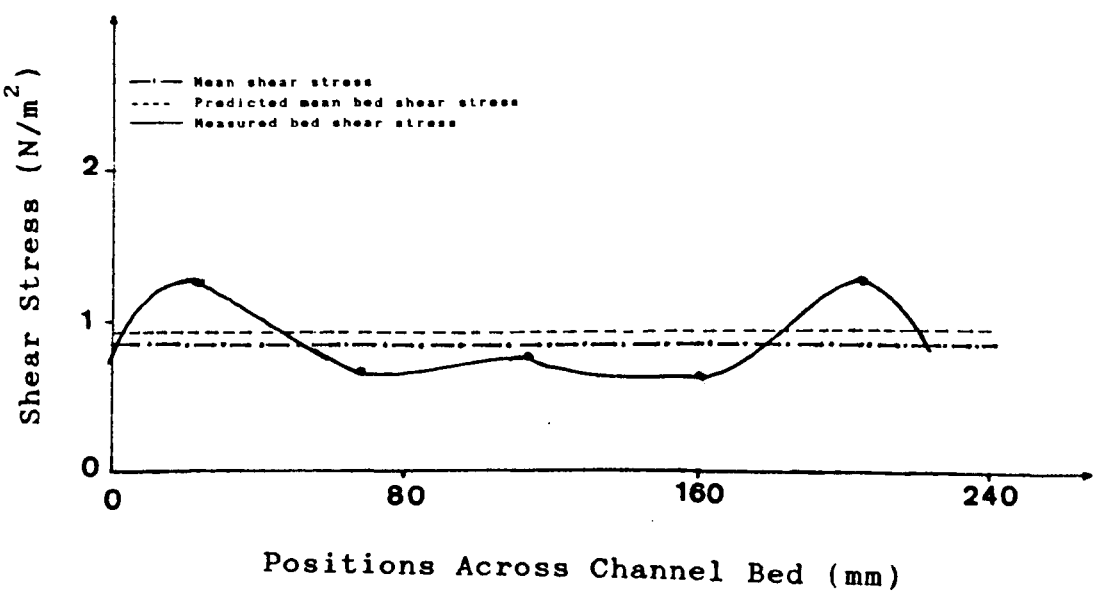

FIGURE 5.14 VELOCITY AND SHEAR DISTRIBUTION CURVES (y_o=107.5mm, S=0.0013, k_s=0.00)

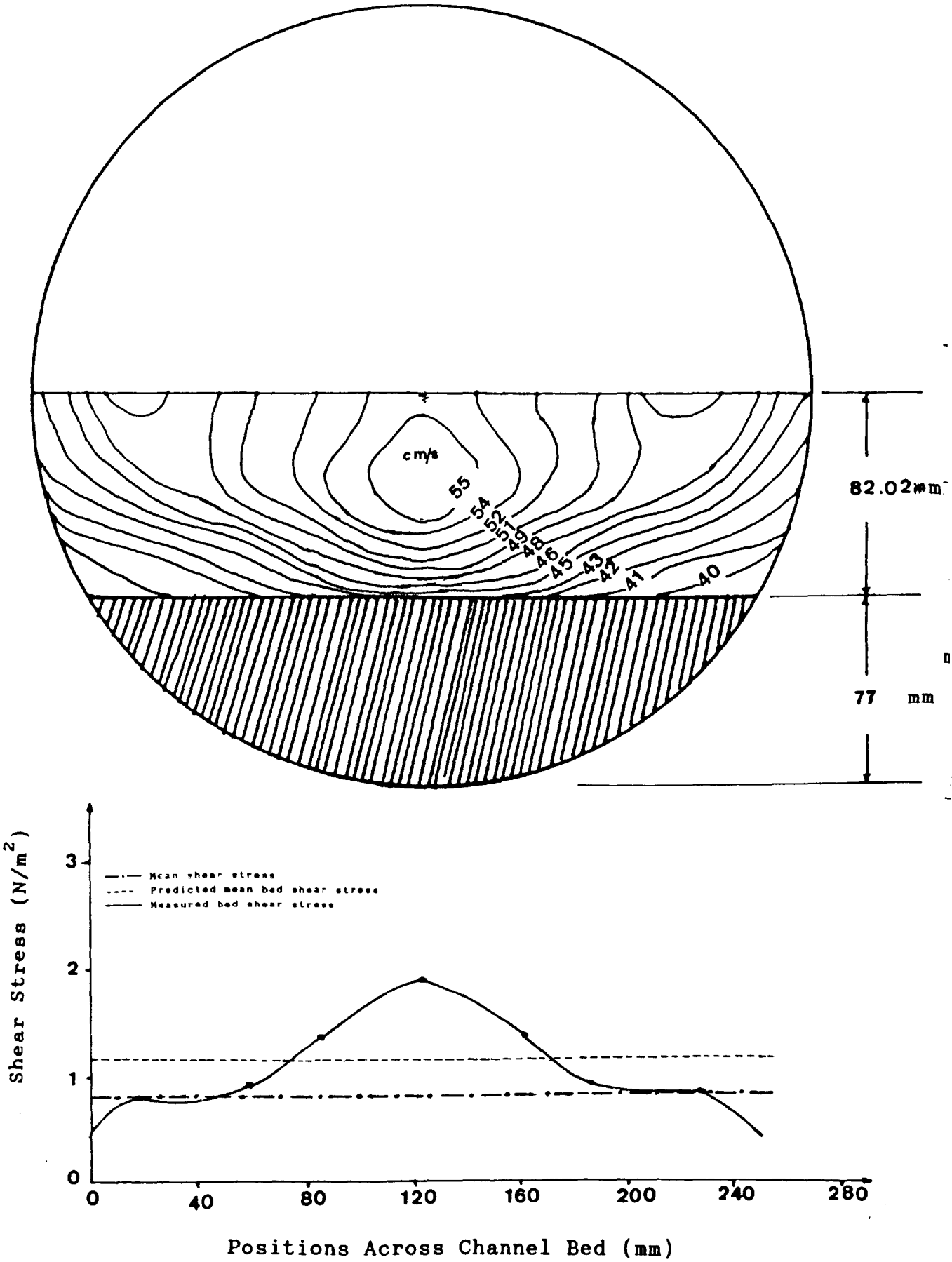

FIGURE 5.15 VELOCITY AND SHEAR DISTRIBUTION CURVES
(y_o=82.02mm, S=0.0014, k_s=0.80)

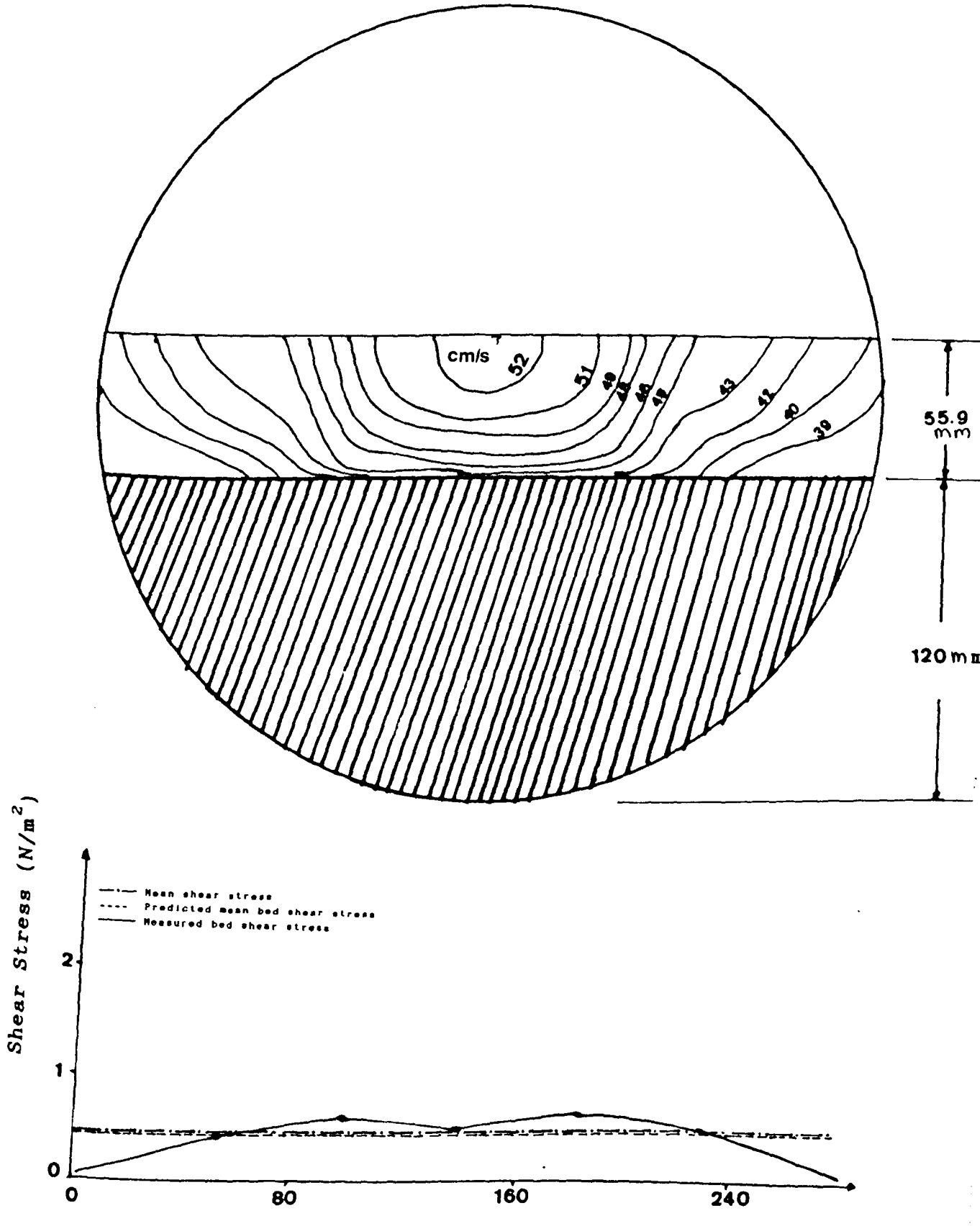

FIGURE 5.16 VELOCITY AND SHEAR DISTRIBUTION CURVES
(y_o=55.9mm, S=0.0011, k_s=0.00)

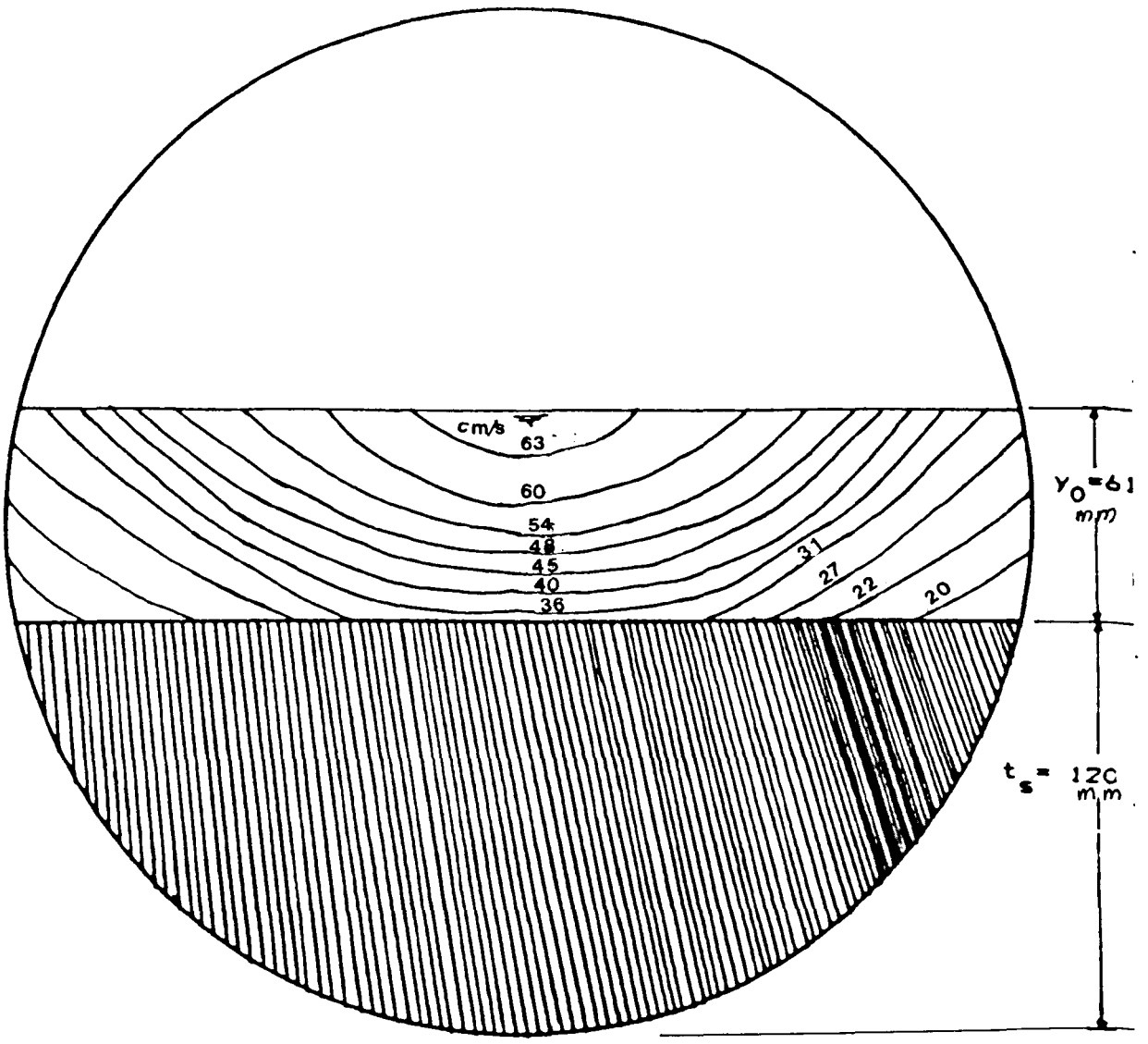

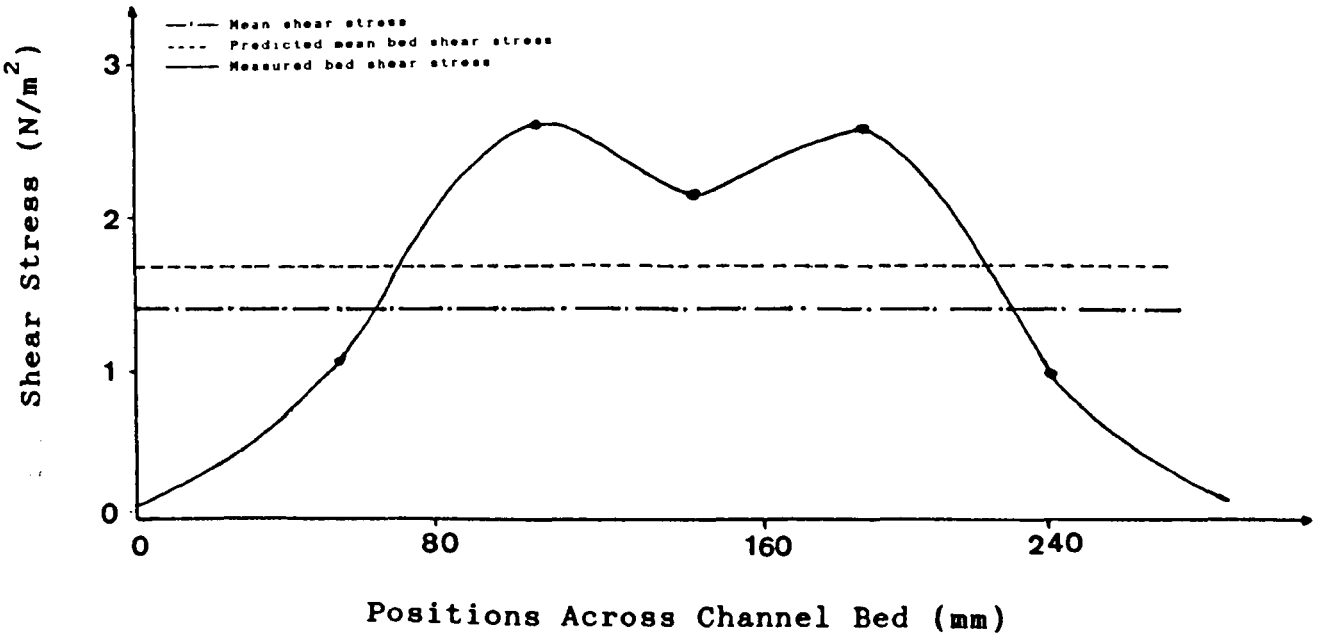

FIGURE 5.17 VELOCITY AND SHEAR DISTRIBUTION CURVES
(y_o=61.5mm, S=0.0032, k_s=1.40)

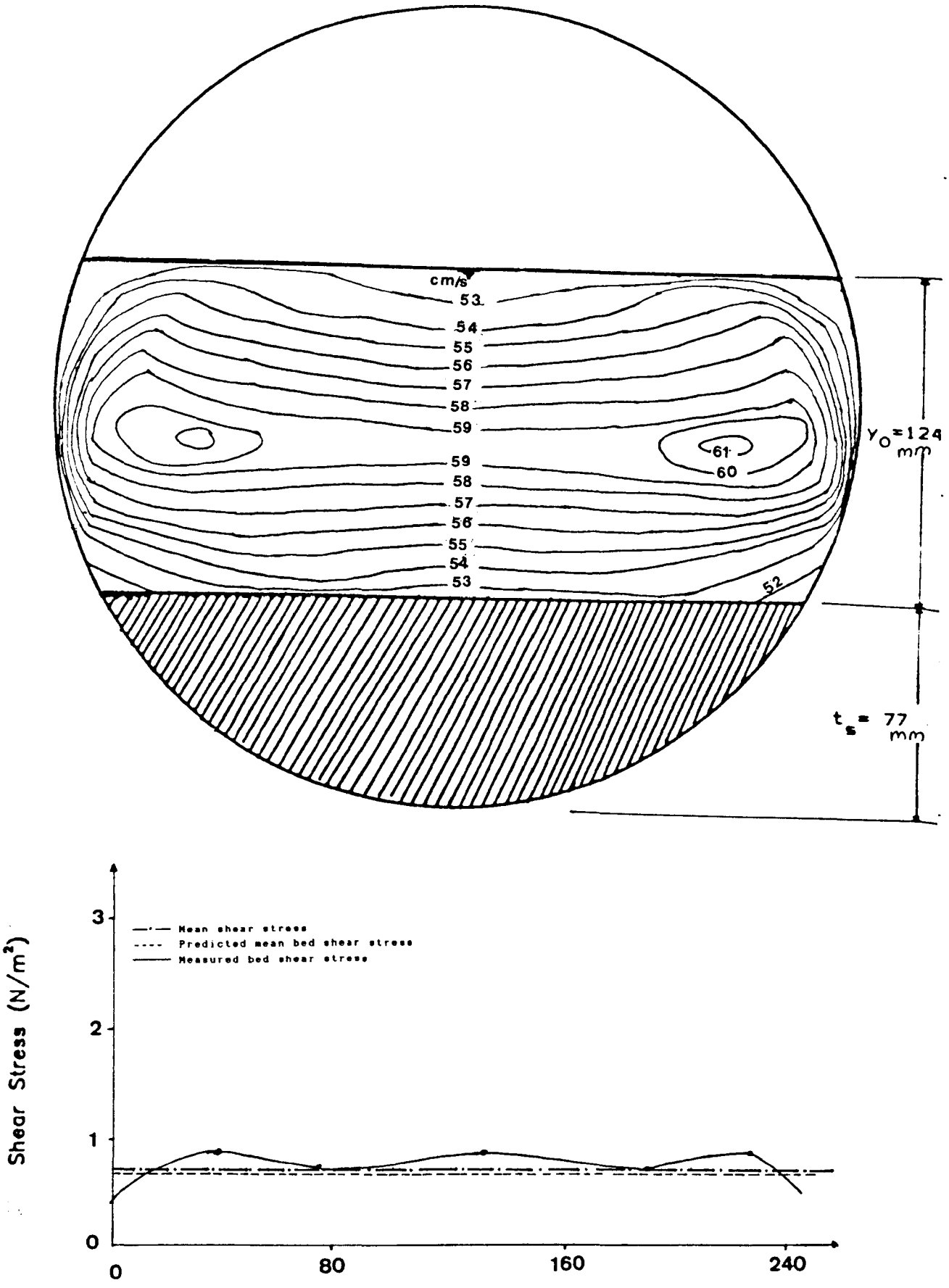

FIGURE 5.18 VELOCITY AND SHEAR DISTRIBUTION CURVES (y_o=124.3mm, S=0.001, k_s=0.00)

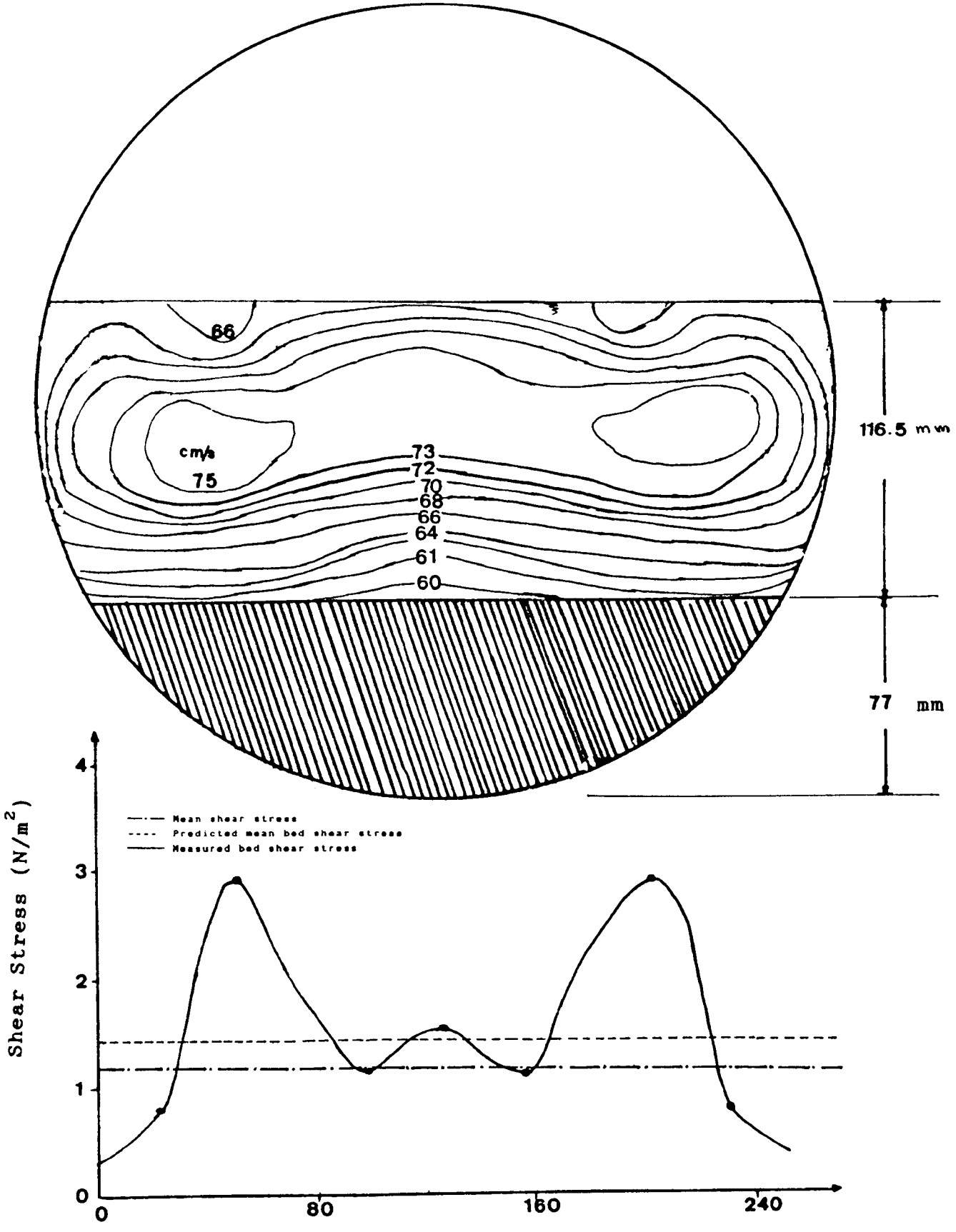

FIGURE 5.19 VELOCITY AND SHEAR DISTRIBUTION CURVES (y_o=116.5mm, S=0.00169, k_s=0.80)

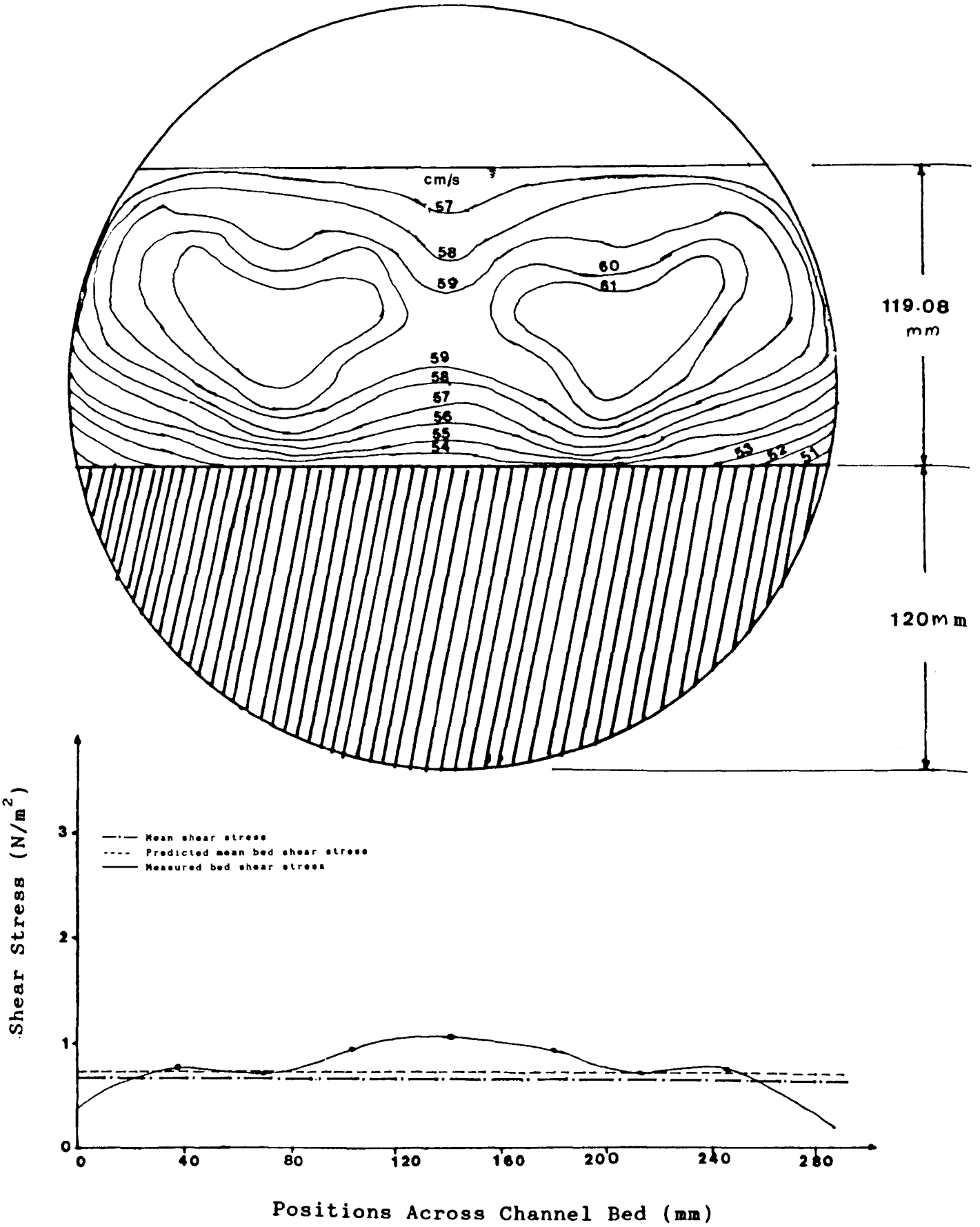

FIGURE 5.20 VELOCITY AND SHEAR DISTRIBUTION CURVES
(y_o=119.08mm, S=0.0011, k_s=0.00)

The exact location of maximum velocity distributions could not be determined. Measurements indicated that the maximum velocity for upper flow depths (above half-full), where the side wall effect became predominant, usually appeared below the free surface, while for shallow depths of smooth beds, it was found that the maximum velocity occurred at the water surface. The secondary currents appear to play an important role in the distributions of velocity in rough beds and geometry appears to play the major role in triggering and establishing the secondary currents which are believed to influence the location of the maximum velocity filament.

Nezu & Rodi (1985) argued that the most important feature related to secondary currents in narrow open channels is that the maximum velocity does not appear at the free surface, but below it. This phenomenon is called the "velocity-dip" and is peculiar to open channel flow.

5.4 Bed Shear Stress Distributions

5.4.1 General

Information regarding the nature of boundary shear stress distribution in a flowing stream is needed for various purposes; firstly, to give a basic understanding of the resistance relationship and secondly, to understand the mechanism of sediment transport, for designing stable channels.

The distribution of bed shear stress is of great importance, because it offers an opportunity to identify the region of

high shear stress where the possibility of deposition is minimal.

Uniform distribution of shear stress can be expected only in infinitely wide rectangular channels and in circular pipes flowing full. A considerable part of the erosion and sedimentation damage caused by channels depends upon the inequality of shear stress exerted on different parts of the wetted perimeter.

5.4.2 Determination of Bed Shear Stress

The bed shear stress has been estimated through the use of velocity profiles, which is an indirect method commonly used in experimental studies of flow in pipes and open channels. Patel (1984) found that the boundary shear stress obtained from semi-log plots of velocity data agreed reasonably well with those obtained by the Preston tube technique. For a steady and uniform two dimensional flow, the logarithmic velocity law can be written as:

$$\frac{u}{u_*} = \frac{1}{\kappa} \ln (y) + \text{constant} \qquad (5.16)$$

in which $u_*=\sqrt{\tau_o/\rho}$ is the shear velocity, u is the velocity in longitudinal direction at depth y, κ is Von Karman's universal constant. For open channel flow Eq. 5.16 can be expressed for smooth surfaces, as:

$$\frac{u}{u_*} = 5.75 \log \left[\frac{9yu_*}{\upsilon}\right] \qquad (5.17)$$

where υ is the kinematic viscosity and, for rough surfaces, as:

$$\frac{u}{u_*} = 5.75 \log \left[\frac{30.2\ y}{k_s} \right] \qquad (5.18)$$

where k_s is Nikurade's equivalent sand roughness. For the position of maximum velocity (y=h) Eq. 5.18 can be written as:

$$\frac{u_{max}}{u_*} = 5.75 \log \left[\frac{30.2\ h}{k_s} \right] \qquad (5.19)$$

Subtracting Eq. 5.18 from Eq. 5.19 yields,

$$\frac{u_{max} - u}{u_*} = -5.75 \log \left[\frac{y}{h} \right] \qquad (5.20)$$

The value of u_* can be obtained by the best fit line method (see Fig. 5.21) from which the bed shear stress, $\bar{\tau}_b$ can be obtained directly from:

$$\bar{\tau}_b = \rho\ u_*^2 \qquad (5.21)$$

The limit of applicability of the logarithmic law in a two-dimensional flow is the relative scale of the roughness. If the individual roughness elements are large in relation to the flow depth the wake eddies disrupt the velocity profile. However, in small scale roughness the velocity profile is similar to that in a boundary layer and the logarithmic law applies. It was considered that this indirect method would be applicable only in the bottom 20% of the flow depth, with the Von-Karman constant at its usual value of 0.4.

An example of the velocity profile and logarithmic velocity distribution for a particular flow are shown in Fig. 5.21. By measuring several vertical velocity profiles across the width of the flume it was possible to obtain the distribution of shear stress on the bed (see Table 5.2 for typical measurement).

5.4.3 Experimental Results

Measurements of bed shear stress were undertaken with smooth beds and with beds roughened with uniform sands (d_{50}= 0.53 mm and 1.0 mm). Bed shear stresses were measured, and averaged (using "trapezoidal rule" numerical method) in some cases to give bed mean values $\bar{\tau}_{bm}$, which were then compared with the mean shear stresses calculated from energy slope ($\tau_o=\rho gRS$) and with bed shear stresses obtained by the separation technique for rough beds ($\bar{\tau}_b$) (see Table 5.3).

In the case of a channel with a rough bed and smooth walls, the hydraulic radius and areas of the bed were determined by using Einstein-Vanoni's method (see Appendix G) to eliminate the side wall effects. The mean bed shear stress was then determined from the equation, $\bar{\tau}_b=\rho gR_bS$. Table 5.3 shows that this mean bed shear stress agreed reasonably well with the measured bed shear stress obtained indirectly from velocity data.

It was found that the shear stress distribution along the channel beds was markedly non-uniform. This was observed for all three bed thicknesses. In most of the cases the maximum

TABLE 5.2 TYPICAL SHEAR STRESS DISTRIBUTION COMPUTATION

Velocioty profile to obtain bed shear stress
pipe (D=305 mm) with smooth flat bed
Bed thickness =47 mm
Bed width =220 mm
Discharge =0.00681 m
Slope =0.001452
Normal Depth =57.15 mm

Date:18/7/89
At centre line

Y mm	. cm/s	.max cm/s	max-. cm/s	-5.75 LOG(Y/Ym)
2	28.5	49.3	20.8	8.23
3	32	49.3	17.3	7.22
4	33.3	49.3	16	6.50
6	36.3	49.3	13	5.49
10	39.2	49.3	10.1	4.21
15	40.7	49.3	8.6	3.20
25	43.4	49.3	5.9	1.92
35	45.3	49.3	4	1.06
45	47.3	49.3	2	0.46
54	49.3	49.3	0	0.00

Regression Output:

Constant	-1.19344
Std Err of Y Est	0.397179
R Squared	0.992934
No. of Observations	5
Degrees of Freedom	3
X Coefficient(s)	2.628069
Std Err of Coef.	0.128002

Shear velocity $u_* =$ 0.026281 m/s
Measured bed shear stress $\tau_{bm} =$ 0.69 N/m2

Mean shear stress $\tau_o =$ 0.59 N/m2

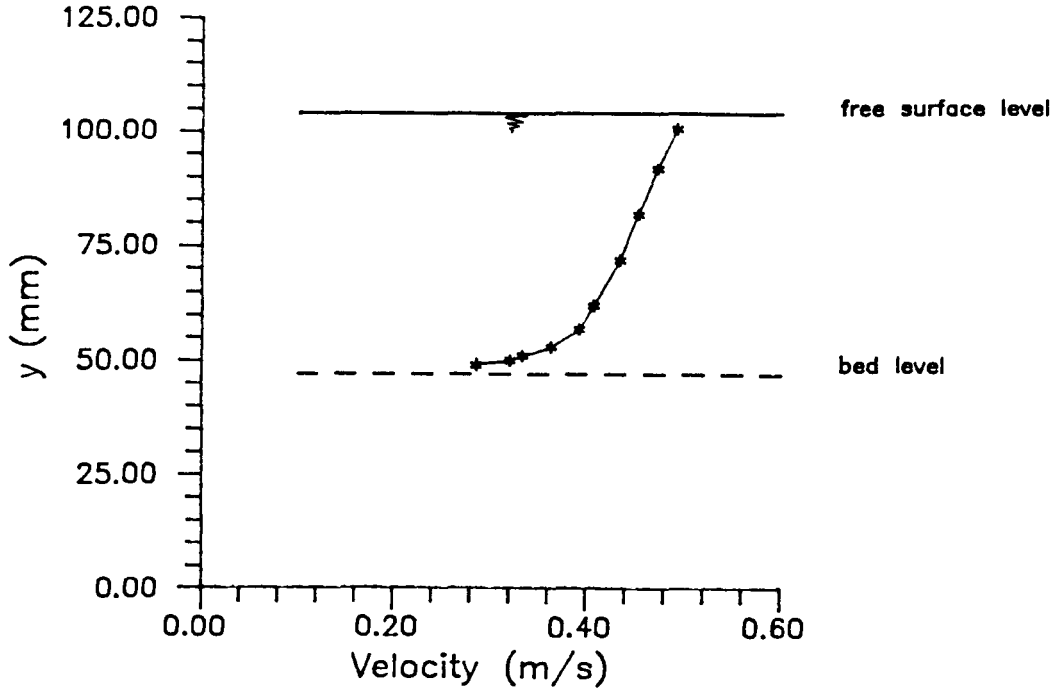

a) Velocity distribution

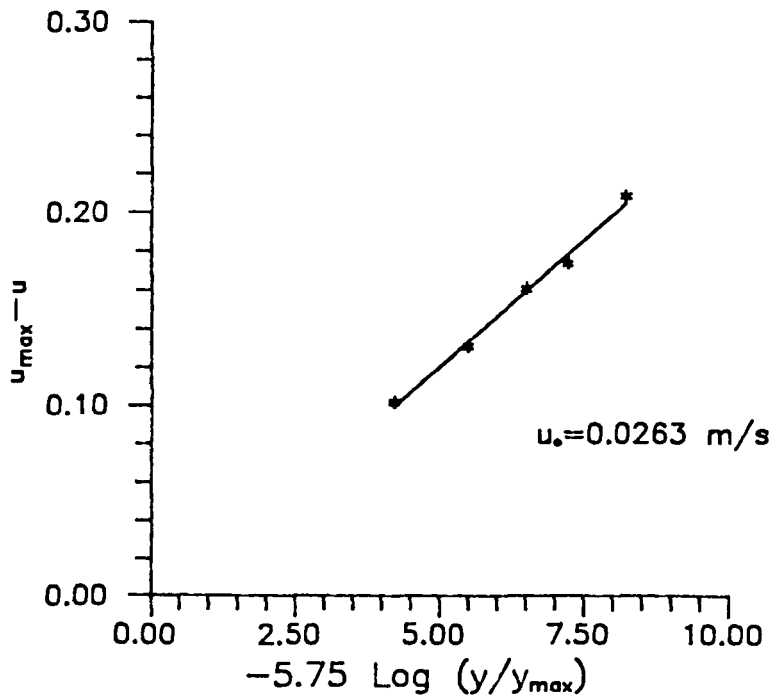

b) Log. velocity distribution

FIGURE 5.21 TYPICAL VELOCITY DISTRIBUTION ON CENTRELINE
($Q = 0.0068$ m^3/s; $S = 0.00145$; $y_o = 57.15$ mm)

bed shear stress did not necessarily occur below the point of maximum velocity but instead at some intermediate position between the centreline and the corner (see Figs 5.14 and 5.15). This phenomenon has been confirmed by several researchers (Bathurst et al 1979, Gosh and Roy 1970, Knight et al,1982 and Choa-lin and Gwo-fang 1983) in the case of wide channels; however, the maximum bed shear stress for full-flow conditions is found to be at the centreline of the channel (Alvarez 1990).

The results presented in Fig. 5.17 show the complexity of the bed shear stress, and how they are affected by variations in bed roughness. From Table 5.3, it would appear that $\bar{\tau}_{bm}/\tau_o$ varies relatively little with y_t/D for the three roughness cases and increases with increasing bed roughness (although only a few experiments were conducted on rough beds).

The bed shear stress distribution influences the initial movement of bed load materials. It was observed during the initiation of motion experiments that at flows of depths up to one third full and two-thirds full the particles that started to move were those close to the side wall while for flows at half-full depths the particles at the centre line of the channel bottom were seen to move earlier than those close to the side walls. Similar observations were seen during bed load experiments where the initiation of deposition was found to occur at the middle part of the channel for flows at a third-full and two-thirds full depths and for flows at half-full depth the initiation of deposition was found to be

close to the side walls.

The flow depth and boundary roughness was found to be affecting the bed shear stress distributions.

The average (measured) bed shear stresses were found to be approximately 20% greater than the average shear stress obtained from equation $\tau_o = \rho g R S$. Figure 5.22a shows the relationship between average shear stress and measured mean bed shear stress for different bed thicknesses ($0.15 < \frac{t_s}{D} < 0.4$) and roughnesses ($0.0 < k_{s(mm)} < 1.4$). The data was found to be represented by the best fit line:

$$\bar{\tau}_{bm} = 1.2 \ \tau_o^{1.25} \qquad (5.22)$$

with r=0.9.

TABLE 5.3 BED SHEAR STRESS DATA

a) For $y_t/D < 1/2$

	t_s mm	y_o mm	Q m^3/s	k_s mm	τ_o N/m^2	Meas. $\bar{\tau}_{bm}$ N/m^2	Comp. $\bar{\tau}_b$ N/m^2	$\bar{\tau}_{bm}/\tau_o$
1	47	55.70	0.009	smooth	1.08	1.1		1.02
2	47	57.15	0.0068	smooth	0.59	0.75		1.27
3	47	60.5	0.0064	0.80	0.55	0.55		1.00
4	47	67.17	0.0087	smooth	0.39	0.32		0.82
5	47	71.25	0.012	smooth	1.01	1.14		1.13
6	77	32.13	0.0042	smooth	0.64	0.40		0.63
7	77	53.88	0.0078	1.4	1.15	1.37	1.36	1.19
8	77	60.84	0.008	1.40	1.00	1.22	1.219	1.22

b) For $y_t/D > 1/2$

	t_s mm	y_o mm	Q m^3/s	k_s mm	τ_o N/m^2	Meas. $\bar{\tau}_{bm}$ N/m^2	Comp. $\bar{\tau}_b$ N/m^2	$\bar{\tau}_{bm}/\tau_o$
9	47	157.60	0.0304	smooth	0.73	0.78		1.11
10	47	107.5	0.0181	smooth	0.84	0.92		1.10
11	47	155.10	0.0271	smooth	0.76	1.06		1.39
12	47	104.70	0.0173	0.80	1.01	1.49	1.30	1.48
13	77	82.10	0.0174	smooth	1.24	1.33		1.07
14	77	124.4	0.0255	smooth	0.69	0.74		1.07
15	77	124.7	0.0222	smooth	0.83	0.83		1.00
16	77	78.95	0.0186	smooth	1.49	1.61		1.08
17	77	82.02	0.0012	0.80	0.81	1.10	1.20	1.36
18	77	116.5	0.0219	0.80	1.13	1.60	1.40	1.42
19	120	55.94	0.0076	smooth	0.45	0.45		1.00
20	120	119.1	0.0191	smooth	0.70	0.79		1.13
21	120	125.7	0.0188	0.80	0.91	1.07	1.16	1.18
22	120	83.24	0.0147	0.80	1.08	1.20	1.30	1.11
23	120	105.9	0.0198	1.40	1.57	2.9	2.10	1.85
24	120	61.50	0.0103	1.40	1.39	1.67	1.65	1.20

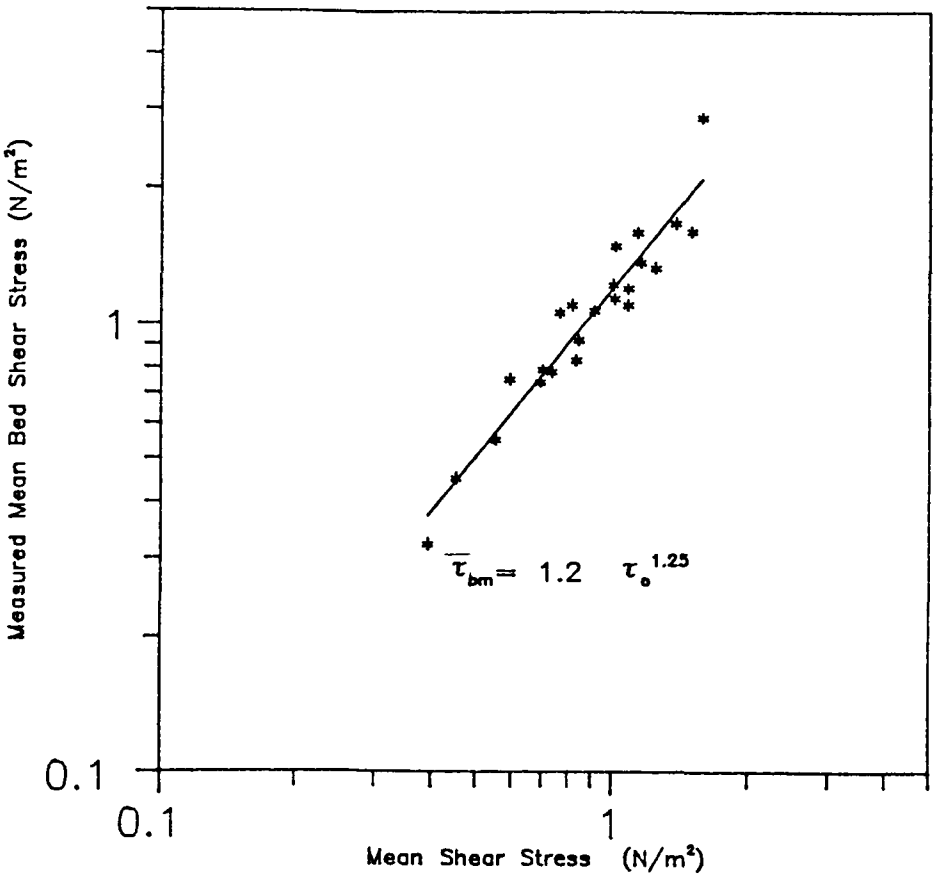

FIGURE 5.22 MEAN SHEAR STRESS VS. MEASURED MEAN BED SHEAR STRESS FOR ALL BEDS

5.5 Turbulence Measurements:

5.5.1 General

Turbulence is one of the important features in the movement of sediment. Turbulence is the irregular motion of flowing fluid that one observes commonly in streams. The turbulent motion results from eddies that are swirling in an irregular manner as they are carried along by the flow. The eddies are formed continuously by the shearing action of the fluid. Sediment transport mechanics is one field in hydraulic engineering where turbulence structure plays the dominant role. The self sustaining turbulent motion strongly influences the rate of removal, deposition and entrainment of

sediment. The frequencies at which particles are removed and deposited are associated with the hydrodynamic lift and drag forces on such particles.

In steady turbulent flow, the velocity fluctuates with time, both in magnitude and in direction. The components of the velocities can be expressed by a time averaged velocity and instantaneous fluctuations as

$$u = \bar{u} + u' \tag{5.23}$$

$$V = \bar{V} + v' \tag{5.24}$$

$$W = \bar{W} + w' \tag{5.25}$$

where $\bar{u}$, $\bar{V}$, $\bar{W}$ are the time averaged values of the u, V, and W components and u′, v′, w′ are the instantaneous fluctuations in the respective directions.

The root mean square $\sqrt{\overline{u'^2}}$ is taken as a measure of the intensity of turbulence.

5.5.2 Brief Review Of Previous Investigations

Richardson and McQuivey (1968) conducted extensive turbulence measurements in water flowing in an open channel with smooth side walls and smooth and rough beds, with only one size roughness. The purpose of their study was to determine the effect of the Reynolds number and boundary roughness on turbulence intensities. They found that the relative turbulence intensity in the direction of flow, $\sqrt{\overline{u'^2}}/V$ with respect to the average gross flow velocity increases with

decreasing relative distance, y/y_o, particularly for a relative distance smaller than 0.1. The same intensity increases with decreasing Reynolds number and vice versa for both smooth and rough boundaries. The bed roughness causes a strong increase of $\sqrt{\overline{u'^2}}/V$ at a particular relative distance.

Blinco and Partheniades (1971), conducted experiments in a wooden rectangular flume with glass side walls. Three types of bed surfacing were used: smooth; moderately rough, made by gluing uniform 0.345 mm sand to 0.32 mm thick plexiglas plates; and very rough, made by gluing 2.45 mm silicon carbide particle to similar plates. They found that there was a clear tendency for the relative intensity to decrease with increasing Reynolds number. The Reynolds number effect was more pronounced near the bed. For relative depths larger than 0.1, the Reynolds number effect appeared to be small. The average turbulence intensity for all runs at $y/y_0=0.1$ was approximately 12% and dropped to about 4% near the free surface. The turbulence intensity was found to be maximum at a relative distance (y/y_o) between 0.36 and 0.4.

Nalluri & Novak (1974), conducted turbulence measurements in a smooth open channel of circular cross section using a hot film anemometer and concluded that the relative turbulence intensities range from about 4% of mean velocities at free water surface to about 10% near the channel bottom. At greater depths the "crowing effect" of the channel cross section causes an appreciable increase of turbulence levels

towards the free surface.

The purpose of the present investigation was to provide detailed measurements, which would increase understanding of the physical process governing the flow in circular channels with flat beds. The experimental equipment and experimental techniques used to obtain the measurements are described in Section 4.4 and Appendix C.

5.5.3 Experimental Results

A total of **11** tests were carried out with the LDA. The mean (u-component only) and fluctuating velocity measurements were made in the flow direction for various uniform open channel flow conditions, and two flat bed thicknesses (t_s- 47mm and t_s-120mm). Several vertical profiles were taken for each test with about 10 to 15 points on each vertical profile depending on flow depth. The spacing of the points ranged 1.0 mm near the bed to about 5.0 t0 10.0 mm through the upper part of the flow.

Measurements of turbulence intensity were classified into two groups according to the bed depths and bed roughness conditions:

group (A) : For flow at up to half-full depths

A-1 Smooth bed (series T_1-T_2)

A-2 Rough bed (series T_3-T_5)

group (B) : For flow at more than half-full depths

B-1 Smooth bed (series T_6-T_9)

B-2 Rough bed (series T_{10}-T_{11})

Table 5.4 shows the flow characteristics from all 11 tests. The turbulence intensity computations are shown in appendix F.

Figures 5.23 through 5.26 show the turbulence intensities, made dimensionless with the local velocity (u), plotted against the relative depth $\frac{y}{y_o}$ in the vertical elevation at different positions across the channel. The plots indicate that turbulence intensity is dependent on measuring position as well as flow depth and bed roughness.

TABLE 5.4 FLOW CHARACTERISTICS OF THE TURBULENCE TESTS

EX. NO.	t_s (mm)	Q (m^3/s)	y_o mm	y_t/D	S	τ_o (N/m^2)	k_s (mm)	R_e	F_r
T1	47	0.0090	55.7	0.336	0.0027	1.08	smooth	97854.9	0.88
T2	47	0.0068	57.2	0.342	0.0015	0.597	smooth	73746.9	0.65
T3	47	0.0067	59.5	0.349	0.0015	0.653	0.80	73397.2	0.59
T4	47	0.0064	60.5	0.352	0.0013	0.554	0.80	69494.7	0.54
T5	47	0.0173	104.7	0.50	0.0016	1.014	0.80	151020.3	0.61
T6	47	0.0181	107.5	0.51	0.0013	0.842	smooth	156004.0	0.62
T7	120	0.0097	66.7	0.61	0.0011	0.500	smooth	75744.4	0.59
T8	47	0.0271	155.1	0.66	0.001	0.756	smooth	199715.7	0.50
T9	120	0.0183	104.4	0.736	0.0011	0.660	smooth	117676.0	0.56
T10	120	0.010	61.5	0.60	0.0032	1.390	1.40	83581.4	0.71
T11	120	0.018	105.9	0.74	0.0027	1.575	1.40	126059.0	0.59

As far as the measuring positions across the channel bottom are concerned, it was found that for shallow flow depths up to one third full (see Figs. 5.23 and 5.24) the maximum turbulence occurred not in the centreline but near to the side wall. The result shows that the turbulence decreases towards the centre line of the channel. The same trend was observed for higher flow depths ($\frac{y_t}{D} \geq 2/3$) (see Figs. 5.27, 5.30 and 5.31). However, for flow at half-full depths maximum turbulence intensities occurred at the centre of the channel (see Figs. 5.25 and 5.26).

In general it was observed that in bed 1 ($t_s/D=0.15$) the turbulence intensities were maximum near the bed and decreased gradually to the water surface, and in bed 3 ($t_s/D=0.39$) (see Figs. 5.28 to 5.31) the turbulence intensities were maximum near the bed and decreased towards the water surface to a relative depth of about 0.8 and thereafter increased gradually to the top of the water surface.

The difference in the distribution of the turbulence intensities near the water surface for the two bed depths could be attributed to the surface-air interface where waves affect the flow and to the effect of secondary currents. In bed 3, the bed depth is about 40% of the channel diameter which means that the flow depth is shallow; therefore the wave fluctuations are more pronounced leading to increased turbulence.

The turbulence quantities are dependent on the bed roughness especially near the channel bed. However, this dependence practically disappears at locations away from the bed. The magnitude of the turbulence intensities on rough beds is found to be higher than those on smooth beds. The same results were observed by Alvarez (1990). The effect of bed roughness seems to be strongest at low flow depth particularly in bed 3 (see Fig. 5.29).

It is clear that the initial movement of sediment particles is a function of the intensity of turbulence and the stability of the grain on the bed. The sediment particles are very sensitive to any increase in turbulence around them. It was observed during the initiation of movement experiments that near to the critical condition, the particles of the first row (upstream row) were rolling but not moving, thus increasing the friction between the particles and further increasing the turbulence levels. For flow at one-third full depth, the weakest area that is subjected to the highest turbulence (usually the first row of particles) began to move from the two sides of the channel bed. That was due to the high turbulence levels which occurred near the side walls. Similar trends were observed at flow of two-third full depths, where the particles which start to move were those away from the centre.

However, different trends were observed for flows at half-full depths, where the turbulence level was found to be maximum in the middle part of the channel bed. The critical conditions seem to reach the sediment particles in the

centre of channel bed earlier than those near the side walls. It was observed in most of the tests that the turbulence intensity increased as the free water surface approached. This tendency, which is clearer at high flow depths, can be attributed to the shape effect (crowning) of the channel and to the effect of secondary currents between the side walls and the free surface.

An attempt has been made to compare the distribution of turbulence intensities for the two beds (1 and 3) at approximately the same degree of filling (y_t/D).

Figure 5.32 shows the turbulence intensities against relative depths at medium flow depths. It was observed that the turbulence intensities at the centre line are higher in bed 3 (b=298 mm) than in bed 1 (b=220 mm) for the same degree of filling. Away from the centre line the results showed no difference. The width of the bed is believed to be responsible for that difference, as the turbulence intensity increases with the increase in bed width. Furthermore, the water depth (y_o) in bed 3 is far less than that in bed 1 and the secondary currents (vortices) are believed to be higher in shallow water as the bottom and free surface vortices are closer to each other than in deep water. It has to be mentioned here that during initiation of motion experiments (see Ch. 6), it was observed that on high water depth (y_o>0.5D) the sediment particles resting at the channel bed needed more shear stress to be eroded than the same particles at low water depth (y_o<0.5D).

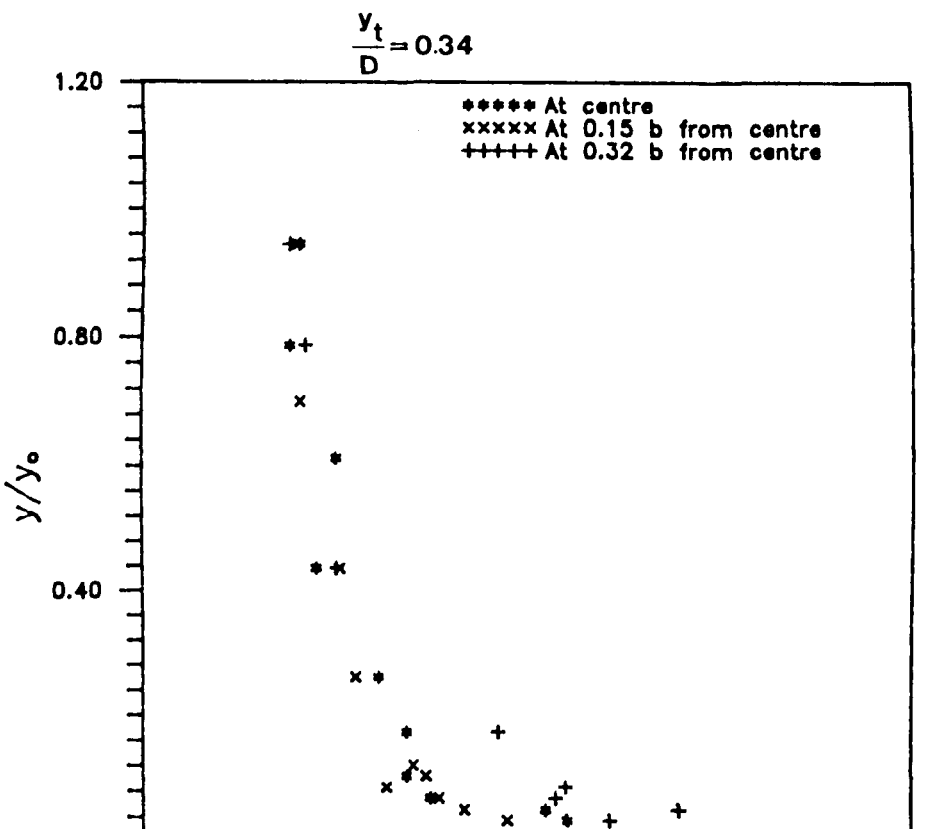

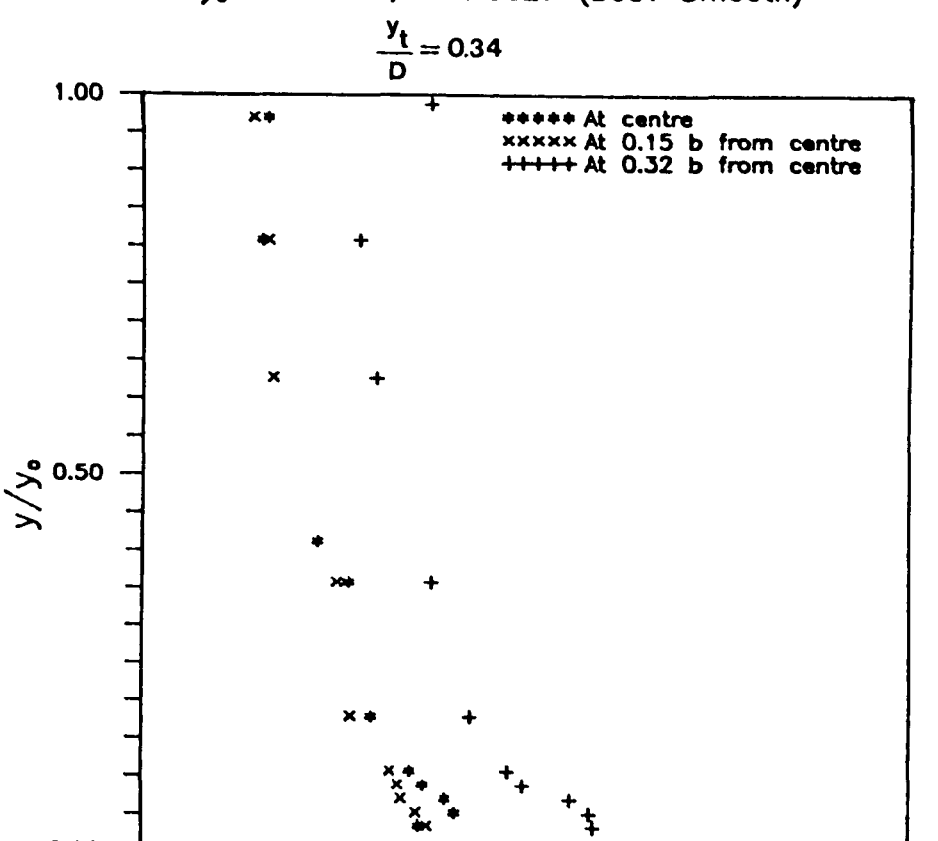

FIGURE 5.23 VARIATION OF RELATIVE TURBULENCE (WITH RESPECT TO LOCAL VELOCITY) WITH RELATIVE DEPTHS. (bed 1; smooth)

141

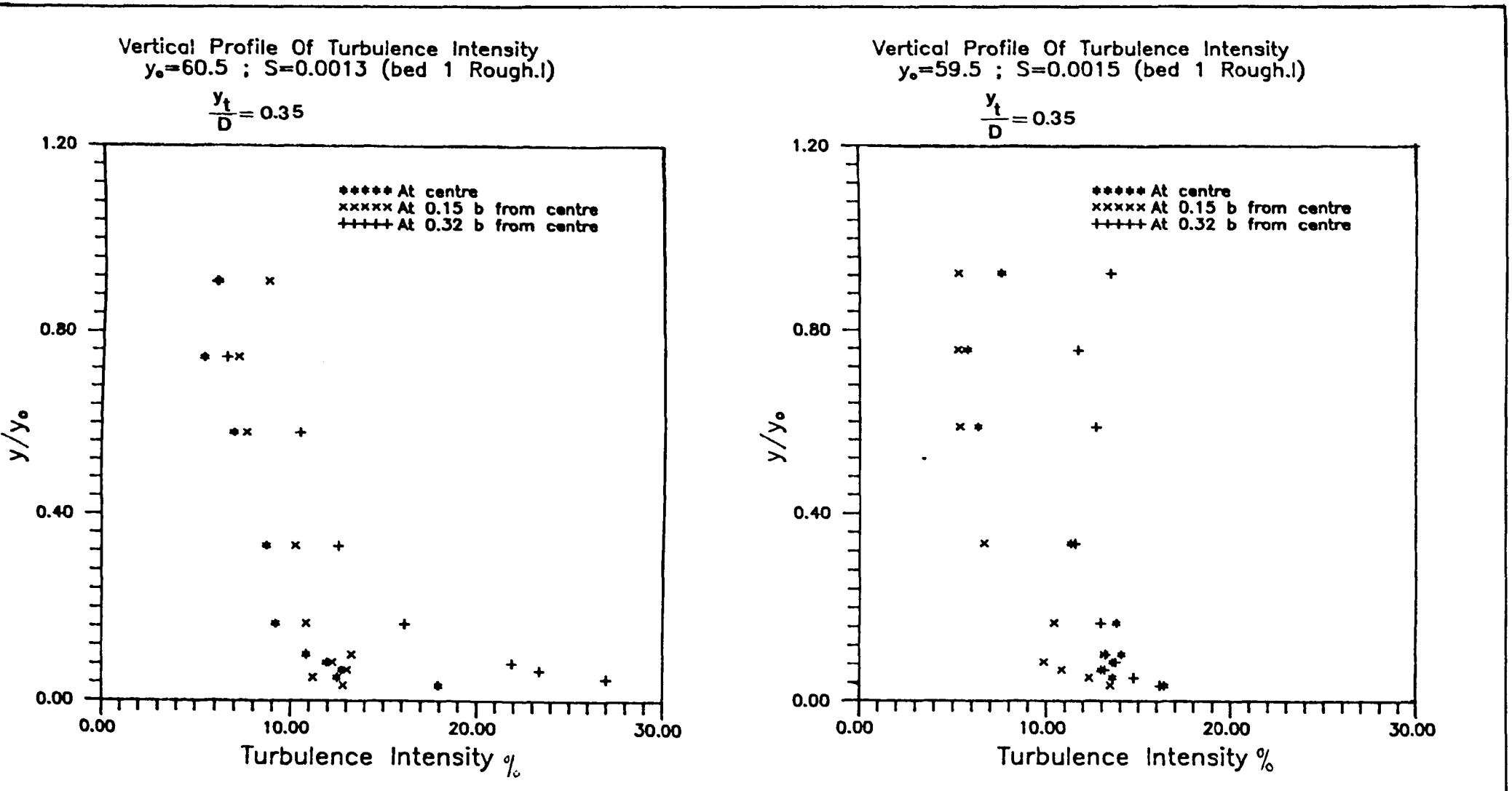

FIGURE 5.24 VARIATION OF RELATIVE TURBULENCE (WITH RESPECT TO LOCAL VELOCITY) WITH RELATIVE DEPTHS. (bed 1; roughness I)

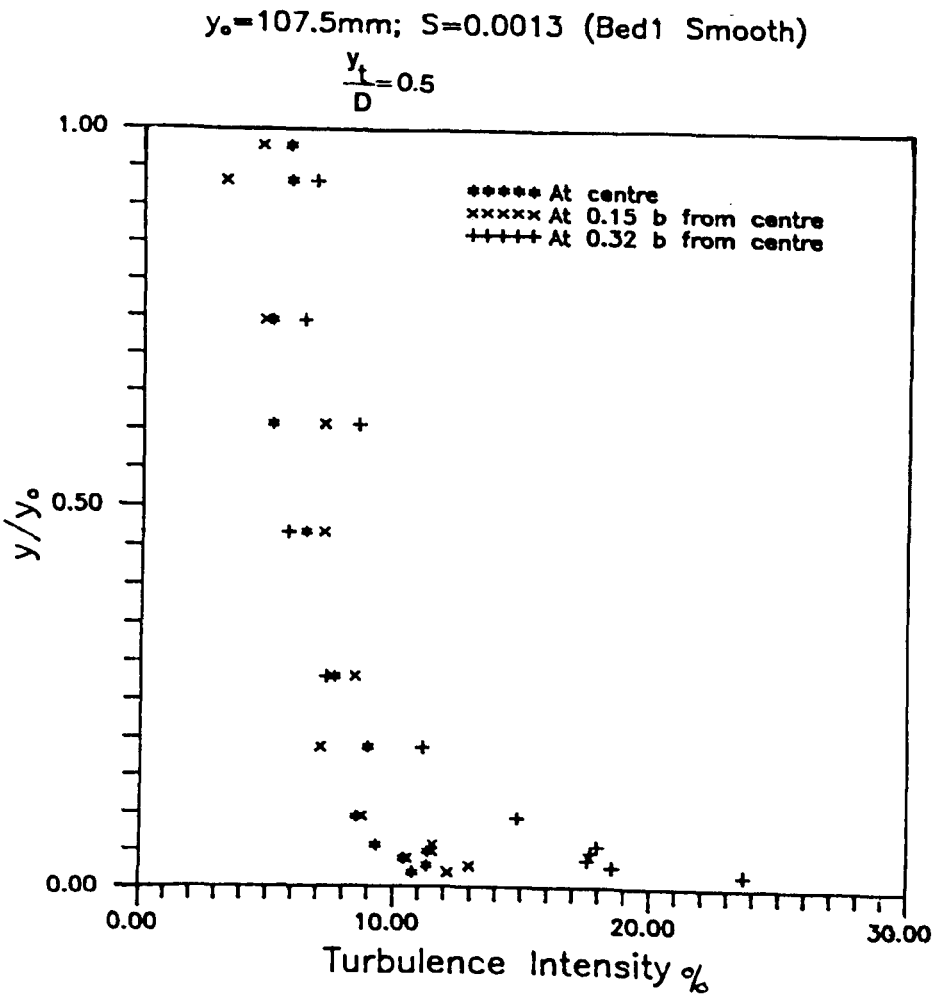

FIGURE 5.25 VARIATION OF RELATIVE TURBULENCE (WITH RESPECT TO LOCAL VELOCITY) WITH RELATIVE DEPTHS. (bed 1; smooth)

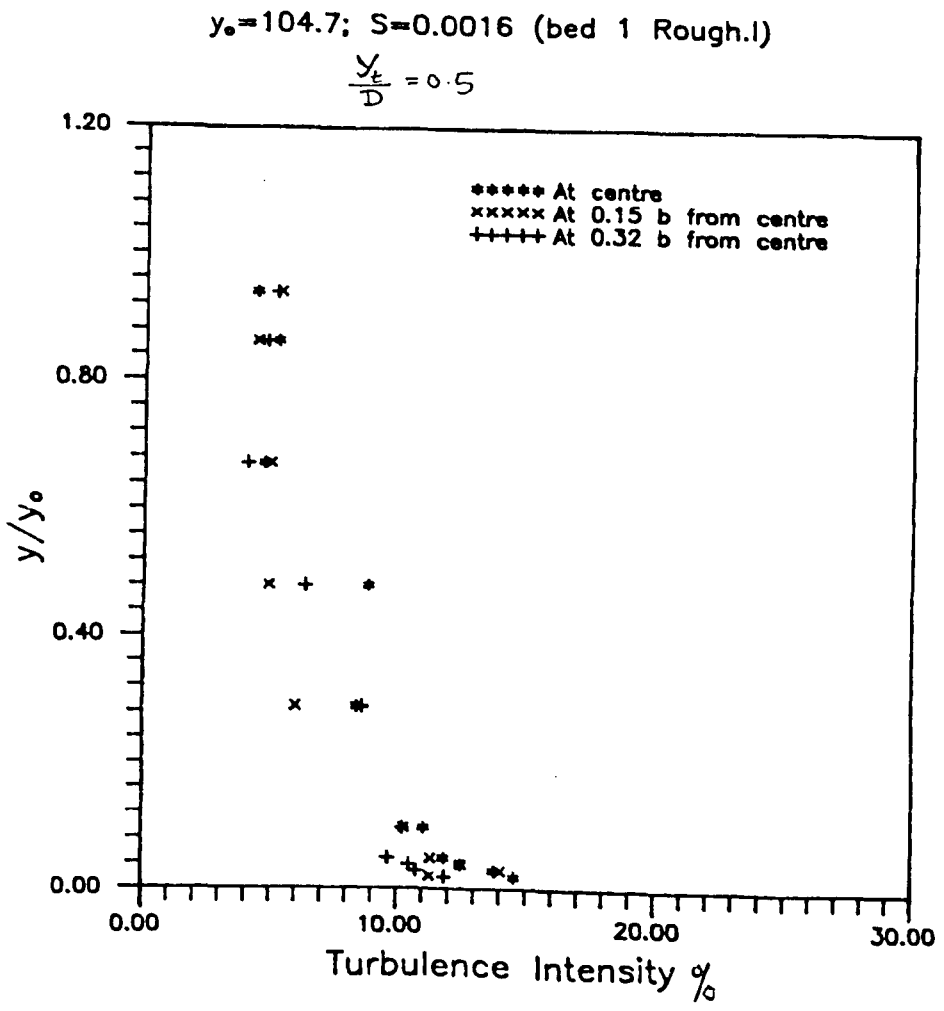

FIGURE 5.26 VARIATION OF RELATIVE TURBULENCE (WITH RESPECT TO LOCAL VELOCITY) WITH RELATIVE DEPTHS. (bed 1; roughness I)

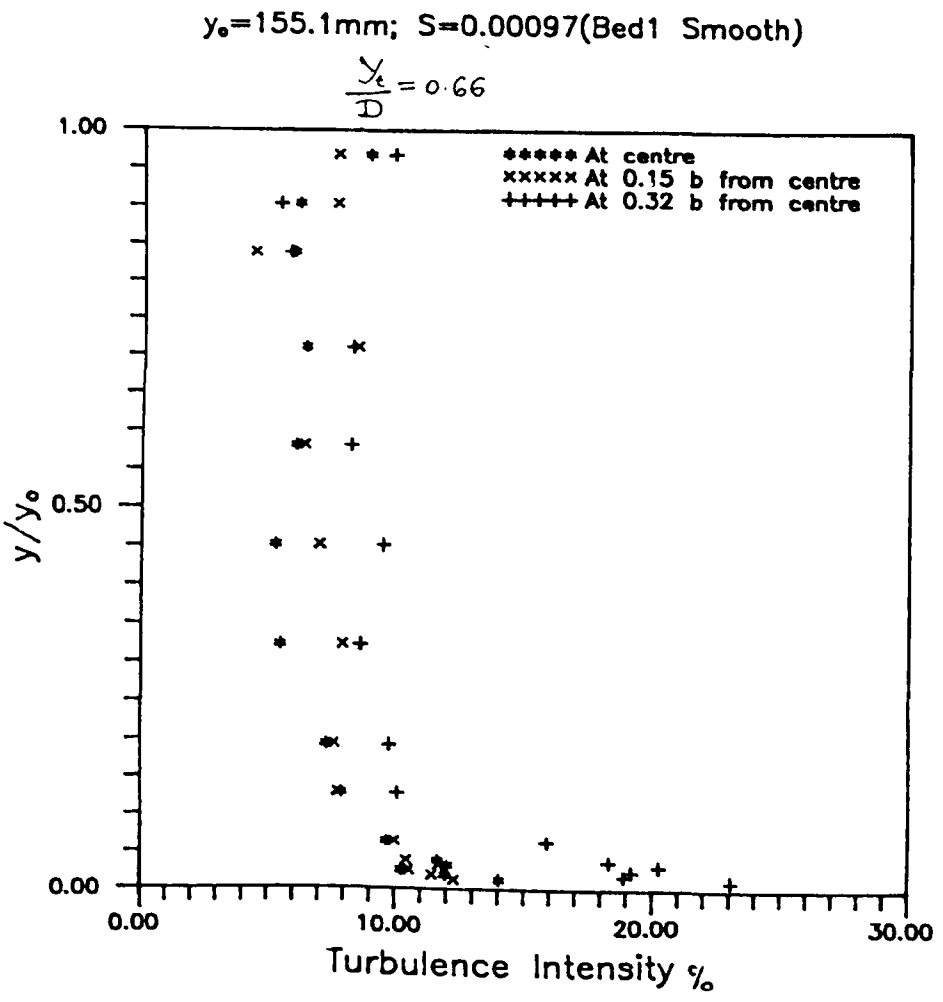

FIGURE 5.27 VARIATION OF RELATIVE TURBULENCE (WITH RESPECT TO LOCAL VELOCITY) WITH RELATIVE DEPTHS. (bed 1; smooth)

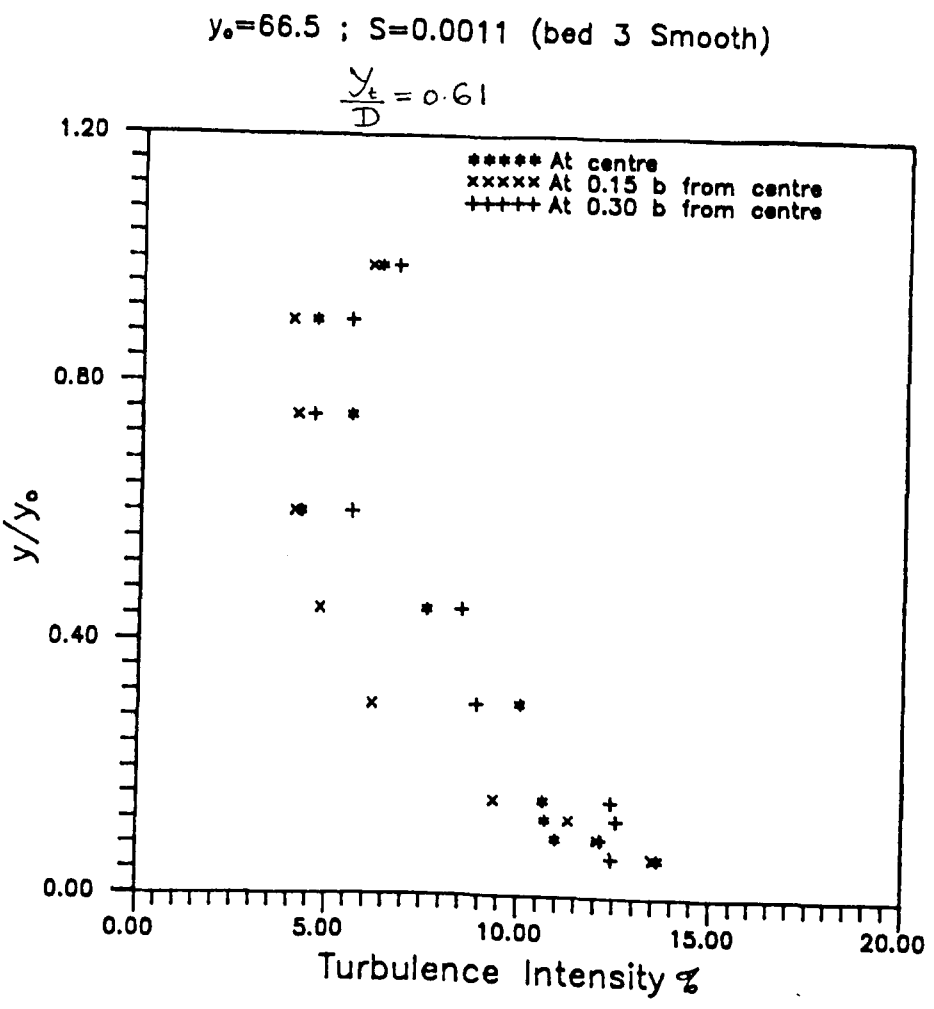

FIGURE 5.28 VARIATION OF RELATIVE TURBULENCE (WITH RESPECT TO LOCAL VELOCITY) WITH RELATIVE DEPTHS. (bed 3; smooth)

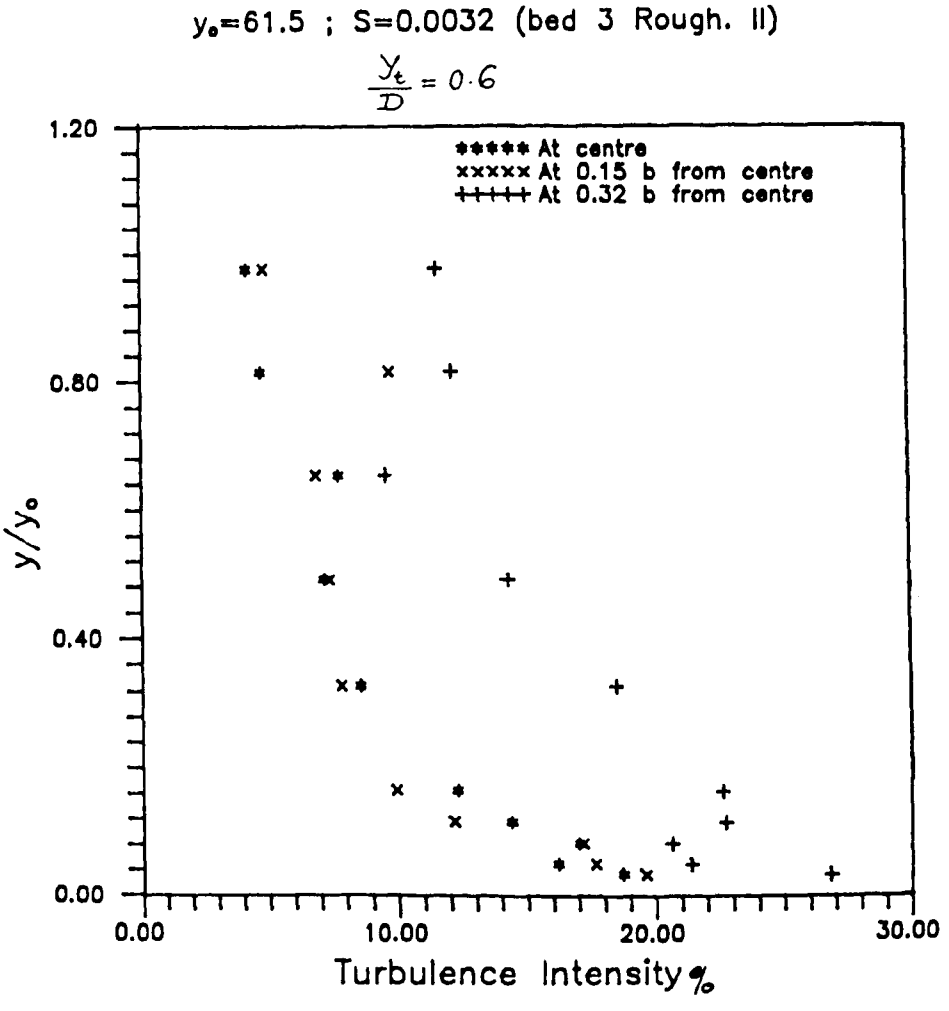

FIGURE 5.29 VARIATION OF RELATIVE TURBULENCE (WITH RESPECT TO LOCAL VELOCITY) WITH RELATIVE DEPTHS. (bed 3; roughness II)

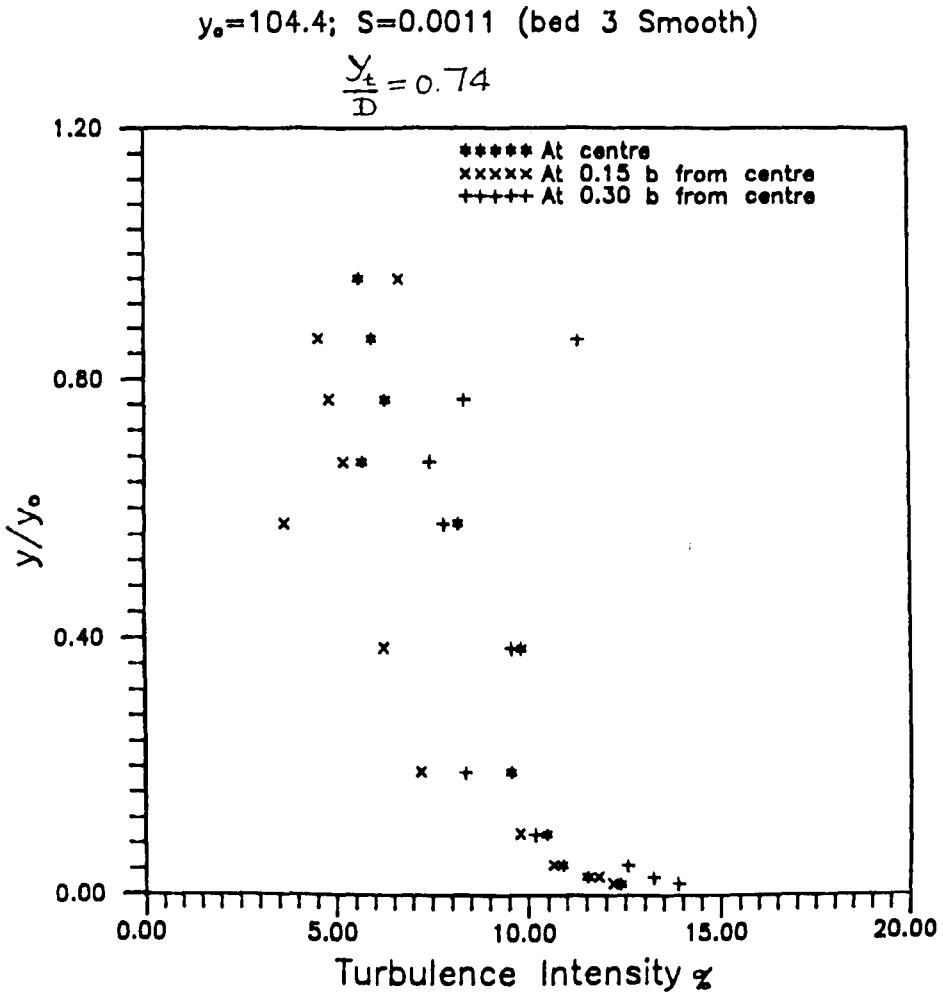

FIGURE 5.30 VARIATION OF RELATIVE TURBULENCE (WITH RESPECT TO LOCAL VELOCITY) WITH RELATIVE DEPTHS. (bed 3; smooth)

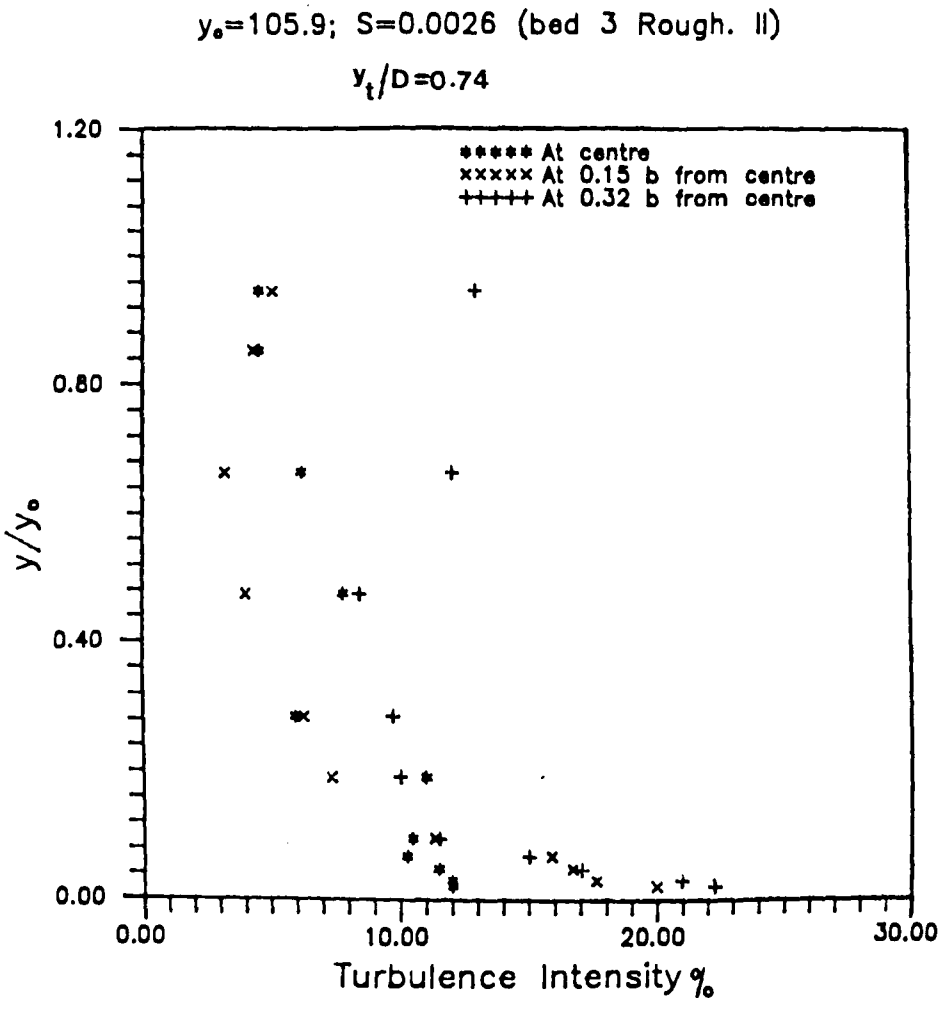

FIGURE 5.31 VARIATION OF RELATIVE TURBULENCE (WITH RESPECT TO LOCAL VELOCITY) WITH RELATIVE DEPTHS. (bed 3; roughness II)

For larger flow depths (see figure 5.33) the turbulence intensities for both beds at the centre line show no significant differences, while near to the side wall the results show that the turbulence intensity for bed 3 (t_s=120 mm) is higher than that of bed 1 (t_s= 47 mm).

Velocities at channel bed are subject to random fluctuations with respect to time. Initial movement will be caused by the occasional peak value of bed shear stress. Further increase in bed shear stress will erode the sediment bed, then the sediment will move as bed load. Turbulence in conjunction with bed shear stress or velocity can affect the sediment movement in the channel bed.

In a flow consisting of a parallel mean motion in the direction of x-axis, where the local mean velocity "u" is a function of distance normal to the wall "y" only, the shear stress is mainly due to velocity fluctuations which transfer the momentum from layer to layer. The magnitude of this shear stress is given by $-\rho\overline{u'v'}$, where u' and v' are the velocity fluctuations superimposed on the mean values in the longitudinal direction and transverse direction respectively. (In this study no attempt was made to measure v' because of the limitation of the equipment).

Due to turbulence characteristics which change according to the flow depth, it was observed that the sediment spread all over the channel bed in such a way that when the flow was at up to half-full depths the sediments appeared to move faster in the middle part of the channel bed (high turbulence

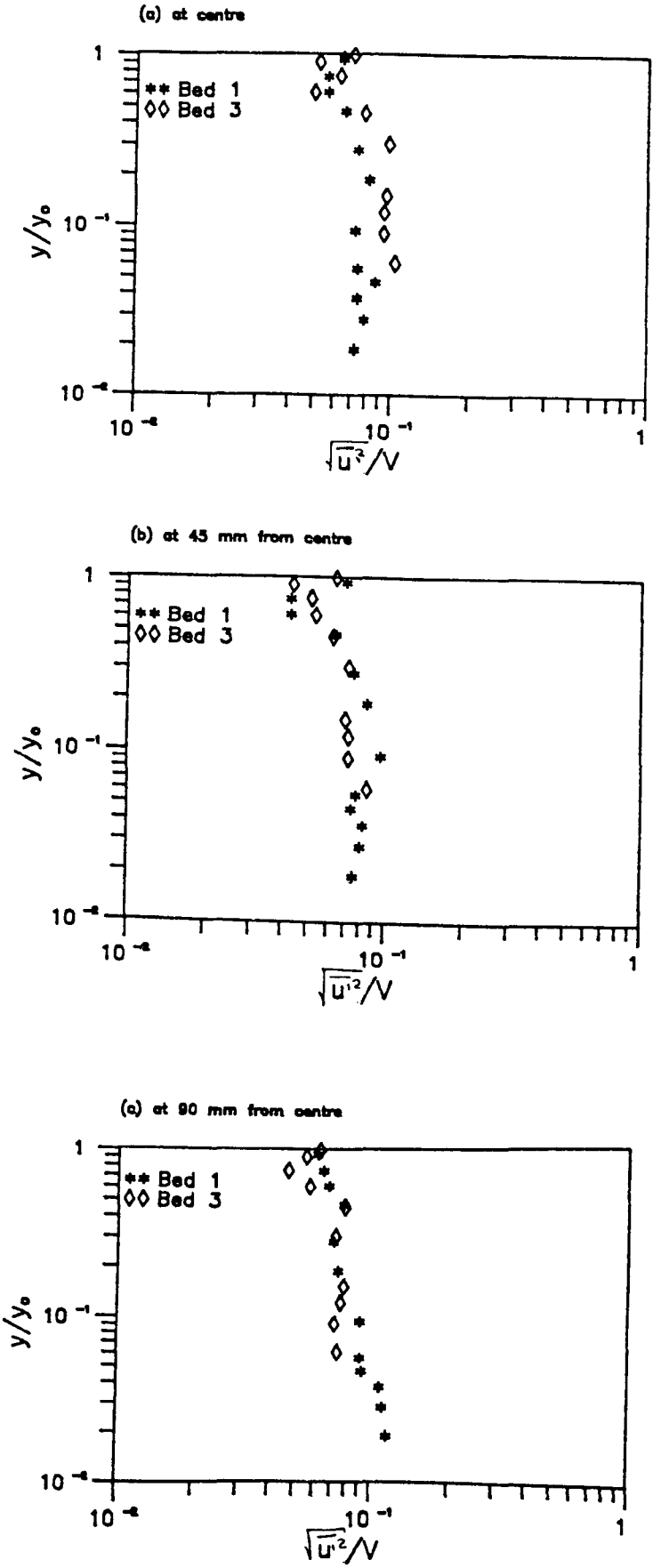

FIGURE 5.32 VARIATION OF RELATIVE TURBULENCE (WITH RESPECT TO MEAN VELOCITY) WITH RELATIVE DEPTHS (smooth beds; $y_t/D \cong 1/2$)

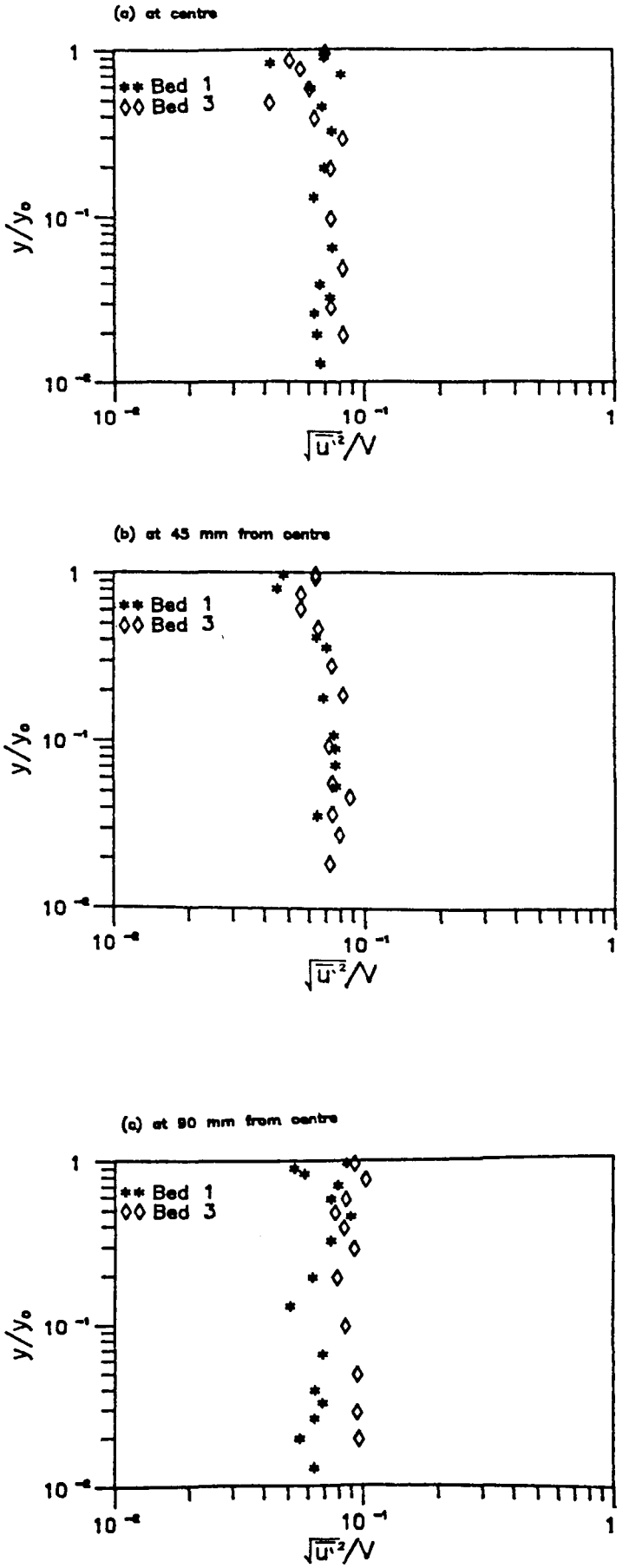

FIGURE 5.33 VARIATION OF RELATIVE TURBULENCE (WITH RESPECT TO MEAN VELOCITY) WITH RELATIVE DEPTHS (smooth beds; $y_t/D \cong 2/3$)

intensity) than those close to the side wall (low turbulence intensity). Therefore, the risk of deposition near side walls at half-full depths is high. At flows up to one-third full and two thirds-full, although the sediment spreads across the channel width, faster movement was observed with those particles close to the side walls than those at the centre of the channel bed.

Although this study led to a deeper understanding of the hydraulic characteristics of circular cross section channels with flat beds, the secondary currents in this type of channel are still far from being well understood. Even though in the present study some attempts have been made to utilize the information already published on secondary currents in rectangular and trapezoidal channels to explain some of the unknown phenomena, comprehensive research of secondary currents in circular cross section channels with flat beds has not been done. There is clearly a great need for further investigation into this phenomena.

In the present study the turbulence intensity measurements were carried out only in the longitudinal direction. It is necessary, in any further study, to measure the turbulence intensity in the transverse direction and to evaluate the shear stress $-\rho\overline{u'v'}$.

CHAPTER 6

INITIATION OF SEDIMENT MOTION

6.1 Introduction

The initiation of motion is a phenomenon that is clearly observable and highly conspicuous since it is characterised by the beginning of movement of bed load particles. In the field of sediment transport the initiation of motion must be regarded as most important.

Under certain conditions the non-cohesive particles covering the bottom of the channel are set into motion. At the moment when movement starts, the forces acting on the bed load particles at rest on the bottom are exactly equal to the resistance of the bed load particles to movement i.e. the particles start to move at the moment when the shear stress has attained the limit value at which the forces acting on the bed load particles are balanced by the resistance of the particles to movement. The boundary condition between movement and no movement is referred to as the critical condition for initiation. The general movement of bed load particles starts as the velocity further increases.

Only a few studies have been attempted (Novak & Nalluri 1975, 1984 and Ojo, 1978) which analyse the incipient motion of touching grouped particles of different sizes on smooth and rough rigid beds in open channels of circular (clean pipe) and rectangular cross section where the roughness is smaller

than the transported sediments. However, the present study of sediment movement in circular cross section channels with flat beds is different from the cases previously studied and it is aiming to investigate the important parameters governing the incipient motion of particles touching each other and resting on a flat bed.

6.2 Theoretical Model of Initiation Of Motion

The major forces which cause a sediment particle to move are drag, F_D, and lift, F_L, while those which counter the movement are submerged particle weight, F_G, and friction, F_R.

Critical conditions for the initiation of particle movement occur when these forces are in balance according to the following equations (see Figure 6.1):

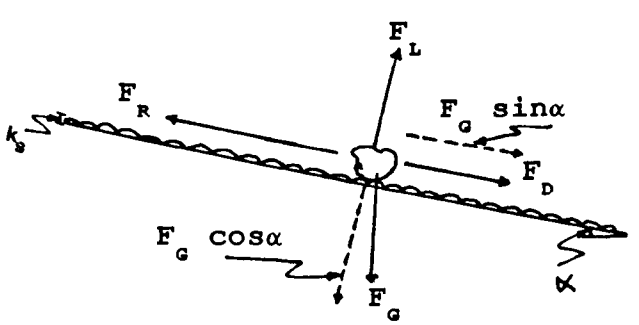

FIGURE 6.1 FORCES ACTING ON A PARTICLE RESTING ON CHANNEL BED

$$F_G \sin\alpha + F_D = F_R \qquad (6.1)$$

$$F_L = F_G \cos \alpha \qquad (6.2)$$

The drag and lift forces exerted on a particle by fluid are:

$$F_D = \frac{1}{2} \rho C_D \beta_1 d^2 (u_b^2) \qquad (6.3)$$

and

$$F_L = \frac{1}{2} \rho C_L \beta_1 d^2 (u_b^2) \qquad (6.4)$$

where $\beta_1 d^2$ is the cross sectional area of the particle (β_1 is the shape factor for a cross sectional area of sediment and is equal to $\pi/4$ for spherical particles), and C_D and C_L are the drag and lift coefficients; u_b represents the bottom velocity (velocity at the top of the particles, to which the upper portion of a particle is exposed and which is primarily responsible for the drag and lift forces exerted) in turbulent flows with solid-liquid mixtures and can be expressed as:

$$u_b = u_* f \text{ (fall velocity, hydraulic conditions, channel shape)} \qquad (6.5)$$

Where the fall velocity of particles (in turbulent flow) is a function of R_{*} (Reynolds' number of the particle), hydraulic conditions can be defined by the parameter d_{50}/k_s and the channel shape can be represented by the parameter y_o/b. Thus Eq. 6.5 can be written as:

$$u_b = u_* f \left(\frac{u_* d_{50}}{\upsilon}, \frac{d_{50}}{k_s}, \frac{y_o}{b}\right) \qquad (6.6)$$

The frictional force, resulting from friction between the bed and the particles can be expressed as

$$F_R = c\ (\rho_s - \rho)\ g\ \beta_2 d^3 \qquad (6.7)$$

where c is the friction coefficient (= $\tan\phi$, ϕ being friction angle between the channel surface and the grain) and β_2 is the shape factor for sediment particle volume.

The submerged weight force (gravitational force) is given by

$$F_G = (\rho_s - \rho)\ g\ \beta_2 d^3 \qquad (6.8)$$

For small channel slope ($\tan\alpha$), $\sin\alpha$ will be very small and approach zero and $\cos\alpha$ will approach unity. Incorporating equations 6.3 to 6.8 into equation 6.1 and 6.2 gives:

$$(u_b^2) = 2(S_s - 1)\ g\ (\beta_2/\beta_1)(c/C_D)d \qquad (6.9)$$

$$(u_b^2) = 2(S_s - 1)\ g\ (\beta_2/\beta_1)(1/C_L)d \qquad (6.10)$$

The phenomenon of lift on bed particles is not well understood and insufficient experimental data is available to formulate reliable numerical relationships between the drag and lift forces. Therefore, in this analysis the lift force will be ignored.

Bagnold (1966) stated that the friction angle (ϕ) for most

sands is approximately 33°, for which $\tan\phi = 0.65$.

The drag coefficient C_D is a function of the particle Reynolds' number and of a particle shape factor. For turbulent flow, the fall velocity (W_o) is expected to be a function of the friction velocity (u_*) thus C_D can be written as:

$$C_D = f\left\{\frac{u_* d_{50}}{\upsilon}, \text{ particle shape factor}\right\} \qquad (6.11)$$

Combining equations 6.6, 6.9 and 6.11 gives

$$\frac{u_{*c}^2}{(s_s-1)gd_{50}} = f\left[R_{*}, \frac{d_{50}}{k_s}, \frac{y_o}{b}\right] \qquad (6.12)$$

or

$$\frac{\tau_c}{(\rho_s-\rho)gd_{50}} = f\left[R_{*}, \frac{d_{50}}{k_s}, \frac{y_o}{b}\right] \qquad (6.13)$$

The dimensionless variables are:

i) **Dimensionless shear stress** ($\frac{\tau_c}{(\rho_s-\rho)gd_{50}}$), which describes the effect of shear stress on the initiation of sediment motion,

ii) **Shear Reynolds' number** ($R_{*} = \frac{u_{*c} d_{50}}{\upsilon}$) which describes the effect of bed sediments and viscosity,

iii) **Roughness to particle size ratio** (d_{50}/k_s), reflects the effect of roughness which has a more definite effect on the initiation of sediment motion and

iv) **flow depth to bed width ratio** (y_o/b) which is

incorporated in the equation to show the influence of the channel shape,

where τ_c is the critical shear stress at the point of initiation of motion, y_o is the normal flow depth, d_{50} is the median particle size, ρ_s is the sediment density, ρ is the water density and R_{*} is the shear Reynolds' number.

6.3 Experimental Work

Eighty four tests were carried out in the flume of a circular cross section (D=305 mm) with three different flat smooth and rough beds (bed 1, bed2 and bed 3).

These tests were intended only as a measure of the threshold conditions of particles laid over the whole width of the channel perpendicular to flow direction. The number of touching particle rows in this study was equal to 15 (see figure 6.2). The study was carried out using uniformly graded particles for a range of particle sizes ($2.9 < d_{50}(mm) < 8.4$) with $0.0 < k_s(mm) < 1.40$.

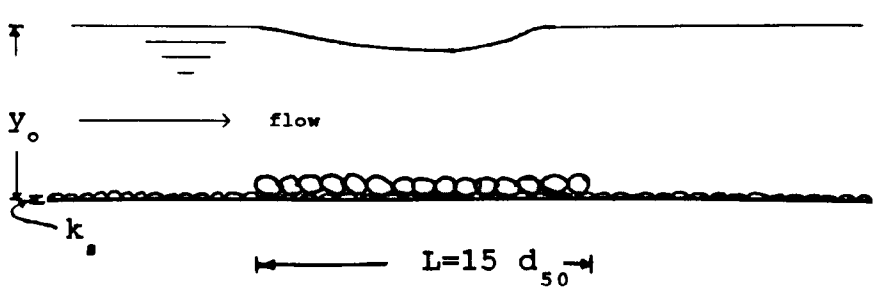

FIGURE 6.2 TYPICAL CONFIGURATION OF TOUCHING PARTICLES FOR INITIATION STUDIES.

6.4 Experimental Procedures

After introducing a flow of about twice the particle size in depth into the flume, the particles were gently placed on the bed, either by hand or by a thin forceps, touching one another side by side. The water discharge was then slightly increased, while making sure that depths upstream and downstream of the test section were maintained at nearly equal levels by adjusting the slope and downstream gates. This procedure of increasing the discharge slightly and adjusting the slope, tailgate positions and equalising the depths was repeated until some of the particles (two at least) moved.

As soon as movement was noticed, readings of flow depths, discharge, channel slope and water temperature were taken. Total energy lines were used when necessary, in calculating shear stresses (see Sec. 4.3.2) which would take into account any slight non-uniformity of the flow.

6.5 Mode Of Movement Of Particles

During the experiments, various modes of particle movement (at the threshold of motion) were observed very closely and accurately. It was observed that there was no dominant mode of movement: for round ones, the particles start to roll on the spot and then jump and then roll again and move over the adjacent particles while for flat ones, particles start to jump then move by sliding over the adjacent particles.

The same modes of movement were observed in both smooth and rough beds. The shape profile of the side of the particle in contact with the bed at times of critical conditions determined the mode of movement.

It was also observed that, in most of the tests, the movement of a particle took place in the front (upstream) rows of particles.

6.6 Experimental Results And Analysis

The experimental results of the initiation studies are shown in Tables 6.1 to 6.9. Bearing in mind the hydraulic factors of flowing water, a wide variety of methods may be adopted for describing the critical condition. Attempts have been made to relate the critical condition to depths, velocities and channel slopes and even to water discharges. Several investigators have introduced logically the product of slope and depth, i.e. the shear stress as a measure of the critical condition. It should be noticed that the critical condition is controlled not only by the properties of bed load material and by the hydraulic factors of flow, but also by the characteristics of the channel, such as the width (b) as well as roughness (k_s). The most familiar approach to the prediction of the critical conditions for bed load movement in wide alluvial channels, is the Shields (1936) equation. In figure 6.3 the present experimental results for the three different roughnesses (k_s= 0.00mm, 0.80mm and 1.40mm) are compared with the Shields curve for alluvial channels. Also

shown in the figure are results of Novak & Nalluri (1984) of grouped touching particles on smooth beds of rectangular channel. The results of the present study over smooth beds were seen to be well below Shields' curve and even below Novak & Nalluri's rectangular channel results. The definition of critical conditions adopted by Novak & Nalluri is the same as the one adopted in this study; so the reason why the results of the smooth beds study were below that for rectangular channels could be high turbulence intensities in circular cross section channel with flat beds.

It is also seen from Figure 6.3 that $\tau_c/(\rho g d_{50}(S_s-1))$ decreases as $(u_* d_{50}/\upsilon)$ increases. This trend was observed for the different roughnesses employed in this study. It is also noticed that for a given particle diameter, the shear stress required to dislodge the particles is higher on rough beds than on smooth beds.

The critical shear stress for incipient motion can be expressed for the different beds by the following equation

$$\frac{\tau_c}{\rho g d_{50}(S_s-1)} = a\left[\frac{d_{50}\,u_*}{\upsilon}\right]^b \qquad (6.14)$$

where a and b are constants and a function of bed conditions, as summarised in Table 6.10.

The differences in the values of the constants are primarily due to the differences in flow resistance for each bed roughness.

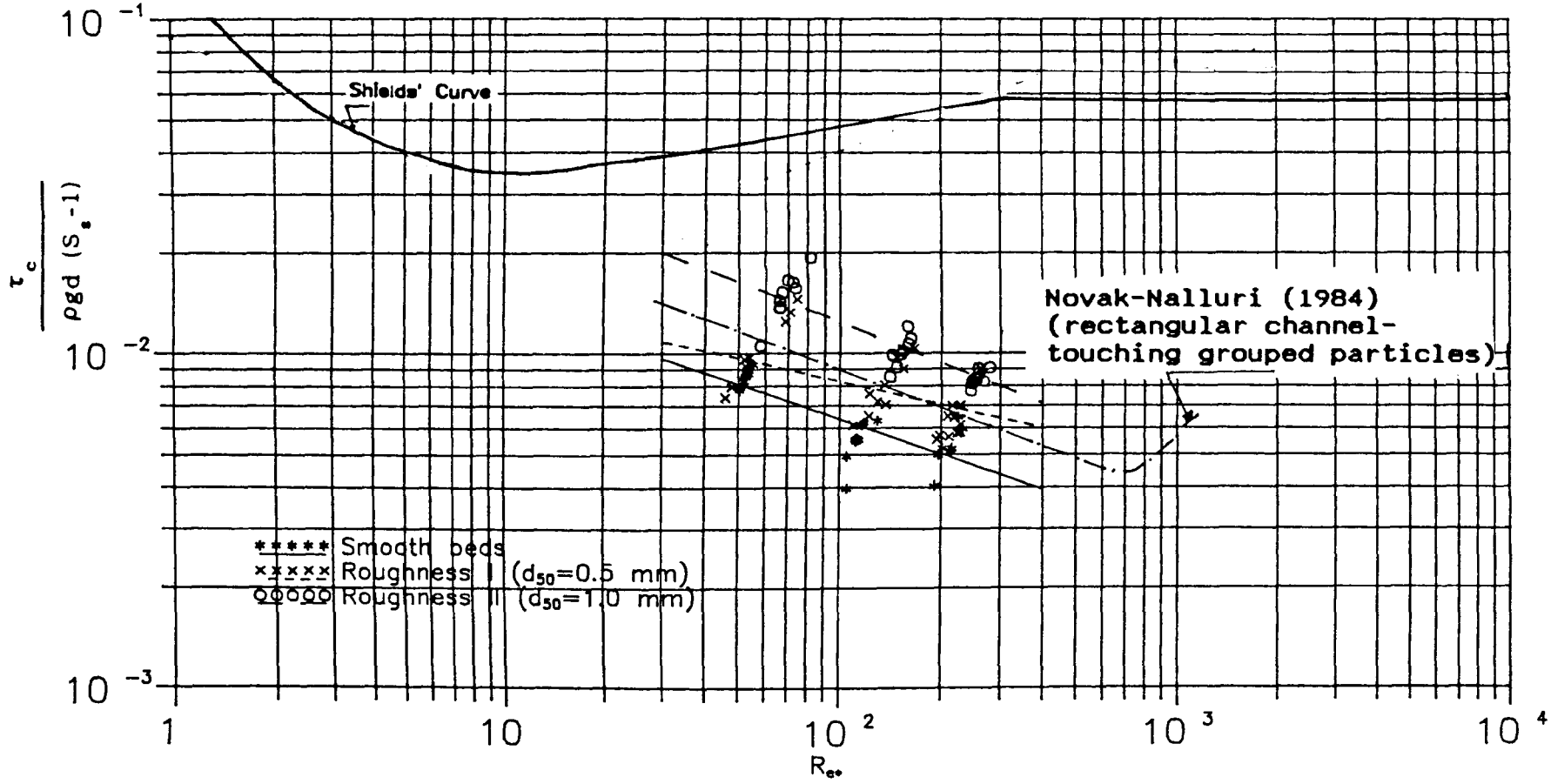

FIGURE 6.3 COMPARISON BETWEEN THE PRESENT STUDY AND NOVAK & NALLURI'S (1984) DATA FOR SMOOTH RECTANGULAR CHANNEL

The roughness (k_s) depends on the nature of the bed material, its grading and properties (particularly shape) and on the spatial variation of these in the channel, and also on the flow depth and velocity which determine the nature of the bed features for a given bed material. The changes in roughness due to the presence of sediment bed features can be substantial.

Fig. 6.4 shows the effect of the ratio of equivalent bed roughness and sand particle (k_s/d_{50}) on the entrainment. The figure shows that the critical shear stress increases with increasing ratio of k_s/d_{50}.

The critical values for large roughness ratio (k_s/d_{50}=0.48) (Fig. 6.4) showed a tendency towards Shields' curve. This can be explained by the fact that the bed roughness was found to affect the critical conditions as more energy had to be used to overcome the higher frictional resistance, apart from the increase in turbulence intensities, which also dissipate more energy.

The results suggest that for channels of circular cross section with fixed sediment bed critical conditions occur at lower values of bed critical shear stress (τ_{bc}) than those of Shields for wide channels. It has to be recalled here that in the present study the particles forming the fixed bed roughness are smaller in size than the transported particles studied ($0.0 < k_s/d_{50} < 0.48$), whereas in Shields' experiments, both were of the same size ($k_s/d = 1.0$).

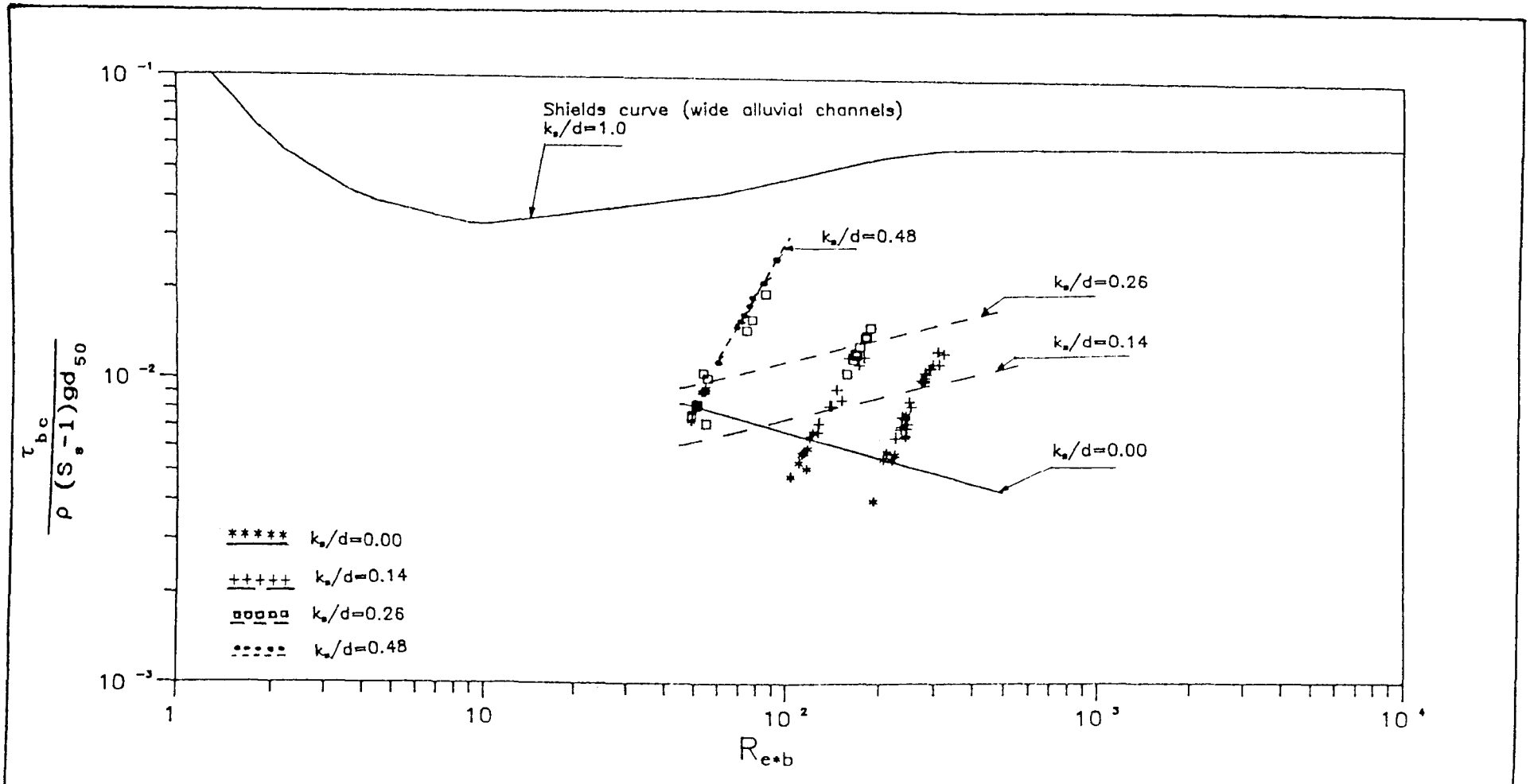

FIGURE 6.4 COMPARISON BETWEEN THE PRESENT DATA (presented in terms of k_s/d) AND SHIELDS CURVE FOR WIDE ALLUVIAL CHANNELS

To study the influence of the flow depths on the critical conditions of the initiation of motion, figure 6.5 shows the comparison between Shields curve and the present study for flows up to half-full and more than half-full depths. In the same figure the results of Novak & Nalluri (1984) for rectangular channels are also shown. It can be seen from the figure that the difference between the two sets of data is not obvious, therefore more experiments are needed to come to any conclusion on the effect of flow depths in the critical conditions.

Fig. 6.5 shows also that the present data of circular cross section channels with flat (smooth and rough) beds are scattering around the line (though most of the data are above the line) represented Novak & Nalluri's (1984) experimental work in smooth rectangular channels. This indicates that when sediment beds in circular channels become fixed then the channel will behave similarly to that of rectangular cross section channels.

An attempt was made to compare the present results with those of Alvarez (1990) for circular channels with loose flat beds ($k_s/d=1$) The results suggest that the critical conditions for touching grouped particles ($n_r=15$) on a circular channel with rigid beds are slightly lower than those for circular channels with loose beds (see figure 6.6). These results agreed well with expectation since in channels with loose

beds particles touch one another, forming layers of sediments over the full channel bed, so there would be greater friction between them which would bind the particles together. Hence a higher value of shear stress or velocity will be required to dislodge the particles and move them in loose beds than in fixed ones.

Equation 6.13 which was derived in section 6.2 describes the initiation of motion of sediment particles theoretically with respect to the shear stress parameter and most of the hydraulic parameters that influence the hydrodynamic movement of the particles.

A multiple correlation analysis was performed on the data of rough beds, and the initiation of motion functional relationship was found to be best described by:

$$\frac{\tau_{bc}}{\rho\,(S_s-1)gd_{50}} = 0.039\,(R_{*b*})^{-0.19}\left[\frac{k_{sb}}{d_{50}}\right]^{0.28} \qquad (6.15)$$

for flows up to half full depths (r=0.85) and,

$$\frac{\tau_{bc}}{\rho\,(S_s-1)gd_{50}} = 0.034\,(R_{*b*})^{-0.19}\left[\frac{k_{sb}}{d_{50}}\right]^{0.19} \qquad (6.16)$$

for flows at more than half-full depths (r=0.8)

where τ_{bc} is the critical bed shear stress, ρ is the density of the water, S_s is the relative density of the sediments, g is the acceleration due to gravity, d_{50} is the median

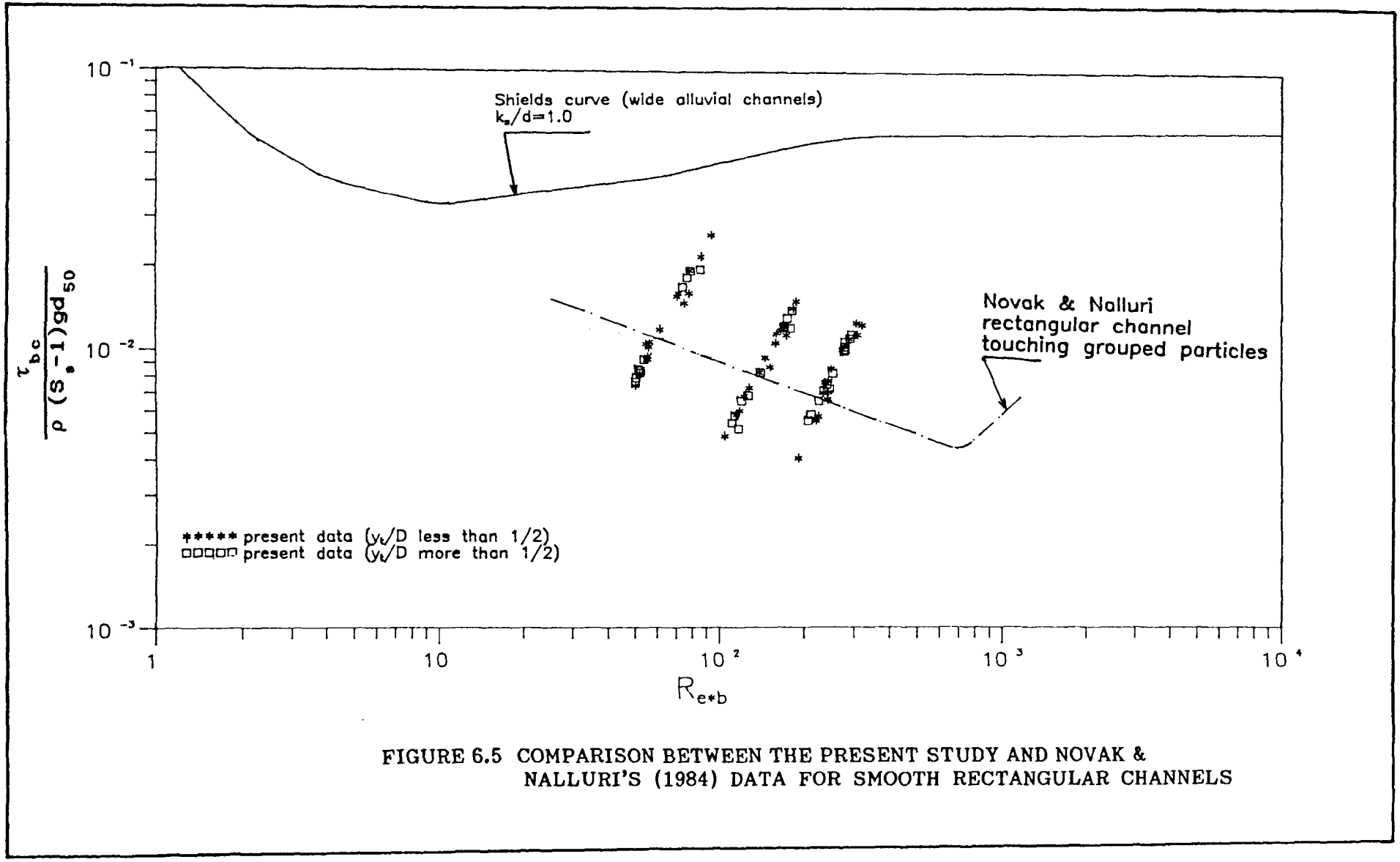

FIGURE 6.5 COMPARISON BETWEEN THE PRESENT STUDY AND NOVAK & NALLURI'S (1984) DATA FOR SMOOTH RECTANGULAR CHANNELS

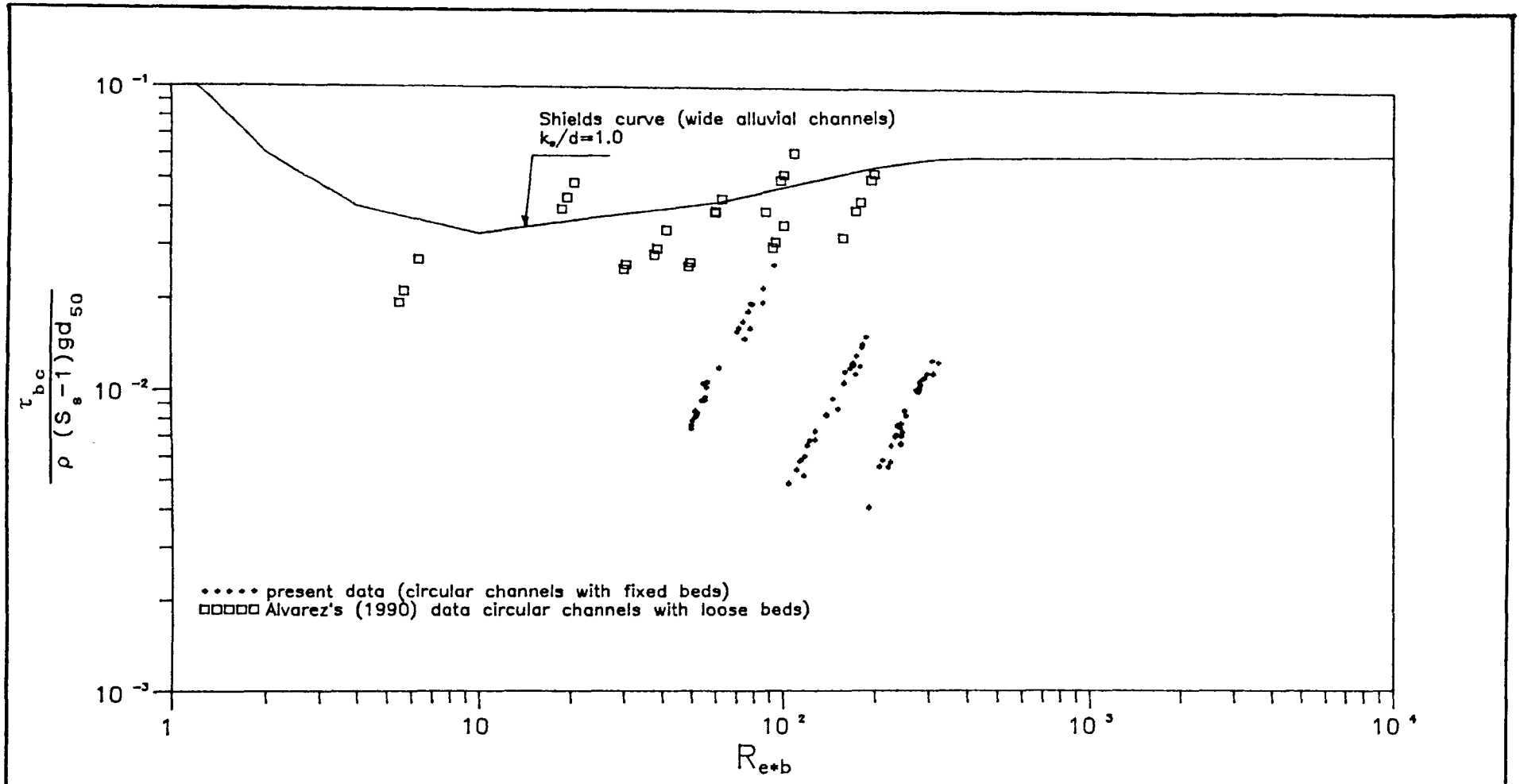

FIGURE 6.6 COMPARISON BETWEEN THE PRESENT STUDY WITH ALVAREZ'S (1990) DATA FOR CIRCULAR CHANNEL WITH LOOSE FLAT BEDS

particle size, k_{sb} is equivalent bed roughness, R_{*b*} $\left[= \frac{u_{b*} d_{50}}{\upsilon}\right]$ is the shear Reynolds' number (it reflects the influence of viscosity), and u_* being the shear velocity.

In order to consider the effects of channel shape the parameter $(\frac{y_o}{b})$ is incorporated in the analysis and the data of rough beds fitted the following equation (see Fig. 6.7):

$$\frac{\tau_{bc}}{\rho\,(S_s-1)gd_{50}} = 0.083\ (R_{*b*})^{-0.28}\left[\frac{k_{sb}}{d_{50}}\right]^{0.24}\left[\frac{y_o}{b}\right]^{0.25} \qquad (6.17)$$

which shows a better correlation (r=0.85), and does represent the data better (see Fig. 6.7). Equations 6.15 to 6.17 were derived from experiments in a circular cross section channel with rough beds only.

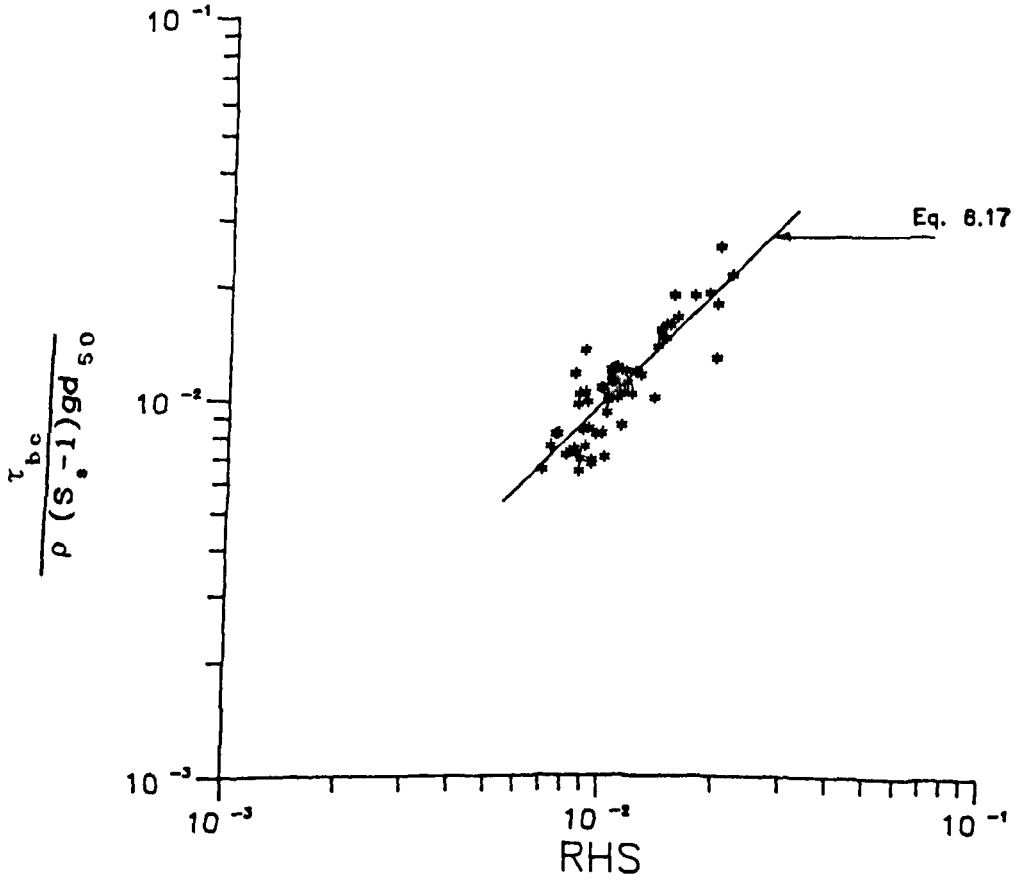

FIGURE 6.7 INITATION OF SEDIMENT MOTION
Multible regression of entrainment function

To develop a universal equation for smooth and rough beds data, the parameter (k_{sb}/d_{50}), in Eq. 6.17,was replaced by the bed friction factor (λ_b) (to avoid the negative values of k_s in smooth beds) and the entrainment function was found to be best described (see Fig 6.8) by:

$$\frac{\tau_{bc}}{\rho\,(S_s-1)gd_{50}} = 5.37\quad (R_{eb*})^{-0.44}\quad (\lambda_b)^{1.0}\left[\frac{y_o}{b}\right]^{0.51} \tag{6.18}$$

for all flow ranges (smooth and rough beds), with r=0.89.

From equations 6.17 and 6.18, it is clear that the bed shear stress required to move the sediment particles increases with the particle size, flow depth and bed roughness and decreases with bed width (i.e. bed thickness). However, the sediment bed width will start decreasing after the sediment bed level exceeds half full pipe. As the experiments covered sediment bed thickness only up to 40%, it can be speculated that a different trend may occur for sediment bed levels above half full pipe (t_s/D >50%).

At the threshold conditions experimental observations showed that at flows of one third and two thirds full depths the sediment particles moved from both sides of the channel width, while for flows at half-full depth the particles moved from the centre line of the channel bed (see Sec. 5.4.3).

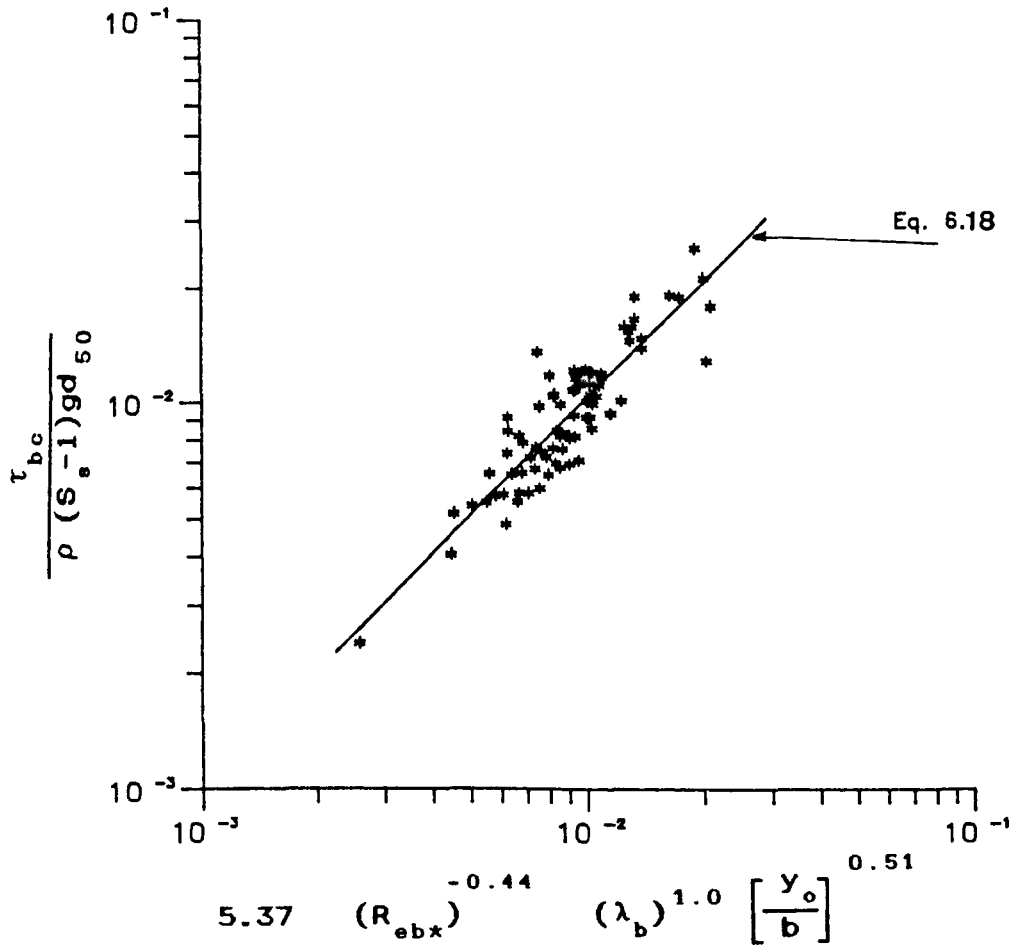

FIGURE 6.8 INITIATION OF SEDIMENT MOTION
multiple regression of entrainment function

Another approach in analysing the data is by using the critical velocity approach.

The following dimensional analysis is based on the system of Yalin (1965), except that mean velocity is used instead of shear velocity. It was found that the critical mean velocity required for particle movement is a function of particle diameter (d_{50}), hydraulic radius (R), water density (ρ), sediment density (ρ_s), and acceleration due to gravity (g). Therefore the function can be written as:

$$V_c = f\ (d_{50},\ R,\ \rho,\ \rho_s,\ g) \qquad (6.19)$$

By dimensional analysis equation 6.19 simplifies to:

$$\frac{V_c}{\sqrt{g d_{50}(S_s-1)}} = f\left[\frac{d_{50}}{R}\right] \qquad (6.20)$$

The functional relationship 6.20 was also used by Novak & Nalluri (1984).

Experimental data was separated into two groups according to whether they were obtained at flows below or above half-full depths.

For flows up to half-full depths the critical velocity parameter was found to be best described by

$$\frac{V_c}{\sqrt{g d_{50}(S_s-1)}} = 0.74\left[\frac{d_{50}}{R}\right]^{-0.339} \qquad (6.21)$$

with r= 0.92, and for flows at more than half full depths

$$\frac{V_c}{\sqrt{g d_{50}(S_s-1)}} = 0.752\left[\frac{d_{50}}{R}\right]^{-0.33} \qquad (6.22)$$

with r=0.82.

The equations indicate that the critical velocity decreases with the particle size and increases with the hydraulic radius of the channel. The differences between equations

6.21 and 6.22 (though very small) reflect the probable shape effects of the circular cross section channel at different degrees of filling.

The whole experimental data of the three different beds were combined to produce universal equation. Figure 6.9, shows the results for the three bed thicknesses and for all roughnesses, from which the following empirical relationship was obtained:

$$\frac{V_c}{\sqrt{g d_{50}(S_s-1)}} = 0.747 \left[\frac{d_{50}}{R}\right]^{-0.336} \qquad (6.23)$$

with r=0.87

By using separated bed hydraulic radius (R_b), Eq. 6.23 becomes

$$\frac{V_c}{\sqrt{g d_{50}(S_s-1)}} = 0.76 \left[\frac{d_{50}}{R_b}\right]^{-0.31} \qquad (6.24)$$

with r=0.82.

where V_c is the critical mean velocity, S_s is the relative density of sediments, g is the acceleration due to the gravity, d_{50} is the median particle size, R is the hydraulic radius and R_b is the separated bed hydraulic radius.

In Fig. 6.9, the resultant line (Eq. 2.23.3) for touching grouped particles on smooth and rough rectangular channel

beds according to Novak & Nalluri (1984) is also shown. It is easily seen that the rectangular channels equation lies below the present study which indicates that in general the critical velocity required to move the 10 rows of touching particles on smooth and rough rectangular channel beds is less than that for 15 rows of touching particles in a circular channel with smooth and rough flat bed. The difference could be attributed to the high resistance to flow as the number of rows increase. As the number of rows decreases, strong irregularities in the water surface become obvious. These irregularities increase the acceleration above the particles and force early motion.

Alvarez's (1990) experimental results in a circular channel with loose beds are also compared with the present study (figure 6.9). It is clear that Alvarez's data fall just above the line represented by equation 6.23 but far above the line represented by equation 2.23.3 (according to Novak & Nalluri, 1984) for a rectangular channel. Shields' curve (Eq. 2.6) for wide alluvial channels is also shown in the figure.

From Fig. 6.9 the following points can be deduced:

1- The higher the number of rows of touching grouped particles, the greater is the possibility that the initiation of motion follows the same trend as that of loose beds especially at low values of d/R, as part of the flow energy is spent in overcoming the friction between the sediment

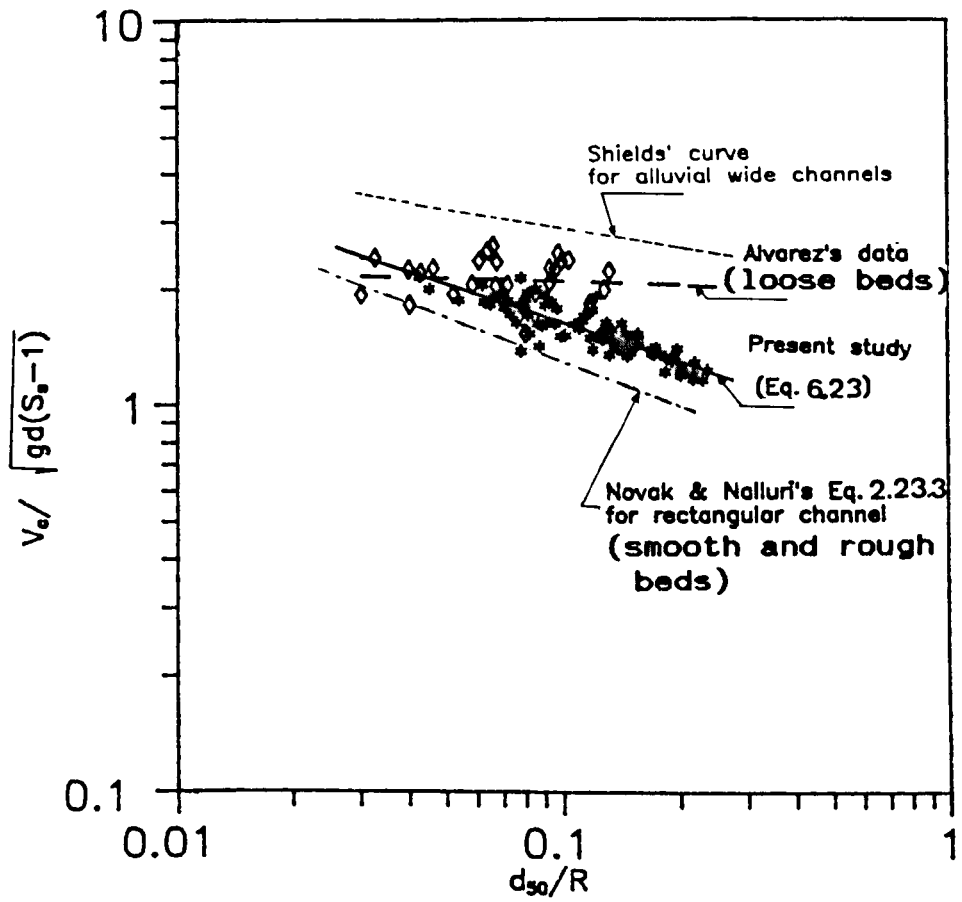

FIGURE 6.9 PLOT REPRESENTING THE PRESENT EQUATION 6.23 WITH NOVAK-NALLURI EQ. 2.23.3 AND ALVAREZ'S (1990) DATA

particles. The consumed energy is increased with increasing number of rows.

2- The critical velocity decreases as the particle diameter decreases. This fact was also noticed by Ojo (1978) and by Novak & Nalluri (1984), and can be seen clearly from the almost identical slope of equations 6.23 and 2.23.3 which indicates a similarity in the behaviour of the particles filling only a small part of the channel bed.

3- Alvarez's (1990) data suggests that the sediment size has

no significant effect on the critical velocity. This could be explained by the complex nature of the initiation of motion in loose beds and to the way the critical conditions in loose beds are determined, which is by extrapolating the bed load transport to the time when bed load ceases or to the lower limit of volumetric sediment concentration (C_v) i.e, $1X10^{-6}$. The extrapolation method of determining the critical conditions is highly questionable.

No attempt was made (in this study) to develop equations for the incipient motion condition by extrapolating the bed load transport to lower values ($C_v = 1x10^{-6}$), as experimental work with these extremely low concentrations is not only very difficult but also unreliable. Moreover, at very low sediment concentration the movement of the particles is similar to the situation of initiation of motion of isolated rather than touching particles.

The influence of the channel shape on critical conditions can be investigated by incorporating the parameter $\frac{y_o}{b}$ (where y_o is the normal flow depth and b is the bed width) in equation 6.20. Regression analysis was made and the best fit equation obtained can be expressed as (see Fig. 6.10):

$$\frac{V_c}{\sqrt{gd_{50}(S_s-1)}} = 0.80 \left[\frac{d_{50}}{R}\right]^{-0.328} \left[\frac{y_o}{b}\right]^{0.04} \qquad (6.25)$$

with r=0.88, and for separated hydraulic radius (R_b) the

following equation was obtained

$$\frac{V_c}{\sqrt{g d_{50}(S_s-1)}} = 0.79 \left[\frac{d_{50}}{R_b}\right]^{-0.306} \left[\frac{y_o}{b}\right]^{0.02} \qquad (6.26)$$

with r=0.81.

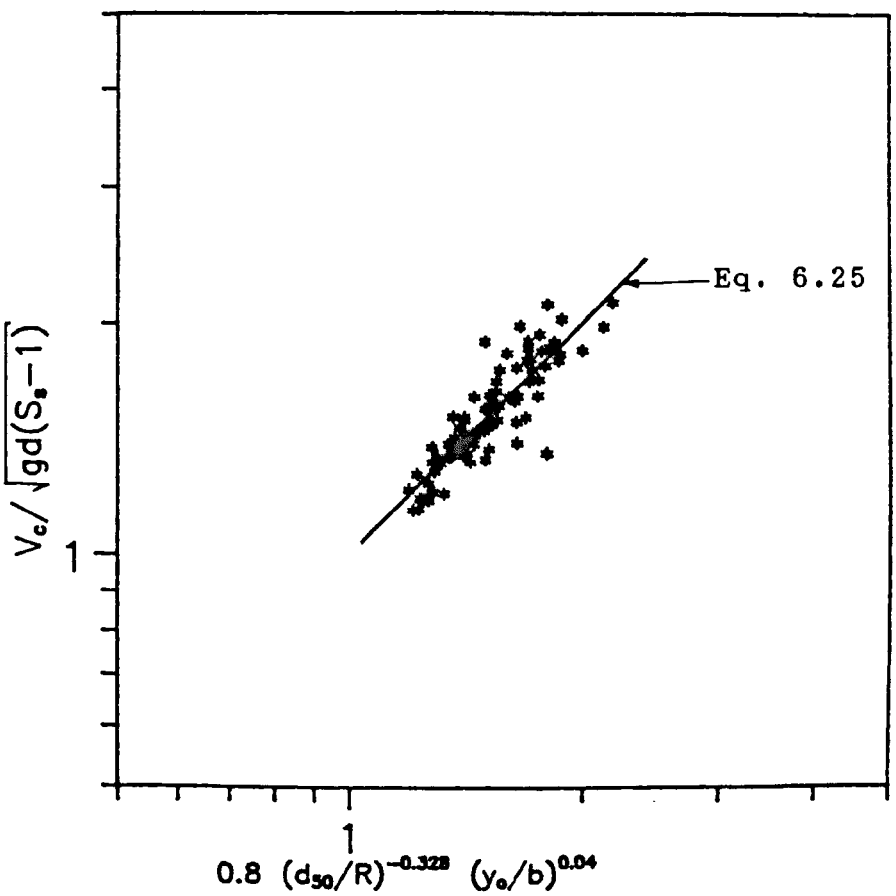

FIGURE 6.10 PLOT REPRESENTING THE PRESENT EQUATION 6.25 WITH COMBINED DATA FOR THE THREE BEDS

Equations 6.25 and 6.26 are valid for sand sizes $2.9 < d_{50(mm)} < 8.4$, sediment density $2.6 < S_s < 2.61$, bed thickness ratios $0.15 < t_s/D < 0.4$, and equivalent sand roughness $0.0 < k_{s(mm)} < 1.40$.

To demonstrate the influence of the degree of filling in the initial movement of the particles the experimental results were separated into two groups.

For a degree of filling up to half-full depth the following equation was obtained (see Figure 6.11).

$$\frac{V_c}{\sqrt{g d_{50}(S_s-1)}} = 0.78 \left[\frac{d_{50}}{R}\right]^{-0.337} \left[\frac{y_o}{b}\right]^{0.036} \qquad (6.27)$$

with r=0.92.

For a degree of filling to more than half-full depth the following equation was found to be the best fit (see Fig. 6.12):

$$\frac{V_c}{\sqrt{g d_{50}(S_s-1)}} = 0.83 \left[\frac{d_{50}}{R}\right]^{-0.32} \left[\frac{y_o}{b}\right]^{0.046} \qquad (6.28)$$

with r=0.83.

The above equations indicate the strong dependency of the critical conditions on d_{50}/R. The results also show that the critical velocity decreases as the bed width (or deposited bed thickness) increases, although this increase is not very pronounced.

In equations 6.25 to 6.28, the parameter y_o/b shows a weak dependence, due to the fact that the parameter d/R is in itself representing the shape effect of the channel and the hydraulic radius (R) incorporates the flow depth as well as the bed width.

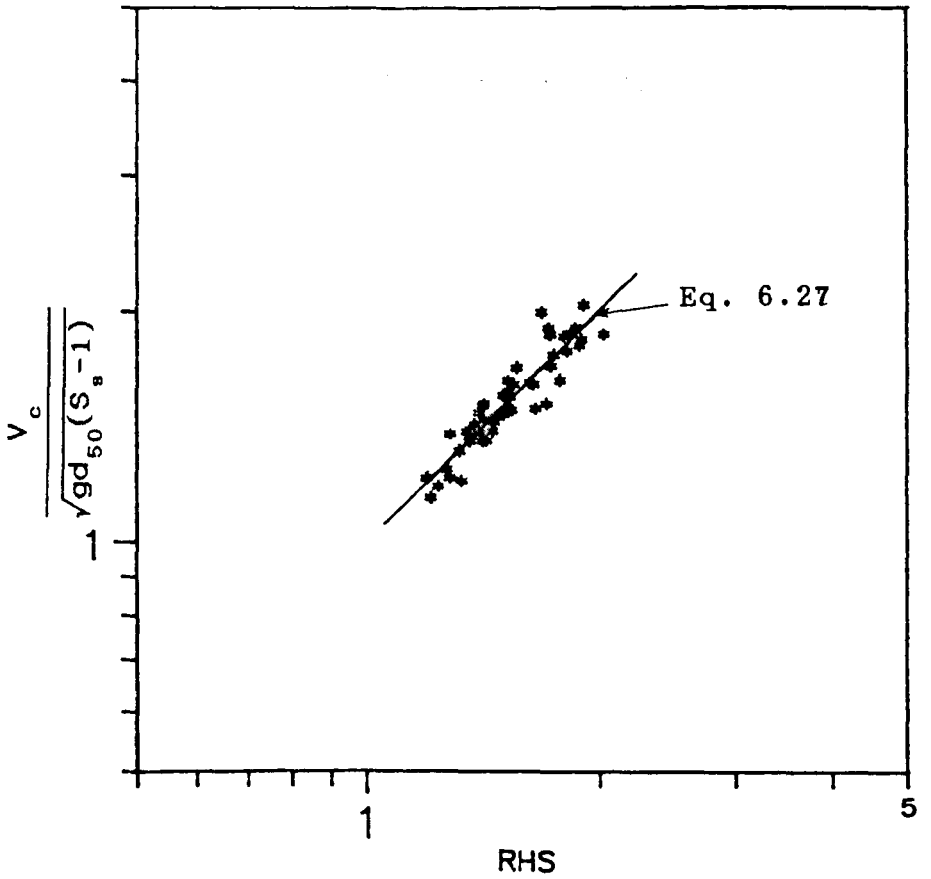

FIGURE 6.11 PLOT REPRESENTING THE PRESENT EQUATION 6.27 FOR FLOWS UP TO HALF-FULL.

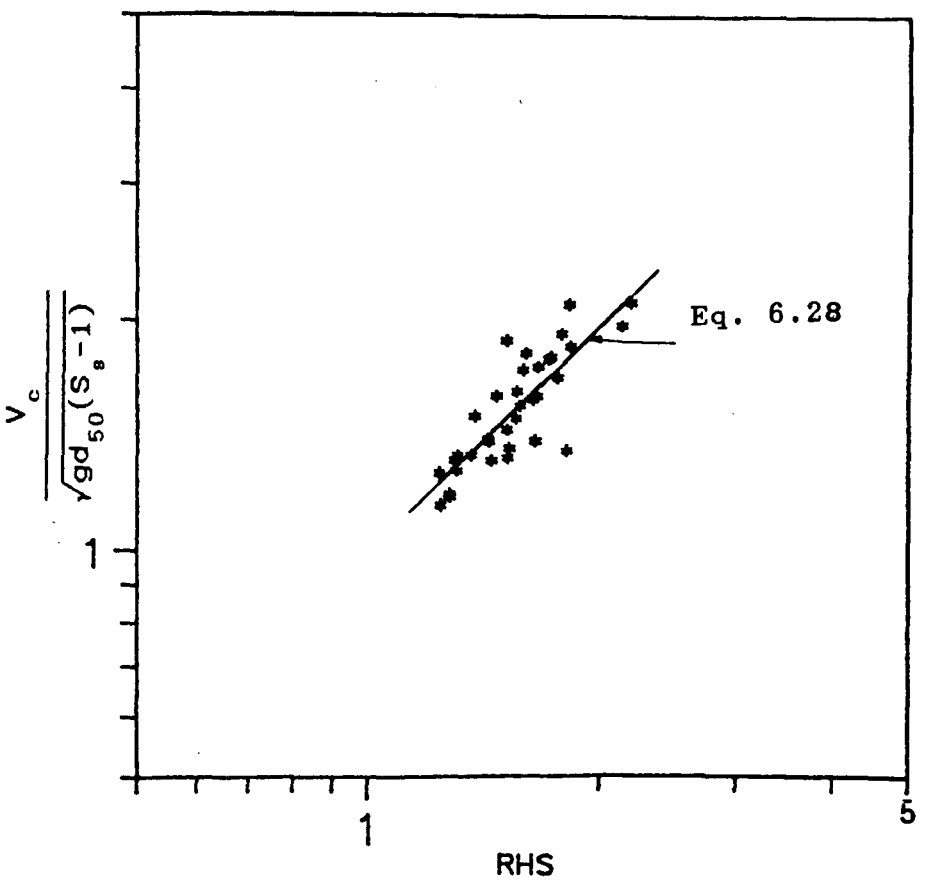

FIGURE 6.12 PLOT REPRESENTING THE PRESENT EQUATION 6.28 FOR FLOWS MORE THAN HALF-FULL.

An attempt was made to reanalyse Alvarez's (1990) data using the same parameters as in equation 6.25; the best fit equation found to describe the initiation of motion of loose beds in circular channel (D=154 mm) is (see figure 6.13):

$$\frac{V_c}{\sqrt{g d_{50}(S_s-1)}} = 2.12 \left[\frac{d_{50}}{R}\right]^{-0.053} \left[\frac{y_o}{b}\right]^{0.168} \qquad (6.29)$$

with r=0.83.

Equation 6.29 is valid for sand sizes $0.5 < d_{50\,(mm)} < 4.1$, relative density $2.48 < S_s < 2.61$, and sediment bed thickness of 0.12 D (where D is the pipe diameter)

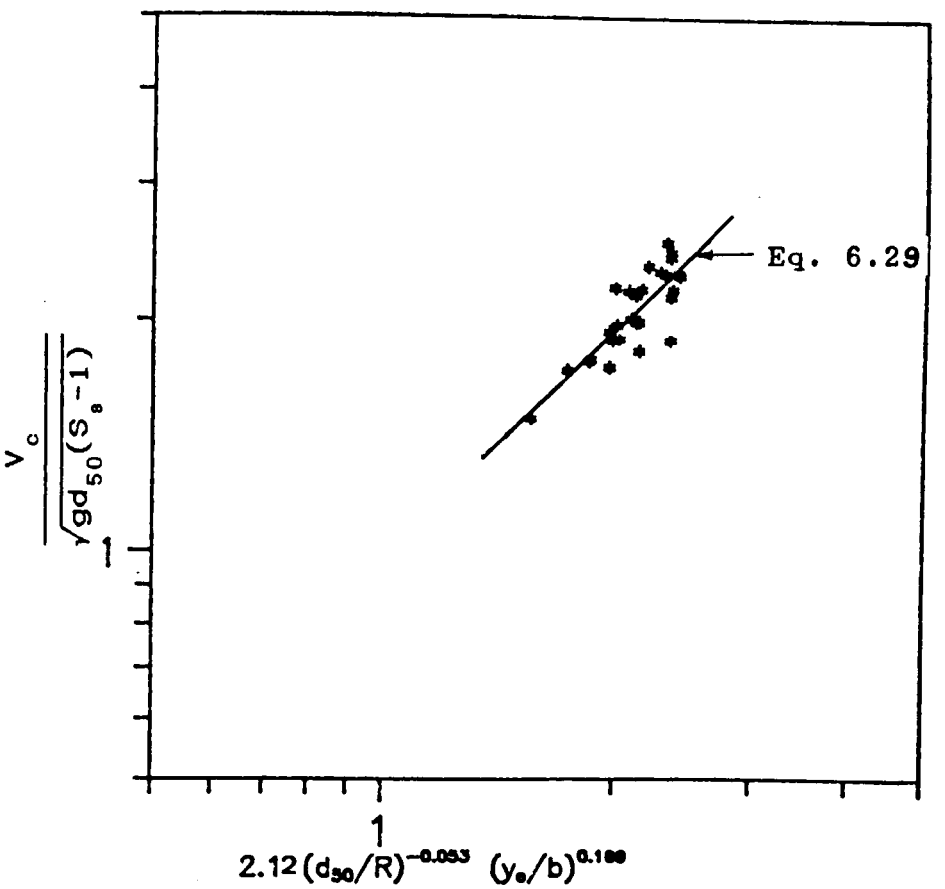

FIGURE 6.13 COMPARISON BETWEEN EQUATION 6.29 AND ALVAREZ'S (1990) DATA FOR CIRCULAR CHANNEL WITH LOOSE FLAT BEDS

6.7 Conclusions

From the foregoing analysis it can be concluded that:

1- In a situation where particles are touching, there would be greater friction between them, which tends to bind the particles together. Hence a higher value of shear stress or velocity will be required to dislodge the larger particles, and move them, than for small particles.

2- From the figure (6.3), it is easily seen that when the bed roughness increases, the functions defined by F_d^2- f (R_{e*}) plots move farther away from smooth fixed bed results towards the Shields' curve for movable beds. Thus, the results show that critical shear stress increases as the particle diameter and roughness increase, as more energy has to be used to overcome the higher friction between the particle and the bed roughness.

3- The more the number of touching particle rows, the greater the shear stress required to move the particles which can be attributed to the increase in flow resistance. Therefore, the equation due to Novak and Nalluri (Eq. 2.23.3) predicts smaller velocities than the measured ones.

TABLE 6.1 INITIATION OF MOTION EXPERIMENTAL DATA
IN CIRCULAR CHANNEL (D=305 mm) WITH FLAT BED 1 (ts=47 mm)
SMOOTH BED

Ex. No.	Q m^3/s	y_o mm	S	A m^2	R m	V_e m/s
1	0.0070	62.17	0.0011	0.0163	0.0447	0.431
2	0.0051	50.00	0.0013	0.0128	0.0377	0.398
3	0.0156	99.50	0.0014	0.0275	0.0624	0.565
4	0.0032	38.02	0.0012	0.0095	0.0302	0.343
5	0.0042	46.32	0.0011	0.0118	0.0355	0.360
6	0.0045	50.36	0.0010	0.0129	0.0380	0.345
7	0.0062	61.70	0.0009	0.0162	0.0444	0.384
8	0.0062	56.43	0.0011	0.0147	0.0415	0.423
9	0.0055	50.64	0.0014	0.0130	0.0381	0.426

τ_c N/m^2	d_{50} mm	S_s	$1/\psi$	R_{e*}	$V_c/\sqrt{g d_{50}(Ss-1)}$	d_{50}/R
0.476	5.70	2.56	0.00546	111.28	1.46	0.128
0.481	5.70	2.56	0.00552	113.33	1.35	0.151
0.856	8.40	2.61	0.00645	224.69	1.55	0.135
0.353	2.90	2.60	0.00776	50.09	1.61	0.096
0.392	2.90	2.60	0.00861	52.61	1.69	0.082
0.388	2.90	2.60	0.00852	52.35	1.62	0.076
0.395	2.90	2.60	0.00869	53.52	1.80	0.065
0.429	5.70	2.56	0.00492	104.75	1.43	0.137
0.541	5.70	2.56	0.00621	117.62	1.44	0.150

k_s/d_{50}	λ_c	d_{50}/b	y_o/b	y_t/D	y_o/P
0.00	0.021	0.026	0.283	0.358	0.170
0.00	0.024	0.026	0.227	0.318	0.147
0.00	0.021	0.038	0.452	0.480	0.226
0.00	0.024	0.013	0.173	0.279	0.121
0.00	0.024	0.013	0.211	0.306	0.140
0.00	0.026	0.013	0.229	0.319	0.148
0.00	0.021	0.013	0.280	0.356	0.169
0.00	0.019	0.026	0.256	0.339	0.160
0.00	0.024	0.026	0.230	0.320	0.149

TABLE 6.2 INITIATION OF MOTION EXPERIMENTAL DATA
IN CIRCULAR CHANNEL (D=305 mm) WITH FLAT BED 1 (ts=47 mm)
BED ROUGHNESS I (ks=0.80 mm)

Ex. No.	Q m^3/s	y_o (mm)	S	A m^2	R m	V_o m/s
1	0.0064	56.06	0.0019	0.0146	0.0413	0.440
2	0.0073	63.30	0.0017	0.0167	0.0453	0.438
3	0.0172	105.00	0.0019	0.0292	0.0646	0.589
4	0.0169	108.03	0.0012	0.0301	0.0658	0.561
5	0.0106	87.72	0.0011	0.0240	0.0574	0.441
6	0.0064	57.23	0.0019	0.0149	0.0419	0.428
7	0.0228	128.75	0.0013	0.0364	0.0729	0.626
8	0.0146	114.10	0.0010	0.0320	0.0680	0.455
9	0.0059	56.68	0.0015	0.0147	0.0416	0.399
10	0.0045	47.38	0.0016	0.0121	0.0362	0.373

τ_c N/m^2	τ_{cb} N/m^2	d_{50} mm	S_s	$1/\psi$	R_{e*}	$V_c/\sqrt{g d_{50}(Ss-1)}$
0.766	0.9115	8.40	2.61	0.00577	223.22	1.21
0.747	0.9068	8.40	2.61	0.00563	210.69	1.20
1.191	1.6066	8.40	2.61	0.00898	263.03	1.62
0.768	0.8600	8.40	2.61	0.00579	227.55	1.54
0.612	0.7371	5.70	2.56	0.00702	136.43	1.49
0.785	0.9565	5.70	2.56	0.00900	154.49	1.45
0.901	1.0378	5.70	2.56	0.01033	166.40	2.12
0.660	0.8560	2.90	2.60	0.01451	73.89	2.13
0.602	0.7044	2.90	2.60	0.01323	70.57	1.87
0.564	0.6490	2.90	2.60	0.01239	68.30	1.75

d_{50}/R	k_s/d_{50}	λ_c	d_{50}/b	y_o/b	y_t/D	y_o/P
0.203	0.10	0.032	0.038	0.255	0.338	0.159
0.185	0.10	0.031	0.038	0.288	0.362	0.172
0.130	0.10	0.027	0.038	0.477	0.498	0.232
0.128	0.10	0.020	0.038	0.491	0.508	0.236
0.099	0.14	0.025	0.026	0.399	0.442	0.210
0.136	0.14	0.034	0.026	0.260	0.342	0.161
0.078	0.14	0.018	0.026	0.585	0.576	0.258
0.043	0.28	0.025	0.013	0.519	0.528	0.243
0.070	0.28	0.030	0.013	0.258	0.340	0.160
0.080	0.28	0.032	0.013	0.215	0.309	0.142

TABLE 6.3 INITIATION OF MOTION EXPERIMENTAL DATA
IN CIRCULAR CHANNEL (D=305 mm) WITH FLAT BED 1 (ts=47 mm)
BED ROUGHNESS II (ks=1.40 mm)

Ex. No.	Q m^3/s	y_o (mm)	S	A m^2	R m	V_c m/s
1	0.0165	103.88	0.0017	0.0289	0.0642	0.570
2	0.0214	119.50	0.0016	0.0337	0.0699	0.635
3	0.0116	78.68	0.0023	0.0213	0.0532	0.545
4	0.0158	100.63	0.0013	0.0281	0.0631	0.562
5	0.0076	64.57	0.0021	0.0173	0.0463	0.439
6	0.0059	54.87	0.0023	0.0144	0.0410	0.412
7	0.0063	58.77	0.0021	0.0155	0.0432	0.405
8	0.0085	79.20	0.0014	0.0216	0.0537	0.396

τ_c N/m^2	τ_{cb} N/m^2	d_{50} mm	S_s	$1/\psi$	R_{e*}	$V_c/\sqrt{g d_{50}(Ss-1)}$
1.096	1.4560	8.40	2.61	0.00826	267.04	1.57
1.097	1.3700	8.40	2.61	0.00827	248.03	1.74
1.201	1.5760	8.40	2.61	0.00905	279.08	1.50
0.793	0.8939	5.70	2.56	0.00909	147.23	1.90
0.964	1.2634	5.70	2.56	0.01105	162.06	1.49
0.931	1.1890	5.70	2.56	0.01067	159.38	1.39
0.881	1.1370	2.90	2.60	0.01935	81.15	1.90
0.711	0.9499	2.90	2.60	0.01563	72.98	1.86

d_{50}/R	k_s/d_{50}	λ_c	d_{50}/b	y_o/b	y_t/D	yo/P
0.131	0.17	0.027	0.038	0.472	0.495	0.231
0.120	0.17	0.022	0.038	0.543	0.546	0.248
0.158	0.17	0.032	0.038	0.358	0.412	0.197
0.090	0.25	0.020	0.026	0.457	0.484	0.226
0.123	0.25	0.040	0.026	0.294	0.366	0.173
0.139	0.25	0.044	0.026	0.249	0.334	0.156
0.067	0.48	0.043	0.013	0.267	0.347	0.163
0.054	0.48	0.036	0.013	0.360	0.414	0.197

TABLE 6.4 INITIATION OF MOTION EXPERIMENTAL DATA
IN CIRCULAR CHANNEL (D=305 mm) WITH FLAT BED 2 (ts=77 mm)
SMOOTH BED

Ex. No.	Q m3/s	y_o mm	S	A m^2	R m	V_c m/s
1	0.0101	69.35	0.0014	0.0202	0.0491	0.501
2	0.0081	56.33	0.0019	0.0161	0.0422	0.502
3	0.0086	62.08	0.0012	0.0180	0.0453	0.479
4	0.0138	90.36	0.0006	0.0266	0.0587	0.519
5	0.0081	64.50	0.0008	0.0187	0.0466	0.433
6	0.0051	42.36	0.0013	0.0120	0.0338	0.424
7	0.0056	44.50	0.0020	0.0127	0.0351	0.442
8	0.0208	123.00	0.0008	0.0363	0.0699	0.573

τ_c N/m^2	d_{50} mm	S_s	$1/\psi$	R_{e*}	$V_c/\sqrt{gd(Ss-1)}$	d_{50}/R
0.675	8.40	2.61	0.00509	212.58	1.37	0.171
0.786	8.40	2.61	0.00593	231.84	1.38	0.199
0.534	8.40	2.61	0.00402	190.69	1.31	0.185
0.345	5.70	2.56	0.00396	104.77	1.76	0.097
0.366	2.90	2.60	0.00804	51.59	2.03	0.062
0.422	2.90	2.60	0.00927	54.99	1.99	0.086
0.689	8.40	2.61	0.00519	215.01	1.21	0.239
0.548	5.70	2.56	0.00629	128.92	1.94	0.082

k_s/d_{50}	λ_c	d_{50}/b	y_o/b	y_t/D	y_o/P
0.00	0.022	0.032	0.262	0.480	0.169
0.00	0.025	0.032	0.213	0.437	0.147
0.00	0.019	0.032	0.234	0.456	0.157
0.00	0.010	0.022	0.341	0.549	0.200
0.00	0.016	0.011	0.243	0.464	0.161
0.00	0.019	0.011	0.160	0.391	0.119
0.00	0.028	0.032	0.168	0.398	0.123
0.00	0.013	0.022	0.464	0.656	0.237

TABLE 6.5 INITIATION OF MOTION EXPERIMENTAL DATA
IN CIRCULAR CHANNEL (D=305 mm) WITH FLAT BED 2 (ts=77 mm)
BED ROUGHNESS I (ks=0.80 mm)

Ex. No.	Q m^3/s	y_o mm	S	A m^2	R m	V_c m/s
1	0.0038	39.25	0.0014	0.0111	0.0317	0.342
2	0.0059	54.30	0.0011	0.0156	0.0410	0.378
3	0.0041	44.55	0.0012	0.0127	0.0351	0.323
4	0.0086	67.75	0.0012	0.0197	0.0482	0.436
5	0.0060	48.48	0.0023	0.0139	0.0375	0.433
6	0.0060	52.23	0.0016	0.0150	0.0398	0.400
7	0.0057	48.67	0.0019	0.0139	0.0376	0.407
8	0.0055	46.34	0.0024	0.0132	0.0362	0.417
9	0.0124	82.36	0.0015	0.0242	0.0552	0.511
10	0.0099	69.46	0.0019	0.0202	0.0491	0.490
11	0.0062	49.95	0.0029	0.0143	0.0384	0.431

τ_c N/m^2	τ_{cb} N/m^2	d_{50} mm	S_s	$1/\psi$	R_{e*}	$V_c/\sqrt{gd\ (Ss-1)}$
0.435	0.4660	2.90	2.60	0.00956	51.69	1.60
0.442	0.4700	2.90	2.60	0.00971	53.55	1.77
0.413	0.4526	2.90	2.60	0.00908	52.50	1.51
0.568	0.6200	5.70	2.56	0.00651	121.50	1.48
0.846	0.9736	5.70	2.56	0.00970	147.46	1.47
0.624	0.7030	5.70	2.56	0.00715	128.94	1.35
0.701	0.7950	5.70	2.56	0.00804	135.70	1.38
0.852	0.9858	8.40	2.61	0.00643	219.36	1.14
0.812	0.9380	8.40	2.61	0.00612	228.27	1.40
0.928	1.1050	8.40	2.61	0.00699	228.08	1.35
1.078	1.2900	8.40	2.61	0.00812	247.06	1.18

d_{50}/R	k_s/d_{50}	λ_c	d_{50}/b	y_o/b	y_t/D	y_o/P
0.092	0.28	0.030	0.011	0.148	0.381	0.112
0.071	0.28	0.025	0.011	0.205	0.430	0.142
0.083	0.28	0.032	0.011	0.168	0.399	0.123
0.118	0.14	0.024	0.022	0.256	0.475	0.166
0.152	0.14	0.036	0.022	0.183	0.411	0.131
0.143	0.14	0.031	0.022	0.197	0.424	0.138
0.151	0.14	0.034	0.022	0.184	0.412	0.132
0.232	0.10	0.039	0.032	0.175	0.404	0.127
0.152	0.10	0.025	0.032	0.311	0.522	0.188
0.171	0.10	0.031	0.032	0.262	0.480	0.169
0.219	0.10	0.046	0.032	0.188	0.416	0.134

TABLE 6.6 INITIATION OF MOTION EXPERIMENTAL DATA
IN CIRCULAR CHANNEL (D=305 mm) WITH FLAT BED 2 (ts=77 mm)
BED ROUGHNESS II (ks=1.40 mm)

Test No.	Q m^3/s	y_o mm	S	A m^2	R m	V_c m/s
1	0.0031	32.54	0.0023	0.0092	0.0270	0.342
2	0.0052	45.90	0.0021	0.0131	0.0360	0.397
3	0.0059	52.28	0.0016	0.0150	0.0400	0.395
4	0.0072	63.10	0.0011	0.0183	0.0460	0.391
5	0.0160	135.08	0.0010	0.0398	0.0726	0.402
6	0.0105	72.13	0.0018	0.0211	0.0500	0.498
7	0.0056	46.53	0.0025	0.0133	0.0360	0.420
8	0.0066	51.50	0.0023	0.0148	0.0390	0.447
9	0.0070	54.18	0.0028	0.0156	0.0410	0.451
10	0.0099	67.14	0.0024	0.0195	0.0480	0.507
11	0.0160	102.56	0.0017	0.0303	0.0632	0.528

τ_c N/m^2	τ_{cb} N/m^2	d_{50} mm	S_s	$1/\psi$	R_{e*}	$V_c/\sqrt{g d_{50}(Ss-1)}$
0.620	0.6880	2.90	2.60	0.01362	65.63	1.60
0.742	0.8500	2.90	2.60	0.01629	71.80	1.86
0.624	0.7100	2.90	2.60	0.01371	65.85	1.85
0.478	0.5200	2.90	2.60	0.01051	57.66	1.83
0.741	1.0970	5.70	2.56	0.00849	141.03	1.36
0.883	1.0400	5.70	2.56	0.01012	153.97	1.68
0.883	1.0300	5.70	2.56	0.01012	153.97	1.42
0.861	0.9960	5.70	2.56	0.00987	152.03	1.51
1.110	1.3430	8.40	2.61	0.00837	254.43	1.24
1.149	1.4000	8.40	2.61	0.00866	258.84	1.39
1.023	1.3180	8.40	2.61	0.00771	244.24	1.45

d_{50}/R	k_s/d_{50}	λ_c	d_{50}/b	y_o/b	y_t/D	y_o/P
0.107	0.4828	0.042	0.011	0.123	0.359	0.096
0.081	0.4828	0.038	0.011	0.173	0.403	0.126
0.073	0.4828	0.032	0.011	0.197	0.424	0.139
0.063	0.4828	0.025	0.011	0.238	0.459	0.159
0.079	0.2456	0.037	0.022	0.510	0.695	0.246
0.114	0.2456	0.029	0.022	0.272	0.489	0.171
0.158	0.2456	0.040	0.022	0.176	0.405	0.126
0.146	0.2456	0.034	0.022	0.194	0.421	0.136
0.205	0.1667	0.044	0.032	0.204	0.430	0.142
0.175	0.1667	0.036	0.032	0.253	0.473	0.165
0.133	0.1667	0.029	0.032	0.387	0.589	0.214

TABLE 6.7 INITIATION OF MOTION EXPERIMENTAL DATA
IN CIRCULAR CHANNEL (D=305 mm) WITH FLAT BED 3 (ts=120 mm)
SMOOTH BED

Test No.	Q m^3/s	y_o (mm)	S	A m^2	R m	V_c m/s
	0.0045	38.08	0.0013	0.0115	0.0308	0.391
2	0.0057	48.75	0.0010	0.0148	0.0373	0.385
3	0.0152	123.20	0.0007	0.0358	0.0641	0.425
4	0.0047	39.30	0.0017	0.0119	0.0316	0.395
5	0.0068	53.83	0.0012	0.0163	0.0402	0.417
6	0.0110	75.50	0.0010	0.0228	0.0505	0.482
7	0.0073	55.50	0.0017	0.0168	0.0411	0.435
8	0.0073	56.00	0.0016	0.0170	0.0413	0.429

τc N/m^2	d_{50} mm	S_s	$1/\psi$	R_{e*}	$V_c/\sqrt{g d_{50}(Ss-1)}$	d_{50}/R
0.384	2.90	2.60	0.00843	50.74	1.83	0.094
0.359	2.90	2.60	0.00788	49.84	1.81	0.078
0.409	2.90	2.60	0.00898	52.80	1.99	0.045
0.533	5.70	2.56	0.00611	116.44	1.34	0.180
0.481	5.70	2.56	0.00552	110.49	1.41	0.142
0.485	5.70	2.56	0.00557	112.11	1.63	0.113
0.689	8.40	2.61	0.00520	200.70	1.19	0.204
0.656	8.40	2.61	0.00495	195.74	1.18	0.203

k_s/d_{50}	λ_c	d_{50}/b	y_o/b	y_t/D	y_o/P
0.00	0.020	0.010	0.128	0.518	0.102
0.00	0.019	0.010	0.164	0.553	0.123
0.00	0.018	0.010	0.413	0.797	0.221
0.00	0.027	0.019	0.132	0.522	0.104
0.00	0.022	0.019	0.181	0.570	0.133
0.00	0.017	0.019	0.253	0.641	0.167
0.00	0.029	0.028	0.186	0.575	0.136
0.00	0.029	0.028	0.188	0.577	0.136

TABLE 6.8 INITIATION OF MOTION EXPERIMENTAL DATA
IN CIRCULAR CHANNEL (D=305 mm) WITH FLAT BED 3 (ts=120 mm)
BED ROUGHNESS I (ks=0.80 mm)

Test No.	Q m^3/s	y_o (mm)	S	A m^2	R m	V_c m/s
1	0.0058	52.68	0.0009	0.0160	0.0395	0.363
2	0.0044	42.23	0.0011	0.0128	0.0334	0.344
3	0.0042	40.84	0.0011	0.0124	0.0326	0.339
4	0.0063	46.55	0.0019	0.0141	0.0361	0.447
5	0.0084	68.57	0.0011	0.0207	0.0475	0.406
6	0.0064	50.40	0.0025	0.0153	0.0383	0.418
7	0.0085	60.20	0.0020	0.0182	0.0435	0.467
8	0.0134	93.13	0.0013	0.0278	0.0570	0.482
9	0.0169	119.38	0.0012	0.0348	0.0635	0.486

τ_c N/m^2	τ_{cb} N/m^2	d_{50} mm	S_s	$1/\psi$	R_{e*}	$V_c/\sqrt{g d_{50}(Ss-1)}$
0.360	0.3700	2.90	2.60	0.00792	47.34	1.70
0.364	0.3740	2.90	2.60	0.00799	47.53	1.61
0.336	0.3400	2.90	2.60	0.00738	45.44	1.59
0.662	0.7040	5.70	2.56	0.00759	121.91	1.51
0.531	0.5830	5.70	2.56	0.00609	109.20	1.37
0.924	1.1000	8.40	2.61	0.00697	215.87	1.15
0.858	0.9700	8.40	2.61	0.00647	208.81	1.28
0.733	0.8500	8.40	2.61	0.00552	193.09	1.32
0.754	0.9224	8.40	2.61	0.00568	197.74	1.33

d_{50}/R	k_s/d_{50}	λ_c	d_{50}/b	y_o/b	y_t/D	y_o/P
0.073	0.28	0.022	0.010	0.177	0.566	0.130
0.087	0.28	0.025	0.010	0.142	0.532	0.110
0.089	0.28	0.023	0.010	0.137	0.527	0.107
0.158	0.14	0.027	0.019	0.156	0.546	0.119
0.120	0.14	0.026	0.019	0.230	0.618	0.157
0.219	0.10	0.042	0.028	0.169	0.559	0.126
0.193	0.10	0.031	0.028	0.202	0.591	0.144
0.147	0.10	0.025	0.028	0.313	0.699	0.191
0.132	0.10	0.026	0.028	0.401	0.785	0.218

TABLE 6.9 INITIATION OF MOTION EXPERIMENTAL DATA
IN CIRCULAR CHANNEL (D=305 mm) WITH FLAT BED 3 (ts=120 mm)
BED ROUGHNESS II (ks=1.40 mm)

Test No.	Q m^3/s	y_o (mm)	S	A m^2	R m	V_c m/s
1	0.0070	49.98	0.0030	0.0152	0.0380	0.463
2	0.0085	58.71	0.0028	0.0178	0.0428	0.480
3	0.0173	99.50	0.0019	0.0296	0.0589	0.585
4	0.0104	70.63	0.0025	0.0213	0.0485	0.488
5	0.0109	78.46	0.0017	0.0236	0.0517	0.462
6	0.0182	117.24	0.0014	0.0343	0.0631	0.531
7	0.0112	65.83	0.0023	0.0199	0.0463	0.560
8	0.0034	34.63	0.0027	0.0105	0.0285	0.320
9	0.0038	41.90	0.0021	0.0127	0.0332	0.299
10	0.0073	60.48	0.0015	0.0183	0.0437	0.398

τ_c N/m^2	τ_{cb} N/m^2	d_{50} mm	S_s	$1/\psi$	R_{e*}	$V_c/\sqrt{gd_{50}(Ss-1)}$
1.118	1.2900	8.40	2.61	0.00843	255.37	1.27
1.192	1.4000	8.40	2.61	0.00899	258.94	1.32
1.075	1.2700	8.40	2.61	0.00810	245.88	1.61
1.194	1.4600	8.40	2.61	0.00900	258.11	1.34
0.857	1.0230	5.70	2.56	0.00983	143.12	1.56
0.854	1.0270	5.70	2.56	0.00979	143.35	1.80
1.045	1.1680	5.70	2.56	0.01198	158.68	1.90
0.752	0.8500	2.90	2.60	0.01652	69.35	1.50
0.690	0.7990	2.90	2.60	0.01517	66.75	1.40
0.652	0.7400	2.90	2.60	0.01432	65.59	1.87

d_{50}/R	k_s/d_{50}	λ_c	d_{50}/b	y_o/b	y_t/D	y_o/P
0.221	0.17	0.042	0.028	0.168	0.557	0.125
0.196	0.17	0.041	0.028	0.197	0.586	0.141
0.143	0.17	0.025	0.028	0.334	0.720	0.198
0.173	0.17	0.040	0.028	0.237	0.625	0.161
0.110	0.25	0.032	0.019	0.263	0.651	0.172
0.090	0.25	0.024	0.019	0.393	0.778	0.216
0.123	0.25	0.027	0.019	0.221	0.609	0.153
0.102	0.48	0.059	0.010	0.116	0.507	0.094
0.087	0.48	0.062	0.010	0.141	0.531	0.110
0.066	0.48	0.033	0.010	0.203	0.592	0.144

TABLE 6.10 - COEFFICIENTS a AND b IN EQUATION 6.14

Bed Condition	average k_s (mm)	a	b
Smooth beds	0.00	0.032	-0.35
Rough Beds (roughness I)	0.80	0.024	-0.23
Rough Beds (roughness II)	1.40	0.064	-0.30

CHAPTER 7

BED LOAD TRANSPORT

7.1 Development of Sediment transport Equations

There are three principal approaches to analysing problems involving two phase flow phenomena. These are:

- empirical methods based on practical experiments
- careful and exact correlation of experimental data (dimensional analysis)
- complete mathematical analysis leading to the development of sediment transport models.

While there has been some attempt, recently, to utilize the last approach, most work on sediment transport has tended to employ mainly the first two approaches.

It is recognized that even if the nature of the transport problem could be expressed fully in mathematical form, the resulting equation would be too complicated to solve and usually this kind of form has some empirical coefficients and assumptions.

Dimensional analysis has proved to be a very useful technique in the study of sediment transport. The technique involves developing equations to describe a particular phenomenon by combining dimensionless groups of the quantities characterising the phenomenon.

The variables that govern the rate of sediment transport in circular cross section channels with flat beds are many and

varied. These are: densities of the water (ρ) and solids (ρ_s), viscosity of the fluid (μ), particle size (d), flow depth (y_o) or hydraulic radius (R), pipe diameter (D), bed width (b) or bed thickness (t_s), acceleration due to gravity (g), mean shear stress (τ_o) or bed shear stress (τ_b), mean flow velocity (V), friction factor with sediment transport (λ_s) and turbulence.

All these variables are inter-related, with some of them playing a predominant role. In this study the more important variables will be evaluated as the principal factors governing the sediment transport such as bed shear stress (τ_b), friction factor with sediment transport (λ_s) and the channel bed width (b).

In sediment transport studies it is the statistical parameters, rather than the instantaneous values of individual variables, that can be related to each other. The above variables can be reduced, by dimensional analysis, to a set of basic dimensionless parameters as follows:

i) Shear stress parameter, $\left\{\frac{\tau_o}{\rho g d_{50}(S_s-1)}\right\}$, where d_{50} is median particle size and S_s is relative density (ρ_s/ρ). This parameter can be obtained by analysing the forces at incipient motion of grain.

ii) Sediment volumetric concentration, ($C_v = \frac{Q_s}{Q}$), where Q_s is the transport rate of sediment in volume per unit time, Q is the water discharge.

iii) Friction factor of the channel with sediment transport, (λ_s), which is different from its value for no sediment in

clear water (λ_c).

iv) Width to depth ratio (b/y_o), which reflects the influence of bed width and flow depth on sediment movement.

v) The relative particle size (d_{50}/D), which characterizes the influence of pipe diameter and particle size on sediment movement.

The functional relationship between the above parameters can be written as:

$$\frac{\tau_o}{\rho g d_{50}(S_s-1)} = f\left[C_v, \frac{b}{y_o}, \frac{d_{50}}{D}, \lambda_s \right] \qquad (7.1)$$

The particle Reynolds number has little effect as the sediment used in this study were mainly coarse sands and gravels. The effect of the acceleration due to gravity, g, and the fluid kinematic viscosity are incorporated in the friction factor parameter ,λ_s.

Since some of the present experiments were carried out in a flume with rough beds and smooth walls, the resistance to flow caused by the roughness of the boundary was not uniform throughout the wetted perimeter. In addition, the width to depth ratio b/y_o of experimental data was not sufficiently high because the pipe was not very large. Therefore, hydraulic parameters such as hydraulic radius and friction factor due to bed only, were considered for analysis by splitting the overall parameters into their constituent parts corresponding to bed and side walls (Einstein-Vanoni's

method, see App. G, was used for this). Thus by using the computed bed shear stress (τ_b) and bed friction factor with sediment (λ_{sb}) Eq. 7.1 can be re-written as:

$$\frac{\tau_b}{\rho g d_{50}(S_s-1)} = f\left[C_v, \frac{b}{y_o}, \frac{d_{50}}{D}, \lambda_{sb}\right] \qquad (7.2)$$

The channel friction factor with sediments (λ_s) depends on various factors such as clear water friction factor (λ_o), volumetric sediment concentration in the flow (C_v), flow depth (y_o) and bed width (b). Therefore, the channel friction factor with sediment can be written in the form: relationship of the form

$$\lambda_s = f\left(\lambda_c, C_v, \frac{b}{y_o}\right) \qquad (7.3)$$

All the above relationships imply the generation of models. However, the determination of such functions is only possible by means of experimental results.

It has to be emphasized here that the width to depth parameter (b/y_o) is of great importance because, in some ways, it is describing the channel shape. Some previous researchers (Ackers 1984, Loveless 1986) introduced the concept of effective width (W_e) to account for the effect of bed width on sediment movement. More recently Paul and Sakhuja (1990) stated that effective width is a function of (b/y_o) and sediment size. Therefore, the parameter b/y_o is considered in this study as a key determinant of critical shear stress or velocity necessary to achieve non-deposition condition in circular cross section channels with flat beds.

7.2 Presentation of Experimental Results

The experimental results obtained from the sediment transport experiments in the three flat beds over a range of transport conditions were analysed and presented under the following categorizations:

a) General analysis

b) Comparison with different sediment transport equations

   i) According to degree of filling

   ii) For all flow ranges

Full details of bed load transport experimental data for the three flat beds (bed 1, bed 2 and bed 3) are presented in Appendix H.

7.3 General Analysis

The limit deposition criterion as discussed in Sec. 4.7 was employed in these experiments. For a given uniform flow sediment was fed to the flow in increasing amounts until the point of deposition was reached.

Analysis of the experimental data were performed for the three beds (for all bed roughnesses), however only bed 1 results will be presented in detail in this section and the results for the other beds (bed 2 and bed 3) will be highlighted as well.

Figures 7.1, 7.2 and 7.3 show the experimental results for

bed 1 with smooth surface, roughness I (k_s=0.80mm), and roughness II (k_s= 1.4 mm) respectively. The data are presented in terms of transport parameter, ϕ (= $C_v VR/\sqrt{gd_{50}^3 (S_s -1)}$), against the flow intensity parameter, ψ ($=\tau_o/(\rho_s-\rho)gd_{50}$). Clear trends can be observed from these figures with a power fitting of the form

$$\psi = a\ (\phi)^b \qquad (7.4)$$

where a and b are constants to be obtained from the data. The agreement between experiments is good, resulting in a different function for each sediment size investigated. Similar trends were observed for the three beds. Tables 7.1, 7.2 and 7.3 show the values of a and b (obtained by linear regression analysis) of the Eq. 7.4 for experimental data of bed 1, bed 2 and bed 3 respectively.

In Figures 7.1 and 7.2, the data plotted in terms of ϕ and ψ for bed 1 with smooth surface and bed 1 with roughness I (k_s=0.8 mm) respectively, it can be seen that there is a consistent trend of increasing ϕ with decreasing ψ over the range of the sediment particles employed in this study. It is also seen that almost all observed values fall above Graf-Acaroglu's loose beds curve (Eq. 2.13) while in bed 1 with roughness II (k_s=1.40 mm) as seen in Figure 7.3, Eq. 2.13 line falls between the lines of the small 2.0mm and 2.9 mm particles.

It can be stated here that the rate of transport of the larger sediment particles is higher than that of small ones.

This is due to the greater exposed area of the larger particles, which are subjected to the drag forces of the flow.

An increase in the surface bed roughness is expected to affect the transport of the sediment simply because it increases the hydraulic resistance and causes the local velocity around the particles to decrease relative to the mean velocity of the flow, which reduces the drag force exerted by the flow on the particles. This explains why in going from smooth and small rough bed (rough I, k_s= 0.8 mm) to a relatively larger rough bed (rough II, k_s=1.4 mm), Graf and Acaroglu's loose beds curve (Eq. 2.13) is seen to intersect the line of small particles i.e. predicts higher sediment transport rate for small particles.

It has to be recalled that Graf- Acaroglu's equation was basically derived from open channels, closed conduits and field data. The results in Figures 7.1, 7.2 and 7.3 suggest that the transport capacity of flows in channels of circular cross section (limit of deposition) with a fixed sediment bed is greater than that of similar flows in alluvial channels. This can be explained by the difference in bed roughness and flow resistance. In rigid bed channels bed roughness is uniform and smaller compared with alluvial beds where bed forms also occur.

TABLE 7.1.1 Values of a and b in Eq. 7.4 for smooth bed 1

d_{50} (mm)	a	b
0.5	2.45	-0.44
1.0	2.54	-0.50
2.0	4.21	-0.47
2.9	6.92	-0.43
5.6	9.90	-0.43
8.4	12.01	-0.415

TABLE 7.1.2 Values of a and b in Eq. 7.4 for bed 1 with roughness I (k_s = 0.8mm)

d_{50} (mm)	a	b
2.0	8.36	-0.23
2.9	9.46	-0.25
5.6	22.90	-0.17
8.4	31.23	-0.19

TABLE 7.1.3 Values of a and b in Eq. 7.4 for bed 1 with roughness II (k_s = 1.40 mm)

d_{50} (mm)	a	b
2.0	11.85	-0.11
2.9	9.00	-0.21
5.6	15.80	-0.19
8.4	16.70	-0.23

TABLE 7.2.1 CONSTANTS a AND b OF EQUATION 7.4 FOR SMOOTH BED 2

d_{50} (mm)	a	b
0.50	3.47	-0.36
1.00	3.52	-0.47
2.90	7.59	-0.40
5.60	8.15	-0.47
8.40	22.90	-0.31

TABLE 7.2.2 CONSTANTS a AND b OF EQUATION 7.4 FOR BED 2 WITH ROUGHNESS I (k_s=0.8 mm)

d_{50} (mm)	a	b
1.00	5.8	-0.20
2.0	6.44	-0.29
2.90	7.51	-0.30
5.60	5.60	-0.40
8.40	25.60	-0.22

TABLE 7.2.3 CONSTANTS a AND b OF EQUATION 7.4 FOR BED 2 WITH ROUGHNESS II (k_s= 1.4 mm)

d_{50} (mm)	a	b
2.00	5.14	-0.28
2.90	4.62	-0.36
5.60	12.04	-0.24
8.40	17.92	-0.23

TABLE 7.3.1 COEFFICIENTS OF EQUATION 7.4 FOR SMOOTH BED 3

d_{50}	a	b
1.0	1.23	-0.74
2.9	2.79	-0.62
5.6	2.53	-0.70
8.4	4.2	-0.58

TABLE 7.3.2 COEFFICIENTS OF EQUATION 7.4 FOR BED 3 WITH ROUGHNESS I (k_s= 0.8 mm)

d_{50}	a	b
2.0	4.90	-0.35
2.9	8.45	-0.27
5.6	11.50	-0.33
8.4	25.60	-0.22

TABLE 7.3.3 COEFFICIENTS OF EQUATION 7.4 FOR BED 3 WITH ROUGHNESS II (k_s= 1.4 mm)

d_{50}	a	b
2.0	8.79	-0.18
2.9	10.16	-0.19
5.6	19.14	-0.17
8.4	25.8	-0.15

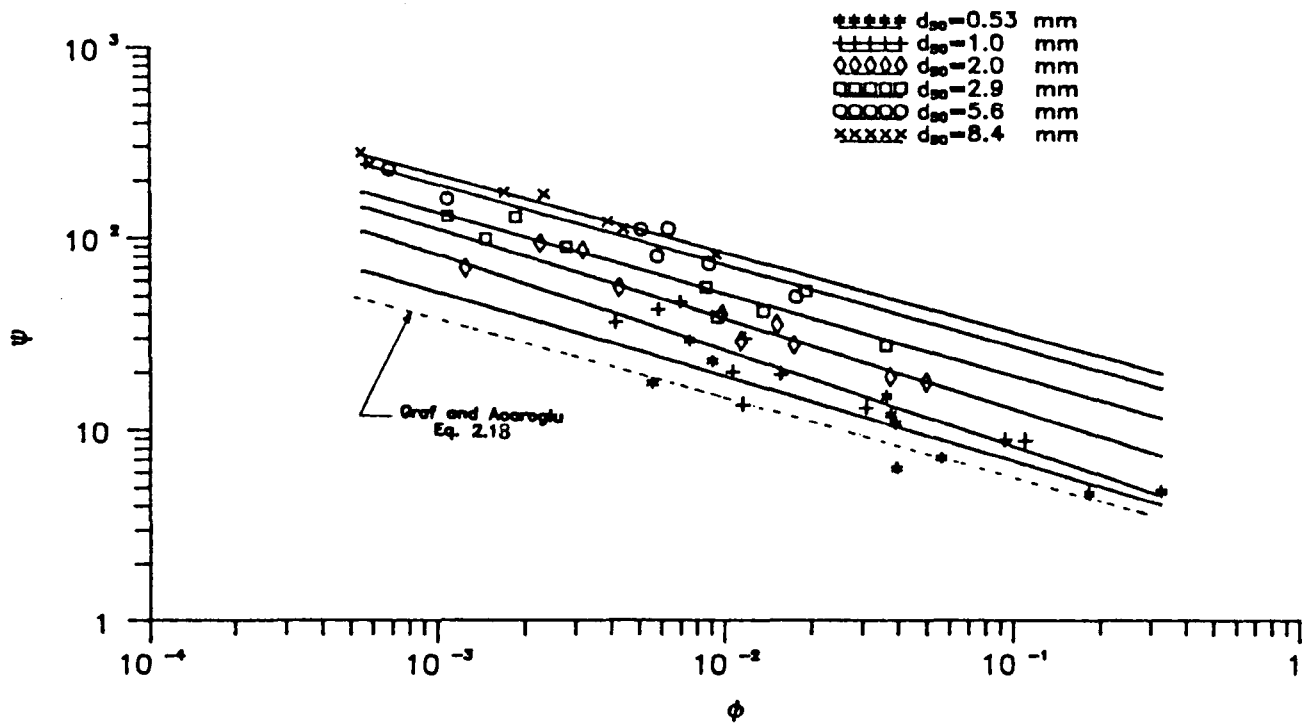

FIGURE 7.1 NON-COHESIVE SEDIMENT TRANSPORT OVER 47 mm THICK BED (smooth bed)

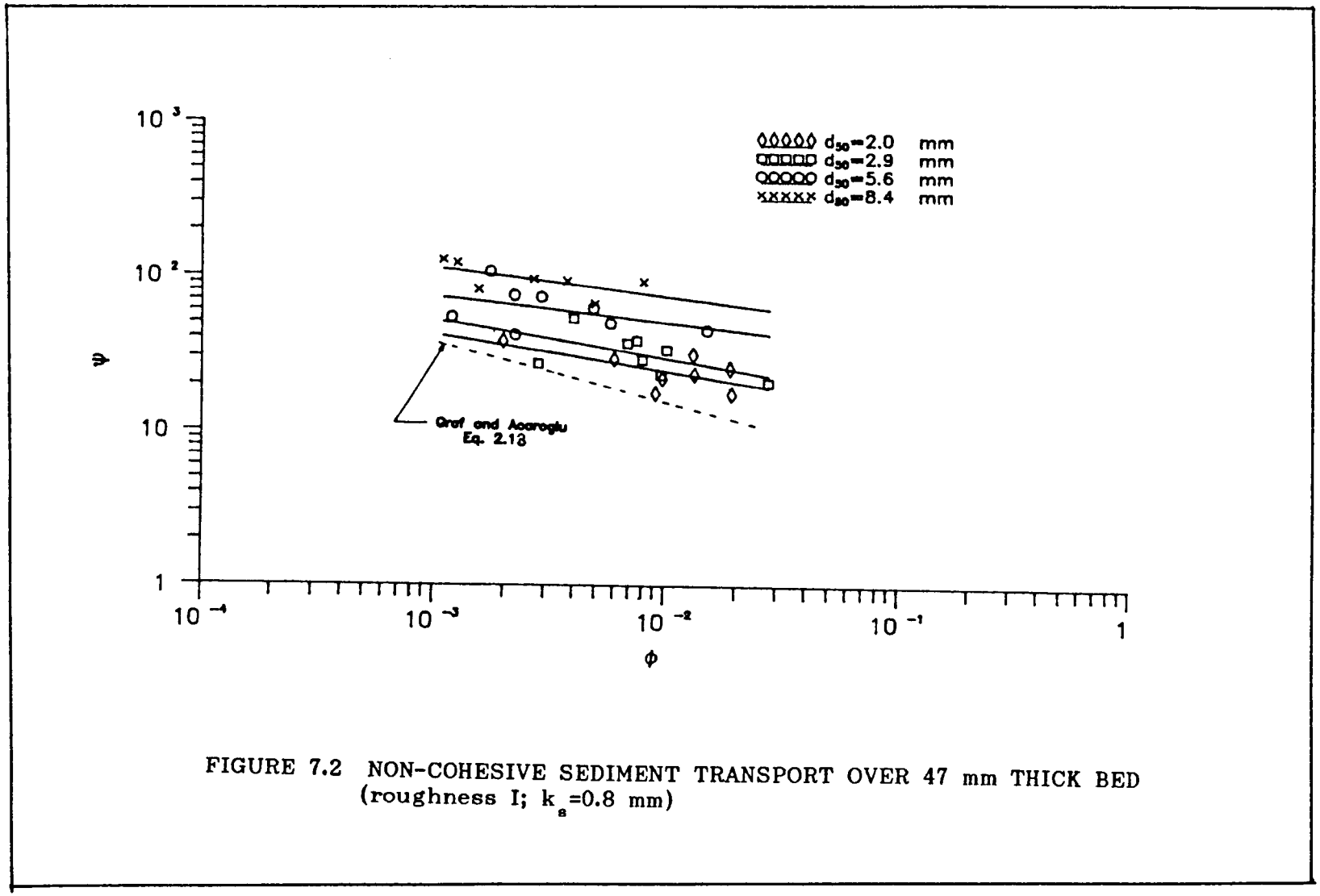

FIGURE 7.2 NON-COHESIVE SEDIMENT TRANSPORT OVER 47 mm THICK BED (roughness I; k_s=0.8 mm)

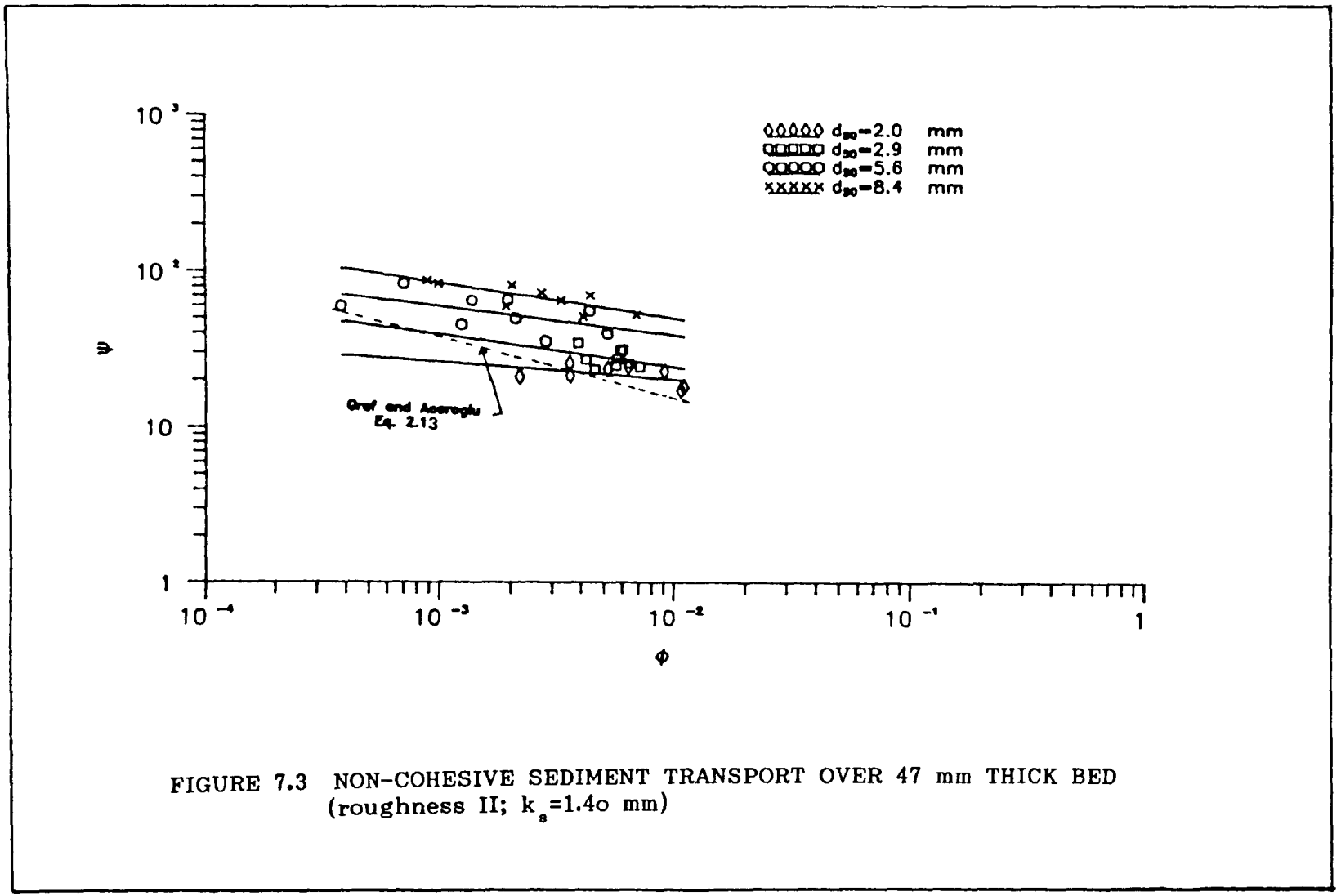

FIGURE 7.3 NON-COHESIVE SEDIMENT TRANSPORT OVER 47 mm THICK BED (roughness II; k_s=1.4o mm)

7.4 Comparisons With Different Sediment Transport Equations

7.4.1 According to Degree of Filling

Circular cross section channels with flat beds can adopt different shapes depending on the flow depths and thickness of deposited beds. For instance, the channel flowing at third-full depths can adopt a trapezoidal-like shape with side walls having a single curvature with a lesser gradient. For flows at half-full depths and at higher sediment deposition, the channel approaches a rectangular-like shape since the gradient of the side wall curvatures increases gradually to infinity at the level of the diameter.
When flowing at more than half-full depth the channel sides here have two curvatures opposing each other which in turn may considerably influence the hydraulic characteristics.

In this section the experimental data (for all roughness cases) will be separated and analysed in two groups according to whether the data was obtained at less or more than half-full flow conditions.

Four sediment transport equations were used in this study to compute the sediment transport rates and to compare them with measured ones. These equations are:
i) Ackers' equation (2.43) for circular channels loose sediment beds
ii) Loveless' equation (2.44) for fixed boundary channels
iii) May et al's equation (3.6) for circular channels with

loose sediment beds and,

iv) Alvarez's equation (3.11) for circular channels with fixed sediment beds.

Figure 7.4 shows the data of bed 1 (for all three roughness cases) with channel flowing at less than half-full depth, plotted as volumetric sediment concentration against the flow velocity and compared with the prediction from Loveless (Eq.2.44), May et al (Eq. 3.6), and Alvarez (Eq. 3.11) equations.

The plot shows that for a given sediment concentration May et al's equation over-predicts and Loveless' equation under-predicts the velocities needed to move the sediment particles. However, Alvarez equation is found to have a fair agreement with the data with differences between the equation and the data decreasing as the volumetric sediment concentration increases.

Fig. 7.5 shows the data of bed 1 with channel flowing more than half-full. In the same figure Loveless, May et al and Alvarez equations have also been plotted. As in the case of the channel flowing less than half-full, Loveless' and May et al's equations do not fit the present data. It can also be seen that the slope of the May et al's equation is steeper than in Fig. 7.4 where the channel is flowing less than half-full. This indicates that for more than half-full flow May et al's equation is predicting even higher velocities.

For the other experimental data of bed 2 and bed 3 as can be

seen in Figs. 7.6, 7.7 and 7.8 the gradients of the lines drawn representing May et al's equation are still steep leading to substantial under-prediction of limiting concentrations especially at low velocities. Agreement could have been better at the higher velocities, but the difference between the values predicted by the equation and the actual measurements are still quite substantial.

Loveless' equation, generally over-predicts the limiting concentration by a factor of 5-10 for all data of the three beds at different flow depths. It should be noted that the effective width term given by Loveless (1986) was taken to be equal to the sediment bed width.

Ackers (1984) combined the Ackers-White (A-W) transport equation with the Colebrook-White resistance equation (as outlined in Appendix I) in a model which was calibrated using May's (1982) experimental data for the limit of deposition. It was also supposed to allow for consideration of deposited beds. Due to the lack of research directly on sediment transport in pipes with bed deposits, Ackers' equation (Eq. 2.43) has never been confirmed as suitable for those conditions.

Ackers' equation (Eq. 2.43) was tested against present data of bed 1, bed 2 and bed 3 (for all three roughness cases) for flow depths at less than half-full flow (see Figs. 7.9 and 7.11) and for flow depths at more than half-full flow (see

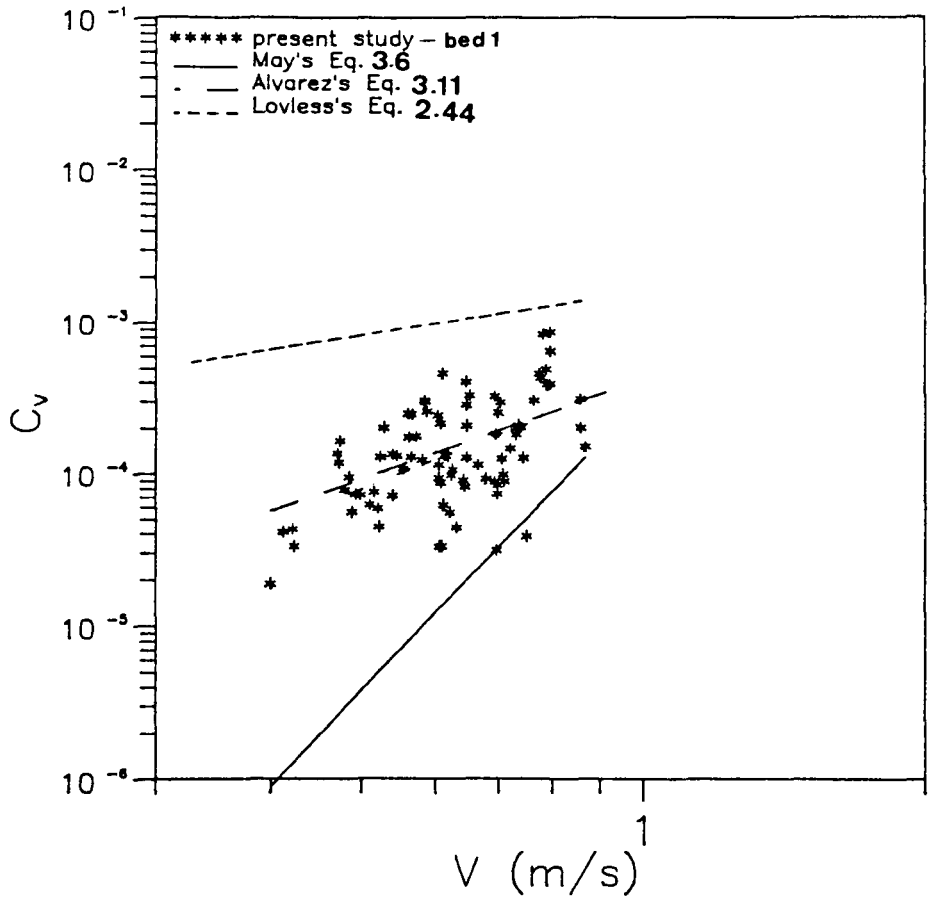

FIGURE 7.4 LIMIT OF DEPOSITION: EXPERIMENTAL DATA AT UP TO HALF-FULL FLOW COMPARED WITH SEDIMENT TRANSPORT EQUATIONS (BED 1)

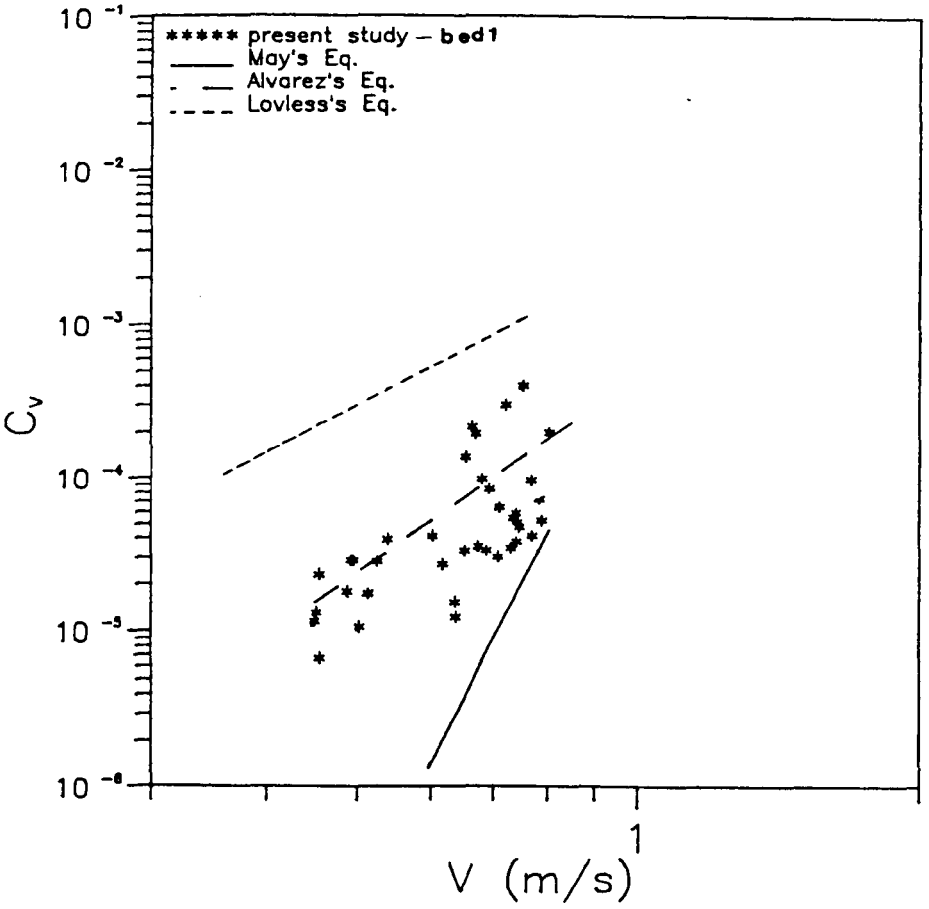

FIGURE 7.5 LIMIT OF DEPOSITION: EXPERIMENTAL DATA MORE THAN HALF-FULL FLOW COMPARED WITH SEDIMENT TRANSPORT EQUATIONS (BED 1)

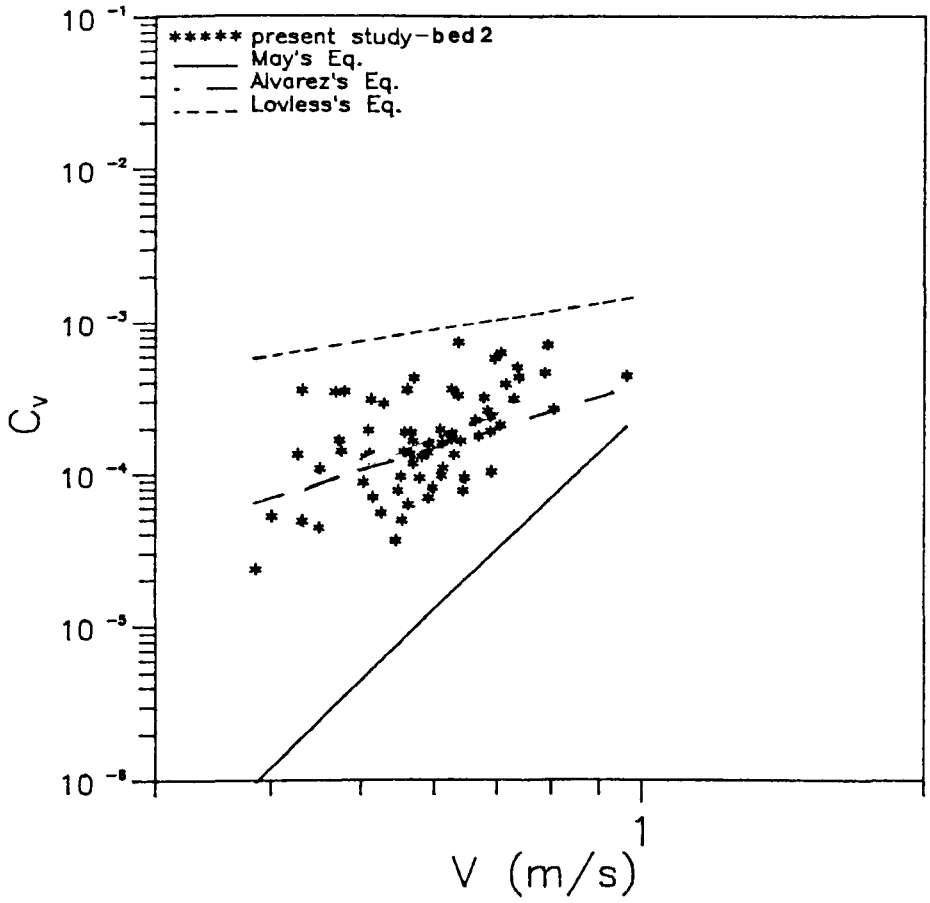

FIGURE 7.6 LIMIT OF DEPOSITION: EXPERIMENTAL DATA AT UP TO HALF-FULL FLOW COMPARED WITH SEDIMENT TRANSPORT EQUATIONS (BED 2)

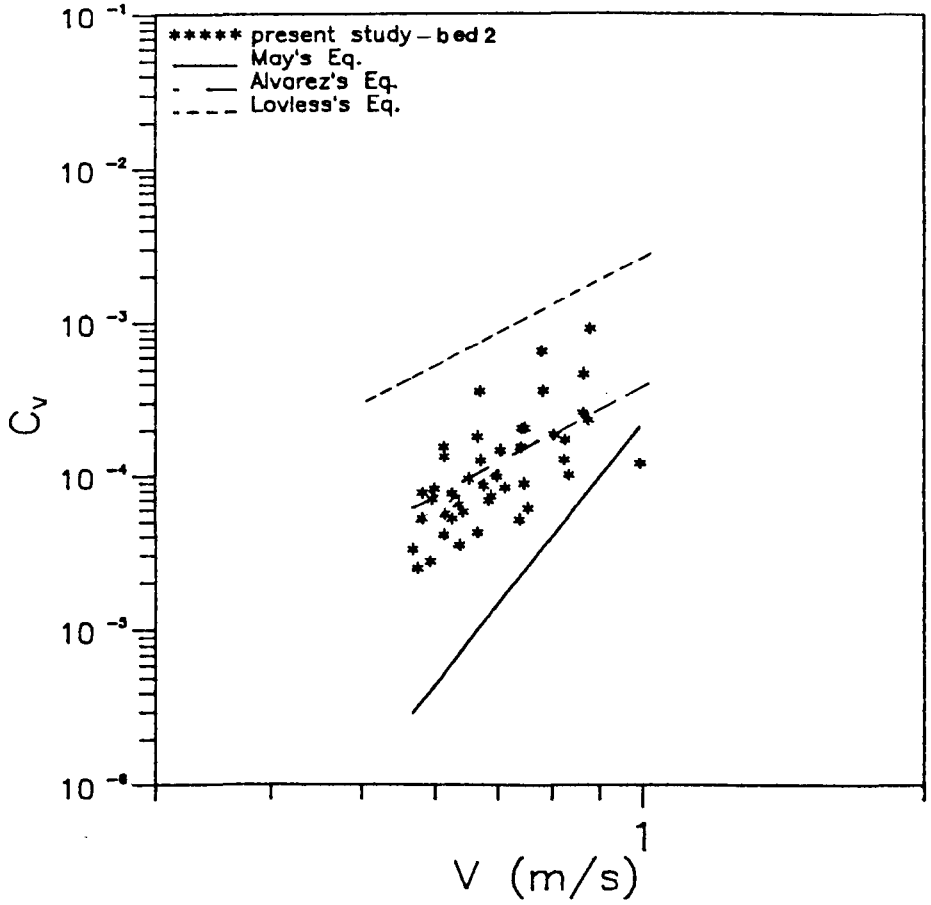

FIGURE 7.7 LIMIT OF DEPOSITION: EXPERIMENTAL DATA AT MORE THAN HALF-FULL FLOW COMPARED WITH SEDIMENT TRANSPORT EQUATIONS (BED 2)

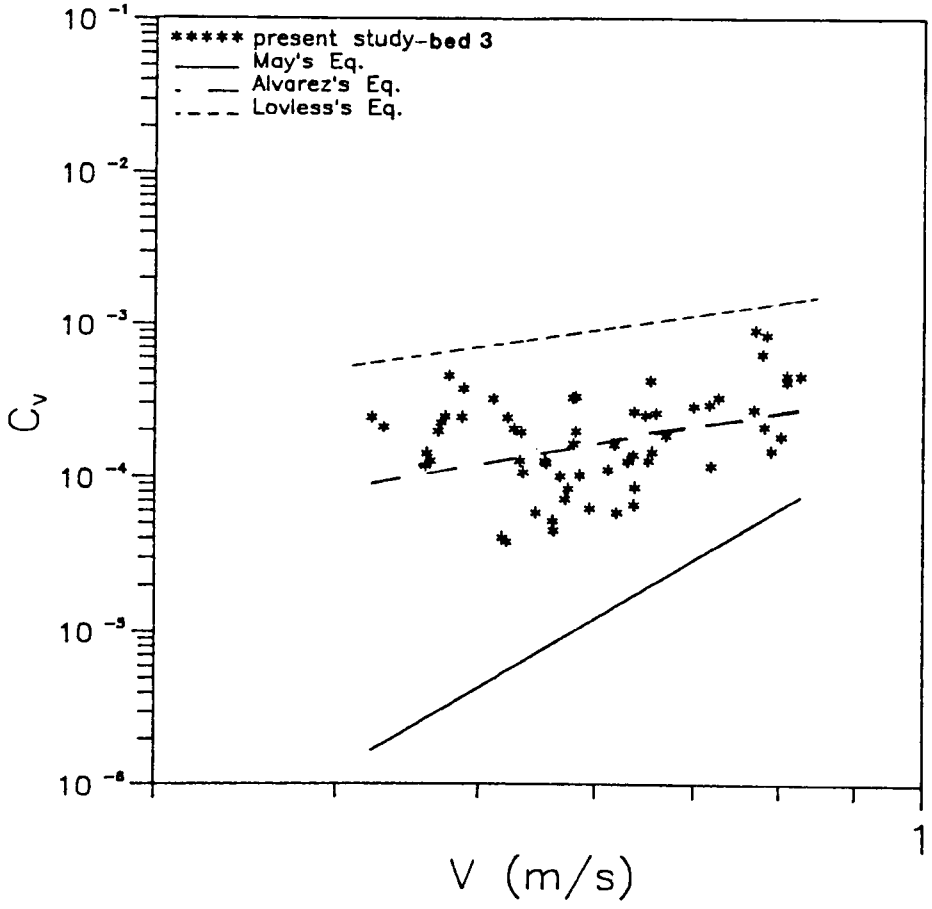

FIGURE 7.8 LIMIT OF DEPOSITION: EXPERIMENTAL DATA AT MORE THAN HALF-FULL FLOW COMPARED WITH SEDIMENT TRANSPORT EQUATIONS (BED 3)

Figs. 7.10, 7.12 and 7.13). It can be seen that Ackers equation for effective width equal to pipe diameter (as assumed by Ackers for flow depth at more than half full flow) generally-over estimates the limiting concentrations by a factor of 6-8; in other words it predicts lower velocity requirements for all sediment concentrations.

For an effective width calculated as the width corresponding to a sediment depth (see Appendix B), the line representing Ackers equation lies close to the present data (for both less and more than half-full flow depths). However, it still overestimates the limiting concentrations.

Ackers (1984) argued that for "clean pipe" transport calculations, it is necessary to select a suitable value of effective width (W_e). He suggested that the value should be equal to 10d (where d is the sediment particle size). It can be seen from Figs. 7.9 to 7.13 that his latest approach (W_e=10d) is in reasonable agreement with the present data. However, at higher sediment bed thickness (i.e. higher bed width) as bed 3 (t_s/D=0.39) Ackers' equation becomes inapplicable as seen in Fig. 7.13 which shows that the bed 3 data fall between the two lines representing Ackers' equation for effective width equal to bed width (or pipe diameter) and 10d respectively.

It is important to mention here that Ackers found the value of effective width to be 10d by utilizing May's (1982) experimental results which were obtained from full pipe experiments in 77 mm and 158 mm pipes. The reason why Ackers' equation with effective width equal to 10d (which was assumed for clean pipe at a limit of deposition) fits bed 1 and bed 2 data could be attributed to the fact that for a particular sediment concentration the required cleansing velocity reduces when the size of the pipe reduces and when the channel is flowing full. This indicates that the Ackers approach for effective width equal to 10d is not valid for a large pipe when flowing part-full.

Therefore, it is advisable that Ackers' equation (Eq. 2.43) be treated with caution when applied to sewers with fixed depositions (open channel flow) filling its invert up to 39%

of the diameter

Apart from Alvarez's equation which was developed for similar conditions but with a small pipe and few experiments. the preceding comparisons show that the sediment movement in circular cross section channel with deposited beds filling its invert up to 39% of the pipe diameter is not fully understood and therefore, not properly formulated by researchers.

The failure of the equations of Loveless, May et al and Ackers (for effective width equal to bed width) to agree with the present data can be attributed to the fact that these equations were developed either for loose deposited beds (Ackers and May et al) or for different cross section shapes other than circular cross section channels with flat beds (Loveless).

7.4.2 For all flow ranges

In this section, another approach is adopted to test the applicability of the sediment transport equations (Ackers 1984, Loveless 1986, May et al 1989 and Alvarez 1990). Only the data of bed 1 will be presented and any particular deviations in the results of bed 2 and bed 3 from that of the general observations will be pointed out.

Measured sediment rates for all flow depths of bed 1 (for all roughness cases) were compared with those predicted by different sediment transport methods. The experimental

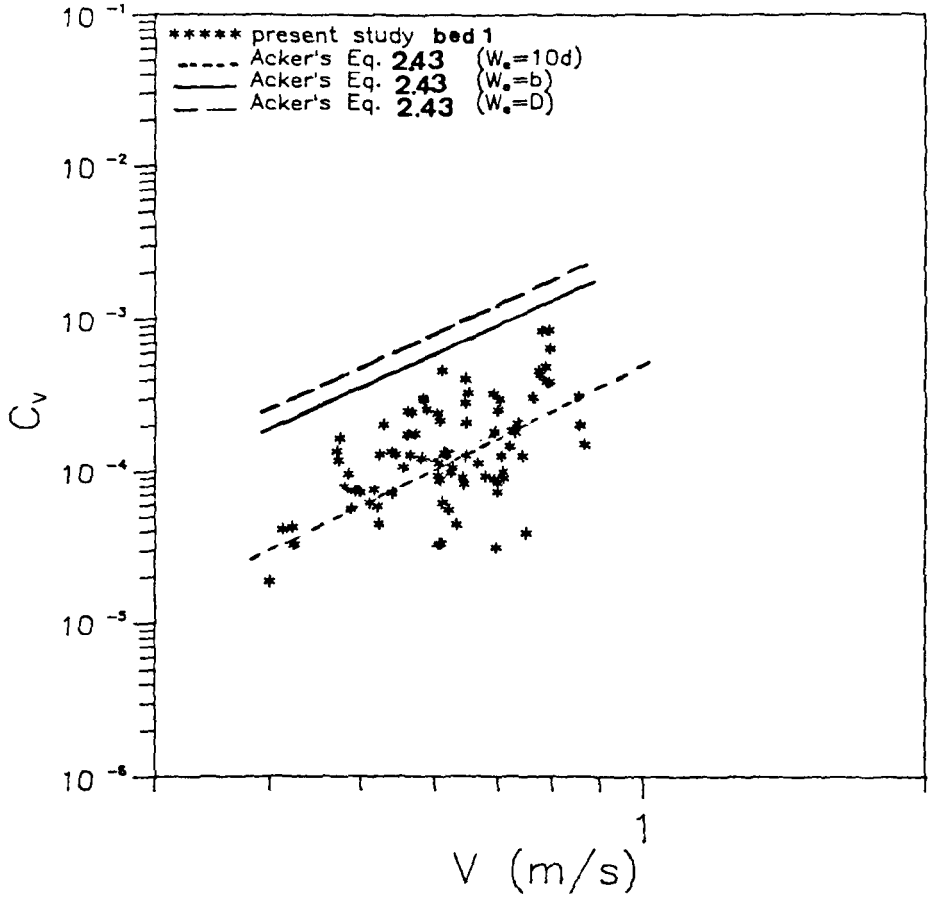

FIGURE 7.9 LIMIT OF DEPOSITION: EXPERIMENTAL DATA AT UP TO HALF-FULL FLOW COMPARED WITH ACKERS' EQUATION (2.43) (BED 1)

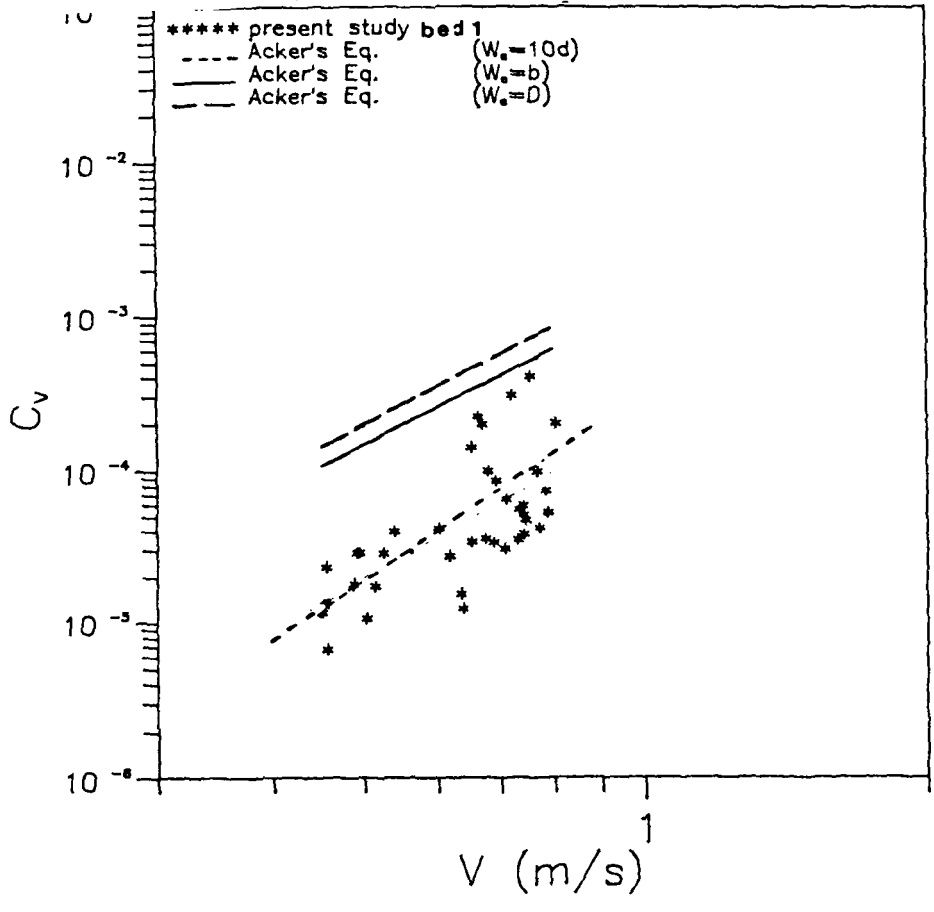

FIGURE 7.10 LIMIT OF DEPOSITION: EXPERIMENTAL DATA AT MORE THAN HALF-FULL FLOW COMPARED WITH ACKERS' EQUATION (2.43) (BED 1)

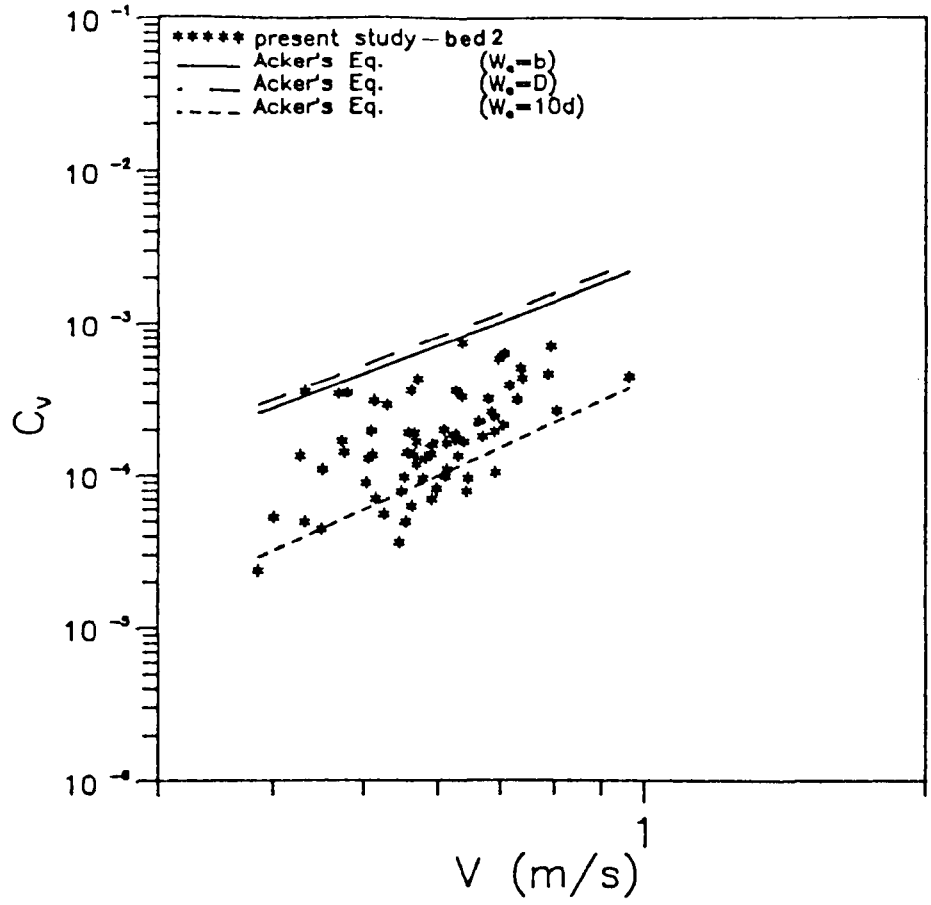

FIGURE 7.11 LIMIT OF DEPOSITION: EXPERIMENTAL DATA AT UP TO HALF-FULL FLOW COMPARED WITH ACKERS' EQUATION (2.43) (BED 2)

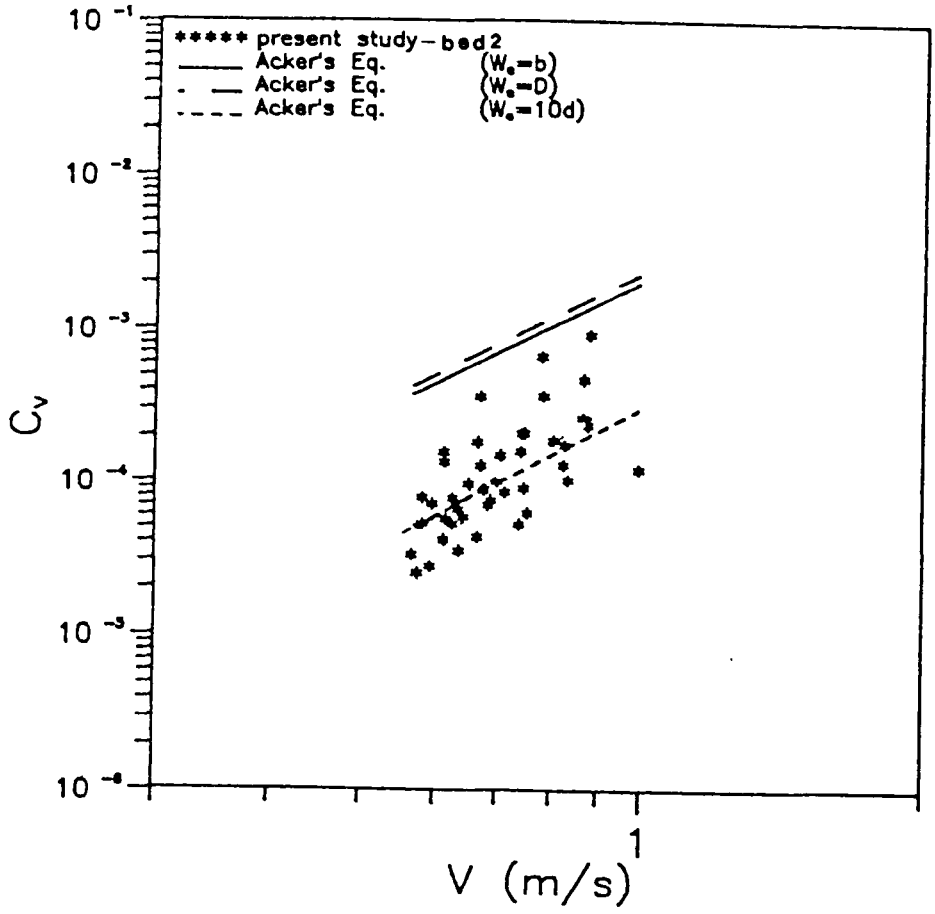

FIGURE 7.12 LIMIT OF DEPOSITION: EXPERIMENTAL DATA AT MORE THAN HALF-FULL FLOW COMPARED WITH ACKERS' EQUATION (2.43) (BED 2)

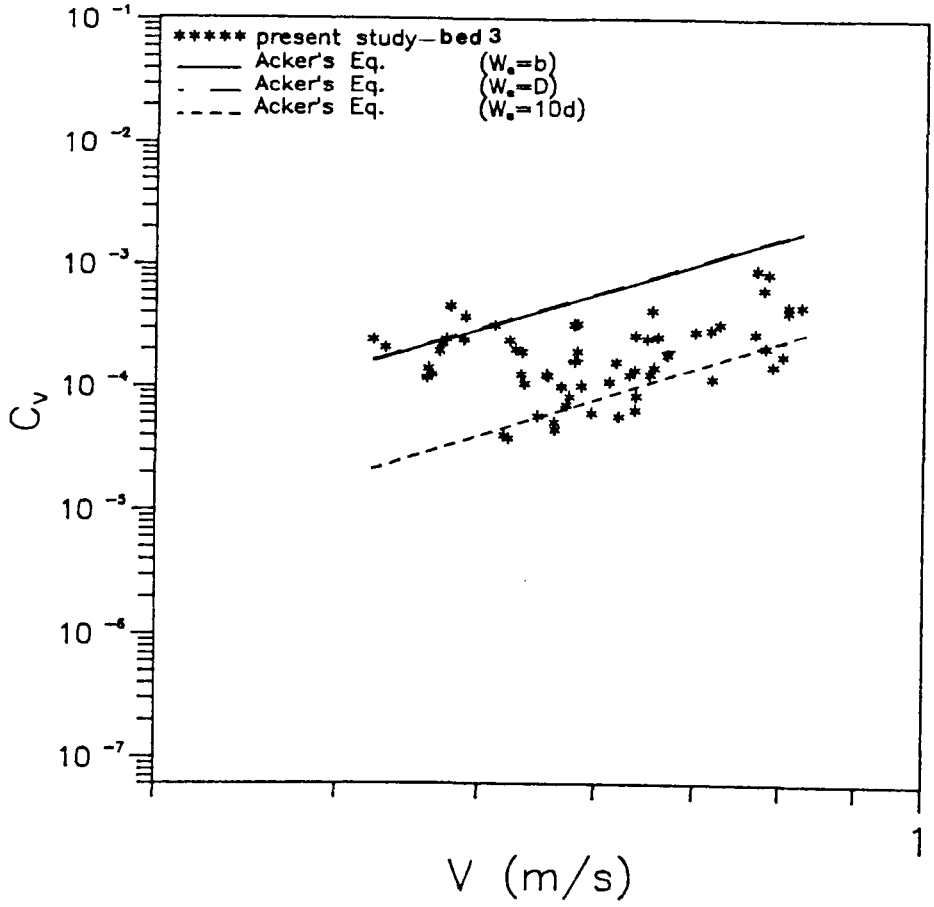

FIGURE 7.13 LIMIT OF DEPOSITION: EXPERIMENTAL DATA AT MORE THAN HALF-FULL FLOW COMPARED WITH ACKERS' EQUATION (2.43) (BED 3)

hydraulic data were used to calculate the predicted sediment rates.

To examine the effect of bed roughnesses on the performance of Ackers' equation, computed sediment rates (by Ackers' equation) were plotted against measured values for the three different bed roughnesses (smooth, k_s=0.8 mm and k_s=1.4mm) as shown in Figures 7.14. It is seen from the figure that, with effective width equal to bed width, Ackers' equation (Eq. 2.43) in general over-predicts the transport rate for all three roughness cases.

It is important to mention here that Ackers' equation was developed basically for wide open channels and thereafter was modified for application to circular channels with deposited beds simply by introducing the term "effective width".
Similar trends were observed when computed sediment rates for the other two beds (bed 2 and bed 3) were compared with the measured values.

Fig. 7.15 shows a comparison between measured volumetric sediment concentration with predicted values using Loveless' equation (Eq.2.44), which is developed for various channel shapes as stated by Loveless (1986). In Eq. 2.44 the drag coefficient is assumed to be 1.7, the lift force coefficient to be zero, α_2/α_1 to be 1, and spacing coefficient (η) to be 0.5. It must be emphasized here that the above coefficients have been confirmed by Loveless himself (1986) to be fairly correct.
One coefficient for which Loveless could not come to any conclusion about its value, though, is the friction angle. He observed a wide variation in the mean values of the friction angle ranging from 28° for coarse particles on a smooth surface, to 55° for the fine particles on a rough surface. This led to the conclusion that friction angle is strongly dependent on d/k_s and the shape of the particles. The exact relationship is not known. For the purposes of this study the friction angle in Loveless' equation was assumed to be 45°. This value was assumed with the full realisation that it might not be totally right since it could

underestimate or overestimate some values. However, it was essential that the friction angle in Loveless' equation be formulated in such a way as to render the equation easy to solve.

It is clear from Fig. 7.15 (based on the assumption of 45° friction angle) that Loveless' equation over-predicts sediment concentrations. The explanation lies in the fact that Loveless' equation was theoretically derived from a basic balance of forces on the particles and then tested against a very small range of experimental data and with small particles. Therefore, the equation can not be safely applied to predict the sediment concentration in circular cross section channels with flat beds.

It is interesting to mention here that, due to assuming 45° for the friction angle, the Loveless equation predicted negative values in the sediment concentration which are not shown in Fig. 7.15.

Fig. 7.16 compares measured volumetric sediment concentration values against those predicted using May et al's equation (Eq. 3.6) for all three roughness cases of bed 1. It is clear that the present data are not in agreement with May et al's equation which was proposed for circular channel with small deposited loose bed thickness (t_s/D= 1.0%).

Two main reasons contributed to the failure of Eq. 3.6 to fit the measured sediment rate. These are: firstly, May et al (1989), in their experimental work, used a loose bed which

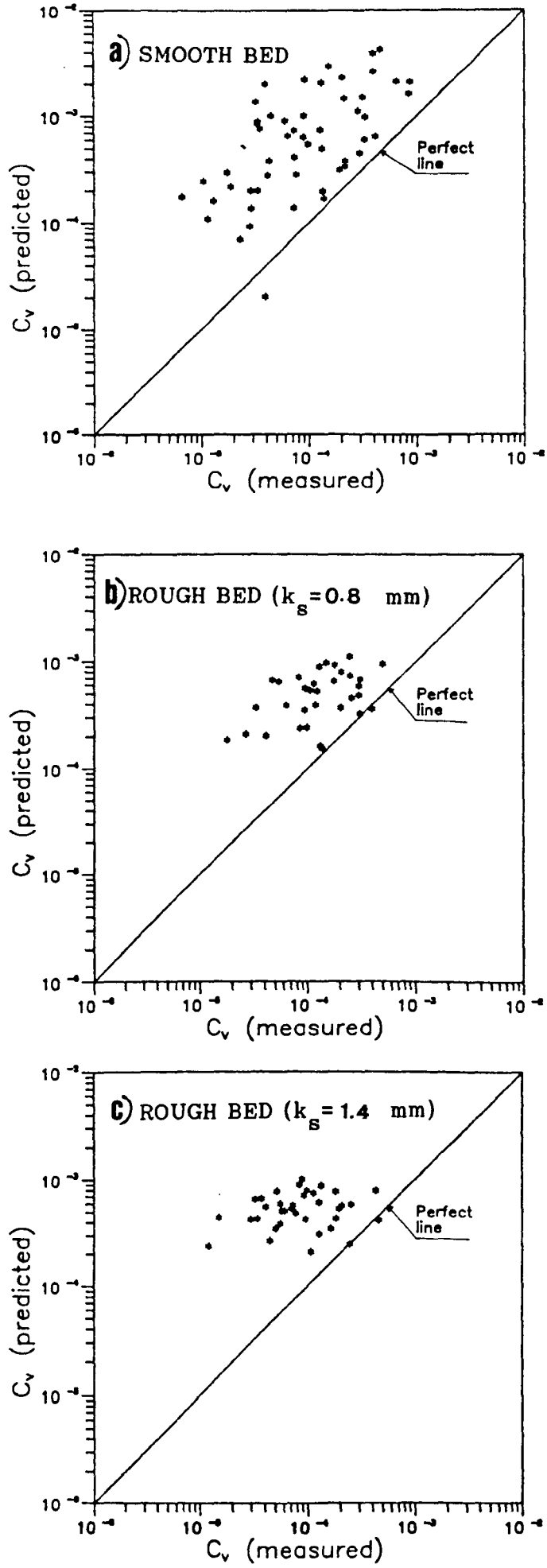

FIGURE 7.14 COMPARISON BETWEEN THE MEASURED SEDIMENT CONCENTRATION VS. COMPUTED SEDIMENT CONCENTRATION BY ACKERS' EQUATION 2.43 (BED 1) (W_e=6)

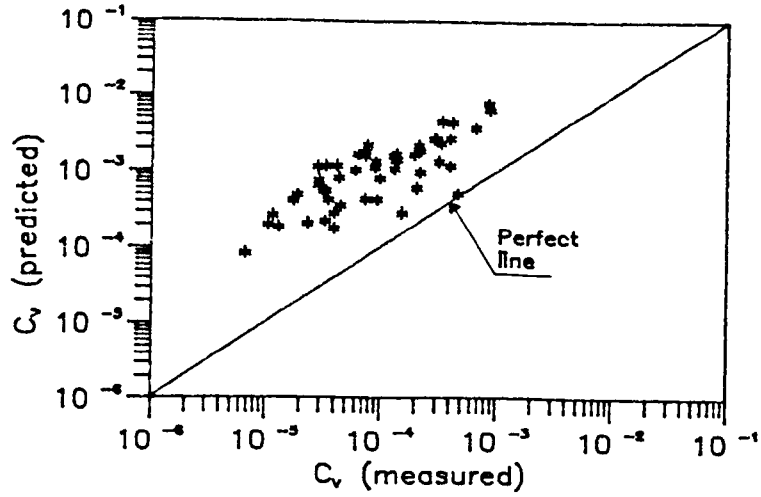

a) smooth bed

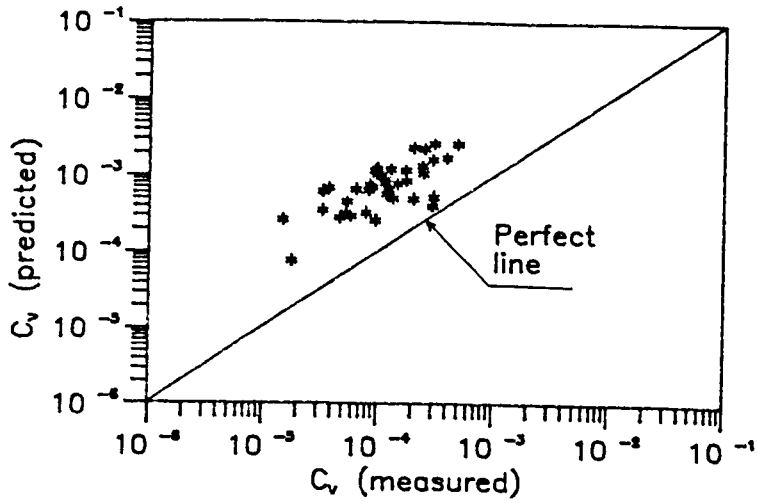

b) roughness I (k_s=0.8 mm)

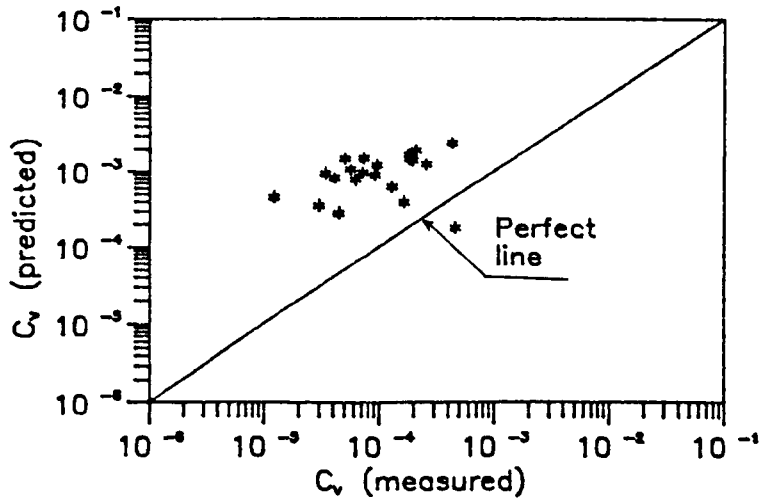

c)roughness II (k_s=1.4 mm)

FIGURE 7.15 COMPARISON BETWEEN THE MEASURED SEDIMENT CONCENTRATION VS. COMPUTED SEDIMENT CONCENTRATION BY LOVELESS EQUATION 2.44 (BED 1)

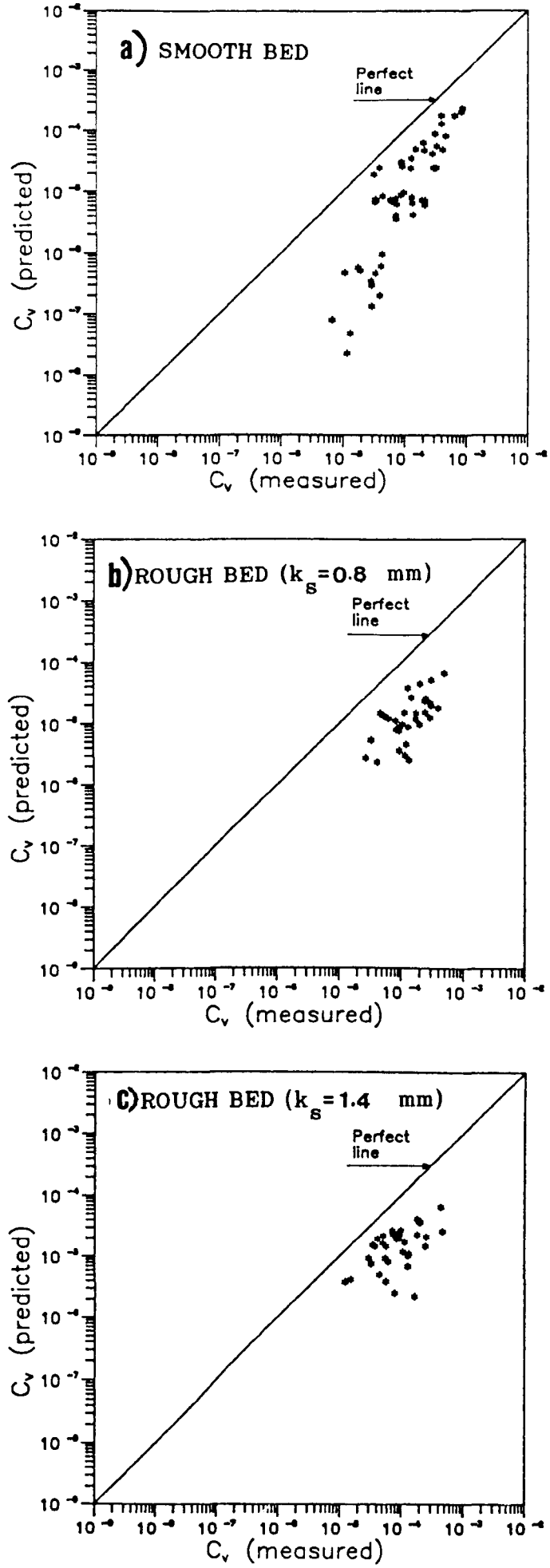

FIGURE 7.16 COMPARISON BETWEEN THE MEASURED SEDIMENT CONCENTRATION VS. COMPUTED SEDIMENT CONCENTRATION BY MAY ET AL'S EQUATION 3.6 (BED 1)

presents a higher flow resistance than a fixed bed thus requiring some of the flow energy to be dissipated in overcoming the increased resistance. Secondly the bed width of the channel employed was very small, compared with that used in the present study, which could affect the sediment transport capacity of the channel as the sediment rate increases with bed width. It seems that more work is needed to improve May et al's equation before it can be safely applied to circular cross section channels with deposited beds.

Alvarez's equation (Eq. 3.11) (which was derived for circular cross section channels with fixed sediment bed, t_s/D-0.26, smooth and rough beds, $0.0<k_s(mm)<2.3$) was tested against the present data for the three bed roughnesses (see Figure 7.17). It can be seen that Alvarez's equation is in reasonable agreement with the present data of smooth bed (see Fig. 7.17a). However, it over-predicts the sediment rate in roughness case II (k_s- 1.40 mm) (see Figure 7.17c).
It must be mentioned here that the same definition of the non-deposition condition used by Alvarez (1990) was adopted by the author. Moreover, as in the case of Alvarez the present study has been over fixed beds. The slight discrepancies between the present study and Alvarez's predictions could be attributed to the fact that only a few experiments were conducted by Alvarez (1990) which makes Eq. 3.11 not highly reliable.

It can be concluded that Ackers' equation (2.43) for effective width equal to bed width over-predicts the limiting concentrations of the three beds. However, when effective width is computed as 10d then Ackers' equation gives more reasonable results especially for the data of the two beds (bed 1 and bed 2) and it underpredicts the limiting concentrations for the data of higher sediment bed (bed 3). Loveless's equation (2.44) gives similar results to Ackers' equation; in other words it also over-predicts the limiting sediment concentrations.

May et al's equation (3.6), although derived for circular cross section channels with loose deposited beds, under-predicts the sediment concentrations. Not surprisingly, Alvarez's equation shows reasonable agreement with the present experimental data since the equation was developed from data collected in circular cross section channels with fixed beds.

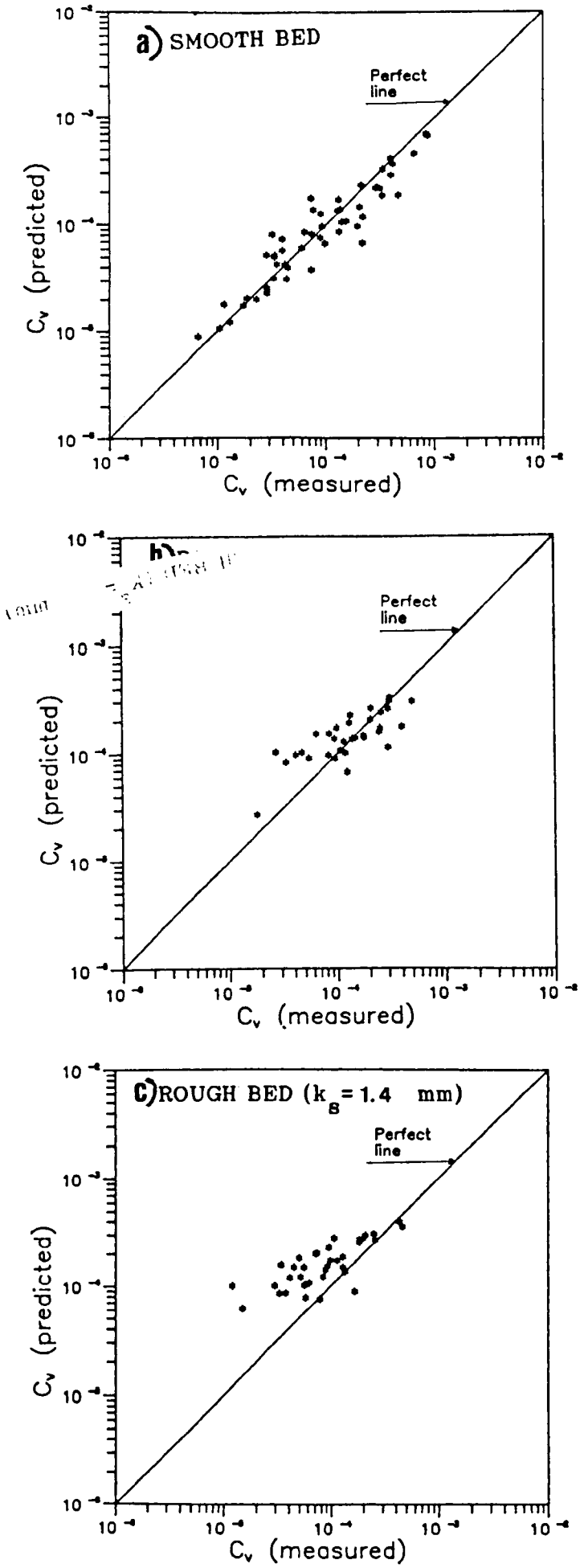

FIGURE 7.17 COMPARISON BETWEEN THE MEASURED SEDIMENT CONCENTRATION VS. COMPUTED SEDIMENT CONCENTRATION BY ALVAREZ'S EQUATION 3.11 (BED 1)

7.5 Modification of Ackers' Equation

It needs to be stated that Ackers' equation was derived basically for wide alluvial channels. In applying it to pipes the difficulty is in defining the applicable effective width. For the limit of deposition condition Ackers used the experimental results of May (1982) which suggested a width of 10 times the particle diameter. CIRIA (1987) reported that this approach gives very high velocity requirements in large sewers. May's (1982) experiments were carried out on a very limited range of pipe sizes and it may be that, in addition to sediment size, the effective width for this condition is also a function of pipe diameter or the bed width.

Therefore, an attempt was made to modify Ackers' equation in order that it could predict limiting concentrations in circular cross section channels with deep deposited beds (t_s up to 0.4 D). Effective width is the only term which could be modified in the equation because it has not get a sharp definition. After modification it was found that the equation could fit the smooth bed 3 ($t_s/D=0.39$) channel data if the effective width became

$$W_e = 8\ d_{50}\ (b/y_o) \qquad (7.5)$$

with r=0.78,

and for bed 3 with roughness I (k_s=0.8 mm), a good fit could be achieved if effective width became

$$W_e = 6\ d_{50}\ (b/y_o) \qquad (7.6)$$

with r=0.83.

For bed 3 with roughness II (k_s=1.4 mm), Ackers equation could give a good fit when

$$W_e = 3\ (d_{50}/y_o)\ b \qquad (7.7)$$

with r=0.87.

When the preceding three equations were combined into a single equation for the three roughness cases of bed 3, the following equation was obtained for effective width

$$W_e = 5.5\ d_{50}\ (b/y_o) \qquad (7.8)$$

with r=0.70.

The effective width in Ackers' equation (2.43) was then replaced by 5.5 $d_{50}(b/y_o)$ and the Ackers' equation is called hereafter "modified Ackers' equation". The modified Ackers' equation was tested against the experimental data of the three beds (bed 1, bed 2 and bed 3) as shown in Figs. 7.18.1, 7.18.2 and 7.18.3. It can be seen from the figures that the equation gives a reasonable estimate of the limiting sediment concentration with correlation coefficients equal to 0.87, 0.67 and 0.70 for the experimental data of bed 1, bed 2 and bed 3 respectively.

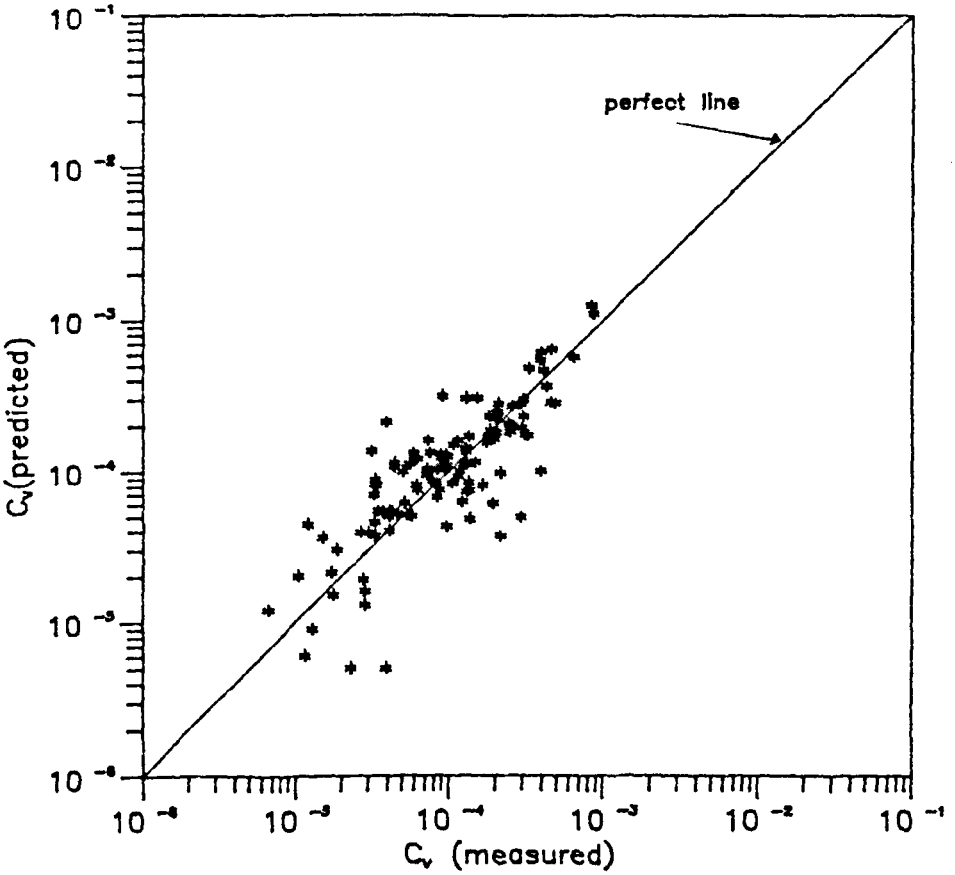

FIGURE 7.18.1 COMPARISON BETWEEN THE MEASURED SEDIMENT CONCENTRATIONS VS. COMPUTED VALUES BY MODIFIED ACKERS' EQUATION $\left\{W_* = 5.5\ d(b/y_o)\right\}$ (bed 1 data)

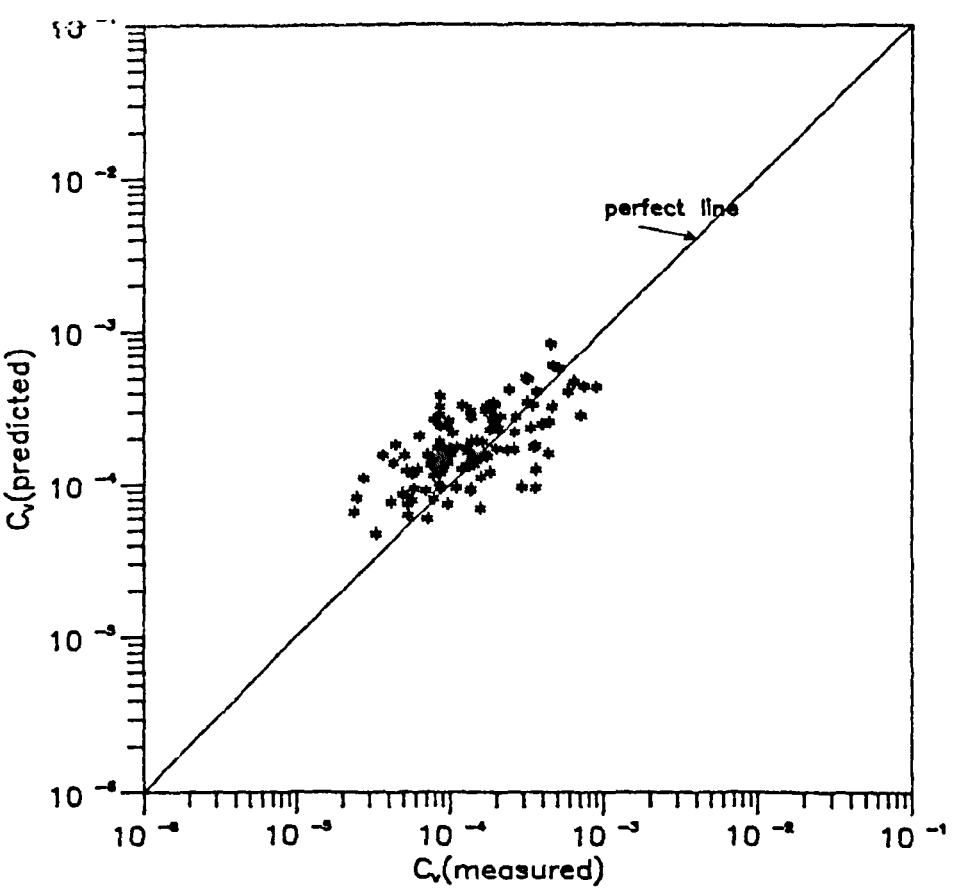

FIGURE 7.18.2 COMPARISON BETWEEN THE MEASURED SEDIMENT CONCENTRATIONS VS. COMPUTED VALUES BY MODIFIED ACKERS' EQUATION $\left\{W_* = 5.5\ d(b/y_o)\right\}$ (bed 2 data)

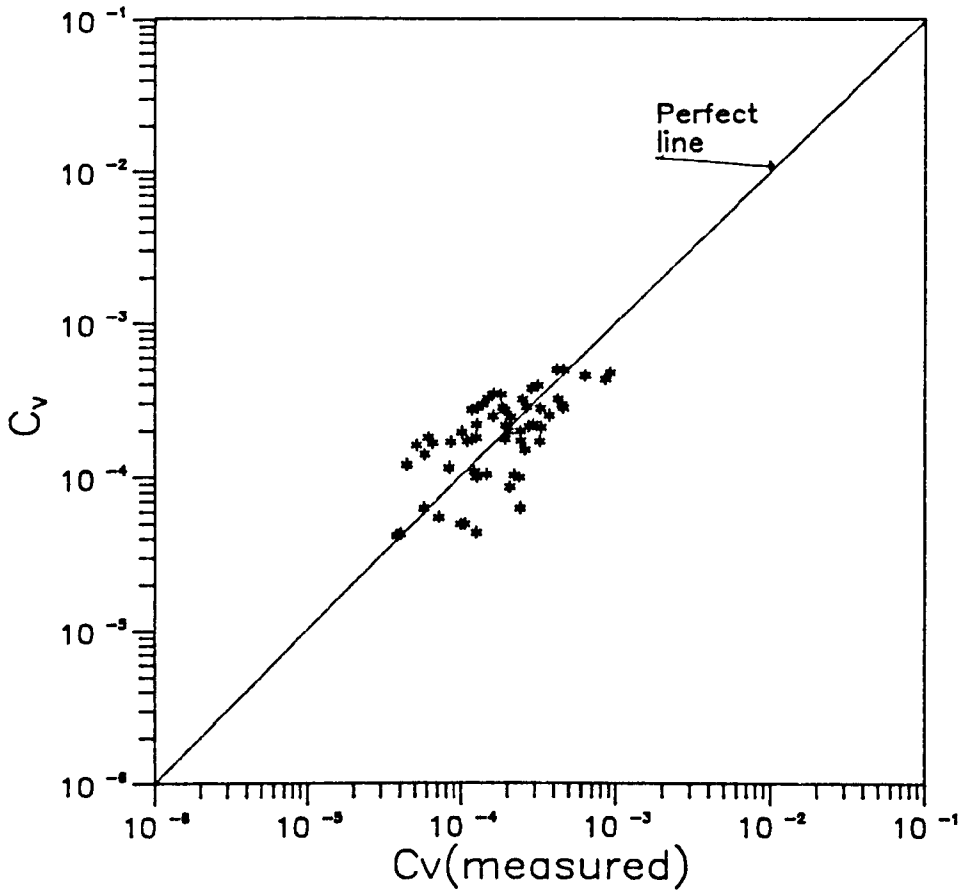

FIGURE 7.18.3 COMPARISON BETWEEN THE MEASURED SEDIMENT CONCENTRATIONS VS. COMPUTED VALUES BY MODIFIED ACKERS' EQUATION $\left\{W_e=5.5\ d(b/y_o)\right\}$ (bed 3 data)

7.6 Effect Of Bed Width

The influence of sediment bed thickness (bed width) on sediment transport is illustrated in Figs 7.19 and 7.20, where the volumetric sediment concentration is plotted against bed shear stress parameter for the various bed thicknesses used, for the sand sizes 1.0 and 8.4 mm respectively. It is apparent in from Figs. 7.19 and 7.20 that for similar levels of bed shear stress the volumetric

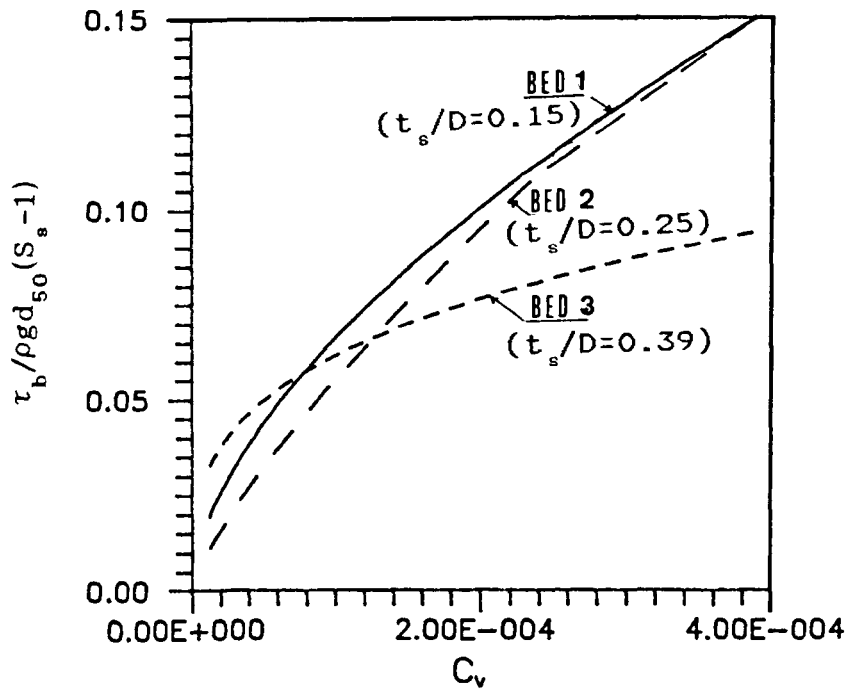

FIGURE 7.19 SHEAR PARAMETER ($\tau_b/\rho g d_{50}(S_s-1)$) AGAINST C_v
(sand size= 1.0 mm, smooth beds)

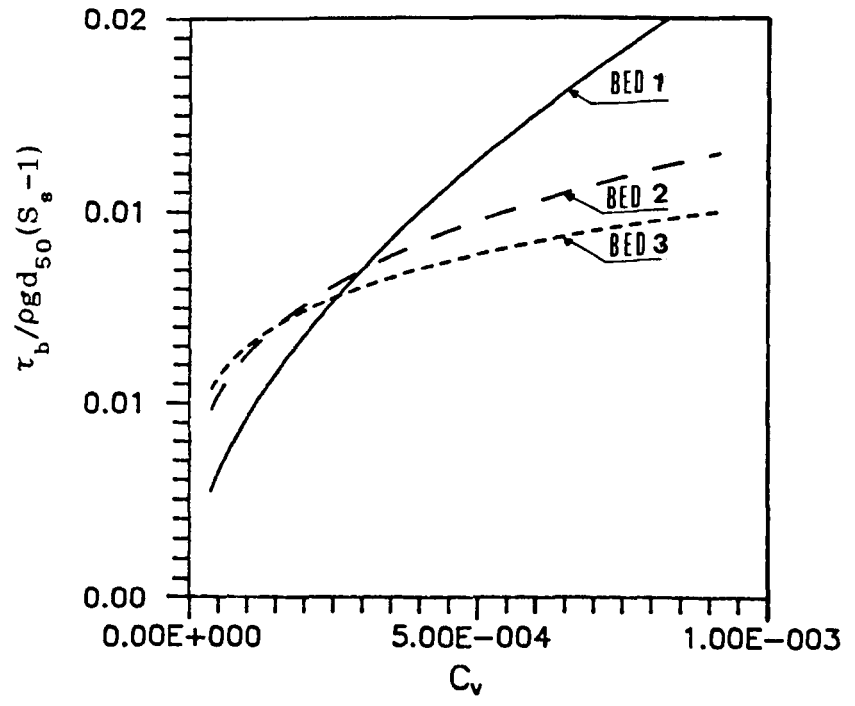

FIGURE 7.20 SHEAR PARAMETER ($\tau_b/\rho g d_{50}(S_s-1)$) AGAINST C_v
(sand size=8.4 mm, smooth beds)

sediment concentration generally increases with bed thickness. However, at very small values of C_v there is no clear relation between critical bed shear stress and sediment bed thickness as the curves tend to cross and overlap. Similar findings were reported by Alvarez (1990).

In Fig. 7.21 Kithsiri's (1990) Eq. 2.32, which was developed from Mayerle's (1988) and Kithsiri (1990) data in rectangular cross section channels with smooth and rough beds, is tested against the present data for flows up to half-full depths for comparison. The bed shear stress parameters $(\frac{\tau_b}{\rho g d_{50}(S_s-1)})$ were calculated using Eq. 2.32 and plotted together with the measured values for limit deposition condition. It can be observed that Kithsiri's equation (2.32) predicts higher values of minimum bed shear stress. The above observation can be explained by the shear stress distribution. In circular cross section channels with fixed beds and at flows up to half-full depths the bed shear stress near the corners could be larger than that of the rectangular channels as high momentum fluid is transported from the free surface region towards the channel corner by downflow vortex, and consequently the wall shear stress increased by this high momentum fluid (see Tominaga et al 1989). Therefore one can conclude that the efficiency of circular cross section channels with flat beds in transporting sediments is higher than that of rectangular ones.

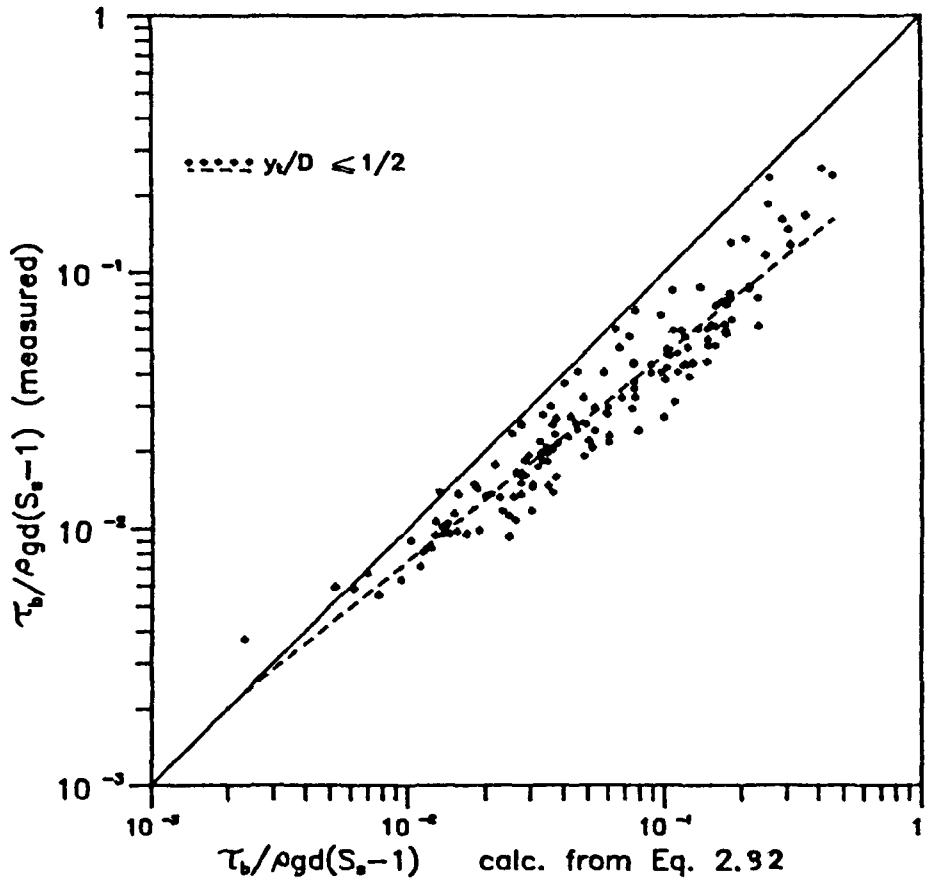

FIGURE 7.21 COMPARISON BETWEEN EQ. 2.32 AND PRESENT STUDY FOR FLOWS UP TO HALF-FULL DEPTH

7.7 Bed Load Models

7.7.1 General

Previous investigations of bed-load transport have generally been carried out either in circular cross section channels (clean pipe) or in circular cross section channel with loose beds. The present experimental results are of particular interest as they were obtained from circular cross section channels with fixed sediment beds.

From the foregoing analysis it can be concluded that almost all the available methods claimed to be applicable to predict sediment transport in circular cross section channels with sediment beds failed to fit the present data. The reason for their failure was explained in earlier sections.

All the analyses discussed in early sections were based mostly on the limiting velocity for non-deposition. However, recent design models favour critical shear stress criterion, (by adopting a single value of shear stress and using Manning's equation, velocity increases with pipe size); thus in this study critical shear stress will be considered instead of critical velocity criterion (i.e. when the shear stress was less than the critical shear stress at the limit of deposition, sediment depositions were considered to be formed).

An ideal method of bed load estimation would be based on four criteria; these are that it should:

(a) consider all important parameters influencing the mechanism of sediment transport

(b) be simple in its solution

(c) require easily obtainable data

(d) give accurate results

It is clear from the analysis in the preceding sections that there is no such ideal method currently in existence for predicting the sediment transport in circular channels with flat beds. Thus, there is need for a new method based on the above criteria. The functional relationships in equations 7.1, 7.2 and 7.3 (see section 7.1) are thought to represent such a method. The data from the three bed thicknesses employed in this study have been utilized to obtain coefficients of the functional relationships (Eqs. 7.1, 7.2 and 7.3). The equations are presented in the following sections.

7.7.2 Proposed Sediment Transport Equations

As mentioned in section 7.1, sediment transport rate in circular cross section channels with flat beds depends on a large number of factors such as flow depth (y_o), slope of the channel (S), sediment particle size (d), density of sediment (ρ_s), kinematic viscosity of fluid (υ), friction factor (λ_s), channel bed width (b) and acceleration due to gravity (g).

With the help of dimensional analysis, these quantities can be reduced to a smaller number of dimensionless parameters as described in section 7.1.

Log-Log plots of non-dimensional shear stress parameter $\tau_o/\rho g d_{50}(S_s-1)$ versus C_v (for the three roughness cases) are shown in Figs. 7.22, 7.23 and 7.24 for bed 1, bed 2 and bed 3 respectively, resulting in a different function for each sediment size investigated on each roughness. It is apparent from Figs. 7.22 to 7.24 that for a given level of mean shear stress the rate of transport for the larger sand is greater. This is due to the greater exposed area of the larger particles, which are subjected to drag forces exerted by the flow. The curves corresponding to sediment particles for smooth and rough beds show a variation in slope, and a decrease in transport rate for increasing bed roughness.

The objective of this study was to develop a model for evaluation of mean or bed shear stress at the limit of deposition for any bed roughness condition. Therefore, the data obtained from 290 experiments carried out in three different bed thicknesses and three different bed roughnesses were combined and utilized to develop equations from the functional relationships in equations 7.1 to 7.3.

A multiple regression analysis was performed to obtain coefficients of the functional relationships 7.1, 7.2, and 7.3 for all beds ($0.15<t_s/D<0.39$) and all roughnesses ($0.0<k_{s\,(mm)}<1.4$). The resulting relations can be expressed for different degrees of filling namely for flows at up to half-full depths and at more than half-full depths (to take into consideration the shape effect due to the change in the

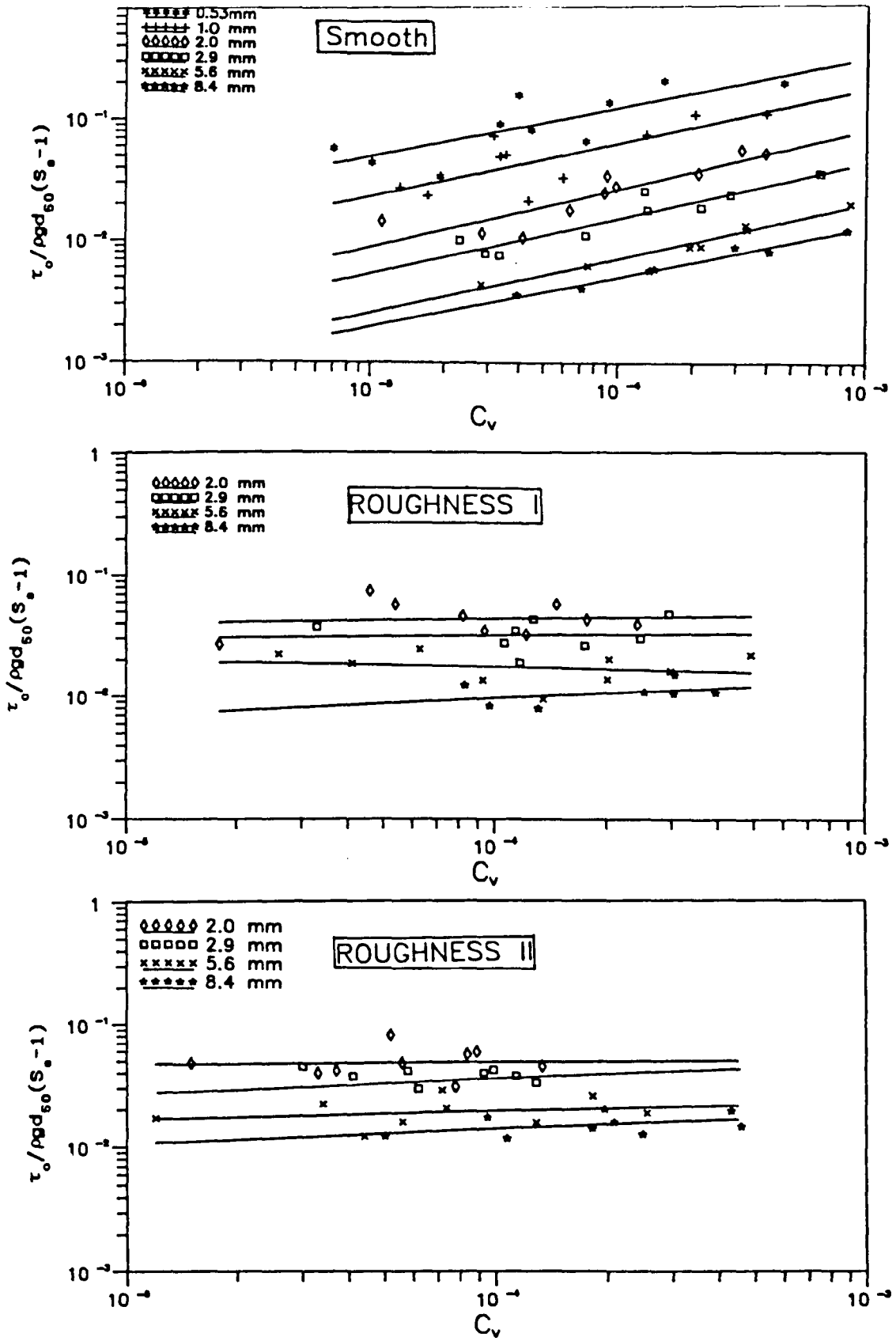

FIGURE 7.22 SHEAR STRESS PARAMETER VS. LIMITING SEDIMENT CONCENTRATION (47 mm thick bed)

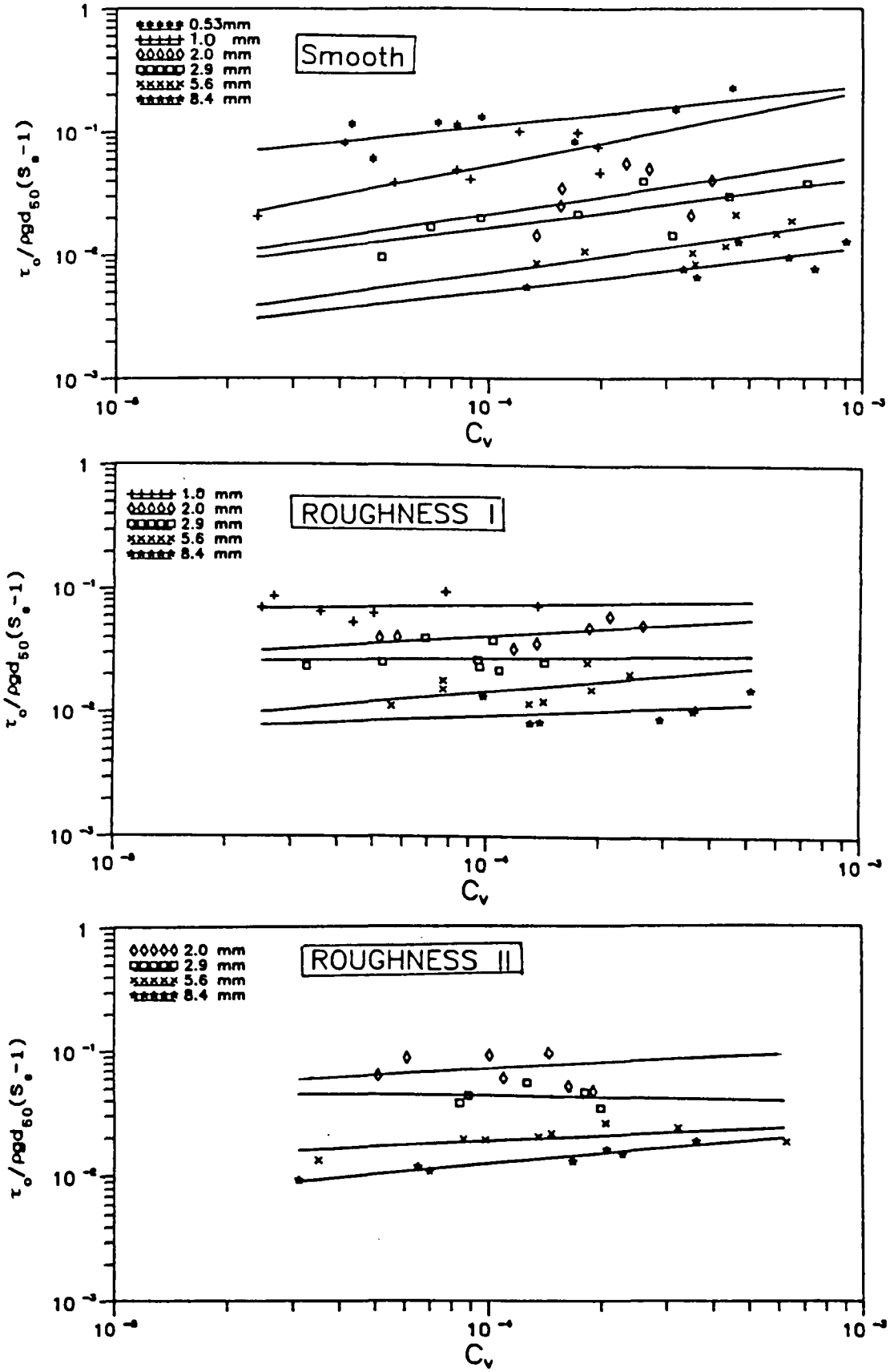

FIGURE 7.23 SHEAR STRESS PARAMETER VS. LIMITING SEDIMENT CONCEMNTRATION
(77 mm thick bed)

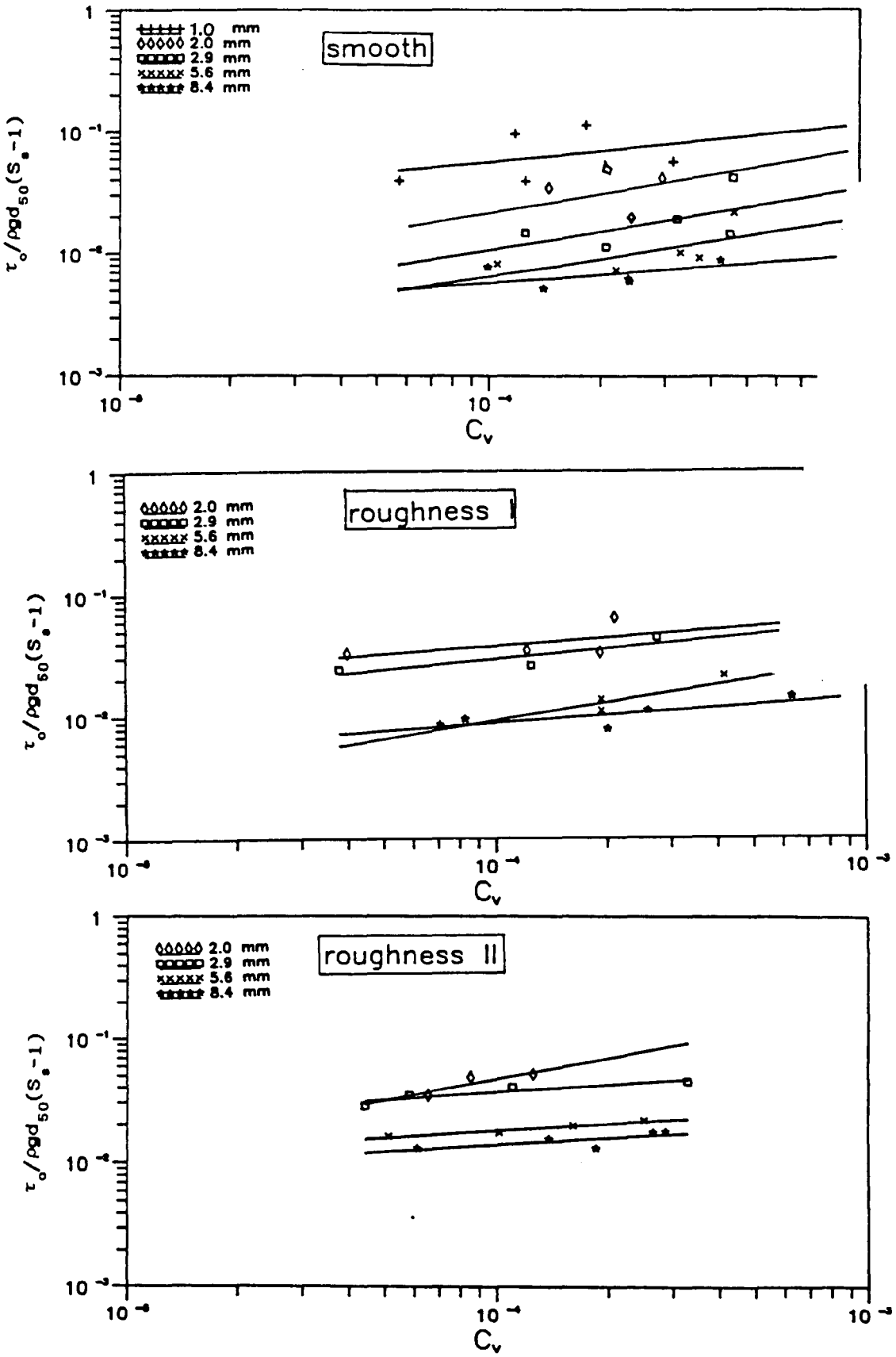

FIGURE 7.24 SHEAR STRESS PARAMETER VS. LIMITING SEDIMENT CONCENTRATION (120 mm thick bed)

flow section corresponding to change in sediment bed and flow depths) and to the entire range of flow depths.

i) For Flows At Up To Half-Full Depth ($0.3 < y_t/D < 0.5$):

Using the mean values (mean shear stresses) a multi-regression was performed and the best fit equation was found to be:

$$\frac{\tau_o}{\rho g d_{50}(S_s-1)} = 0.29 \quad C_v^{0.31} \left[\frac{b}{y_o}\right]^{-0.89} \left[\frac{d_{50}}{D}\right]^{-1.12} \left[\lambda_s\right]^{1.05} \tag{7.9}$$

with r=0.97. Using the separated values (bed shear stresses) Eq. 7.9 becomes:

$$\frac{\tau_b}{\rho g d_{50}(S_s-1)} = 0.34 \quad C_v^{0.31} \left[\frac{b}{y_o}\right]^{-0.92} \left[\frac{d_{50}}{D}\right]^{-1.12} \left[\lambda_{sb}\right]^{1.09} \tag{7.10}$$

with r= 0.98.

Eq. 6.10 can be re-written (using Darcy-Weisbach's equation 2.27) as:

$$\frac{V}{\sqrt{g d_{50}(S_s-1)}} = 1.65 \quad C_v^{0.16} \left[\frac{b}{y_o}\right]^{-0.46} \left[\frac{d_{50}}{D}\right]^{-0.56} \lambda_{sb}^{0.05} \tag{7.11}$$

For the evaluation of the overall friction factor with sediment, λ_s, functional relation 7.3 becomes:

$$\lambda_s = 1.1 \quad C_v^{0.009} \left[\frac{b}{y_o}\right]^{0.081} \left[\lambda_c\right]^{1.0} \tag{7.12}$$

with r= 0.99.

It was found that the bed friction factor with sediment, λ_{sb}, is strongly dependent on the overall friction factor, λ_s, and it was found that

$$\lambda_{sb} = 3.6\ \lambda_s^{1.3} \tag{7.13}$$

with r=0.985.

ii) For Flows At More Than Half-Full Depth ($0.5<y_t/D<0.82$):

$$\frac{\tau_o}{\rho g d_{50}(S_s-1)} = 0.36\ C_v^{0.34} \left[\frac{b}{y_o}\right]^{-0.60} \left[\frac{d_{50}}{D}\right]^{-1.15} \left[\lambda_s\right]^{1.14} \tag{7.14}$$

with r=0.96.

$$\frac{\tau_b}{\rho g d_{50}(S_s-1)} = 0.47\ C_v^{0.34} \left[\frac{b}{y_o}\right]^{-0.67} \left[\frac{d_{50}}{D}\right]^{-1.17} \left[\lambda_{sb}\right]^{1.24} \tag{7.15}$$

with r= 0.96.

By using Darcy-Weisbach's equation (2.27), Eq. 7.15 can be re-written as:

$$\frac{V}{\sqrt{g d_{50}(S_s-1)}} = 1.94\ C_v^{0.17} \left[\frac{b}{y_o}\right]^{-0.34} \left[\frac{d_{50}}{D}\right]^{-0.59} \lambda_{sb}^{0.12} \tag{7.16}$$

$$\lambda_s = 0.824\ C_v^{0.0054} \left[\frac{b}{y_o}\right]^{0.03} \left[\lambda_c\right]^{0.93} \tag{7.17}$$

with r= 0.98.

$$\lambda_{sb} = 12.9 \quad \lambda_s^{1.6} \qquad (7.18)$$

with r=0.97.

iii) For The Entire Range Of Flow Depths:

Having developed equations for the data according to the degree of filling (at up to half-full and more than half-full flow depths), a regression analysis was performed for the different variables appearing in Equations 7.1, 7.2 and 7.3 for the entire data covering flow depths range of $0.3<y_t/D<0.82$. The following relationships were obtained:

The best fit equation for the evaluation of mean shear stress at the limit of sediment deposition in circular cross section channel with flat beds (see Fig. 7.25) could be written in the form

$$\frac{\tau_o}{\rho g d_{50}(S_s-1)} = 0.55 \quad C_v^{0.33} \left[\frac{b}{y_o}\right]^{-0.76} \left[\frac{d_{50}}{D}\right]^{-1.13} \left[\lambda_s\right]^{1.22} \qquad (7.19)$$

with r=0.96.

By using the computed bed shear stress (τ_b) and bed friction factor with sediments (λ_{sb}) (computed using Einstein-Vanoni's separation technique), Eq. 7.19 can be re-written as:

$$\frac{\tau_b}{\rho g d_{50}(S_s-1)} = 0.472 \; C_v^{0.33} \left[\frac{b}{y_o}\right]^{-0.80} \left[\frac{d_{50}}{D}\right]^{-1.14} \left[\lambda_{sb}\right]^{1.2} \qquad (7.20)$$

with r=0.97, (see Fig. 7.26)

In addition to the critical shear stress criterion, the process of sediment transport in circular cross section channel with flat beds can be described in terms of critical velocity as follows. Eq. 7.20 can be re-written (using Darcy-Weisbach's equation 2.27) as:

$$\frac{V}{\sqrt{g d_{50}\,(S_s-1)}} = 1.95\; C_v^{0.17} \left[\frac{b}{y_o}\right]^{-0.40} \left[\frac{d_{50}}{D}\right]^{-0.57} \lambda_{sb}^{0.10} \qquad (7.21)$$

For the evaluation of overall friction factor with sediment (λ_s) the following equation was developed (see Fig. 7.27).

$$\lambda_s = 0.88\; C_v^{0.01} \left[\frac{b}{y_o}\right]^{0.03} \left[\lambda_c\right]^{0.94} \qquad (7.22)$$

with r= 0.984.

The correlation between the bed friction factor with sediments (λ_{sb}), and the overall value of friction factor with sediments (λ_s) is very strong. Therefore, λ_{sb} is best described by the following equation

$$\lambda_{sb} = 6.6\; \lambda_s^{1.45} \qquad (7.23)$$

with r=0.96. It is clear from equation 7.23 that the bed friction factor λ_{sb} is always higher than the overall friction factor with sediments λ_s.

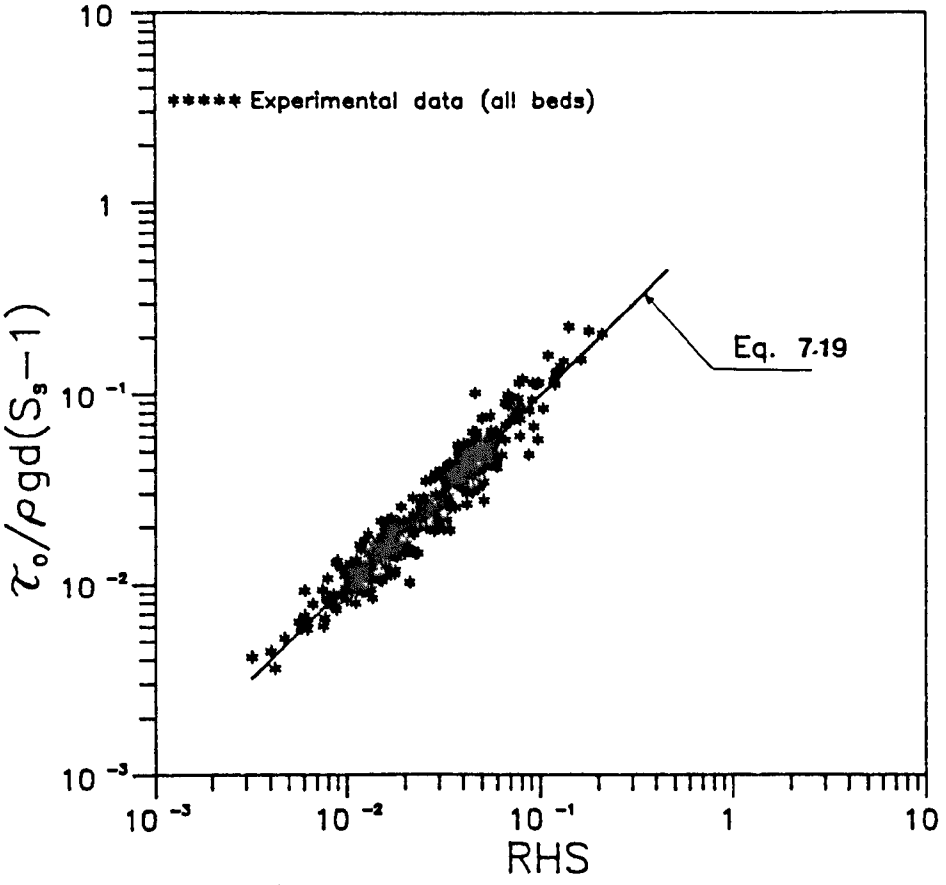

FIGURE 7.25 PLOT REPRESENTING EQ. 7.19 WITH THE COMBINED DATA (for all ranges of flow depths)

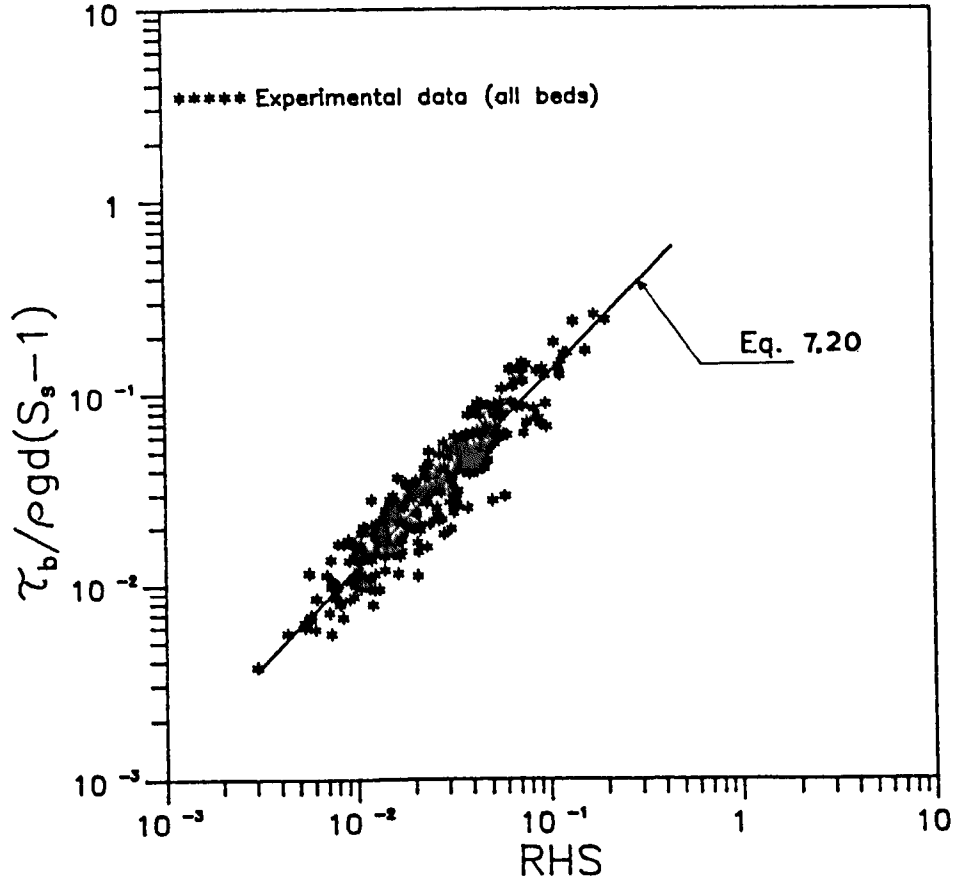

FIGURE 7.26 PLOT REPRESENTING EQ. 7.20 WITH THE COMBINED DATA (for all ranges of flow depths)

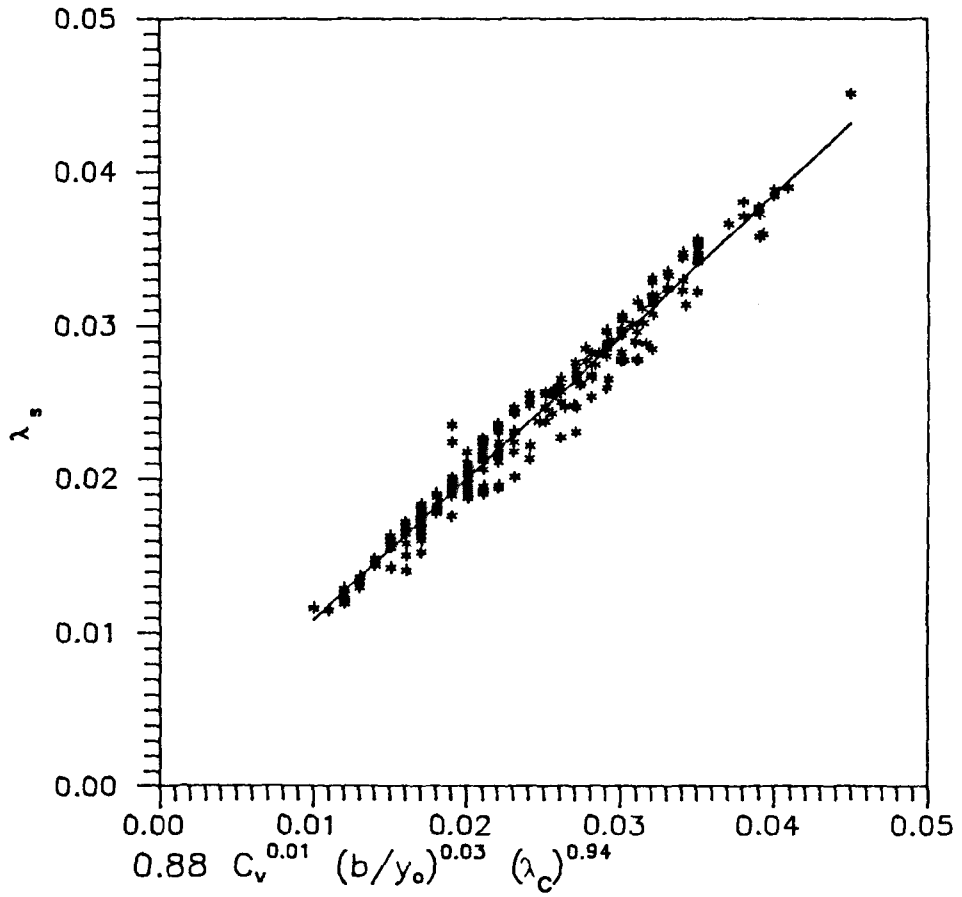

FIGURE 7.27 PLOT REPRESENTING EQ. 7.22

7.8 Model Verification

Equations 7.9 to 7.23, were developed from the present experimental data for three different cases: firstly, for flows up to half-full depths (Eqs. 7.9 to 7.13), secondly for flows of more than half-full depths (Eqs. 7.14 to 7.18) and lastly for the flows covering the entire range of flow depths (Eqs. 7.19 to 7.23). The above equations were obtained from the multiple regression analysis between the different parameters governing the sediment transport in circular cross section channel with flat beds, and the models were considered as being simple and suitable for use in engineering application. Statistical correlation coefficients were found to be strong for all developed equations. However, for the purpose of model verification only the third group of equations (i.e model applicable for all flow depths) will be considered.

The three main reasons behind this decision are:

1) reliability of the multiple regression equations could be improved by increasing the number of data in the sample which is used for developing them. Therefore the third group of equations which were developed from a higher number of experimental (290) tests covering wider parameter ranges can generally be used for computing the bed (or mean) shear stress at the limit of sediment deposition.

2) in sewer networks, the discharge can vary from time to time according to rainfall season and therefore, flow depths can vary accordingly.

3) the available published experimental data intended to be used for the verification of the developed models fits well with the third model (applicable to the entire range of flow depths).

7.8.1) Checking of The Present Equations Using Data Obtained From Circular Cross Section Channels With Fixed Beds

It has to be stressed here that, the problem of permanent deposition in sewers has not been dealt by researchers. However, Alvarez (1990) conducted an investigation in this area (though very limited) during his research work on the influence of cohesion on sediment transport in channels of circular cross section.

The present equations (Eqs.7.19, 7.20 and 7.21) were developed utilizing 290 experimental results; this number is considered high enough to support the model. The investigation was carried out using one circular cross section channel (D=305 mm) with different bed thicknesses.

To check the applicability of the present model to different pipe sizes, Eq. 7.20 (for all flow depths), was chosen to be checked by using Alvarez's (1990) data for non-cohesive sediment ($0.9 < d_{50}(mm) < 5.7$) over fixed smooth and rough beds ($t_s/D \cong 26\%$) in a circular cross section channel of 154 mm diameter. The right hand side of the equation was computed with Alvarez's data and plotted (see Fig. 7.28) against the

observed values of non-dimensional shear stress $(\frac{\tau_b}{\rho g d_{50}(S_s-1)})$.

The correlation coefficients between Alvarez's data and values computed using proposed equations (Eq.7.20) were found to be as high as 0.93. The fairly high correlation coefficient indicates that Alvarez's data agrees reasonably well with the proposed equation which could confirm its applicability for different pipe diameters.

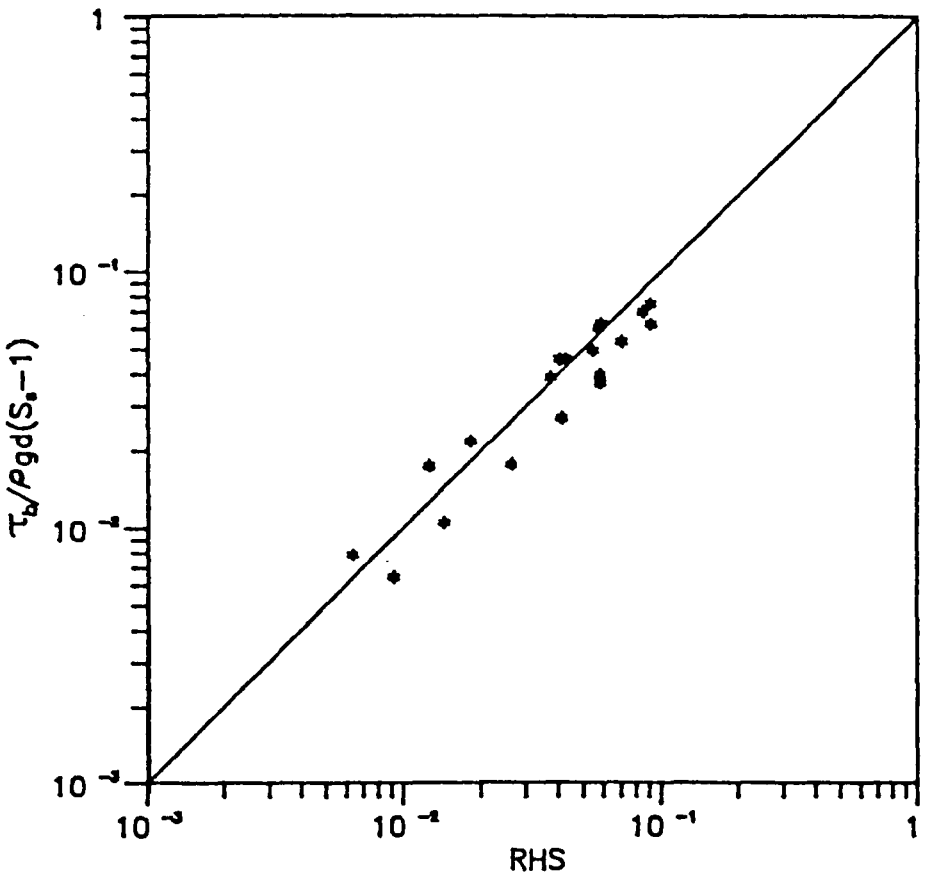

FIGURE 7.28 ALVAREZ'S RESULTS COMPARED TO THE EQ. 7.20

7.8.2 Checking of The Present Equations Using Data Obtained From Clean Pipe

One of the main objectives of this study was to develop a model for evaluation of mean shear stress at the limit of non-deposition for any pipe diameter with and without deposited beds. Therefore, Mayerle's study (1988) of sediment transport in smooth circular channel (D=152 mm) without deposited beds was utilized in this analysis to check the applicability of the proposed equations for circular cross section channel without deposited beds.

In circular cross section channels without flat beds, sediment particles move along the pipe invert over a very narrow band (W_s). Mayerle (1988) measured the width over which the particles were spreading. This spreading width was measured from underneath the channel in the horizontal direction. It has to be emphasized that the spreading width is not dependent on sediment size, but rather on channel shape. Mayerle et al (1991) confirmed that W_s/d can vary greatly (between 1 and 200).

For six sediment sizes ($0.5 < d\ (mm) < 8.74$) the average value of the relative spread (W_s/D, where W_s is the spreading width and D is the pipe diameter) was found to be 0.3 (Mayerle 1988). This value was also confirmed by the author, by conducting a few experiments in circular cross section channel (D=152 mm).

It must be mentioned here, that the value 0.3D is the width which the sediment particles occupy and within which they move close to each other at the invert of the pipe. However, in circular channel with flat beds, it has been observed in this investigation that although the sediment particles are spreading over the whole width of the bed the particles are not touching each other i.e. not as close as in the case of circular channel (clean pipe) and therefore they are not occupying the whole bed surface, but rather the greater part of it. For this reason it is clear that the apparent bed width over which the sediment moves in clean circular channel is not 0.3D but slightly higher.

The best agreement between Eq. 7.19 and Mayerle's data ($0.5<d_{50}$ (mm)<8.74) has been found when the bed width value (b) was replaced by 0.5D (equivalent bed width), where D is the pipe diameter.

In order to check the applicability of Equation 7.19 for bed width equal to 0.5D, the right hand side of the equation was computed and plotted against Mayerle's observed values of $\tau_o/\rho g d_{50}(S_s-1)$ as shown in Figure 7.29. This plot confirms that the data of Mayerle's for smooth circular channels is in good agreement, (r=0.97), with Equation 7.19 for bed width equal 0.5D.

In Fig. 7.30 Mayerle's data for smooth circular channel (clean pipe) were represented in terms of shear stress

parameter against the parameter b/y_o, where b was replaced by 0.5D, for different values of relative particle size (d/D). It is clear from the figure that good agreement exists between the results, which indicates the strong dependency of the shear stress parameter on the equivalent bed width (0.5D) and the relative particle size.

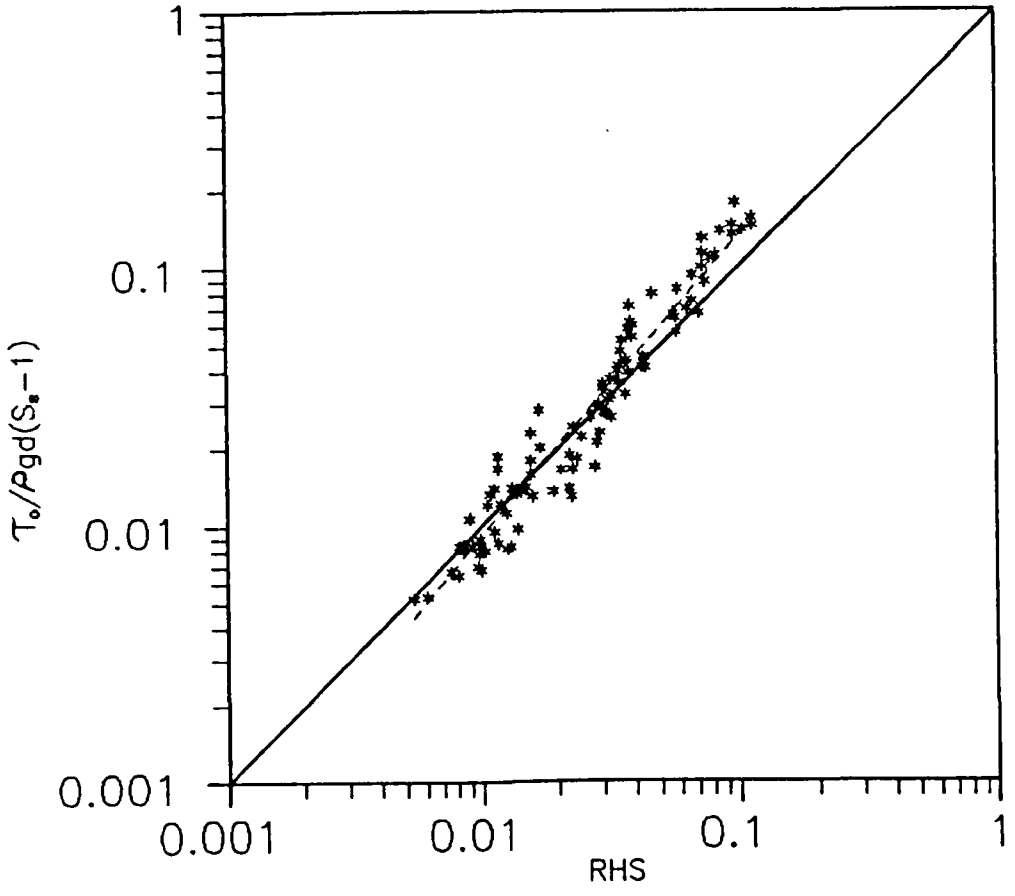

FIGURE 7.29 COMPARISON OF EQUATION 7.19 WITH MAYERLE'S (1988) DATA WITH b= 0.5 D (152 mm PIPE DIAMETER)

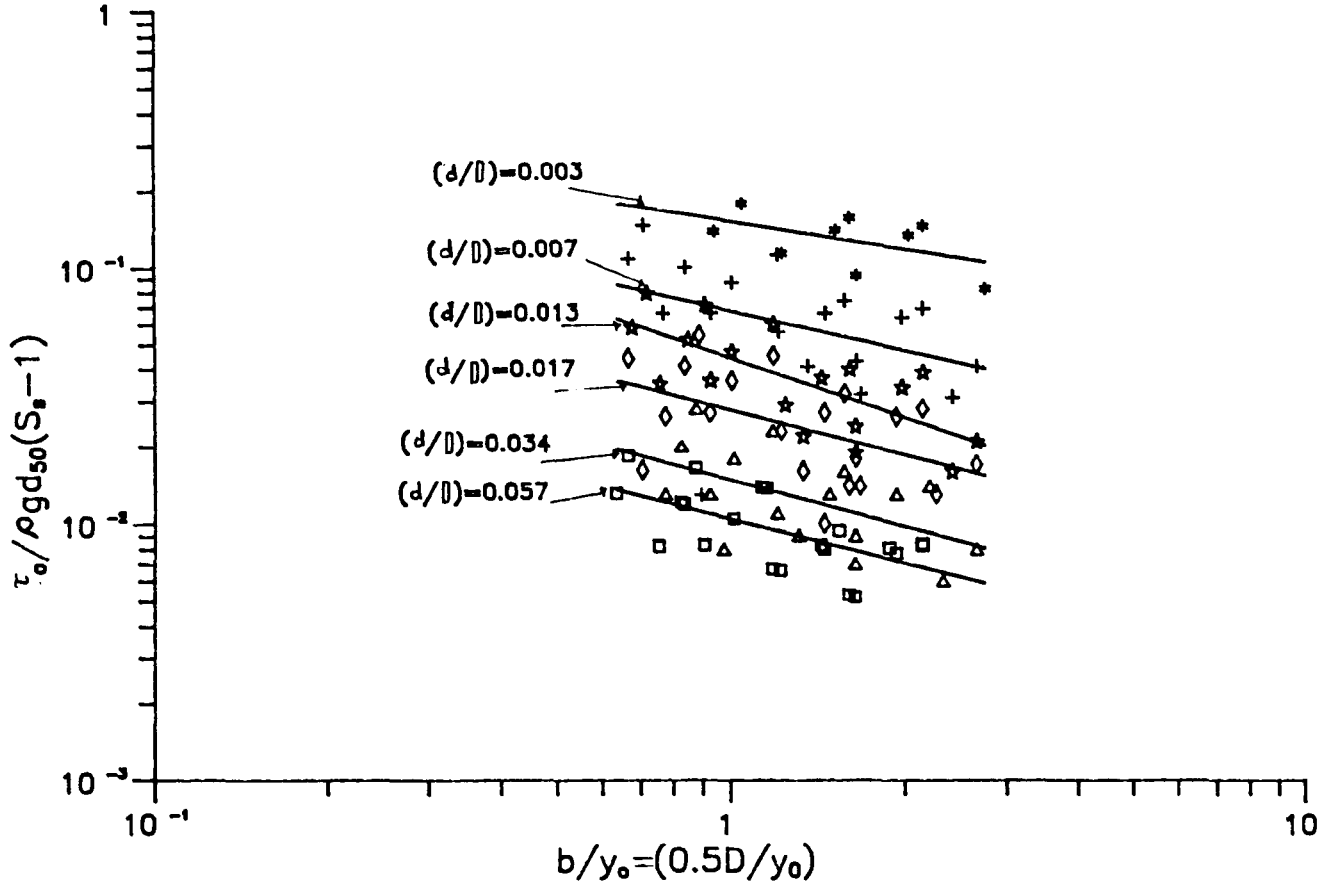

FIGURE 7.30 SHEAR STRESS PARAMETER AGAINST b/y_o
(Mayerle's data for clean pipe)

Further verification of the general application of Eq. 7.19, (with b=0.5D), for circular cross section channels without sediment bed was achieved by utilizing the Hare's (1989) experimental data (d=0.72 mm) from a circular cross section channel of 298.8 mm diameter. It is apparent from Fig. 7.31 that Eq. 7.19 (with b=0.5D) fits the data of full-pipe flows reasonably well, while it under-predicts the mean shear stress at limit of deposition for part-full flow ($0.49 < y_o/D < 1$).

It is important to mention here that Hare's experimental range was not high enough (as only one particle size was tested) to verify the above findings, thus more experiments are needed.

It can be concluded that the proposed equation (Eq. 7.19), is considered to have the following advantages:

(a) it contains all the possible hydraulic parameters such as friction factor with sediment, particle size, pipe diameter, shear stress, etc, that may affect sediment transportation in sewers.

(b) it is applicable to different sizes of sewers with and without sediment beds.

(c) it has been tested against the data obtained from channels without flat bed and proved to fit the data after replacing the bed width by 0.5D (where D is the pipe diameter).

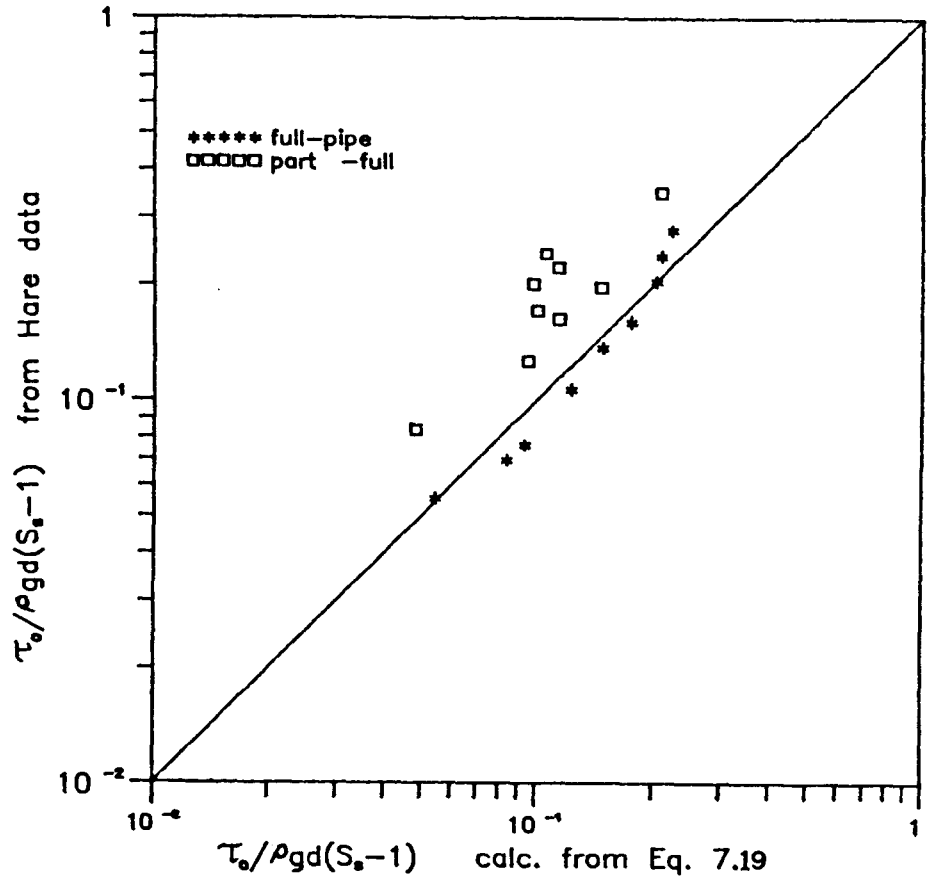

FIGURE 7.31 COMPARISON BETWEEN EQ. 7.19 (b=0.5D) AND HARE'S (1989) DATA FROM CHANNEL WITHOUT FLAT BED (D=298.8 mm)

7.9 Design Criterion

Proposed equations 7.19 to 7.23, in conjunction with the flow resistance equations for smooth channel beds (Eq. 5.14.3) and for rough channel beds (5.15.3), can be effectively used in estimating the bed shear stress for no sediment deposition in circular cross section channels with flat beds.

The following steps have to be followed in design:

(1) For a given flow rate Q, flow depth y_0, bed width b, friction factor for clear water (λ_c) is calculated from Eq. 5.14.3 or Eq. 5.15.3 according to channel roughness.

(2) Sediment friction factor λ_s, is computed from Equation 7.22.

(3) And the bed friction factor with sediment λ_{bs} can then be obtained, according to degree of filling, for all flow ranges by Eq. 7.23.

(4) The value of bed shear stress τ_b , at limit deposition is computed with the equation 7.20.

(5) Bed Hydraulic radius with sediment R_{bs}, is calculated with Eq. 7.23 in step 3 and by using friction factor with sediment λ_s computed in step 2 and applying the following equation

$$\frac{\lambda_s}{\lambda_{bs}} = \frac{R}{R_{bs}}$$

the bed hydraulic radius with sediment, R_{bs}, can be obtained.

(6) The slope, S, required to maintain deposit-free condition is calculated from the definition $\tau_b = \rho\, g\, R_{bs} S$.

Numerical Example:

Problem:

It is proposed to calculate the bed shear stress required to achieve the self-cleansing action and to maintain deposit free flow conditions in circular cross section channels with smooth flat bed under the following conditions:

Data:

Channel diameter (D)	=305 mm
Sediment particle size (d)	=2.80 mm
Relative density of sediments (S_s)	=2.6
Sediment concentration by dry volume (C_v)	$=50 \times 10^{-6}$
Design flow rate (Q)	=20 l/s
Average operating temperature (T)	=16 ^{o}C
Corresponding kinematic viscosity (υ)	$=1.095 \times 10^{-6}$
Sediment bed thickness (t_s)	=47 mm
Sediment bed width (b)	=220 mm

Solution:

a) Consider clear water flow conditions:

Cross sectional area of the flow (A)	$=0.028\ m^2$
Wetted perimeter (P)	=0.442 m
Overall hydraulic radius (R)	=0.063 m
Mean velocity of clear water flow (V)	=0.72 m/s

From flow resistance equation (Eq. 5.14.3) the overall friction factor for clear water conditions (λ_c) =0.0156

b) Consider sediment carrying flow conditions:

b.1) by substituting for C_v, b/y_o and λ_c in equation 7.22, the overall friction factor with sediments (λ_s) **=0.0163**

b.2) From Eq. 7.23, the bed friction factor with sediment (λ_{sb}) can be computed as **=0.017**

b.3) By substituting for d_{50}/D, y_o/b, C_v, and λ_{sb} in equation 7.20:

Bed shear stress for non deposition (τ_b) **=0.655 N/m^2**

b-4) from step 5, the bed hydraulic radius (R_{bs}) **=0.065 m**

Therefore, the slope at which the circular cross section channel with smooth bed sewer should be laid to achieve non-deposit flow conditions (S)= $\tau_b/\rho g R_{bs}$ **=0.001**

Figure 7.32 compares the effect of sediment concentration (C_v) on bed slope (S) computed with the above design criterion. Calculations were done considering a 305 mm pipe diameter, two sediment bed thicknesses (y_t/D=15% and y_t/D=25%), particle size d_{50}=3.0 mm with relative density S_s=2.6, flow depth y_o=100mm, flow rate Q=20 l/s, operating temperature T=16 C° and smooth rigid beds. According to the Figure, slopes computed for bed thickness y_t/D=15% are found to be higher than that of bed thickness y_t/D=25%. The differences in computed designed bed slopes decreases in the case of small sediment concentration and increases in the case of large sediment concentration.

Comparison of the designed slope is done in Figure 7.33 in

the form bed slope (S) versus sediment particle size (d_{50}), for 305 mm pipe diameter and different bed thicknesses (y_t/D=15% and y_t/D=25%), flow rate Q=20 l/s, volumetric concentration C_v=0.00005, flow depth y_o=100 mm, and smooth rigid beds. It can be seen from the Figure that, for small particle size, slopes computed with the above design criterion are steeper than those computed for large particle sizes. This is due to the fact that drag forces (exerted by the flow) acting on the larger particle are higher than those acting on the smaller particles (large particles expose larger areas).

It is also seen from Figure 7.33, that computed bed slope for small bed thickness (y_t/D=15%) is approximately 25% higher than that of higher bed thickness (y_t/D=25%) for the same hydraulic conditions (y_o, S, Q, d_{50}).

From Figures 7.32 and 7.33. it is clear that the bed slope required to maintain deposit free flow conditions in a circular cross section channel with smooth beds, increases as the sediment concentration (C_v) increases and decreases as the particle size of sediment (d_{50}) and sediment bed thickness (t_s) increase.

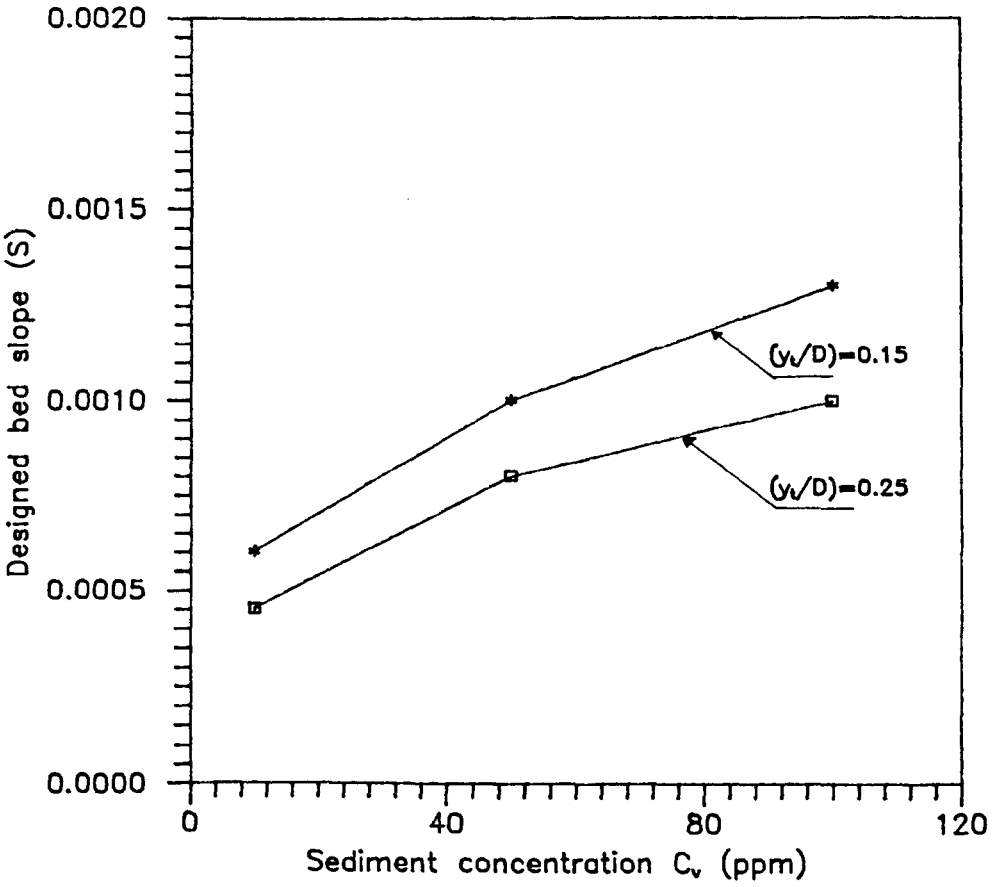

FIGURE 7.32 DESIGN BED SLOPE COMPUTED BY EQ. 7.20 FOR DIFFERENT DEPOSITED BED THICKNESSES (Q=20 l/s; d=3 mm; y_o=100mm smooth channel)

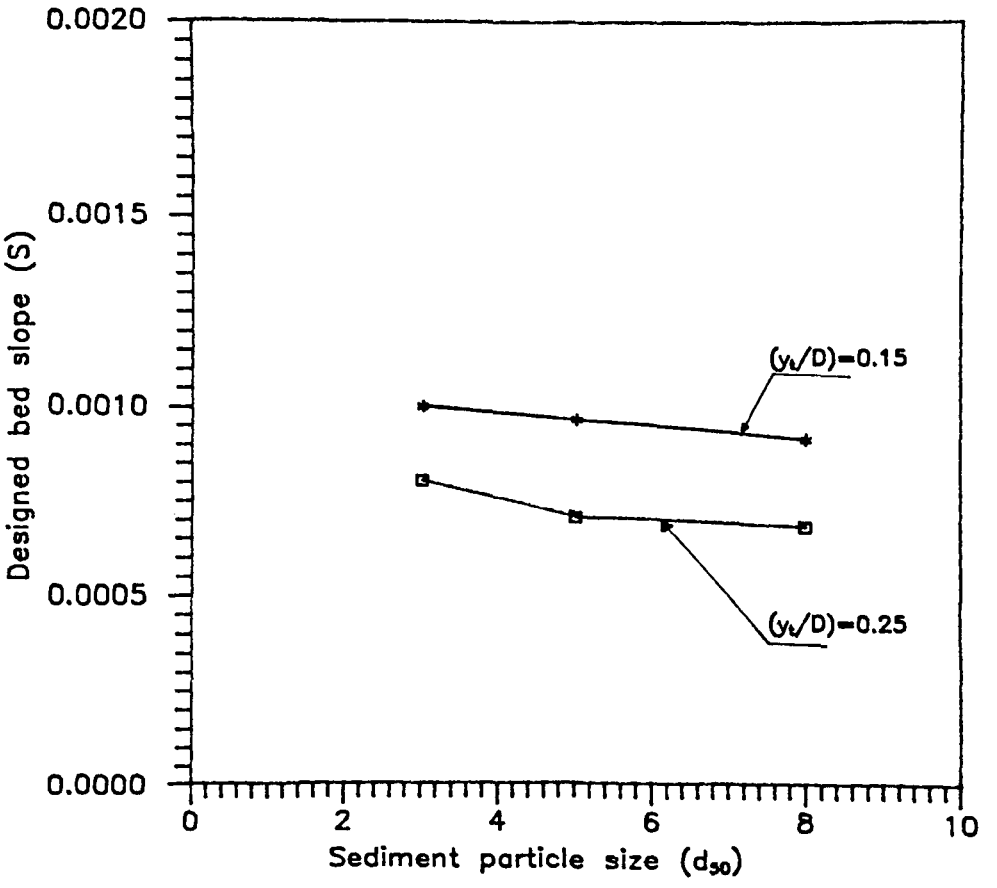

FIGURE 7.33 DESIGN BED SLOPE COMPUTED BY EQ. 7.20 FOR DIFFERENT DEPOSITED BED THICKNESSES (Q=20 l/s; C_v =0.00005; y_o=100 mm; smooth channel)

CHAPTER 8

CONCLUSIONS AND RECOMMENDATIONS FOR FURTHER RESEARCH

This research programme has covered hydraulic characteristics (flow resistance, velocity, bed shear stress and turbulence distributions) and sediment transport (initiation of sediment motion and bed load transport) in circular cross section channels with different bed thicknesses with different roughnesses.

Conclusions on Chapter 5 which deals with hydraulic characteristics of sewers with sediment beds are summarised in section 8.1, those on Chapter 6 dealing with incipient motion of touching grouped particles on smooth and rough beds are summarised in section 8.2. Section 8.3 contains conclusions on Chapter 7 which deals with bed load transport in circular cross section channel sewers with fixed deposited beds.

Recommendations for further research in section 8.4 complete the chapter.

8.1 Hydraulic Characteristics

8.1.1 Flow Resistance

Resistance relationships for circular cross section channels with flat beds are of a more complex nature than those applicable to simple circular cross section channels, indicating the presence of other variables relating to the influence of deposited beds in sewers.

The effect of shape on flow resistance has been examined for smooth rough beds.

It was found that the friction factors (λ_c) in circular cross section channels with smooth flat beds are strongly dependent on flow depth (y_o) and bed width (b). The friction factor was found to decrease with the parameter (y_o/b). This trend is valid for bed thicknesses up to 50% of the pipe diameter. For bed thickness above 50% of pipe diameter the bed width decreases with bed level and a different trend may be expected.

A new method of predicting the friction factor in circular cross section channels with flat beds has been developed. For smooth channels the method (Eq. 5.14.3) incorporates the parameter (y_o/b) and a Reynolds' number with respect to flow depth (R_{ey}) While for channels with rough beds, Eq. 5.15.3 is recommended for evaluating the friction factor which is dependent on y_t/k_s and a flow Reynolds' number (R_{*y}).

8.1.2 Velocity Distributions

The shape of the channel flow-section varies considerably with sediment bed thickness and flow depths, and the velocity distributions are influenced by the associated shape effects.

Velocity distributions over flat beds of circular cross section channels were observed to be dependent on flow depths and bed roughnesses.

For flow at one third-full depth, the side of the flow

section consists of only one curvature on the side wall and therefore the channel will look like a trapezoidal section. The velocity distributions experienced a different pattern according to bed roughness; it was found that in smooth beds the flow is two-dimensional while in rough beds the flow becomes three dimensional. For rough beds, the distribution of velocity is believed to be strongly affected by secondary currents.

For flows at half-full depth, the channel cross section will be in a transition stage from that of trapezoidal section to rectangular. Only one maximum velocity appears below the free surface.

For flows at two-third full depth, the side walls of the channel flow section consist of two curvatures opposing each other, and the flow becomes three-dimensional.

8.1.3 Bed Shear Stress Distributions

Bed shear stresses were measured indirectly from velocity profiles using logarithmic velocity distribution law.

The maximum bed shear stress was found to occur directly below the point of maximum flow velocity but it may also occur instead near the two side walls. Secondary currents are believed to be responsible for such distributions.

The mean bed shear stresses calculated by the standard side-wall correction procedure (Einstein, 1942, Vanoni-Brook 1957) results in small differences from the measured values

on account of the way in which the cross sectional area is divided into sub areas, wall area and bed area, without any momentum exchange between them.
The average bed shear stress was found to be around 20% greater than the average shear stress.

The flow depth and boundary roughness were found to be affecting the bed shear stress distributions considerably.

8.1.4 Turbulence Intensities

Turbulence imposes rapid and significant fluctuations of pressure on the bed surface which have an important effect on the entrainment of sediment as well as on the movement of bed load.
Distribution of turbulence over the flat bed of a channel of circular cross section was found to be strongly dependent on flow depth, bed roughness and bed width. Maximum levels of turbulence intensities were found to be at the centre of the channel bottom for flows at half-full depth while for flows at one third-full and two-third full depths the two maximum levels of turbulence intensities were found to be close to the channel side walls.
The turbulence intensities on rough beds were found to be higher than those of smooth beds. The effect of bed roughness seems to be strongest in the case of low flow depths.
It was found that for the same degree of filling (y_t/D), the

turbulence intensities are higher for large bed thicknesses than for small bed thickness. This increase seems likely to be due to the high bed width in the case of large bed thickness (these findings are valid only for $t_s \leq 0.5D$).
The distribution of turbulence intensities over deposited beds in sewers is an important feature in the erosion process. The beginning of sediment motion was observed to occur at the location of maximum turbulence intensities.

8.2 Initiation Of Sediment Motion

In a situation where particles are touching each other, there would be greater friction between them. This friction increases with the increase in the number of bed particles, and tends to bind the particles together. Hence a higher value of shear stress or velocity will be required to dislodge the larger particles, and move them, than for small particles.
However, for initiation of non-cohesive sediment motion in circular cross section channels with loose bed channels (Alvarez 1990) results show that the size of the aggregates (sand size) has no significant effect on the critical conditions of noncohesive sediments over loose beds (see Fig.6.6).

Experimental results of the initiation of motion of grouped touching particles with number of rows equal to 15 showed that the particles are eroded at lower shear stress than

predicted by Shields' criterion (for wide alluvial channels). The influence of the number of touching grouped particles resting on the channel bed was investigated by comparing the present work with that of Novak and Nalluri (1984) for number of rows equal to 10 in a rectangular channel with smooth and rough beds. The results of the comparison show that the higher the number of rows the higher the velocity needed to erode them (see Fig. 6.9).

The experimental results show that the critical shear stress increases as the bed roughness increases, as more energy has to be used to overcome the higher friction resistance between the particles and the bed roughness.

The critical bed shear stress required to dislodge touching grouped particles resting on the channel bed (smooth and rough) can be calculated from Eq. 6.18.
Another approach in analysing the initiation of motion data was achieved by using the critical velocity approach. Eq. 6.24 can be used to compute the critical velocity at any flow depths and at any bed roughnesses. The influence of the channel shape on critical conditions was investigated by incorporating the parameter y_o/b in Eq. 6.20 and by regression analysis the experimental data was fitted to the Eq. 6.25.

8.3 Bed Load Transport

For the same hydraulic conditions, the results show that the transport of sediments in circular cross section channels with fixed beds (limit deposition conditions) is higher than that in alluvial channels.
The results also show that for a given uniform flow sediment transport increases with particle size. This can be attributed to the increase in exposed area of the particles and to the increase in turbulence intensity surrounding the sediment particles.

Bed roughness was found to affect the sediment transport capacity of a given uniform flow as more energy has to be dissipated to overcome the friction between the rough bed and the sediments.

Four sediment transport equations were used in this study to compute the sediment rate and to compare it with the measured values. These equations are Ackers' (1984), Loveless' (1986), May et al's (1989) and Alvarez's (1990). The comparison showed that Loveless' equation (Eq. 2.44) generally over-predicted the sediment transport rates for all the three different deposited beds, while May et al's equation (Eq. 3.6) under-predicted the volumetric sediment concentrations for all cases.
Ackers' equation (Eq. 2.43) for effective width (W_e) equal to bed width overpredicted the volumetric sediment

concentrations. When Ackers' equation was applied for effective width equal to 10d (d is the particle size) the equation generally underpredicted the measured sediment concentrations for high bed thickness (bed 3) and give a reasonable estimate for small bed thickness (bed 1).

Alvarez's equation (Eq. 3.11) for computing shear stress for the limit deposition in circular cross section channels with fixed sediment beds gave reasonable agreement with the present experimental data.

The definition of the term "limiting deposition" is not unique. Researchers define it according to their own judgment and then develop equations to fit some flow conditions and sediment characteristics. However, no single equation is available to describe the transport capacity for all situations. All the available transport-predicting equations combine the parameters representing the flow and the sediment characteristics used in its derivation.

The results of the present study on the transport of non-cohesive sediments without deposition in circular cross section channels with fixed deposited beds were fitted to equations combining the main variables involved in the problem. Three different approaches were developed to predict the bed load in the channel; firstly for flows up to half-full depth, secondly for more than half-full depth and finally for the entire range of flow depths.

The proposed model is solved iteratively by combining three equations: Eq. 7.19 (or Eq. 7.20) describes the relationship between the mean shear stress (or bed shear stress) for non-deposition, particle size, volumetric concentration, pipe diameter, flow depth, bed width and friction factor with sediments; Eq. 7.22 is the means by which the friction factor with sediments is evaluated at the limit deposition related to its value without sediments, volumetric sediment concentration and bed width; the third equation (5.14.3 for smooth beds or 5.15.3 for rough beds) describes the friction factor without sediment.

The proposed equation (7.20) was tested against Alvarez's experimental results obtained for a circular cross section channel (D=154 mm) with flat deposited beds and found to agree very well; this confirms its validity for other pipe sizes.

The approach suggested in this study can be used to predict the bed load in circular cross section channels without deposited beds simply by replacing the bed width term by the value 0.5D (where D is the pipe diameter). Good agreement is obtained between the proposed approach and Mayerle's experimental data (D=152mm) and Hare et al's data (D=298.8mm).

Ackers' equation (2.43) was modified for use in the prediction of sediment transport concentration in circular cross section channels with fixed deposited beds. This was achieved by replacing the effective width by $5.5\, d_{50}\, (b/y_o)$.

Minimum shear stresses required to maintain non-deposition conditions in circular cross section channel with flat beds were found to be lower than those corresponding to rectangular channels (see Fig. 7.21).

8.4 Recommendations For Further Research

Although this study has led to a deeper understanding of the hydraulic characteristics and sediment movement in circular cross section channels with fixed deposited beds, the problems of sedimentation are still far from being well understood. Even though in the present work some attempts have been made to investigate extensively the hydraulic characteristics (flow resistance, velocity and bed shear stress distributions and turbulence distributions) and the sediment transport (initiation of motion and bed load transport), certain areas remain completely unknown which would particularly benefit from further investigation.

Recommendations for further work are listed below.

1) More clear water experiments with higher bed roughness should be conducted in order to explore the effect of high roughness on flow resistance.

2) A detailed study of boundary shear stress distributions with composite roughness is recommended.

3) Turbulence measurements at higher flow depths, open channel flow, and at full pipe flow are needed to study the

influence of air and free surface on turbulence.

4) The hydr a ulic characteristics study will be more constructive if the secondary currents are measured.

5) More experiments (clear water and sediment transport) are needed at very low deposit thickness (t_s<0.1D) to verify the proposed models and to confirm their validity for circular cross section channels with different deposited bed thicknesses.

6) Experiments at higher bed roughness are required to examine its influence on the sediment transport capacity of circular channels with flat beds.

7) In initiation of sediment motion studies, a higher number of touching grouped particles need to be examined in order to reach the stage at which the the sediment particles behave in a similar manner to those on alluvial beds.

8) The findings in this study show the danger of neglecting shape effects in open channels and underline the need for a more systematic investigation of the influence of cross-sectional shape on sediment transport capacity of sewers with different cross sections.

9) As the flow conditions in sewers is intermittent i.e unsteady, an investigation to study the effect of unsteady flow on the consolidation of deposited beds should be carried out.

10) In real storm sewers, sediment deposits are a mixture of sand, silt, debris, etc with different densities. Although the effect of particle density is considered in the analysis of the present data, more experiments in a similar manner but with particles having different densities are desirable.

11) Field surveys are needed, especially in sewers experiencing deposition, to assess their performance with existing deposits.

APPENDIX A

REFERENCES

1. **Ackers P. (1958)**, "Resistance of fluids flowing in channels and pipes", HMSO, London. Hydraulics Research Paper No.1.

2. **Ackers, p. (1978)**, "Urban Drainage: the Effects of Sediment on Performance and Design criteria",. Proc 1st International Conference on Urban Storm Drainage, Southampton, England.

3. **Ackers,P. (1984)**, "Sediment Transport in Sewers and the Design Implications", International Conference of the planning, Construction, Maintenance and Operation of Sewerage Systems, organised by BHRA , Reading, ENGLAND.

4. **Ackers, P. Crickmore, M.J. and Holmes.D.W. (1964)**, "Effects of Use on the Hydraulic Resistance of Drainage Conduits", Proc. Inst. Civil Engineers,. 28 pp 339-360.

5. **Ackers, P. and White, W.R. (1973)**, "Sediment Transport: New Approach and Analysis", Journal of the Hydraulic Division, ASCE, Vol.99, HY 11.

6. **Al-Saqri, T. (1990)**, "A study of Shape Effect on Flow Characteristics and Incipient Motion of Sediment in Rigid Closed and Open Conduits", MSc Thesis, Dept. of Civil Eng., University of Newcastle upon Tyne, ENGLAND.

7. **Alvarez, E. (1990)**, "The Influence of Cohesion on Sediment Movement in Channels of Circular Cross-Section", PhD Thesis, Dept. of Civil Eng., University of Newcastle upon Tyne, ENGLAND.

8. **Ambrose, H.H. (1953)**, "The Transportation of Sand in Pipes Free Surface Flow", Proceedings of the fifth Hydraulics

Conference, Bulletin 34, State University of Iowa Studies in Engineering, Iowa University, Ames, Iowa.

9. **Arora, A.K. Ranga Raju,K.G. and Grade,R.G. (1984)**, "Criteria for Deposition of Sediment Transported in Rigid Boundary Channels", Proceedings of the first International Conference on Channels and Channel control sections, Southampton, ENGLAND.

10. **Bathurst, J. C Thorne, C. R. and Hey R. D. (1979)**, "Secondary Flow and Shear Stress at River Bends," Journal of Hydraulics Division, ASCE, Vol. 105, No. HY10.

11. **Bayzit, M. (1976)**, "Free Surface Flow in A channel of Large Relative Roughness", Journal of Hydraulic Research Vol. 14(2) pp.115-126.

12. **Blinco, P. H. and Partheniades E.P. (1971)**, "Turbulence Characteristics in Free Surface Flows over Smooth and Rough Boundaries", Journal of Hydraulic Research Vol. 9 No. 1.

13. **Brown, C. B. (1950)**, " Sediment Transport, Chapter XII, *Engineering Hydraulics,* edited by H. Rouse, Wiley & Sons.

14. **Bonapace, A. C. (1981)**, "Critical Lift Velocity of a Particle Placed at the Boundary of a Stream", South African Mech. Engr., Vol. 31, PP 3-19.

15. **Celik, I. and Rodi, W. (1984)**, "A Deposition-entrainment Model for Suspended Sediment Transport", Report no. SFB/T/6, University of Karlsruhe, Karlsruhe. FRG.

16. **Celik, I. and Rodi, W. (1985)**, "Mathematical Modelling of Suspended Sediment Transport in Open Channels", Paper presented at the 21st. congress of International Association of Hydraulic Research on flood flows in channels and flood plains; Sediment transport in rivers; Hydraulic structures, Melbourne, AUSTRALIA.

17. **Chao-Lin C. and Gwo-Fong L. (1983)**, "Computation OF 3-D Flow And Shear In Open Channels" Journal of Hydraulics Division ASCE Vol. 109, No. 11.

18. **Chien N. (1956)**, "The present Status of Research on Sediment Transport" ASCE Hydraulic Division Vol. 121.

19. **Construction Industry Research and Information Association, (1987)**, "Sediment Movement in Combined Sewerage and Storm-water Drainage Systems", CIRIA Project Report 1.

20. **Crabtree, R. W. (1988)**, "A Classification of Combined Sewer Sediment Types and Characteristics", WRC, Swinden.

21. **Craven ,J. P. (1953)**, "The Transportation of Sand in Pipes-full Flow", Proceedings of the Fifth Hydraulic conference, Bulletin 34, Iowa Institute of Hydraulic Research, Iowa State University, USA, Iowa.

22. **Dhillon, G.S. Paul, T.C. and Sakhuja, V.K. (1988)**, "Sediment Transport Capacity of Rigid Boundary Channels", Paper presented at the Indo-British workshop on sediment measurement and control, Chandigarh INDIA.

23. **Durand, R. (1953)**, "Basic Relationships of the Transportation of Solids in Pipes", Experimental research, International Association for Hydraulics Research Fifth Congress, Minneapolis.

24. **Einstein, H.A. (1942)**, "Formulas for the Transportation of Bed-load", Transactions ASCE, Vol. 107.

25. **Einstein, H. A. and El-Samni, S. A. (1949)**, "Hydrodynamic Forces on a Rough Wall", Rev. Mod. Phys. Vol 21, pp. 520-524.

26. **Einstein, H.A. (1950)**, "The Bed-load Function for Sediment Transportation in Open Channel Flows", Technical Bulletin no.

1028, U.S. Department of Agriculture, Soil conservation service, Washington D.C.

27. **Ellis, J. B. (1976)**, "Sediments and Water Quality of Urban Storm Water", Water Services, Dec. 1976., PP 730-234.

28. **Enger P. F. (1961)**, "Tractive Force Fluctuation Around an Open Channel Perimeter as Determined From Point Velocity Measurements", Proc. ASCE Convection Phoenix, Arizona, 1961.

29. **Frohlich, G. R. (1985)**, "Über den Einfluss der Sohlenform auf den sand-transport bei geringen Feststoffkonzentrationen in teil-und Vollgefüllten Rohrleitungen", Disertation, Tech. University Braunchewig, FRG.

30. **Gosh S. N. and Roy N. (1970)**, "Boundary Shear Distribution in Open Channel Flow", Journal Of Hydraulic Division ASCE, 1970, 96, HY4, (April) PP967-994.

31. **Graf W.H. (1971)**, "Hydraulics of Sediment Transport", MC Graw-Hill series in Water Resources and Environmental Engineering, MC Graw-Hill Book co., Inc., New York.

32. **Graf W.H. and Acaroglu E.R. (1968)**, "Sediment Transport in Conveyance Systems", Part 1. Bull IAHR XIII, No2, pp20-39.

33. **Grass, A. J. (1970)**' "The Initial Instability of Fine Sand" Proc. ASCE, Vol. 96, HY 3, 619-632.

34. **Henderson R.J. (1984)**, "The Hydraulic Roughness of Used Sewers", International Conference Of the Planning, Construction, Maintenance and Operation of Sewerage systems. Reading, England.

35. **Hicks, F. E. and Steffler P. M. (1990)**, "Flow Near Sloped Bank in Curved Channel", Journal of Hydraulic Division ASCE, Vol. 116, No.7, Jan 1990, Paper No. 2413.

36. **Hydraulic Research Station, Wallingford** (1981), "Velocity Equations for Hydraulic Design of Pipes", Summary No. 72.

37. **Ippen A. E. and Drinker P. A. (1962)**, "Boundary Shear Stress in Curved Trapezoidal Channels", Journal Of Hydraulic Division ASCE HY 5. (Sept), PP.143-179.

38. **Ippen A.T. and Verma R.P. (1953)**, "The Motion of Discrete Particles along the Bed of a Turbulent Stream", Proceedings of the Minnesota International Convention, Minneapolis.

39. **Jayaraman, V. V. (1970)**, "Resistance Studies on Smooth Open Channels", Journal of Hydraulic Division, Proc. of the ASCE, Vol.96, HY 5.

40. **Kalinske, A. A. (1947)**, "Movement of Sediment as Bed-Load in Rivers", Trans. Am. Geophys. Union, Vol. 28, No. 4, pp 615-620.

41. **Karth V. C. and Leutheusser H. J. (1970)**, "Distribution of Tractive Force in Open Channels", Journal Of Hydraulic Division ASCE, Hy7 (July) 1469-1483 (paper No.7415).

42. **Kazemipour, A.k. and Apelt C. J. (1980)**, "Shape Effects on Resistance to Flow in Smooth Semi-Circular Channels", Research report No. CE 18, University of Queensland.

43. **Kazemipour A. K. and Apelt, C. J. (1982)**, "New Data on Shape Effects in Smooth Rectangular Channels", Journal of Hydraulics Research IAHR, Vol.1. 20, No. 3.

44. **Keulegan, G. H. (1938)**, "Laws of Turbulent Flow in Open Channels", Journal of Research, National Bureau of Standards, Washington D. C., Research paper 1151, Vol 21, No. 6, pp 707-741.

45. **Knight D. W. and Macdonald J. A. (1979)**, "Open Channel Flow

with Varying Bed Roughness", Journal of Hydraulic Division ASCE, HY9 (September) pp. 1167-1183 (Paper No. 14839).

46. **Knight D. W. Patel H.S. Demetriou J. P. and Hamed M. E. (1982)**, "Boundary Shear Stress Distributions in Open Channel and Closed Conduit Flow", Proc. Euromech 156 Conference on Mechanics of Sediment Transport, Istanbul, 12-14 July.

47. **Kuhil Z.S. (1989)**, "Sediment Transport in Storm Sewers", PhD Thesis Department of Civil Engineering, University of Salford, England.

48. **Laplace, Y. Sander D. Dartus, D. and Bachoc, A. (1990)**, "Sediment Movement into The Combined Trunk Sewer No.13 In Marseille", Journal Of Water Science and Technology Vol. 22 No. 110/11 pp.259-266.

49. **Laursen, E.M. (1956)**, "The Hydraulics of Storm-drain System for Sediment-transporting Flow", Bulletin no. 5 , Iowa Highway Research Board.

50. **Loveless, J.H. (1986)**, "Sediment Transport in Circular and Non-circular Conduit", paper presented at the Conference on Hydraulic Design: Land Drainage Southampton, ENGLAND.

51. **Macke ,E. (1982)**, "Determination of Sediment Free Flow Conditions in Sewer Pipes", Korresponenz Abwaser, 30. No. 7.

52. **May, R.W.P. (1982)**, "Sediment Transport in Sewers", Hydraulic Research Station , Report IT 222.

53. **May R.W.P. Brown P.M. Hare G.R. and Jones K.D. (1989)**, "Self-Cleansing Conditions for Sewers Carrying Sediment", Hydraulic Research Station Report SR 221.

54. **Mayerle, R. (1988)**, "Sediment Transport in Rigid Boundary

Channels", PhD Thesis, Department of Civil Engineering, University of Newcastle Upon Tyne, England.

55. **Mayerle, R. Nalluri, C. and Novak, P. (1991)**, "Sediment Transport in Rigid Bed Conveyances" , Journal of the Hydraulics Division, Proc. of the ASCE Vol. 29, HY 4. pp. 475.

56. **McQuivey R.S. and Richardson E. V. (1969)**, "Some Turbulence Measurements in Open Channel Flow", Journal of the Hydraulics Division, ASCE Vol. 95 No. 1441 Proc. paper 6349, pp. 209-223.

57. **Metcalf & eddy (1972)**, "Wastewater Engineering", pp. 2-3. McGraw Hill, New York.

58. **Myers, W. R. C. (1982)**, "Flow Resistance in Wide Rectangular Channels", Journal of Hydraulics Division Proc. of the ASCE Vol. 108., HY 4. pp. 471-482.

59. **Myers, W. R. C. and Brennan, E. K. (1990)**, "Flow Resistance in Compound Channels", Journal of Hydraulic Research, Vol. 28, No. 2.

60. **Nalluri, C. (1986)**, "Sediment Transport in Rigid Boundary Channels", Proceedings of Euromech 192, Transport of suspended solids in open channels, Neubiberg, June, 1985, Balkema Publishers, Boston.

61. **Nalluri, C. and Adepoju B. E. (1985)**, "Shape Effects on Resistance to Flow in Smooth Channels of Circular Cross Section", Journal of Hydraulics Research IAHR 23(1) pp.37-46.

62. **Nalluri, C. and Novak, P. (1973)**, "Turbulence Characteristics in a Smooth Open Channel of Circular Cross Section", Journal of Hydraulics Research IAHR, Vol. 11, No.4.

63. **Neil, C.R. and Yalin, M.S. (1969)**, "Quantitative Definition of

Beginning of Bed Movement", Proc. ASCE, Vol. 95, HY1, 585-588.

64. **Nezu, I. and Rodi, W. (1985)**, "Experimental Study on Secondary Currents in Open Channel Flow", 21st IAHR Congress, Melbourne, Australia, Vol. 2, pp. 19-23.

65. **Novak, P. and Nalluri, C. (1975)**, "Sediment Transport in Smooth Fixed Bed Channels", Journal of the Hydraulics Division, ASCE., Vol. 101, HY 9.

66. **Novak, P. and Nalluri, C. (1978)**, "Sewer Design for no Sediment Deposition", Proceedings of the Institution of Civil Engineers, part 2, Vol.65.

67. **Novak, P. and Nalluri, C. (1984)**, "Incipient Motion of Sediment Particles over Fixed Beds", Journal of Hydraulic Research , Vol. 22, pp 181-197.

68. **Ojo, S.I.A. (1978)**, "Study of Incipient Motion and Sediment Transport over Fixed Beds", PhD Thesis, Department of Civil Engineering, University of Newcastle Upon Tyne, England.

69. **Ojo, S.I.A. (1980)**, "A predictive Formula for Sediment Discharge in a Rectangular Flume", Symposium on River Engineering and it's Interaction with Hydrological and Hydraulic Research, International Association for Hydraulic Research, Belgrade.

70. **Patel, S. H. (1984)**, "Boundary Shear In Rectangular And Compound Ducts" PhD thesis, Dept. of Civil Eng. University of Birmingham.

71. **Paul, T. C. and Sakhuja, V. S. (1990)**", Why Sediment Deposit in Lined Channels", Journal of Irrigation and Drainage Eng. ASCE Vol. 116 No. 5.

72. **Perdoli, R. (1963)**, "Bed-load Transportation in Channels with Fixed and Smooth Inverts", Mitteilung des Eidg. Amets fur Wasserwirtscaft, Dienst Exemplar, No.43, Bern, Switzerland.

73. **Rao, K. K. (1967)**, "Effect of Shape on the Mean Flow Characteristics of Turbulent Flow through Smooth Rectangular Open Channel", PhD thesis presented to the University of Iowa.

74. **Raudkivi, A. J. (1990)**, "Loose Boundary Hydraulics", 3rd Edition, Pergamon Press.

75. **Reinus, E. (1961)**, "Steady Uniform Flow in Open Channels", Transactions of the Royal Institute of Technology, Stockholm, Sweden, No. 179.

76. **Richardson E. V. and McQuivey R.S. (1968)**, "Measurements of Turbulence in Water", Journal of Hydraulics Division ASCE, vol.94, No. HY2 , Proc. paper 5855, pp. 411-429.

77. **Robinson, M.P. and Graf, W.H. (1972)**, "Pipelining of Low Concentration Sand-Water Mixtures", Journal of the Hydraulics Division, Proc. of the ASCE, Vol. 98, HY7, pp. 1221-1241.

78. **Rottner, J. (1959)**, "A Formula for Bed-Load Transportation", La Houille Blanche, No.3.

79. **Rouse, H. (1937)**, "Modern Conceptions of the Mechanics of Turbulence", Trans. ASCE, Vol. 102, PP 463-543.

80. **Rouse, H. (1965)**, "Critical Analysis of Open Channel Resistance", Journal of Hydraulic Division ASCE, Vol. 91 HY4, pp 475-500.

81. **Sarter, J. D. Boyed, G. B. and Agrody, F. J. (1974)**, "Water Pollution Aspects of Street Surface Contaminants", Journal Water Pollution Control Federation, Vol.49, No.3, Part 1.

82. **Sclichtiz, H. (1979),** "Boundary Layer Theory", Mc Graw-Hill Book., Inc, New York, N.Y.

83. **Shields, A. (1936),** "Anwendung der Ahnlickeitsmechanik und Shields, A., Turbulenzforschung auf die Geschiebebewegung", Mitteilungen der Preussichen Veruchsanstaff fur wasserbau und sciffbau, No.26 , Berlin.

84. **Shih, C. C. and Grigg, N. S. (1967),** "A reconsideration of the Hydraulic Radius as a Geometric Quantity in Open Channel

85. Hydraulics", Proc. 12th Int. Congress of IAHR, Vol. 1 (paper A36) pp. 288-296.

86. **Simons, D.B. and Senturk, F. (1977),** "Sediment Transport Technology", Water Resources Publications, Fort collins, Colorado, USA.

87. **Steffler, P. M. Rajaratnam, N. and Peterson A. W. (1985),** "LDA Measurements in Open Channel", Journal of the Hydraulics Division, ASCE vol.1No. 1, PP. 119-130.

88. **Sturm, T. W. and King, D. A. (1988),** "Shape Effects on Flow Resistance in Horseshoe-Conduits", Journal of Hydraulics Division Proc. of ASCE, Vol. 11.

89. **Suki, R.B.M. (1987),** "Sediment Transport in Storm Sewers", PhD Thesis, Department of Civil Engineering, University of Salford, England.

90. **Task Committee for Preparation of Sediment Manual (1966),** "Sediment transportation Mechanics: Initiation of Motion", Journal of the Hydraulics Division, Proc. of ASCE, Vol. 92, No. HY2, Paper 4738, pp.291-314.

91. **Tominaga k. Nezu I. Ezaki K. and Nakagawa H. (1989),**

"Three-Dimensional Turbulent Structure in Straight Open Channel Flows", Journal of the Hydraulic Research, Vol. 27, No.1, pp. 149-173.

92. **Tracy, H. J. and Lester, C. M. (1961)**, "Resistance Coefficients and Velocity Distribution in a Smooth Rectangular Channel", US Geological Survey, Water Supply Paper 1592A. Washington D.C.

93. **Unsöld, G. (1982)**, "Der Transportbeginn rolligen Schlenmaterials in gleichförmigen turbulenten Strömungen: Eine Kritische Überprüfung der Shields-Funktion und ihre experimentelle Erweiterung auf feinkörnige, nicht-bindige Sedimente. Dissertation, Mathematische- Naturwissenschaftlichen Fakultät Universität Kiel, FRG.

94. **Van Rijn, L. C. (1984)**, "Sediment Transport Part II: Suspended Load Transport", Journal of Hydraulic engineering, ASCE, Vol. 110, PP 1613-1641.

95. **Vanoni, V.A. (1975)**, "Sedimentation Engineering", Task Committee for the Preparation Manual on Sedimentation , American Society of Civil Engineers , New York.

96. **Vanoni, V. A. and Brooks, N. H. (1957)**, "Laboratory Studies of the Roughness and Suspended Load of Alluvial Channels". California Institute of Technology, Report No. E-68, USA.

97. **Verbank, M. (1990)**, "Sewer Sediments and its Relation With the Quality Characteristics of Combined Sewer Flows", Journal Of Water Science and Technology Vol.22 No.110/11 Pp.247-257.

98. **Westrich, B. and Jurashek, M. (1985)**, "Flow Transport Capacity for Suspended Sediment", Paper presented at the 21st. Congress of International Association for Hydraulics Research in flood flows in channels and flood plains; Sediment transport in Rivers; Hydraulic structures, Melbourne, Australia.

99. **Yalin M.S. (1965)**, "Similarity in Sediment Transport by Currents", Hydraulic Research Paper No. 6., H.M. Stationary Office London.

100. **Yao K. M. (1974)**, "Sewer Line Design on Critical Shear Stress", Journal of the Environmental Engineering Division, ASCE, Vol 100, EE2.

101. **Zenz, F. A. and Othmer, D. F. (1960)**, "Fluidization and Fluid-Particle Systems", Reinhold Publishing Corp., New York, N. Y.

APPENDIX B

GEOMETRY OF CIRCULAR CROSS SECTION CHANNEL WITH FLAT BEDS

APPENDIX B

GEOMETRY OF CIRCULAR CROSS SECTION CHANNELS WITH FLAT BEDS

Circular channel with flat bed is schematically shown in Figs. B.1 and B.2.

For a given diameter D, flow depth y_o and sediment bed thicknesses t_s, various geometric properties of the circular channel with flat bed can be calculated according to the degree of fillings.

When the channel is flowing partly full and water depth does not exceeded the perimetric part of the channel, i.e $y_t<D/2$, (where y_t is the total depth of sediment and water in the channel). The geometric properties of the cross section are expressed according to Fig. B.1.

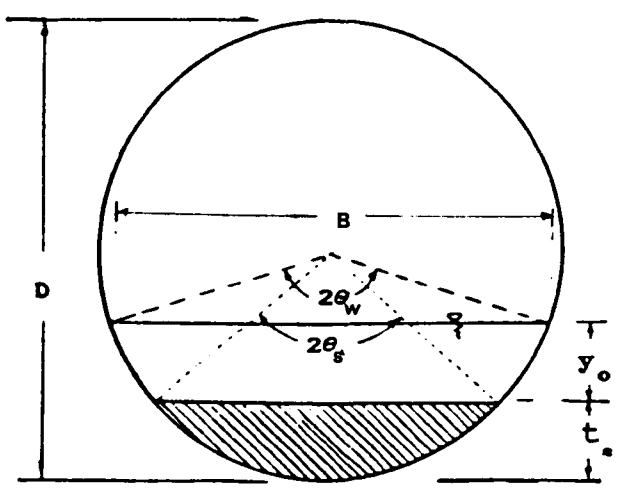

FIG B.1 SCHEMATIC OF THE CHANNEL (up to half-full)

$$\theta_s = \mathrm{Sin}^{-1}\left(\frac{b}{D}\right) \qquad \text{(B.1)}$$

$$b = 2\sqrt{t_s(D-t_s)} \qquad \text{(B.2)}$$

$$\theta_w = \mathrm{Sin}^{-1}\left(\frac{B}{D}\right) \qquad \text{(B.3)}$$

$$B = 2\sqrt{y_t(D-y_t)} \qquad \text{(B.4)}$$

$$y_t = (y_o + t_s) \tag{B.5}$$

$$A_{w1} = \left[\frac{\pi D^2}{4}\right] \left[\frac{\Theta_w}{180} - \frac{\Theta_s}{180}\right] + \left[(B-b)\left(\frac{D}{4} - \frac{t_s}{2}\right)\right] \tag{B.6}$$

$$P_{w1} = (\pi D) \left[\left(\frac{\Theta_w}{180}\right) - \left(\frac{\Theta_s}{180}\right)\right] + b \tag{B.7}$$

where Θ_s is half angle subtended by the sediment bed surface at the centre of a pipe channel, b is sediment bed width, t_s is sediment bed thicknesses, Θ_w is half angle subtended by the water line at the centre of pipe channel, A_{w1} is cross-sectional area of flow (at up to half-full) at, P_{w1} is the wetted perimeter (at up to half-full) , and y_o is the flow depth at the centre line of the channel.

When the channel flowing at a depth more than half-full, then the area and wetted perimeter of the flow can be expressed as (Fig. B.2):

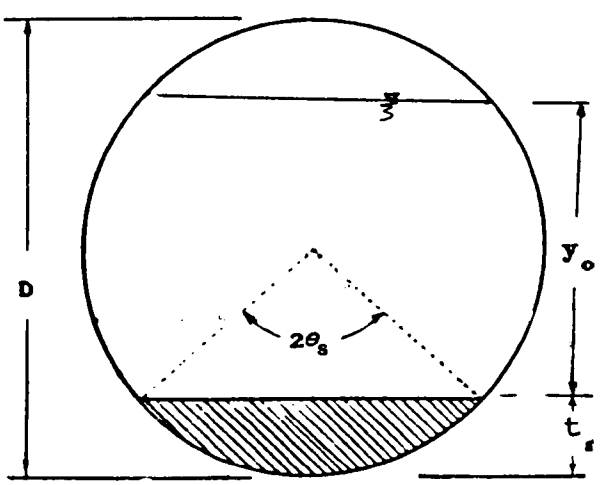

FIG B.2 SCHEMATIC OF THE CHANNEL (more than half-full)

$$A_{w2} = \left[\frac{\pi D^2}{4}\right] - \left[\frac{\pi D^2}{4}\left(\frac{\Theta_w}{180} + \frac{\Theta_s}{180}\right)\right] + \left[(B+b)\left(\frac{D}{4} - \frac{t_s}{2}\right)\right] \tag{B.8}$$

$$P_{w2} = (\pi D) - (\pi D) \left[\left(\frac{\Theta_w}{180}\right) + \left(\frac{\Theta_s}{180}\right)\right] + b \tag{B.9}$$

where A_{w2} is cross-sectional area of flow at a flow depth higher than D/2 and P_{w2} is the wetted perimeter at a flow depth higher than D/2.

The geometrical parameters of the partly full circular cross section channel with flat beds are given in Figures from number B.3 to number B.5.

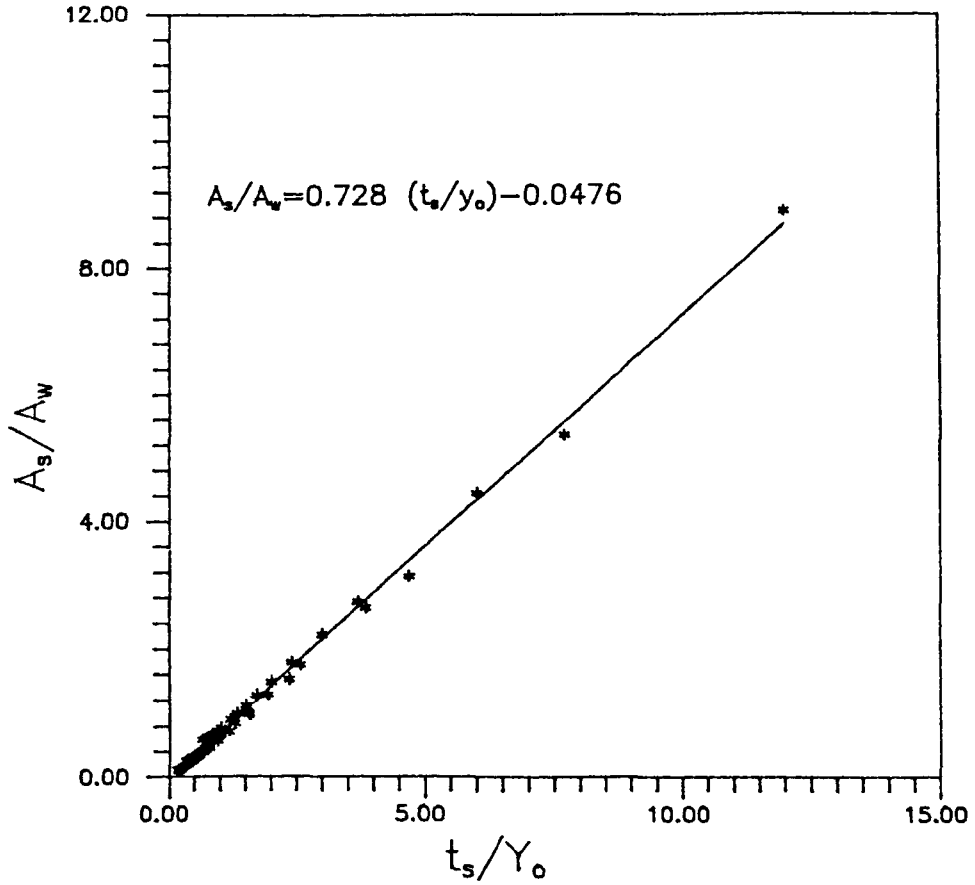

FIGURE B.3 GEOMETRICAL RELATIONSHIP BETWEEN A_s/A_w AND t_s/y_o

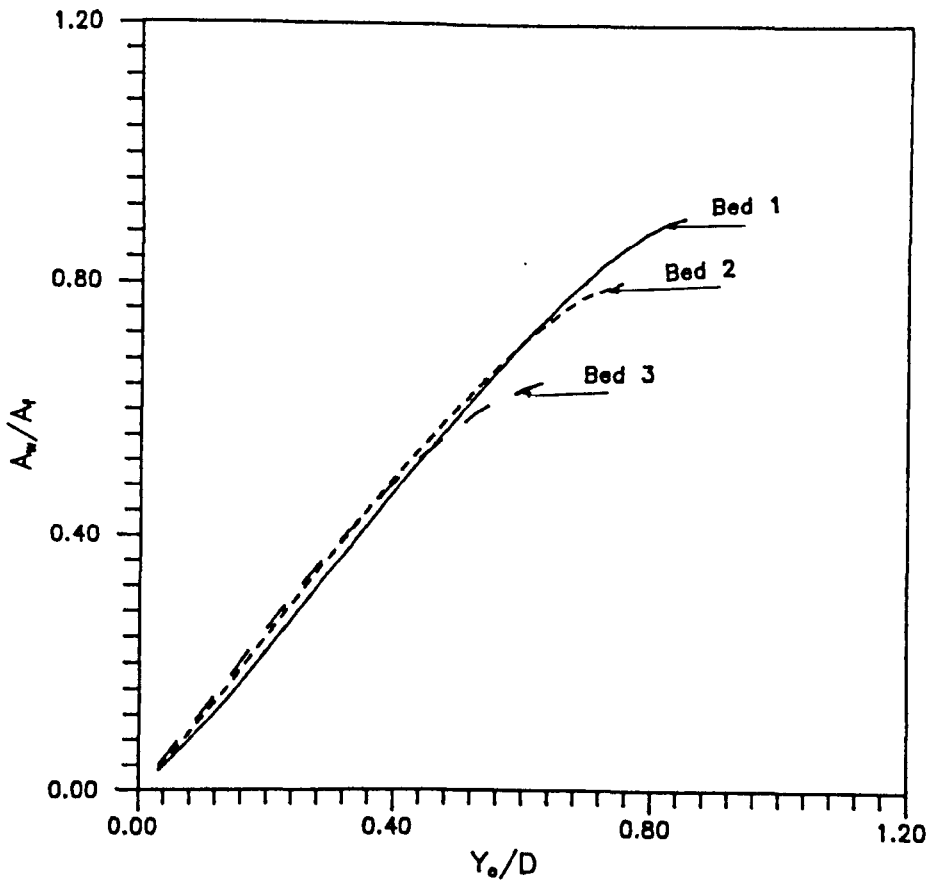

FIGURE B.4 GEOMETRICAL RELATIONSHIP BETWEEN A_w/A_f AND Y_o/D

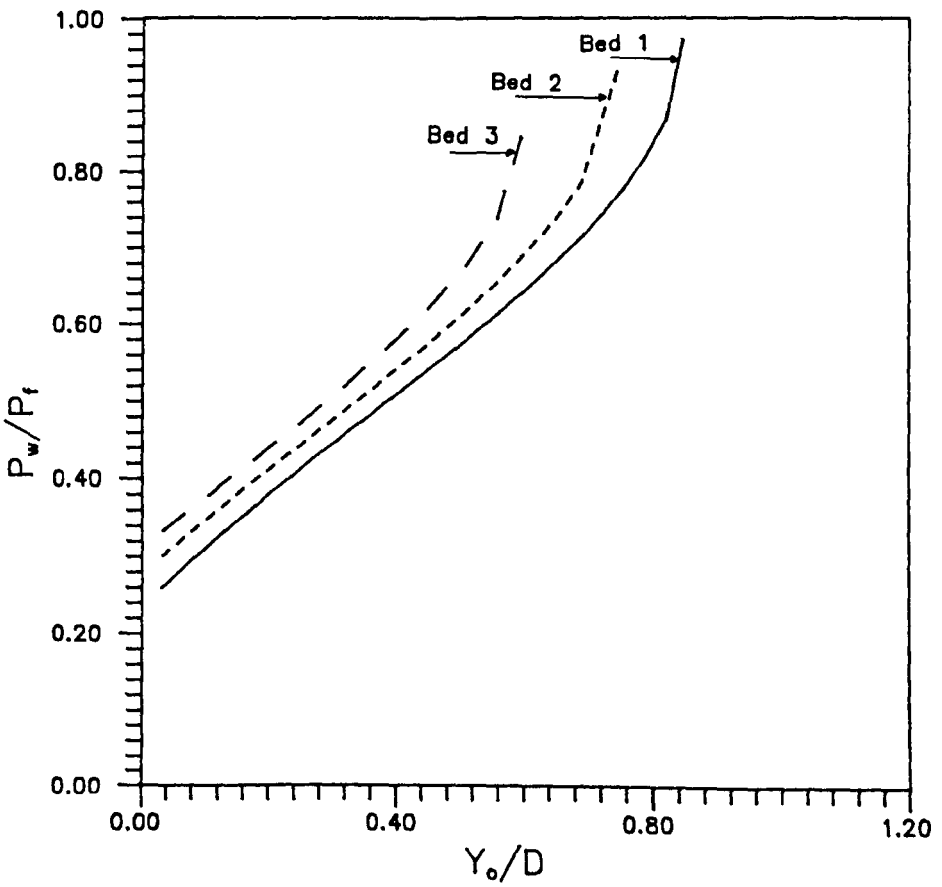

FIGURE B.5 GEOMETRICAL RELATIONSHIP BETWEEN P_w/P_f AND Y_o/D

APPENDIX C

LASER DOPPLER ANEMOMETER

APPENDIX C

LASER DOPPLER ANEMOMETER

a) Laser Doppler Anemometer Principles

In LDA measurements three modes of operation, the Reference Beam Mode, the Differential Doppler Mode and the Dual Scattered Mode have been used, but only the first two have found general acceptance.

A monochromatic coherent beam is produced by the laser which has an extremely high frequency stability. In the Differential Doppler Mode, as used in this study, this beam then passes a beam splitter (see Fig. C.1).

The non-refracted beam then passes through an acousto-optical device known as a Brag cell in which ultrasonic energy is propagated transversely to the laser beam to have the frequency of the light waves upshifted or downshifted. The two beams produced then pass through the beam displacer, beam translator, beam expander, and finally pass through a suitable lens arrangement to cross a convenient position in the fluid flow whose characteristics are to be observed.

At the beam crossing the two laser beams of monochromatic coherent light, each with plane and parallel wave fronts, will form a fringe pattern according to Fig. C.2. The fringes, formed by alternately constructive and destructive superposition of the two beams, define the measuring volume. The particle moves through the fringe pattern creating a Gaussian variation in the scattered light density. This is converted by the photo-multiplier into a voltage signal with

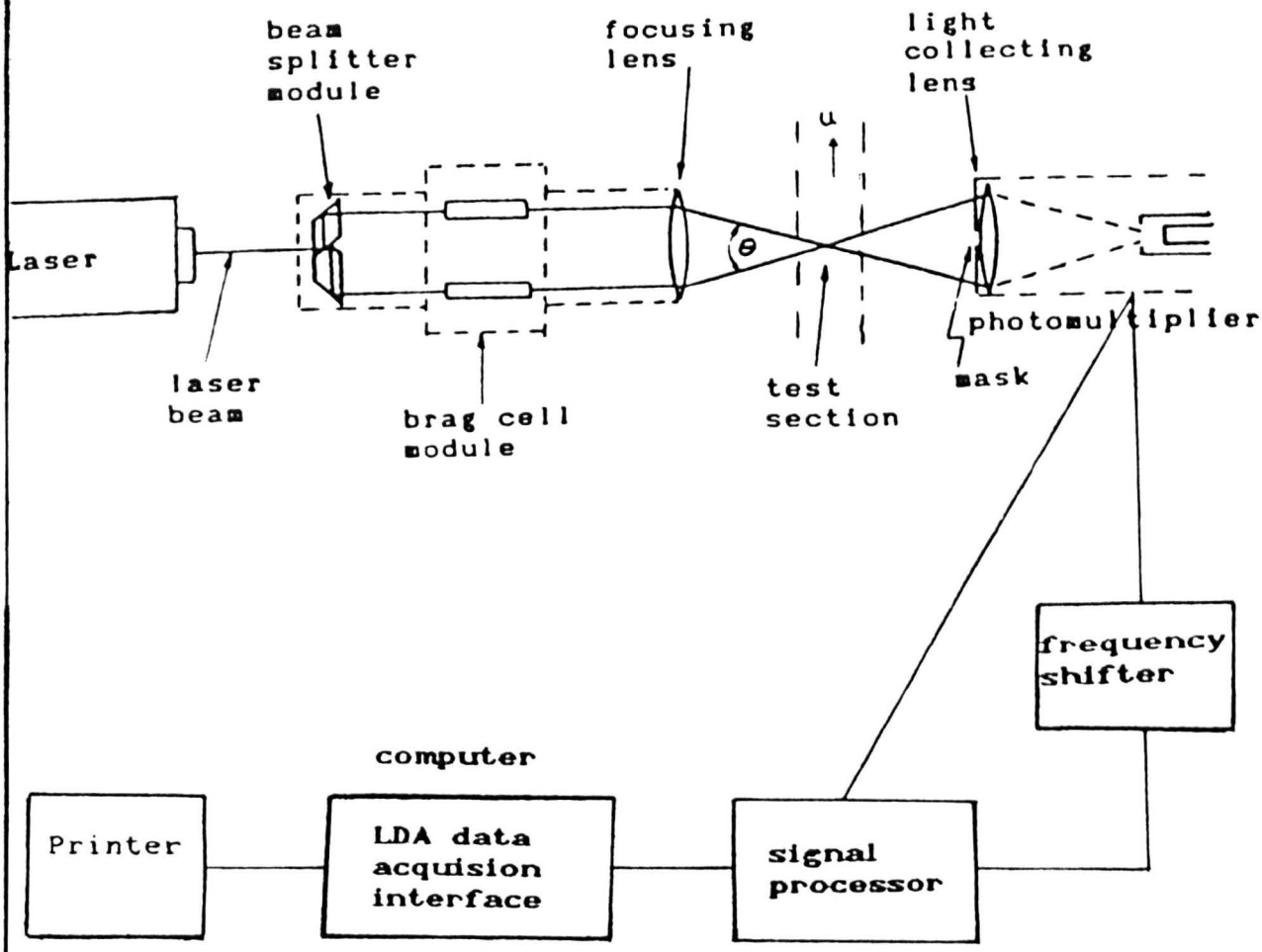

FIGURE C.1 SCHEMATIC LAYOUT OF THE LDA SYSTEM

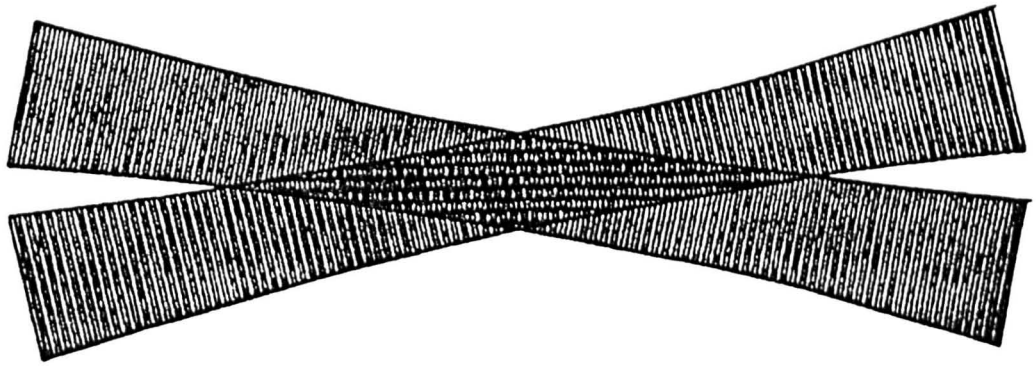

FIGURE C.2 THE FRINGE PATTERN

a time varying amplitude. The velocity measured is always normal to the fringes.

A mask was used to protect the highly sensitive photo-multiplier tube from the direct laser beams. A high voltage supply was used to supply the photo-multiplier with a continuously adjustable voltage.

The output signal from the photo-multiplier was analysed by a signal processor.

The optical part of the LDA system, comprising the laser, optical unit and photo-multiplier, was mounted on a rigid traversing machine capable of moving in the three coordinate directions (see Fig. C.3 and plate C.1). The accuracy of positioning the LDA system in each direction was 0.025 mm.

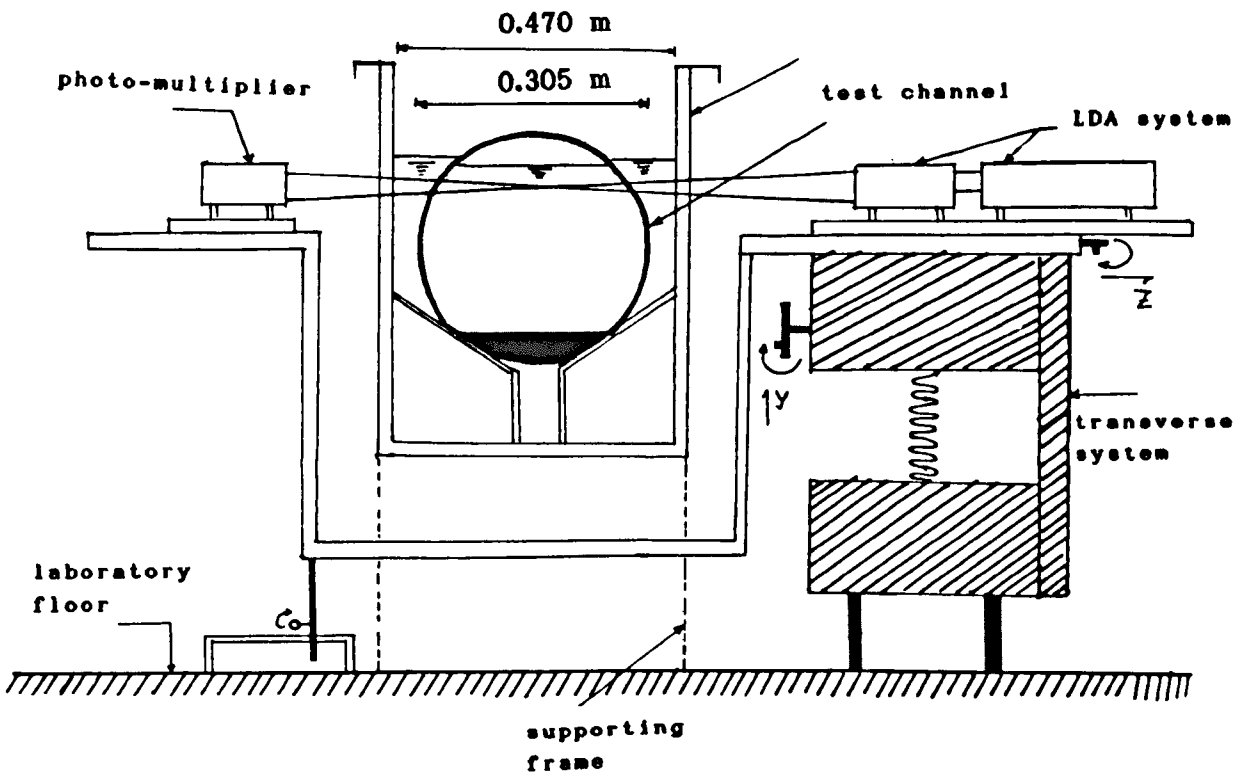

FIGURE C.3 EXPERIMENTAL SET UP AND ARRANGEMENT OF LDA SYSTEM

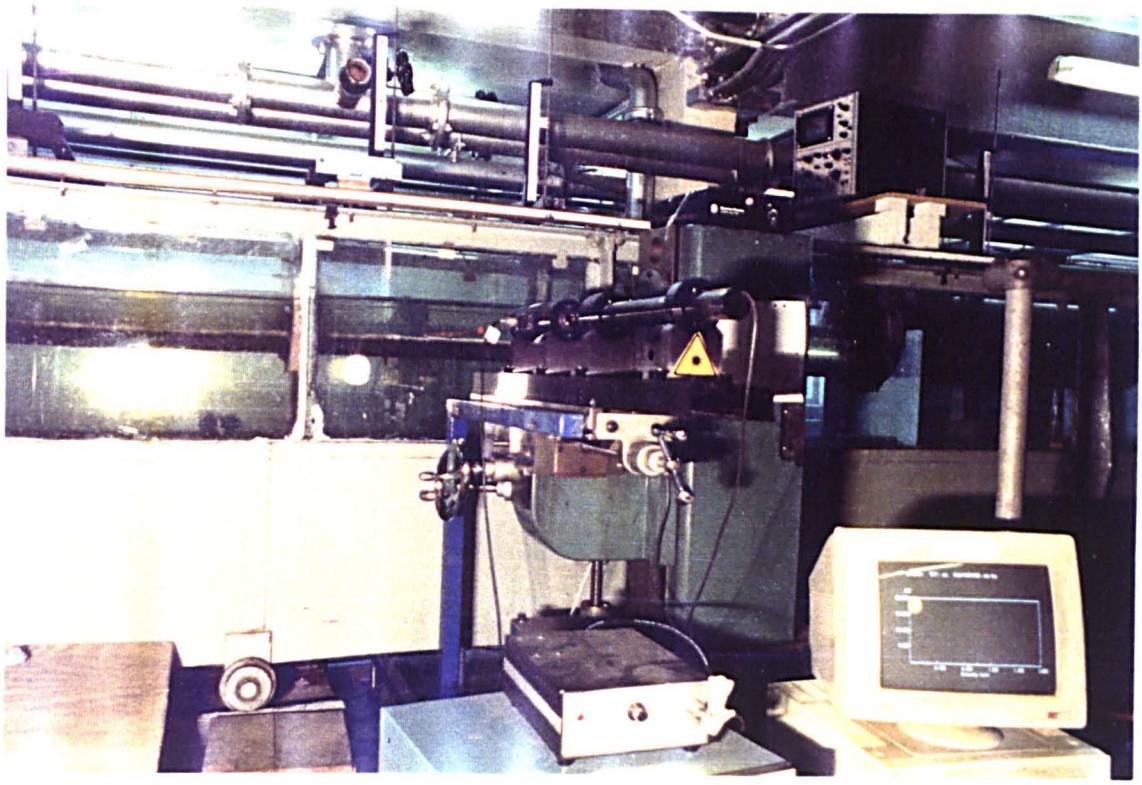

PLATE C.1 SHOWING THE HELIUM NEON LASER

b) Signal Processing

The TSI model IFA 550 Signal Processor was used (see plate C.2). It is designed to extract velocity information from noisy signals derived from a Laser Doppler Anemometer. It operates without operator interaction in a "hand off" mode. In searching for a signal, the IFA 550 combines correlation and a digital form of forward feed control. This combination provides a method whereby an autocorrelation is performed on each half-cycle of the signal to ensure that the cycles correlate in succession. The IFA 550 automatically rejects noise, ensuring that it makes only good measurements.

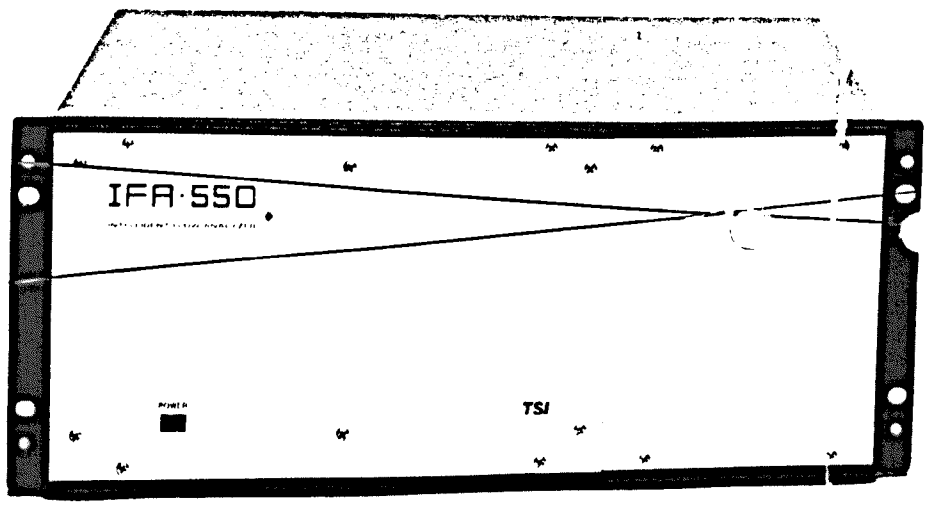

PLATE C.2 THE SIGNAL PROCESSOR

The system is operated with a data analysis and interface package which provides real-time velocity histograms and read out mean velocity and turbulence. Fig. C.4 shows a representative sample of simultaneous filtered data at time intervals, and much of the noise has been eliminated.

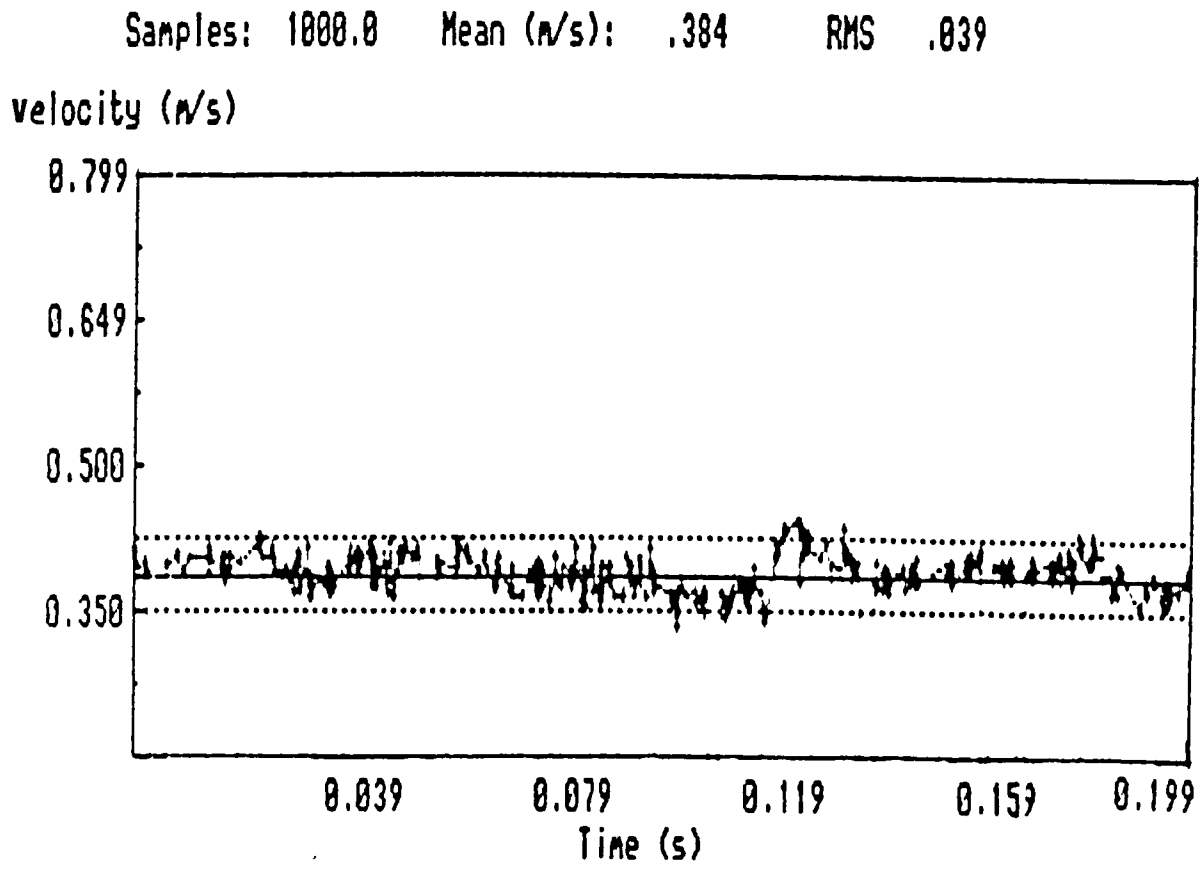

FIGURE C.4 TIME DEPENDENT VELOCITY (trace of velocity, V)

c) Theoretical Background of LDA

The simplest way of explaining the nature of the Laser Doppler signal is the fringe model. The two intersecting beams make up a fringe pattern (see Fig. C.2). Particles

moving across the fringe scatter the light and a signal, consisting of light and dark regions, is detected. The time difference between the light peaks is dependent on the velocity of the particles and the fringe spacing. The latter being determined by the optical set up, the laser light wavelength and the angle between the two incident beams. The fringe spacing is given by:

$$\delta_f = \frac{\lambda}{2} \sin (\ominus/ 2) \qquad (C.1)$$

where λ is the laser light wavelength, $\ominus$ the angle extended by the two incident beams.

The Doppler frequency (f_D) is given by:

$$f_D = f_s - f_i = \frac{1}{\lambda} \vec{V} (\hat{e}_s - \hat{e}_i) \qquad (C.2)$$

where f_s and f_i are the frequencies of the scattered and incident and beams respectively, $\vec{V}$ is the velocity vector of the particle passing through the measuring volume, and $\hat{e}_s$ and $\hat{e}_i$ are the unit vectors of the scattered and incident beam respectively.

By considering the velocity component in the direction of the flow f_D can be written as:

$$f_D = \frac{2 V_x}{\lambda} \sin (\ominus/2) \qquad (C.3)$$

and the velocity is given by:

$$V_x = \frac{\lambda f_D}{2 \sin(\theta/2)} \qquad (C.4)$$

where θ and λ are known parameters of the system and f_D is measured from the signal.

In practical situations there are other factors to take into consideration. For instance if there is more than one particle in the measuring volume.

In a laser beam operating in the fundamental optical mode Transverse Electromagnetic Mode (TEM), the measuring volume is an ellipsoid (see Fig. C.6). The TEM means that the laser may be focused to the smallest spot and the energy can be concentrated in a small measuring volume (i.e., the laser beam has a Gaussian intensity distribution). The probe volume parameters according to Fig. C.6 are:

$$2a = 4\,\delta_x = \frac{d_w}{\cos(\theta/2)} \qquad (C.5)$$

$$2b = 4\,\delta_y = d_w \qquad (C.6)$$

$$2c = 4\,\delta_z = \frac{d_w}{\sin(\theta/2)} \qquad (C.7)$$

where d_w is the diameter of the laser beam waist, which is given by:

$$d_w = (4/\pi)(f\lambda/d_2) = (4/\pi)(f\lambda/Ed_1) \qquad (C.8)$$

where f is the focal distance of the optical system, d_1 is the beam waist diameter, d_2 is the expanded beam waist diameter and E is the beam expansion ratio.

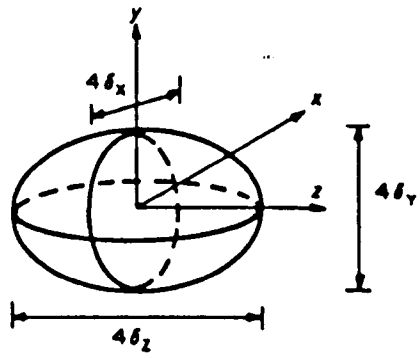

FIGURE C.6 PROBE VOLUME (ELLIPSOID)

The number of fringes (N_f) is given by:

$$N_f = \frac{4D_2}{\pi d_2} \cdot \frac{4ED_1}{\pi E d_1} \qquad (C.9)$$

where D_1 is the beams is the beams separation at front of lens and D_2 is the beams separation in the optics.

The performance of the LDA is described by the same parameters. It is related to the calibration constant, to the dimensions of the measuring volume and to the number and separation of the interference fringe lines in the measuring volume, and to the fixed characteristics of the LDA system such as laser beams separation, laser wavelength, beam expansion ratio and the measuring distance.

d) Experimental Procedure

It is necessary to check that the LDA instruments are set properly before the test started. Therefore a step by step adjustment of the transmitting optics must be carried out before using it for the experimental work.

The adjustments of the laser light beam were performed according to the following sequence:

1- The transmitting optics were mounted on the optical traversing machine, and then the laser was switched on. The Brag cell section was connected to its power supply and the frequency of the laser beam was shifted.

2- The light beams were positioned properly on the prisms, by making adjustments through small ports located on the beam splitter, and the Brag cell section. The best position were indicated by the brightest image on screen (a wide screen made of paper was mounted at the front of the system). Adjustments were made by using an Allen key.

3- To ensure that the laser beam was parallel to the top of the optical bench, the following procedure was used: The beam expander was screwed onto the transmitting optics and a special alignment mask was was placed in front of the beam expander. The beam splitter's adjustment knobs were then used to ensure that the beams were parallel and passed through the middle part of the alignment mask. The alignment mask was then removed.

4- The appropriate front lens was selected and screwed on to the expander.

5- The interaction of the two beams must be checked for every measurement.

APPENDIX D

CLEAR WATER EXPERIMENTAL DATA

TABLE 1 CLEAR WATER EXPERIMENTS IN CHANNEL WITH 47 mm THICK BED
(SMOOTH BOUNDARY)

	Q m^3/s	S	y_o mm	y_t/D	A m^2	R m	n	λ_c	τ_o N/m^2	T C°	R_e	k_s mm	Fr
1	0.0087	0.0011	65.4	0.37	0.0173	0.0465	0.009	0.016	0.51	20.0	92053.9	−0.07	0.66
2	0.0073	0.0006	65.3	0.37	0.0172	0.0464	0.007	0.012	0.28	20.0	77751.7	−0.18	0.56
3	0.0119	0.0040	57.1	0.34	0.0148	0.0419	0.010	0.021	1.64	20.0	131794.8	0.12	1.13
4	0.0106	0.0025	62.0	0.36	0.0163	0.0446	0.010	0.021	1.09	21.0	117106.9	0.12	0.88
5	0.0258	0.0027	105.5	0.50	0.0290	0.0647	0.009	0.017	1.68	20.0	226295.8	0.06	0.92
6	0.0177	0.0010	101.0	0.49	0.0279	0.0630	0.008	0.012	0.62	21.0	160563.1	−0.10	0.67
7	0.0212	0.0021	101.8	0.49	0.0282	0.0633	0.010	0.018	1.27	21.0	191628.5	0.09	0.79
8	0.0089	0.0011	64.6	0.37	0.0171	0.0460	0.008	0.015	0.51	20.0	94331.9	−0.09	0.69
9	0.0073	0.0007	65.4	0.37	0.0173	0.0464	0.008	0.014	0.32	20.0	77403.1	−0.14	0.56
10	0.0120	0.0041	56.8	0.34	0.0148	0.0417	0.009	0.020	1.68	20.0	133454.0	0.11	1.15
11	0.0106	0.0026	62.3	0.36	0.0164	0.0447	0.010	0.022	1.14	20.0	114199.6	0.17	0.88
12	0.0255	0.0026	105.5	0.50	0.0294	0.0648	0.009	0.018	1.65	20.0	221709.6	0.08	0.89
13	0.0177	0.0012	104.7	0.50	0.0291	0.0645	0.009	0.017	0.76	20.0	153972.4	0.00	0.63
14	0.0201	0.0018	103.4	0.49	0.0287	0.0640	0.010	0.018	1.10	20.0	176257.8	0.07	0.73
15	0.0089	0.0011	65.0	0.37	0.0172	0.0462	0.008	0.015	0.50	20.0	94183.7	−0.09	0.68
16	0.0073	0.0007	65.3	0.37	0.0172	0.0464	0.008	0.013	0.30	20.0	77303.6	−0.16	0.56
17	0.0119	0.0038	57.0	0.34	0.0148	0.0418	0.009	0.019	1.56	20.0	132171.0	0.07	1.13
18	0.0106	0.0024	62.0	0.36	0.0163	0.0446	0.009	0.020	1.05	20.0	114359.5	0.08	0.88
19	0.0254	0.0026	104.5	0.50	0.0291	0.0644	0.009	0.017	1.64	20.0	221656.4	0.06	0.90
20	0.0176	0.0012	104.5	0.50	0.0291	0.0644	0.009	0.017	0.76	20.0	153588.7	0.00	0.63
21	0.0201	0.0017	102.0	0.49	0.0283	0.0634	0.009	0.017	1.06	20.0	177372.3	0.03	0.74
22	0.0086	0.0010	65.0	0.37	0.0172	0.0462	0.008	0.014	0.45	18.0	86855.9	−0.12	0.66
23	0.0075	0.0007	65.7	0.37	0.0174	0.0466	0.008	0.014	0.32	18.0	75454.3	−0.16	0.57
24	0.0120	0.0039	57.0	0.34	0.0148	0.0418	0.009	0.020	1.60	19.0	130084.0	0.08	1.14
25	0.0106	0.0024	61.8	0.36	0.0162	0.0445	0.009	0.020	1.05	18.0	109008.8	0.07	0.89
26	0.0179	0.0012	104.4	0.50	0.0290	0.0644	0.009	0.016	0.76	18.5	150669.5	−0.02	0.64
27	0.0202	0.0018	103.3	0.49	0.0287	0.0639	0.010	0.018	1.13	19.0	173221.3	0.08	0.73
28	0.0089	0.0011	65.0	0.37	0.0172	0.0462	0.008	0.015	0.51	18.0	89502.8	−0.09	0.68
29	0.0120	0.0042	56.1	0.34	0.0146	0.0413	0.009	0.020	1.70	18.5	129185.4	0.10	1.17
30	0.0106	0.0025	62.1	0.36	0.0163	0.0447	0.010	0.021	1.10	18.5	110188.0	0.12	0.88
31	0.0177	0.0012	104.6	0.50	0.0291	0.0644	0.009	0.016	0.76	18.0	147021.6	−0.01	0.63
32	0.0201	0.0018	103.4	0.49	0.0287	0.0640	0.010	0.018	1.13	18.0	167859.4	0.09	0.73
33	0.0094	0.0011	65.2	0.37	0.0172	0.0463	0.008	0.013	0.50	18.0	94830.8	−0.12	0.72
34	0.0121	0.0038	58.0	0.34	0.0151	0.0424	0.009	0.020	1.58	17.8	126970.7	0.08	1.12
35	0.0106	0.0024	61.9	0.36	0.0163	0.0445	0.009	0.020	1.05	18.0	108950.0	0.07	0.88
36	0.0177	0.0012	104.7	0.50	0.0291	0.0645	0.009	0.016	0.76	18.0	146950.5	−0.01	0.63
37	0.0205	0.0018	103.9	0.49	0.0289	0.0642	0.010	0.018	1.13	18.0	170809.0	0.07	0.74
38	0.0295	0.0010	157.7	0.67	0.0450	0.0803	0.009	0.014	0.77	18.0	197589.1	−0.05	0.53
39	0.0312	0.0009	157.9	0.67	0.0450	0.0804	0.008	0.012	0.74	20.5	221549.6	−0.08	0.56
40	0.0257	0.0006	200.8	0.81	0.0564	0.0856	0.010	0.018	0.47	20.0	153537.7	0.09	0.30
41	0.0227	0.0005	155.2	0.66	0.0443	0.0798	0.008	0.011	0.36	20.0	161197.5	−0.16	0.42
42	0.0303	0.0010	156.5	0.67	0.0446	0.0801	0.008	0.013	0.75	20.0	214104.0	−0.07	0.55
43	0.0257	0.0005	202.5	0.82	0.0568	0.0856	0.010	0.016	0.42	20.0	152515.3	−0.00	0.29
44	0.0216	0.0005	153.0	0.66	0.0436	0.0793	0.008	0.011	0.35	20.0	154679.6	−0.15	0.41
45	0.0306	0.0010	156.9	0.67	0.0447	0.0802	0.009	0.013	0.79	20.0	215889.7	−0.06	0.55
46	0.0254	0.0005	200.8	0.81	0.0564	0.0856	0.010	0.017	0.42	20.0	151736.9	0.00	0.30
47	0.0300	0.0010	156.5	0.67	0.0446	0.0801	0.009	0.013	0.76	18.7	205375.0	−0.07	0.54
48	0.0258	0.0005	201.9	0.82	0.0567	0.0856	0.010	0.018	0.45	18.5	147954.0	0.05	0.30
49	0.0303	0.0009	156.2	0.67	0.0445	0.0800	0.008	0.013	0.73	18.5	206627.6	−0.09	0.55

TABLE []2 CLEAR WATER EXPERIMENTS IN CIRCULAR CHANNEL WITH 47 mm THICK BED
(ROUGHNESS I (ks=0.80 mm))

	Q m^3/s	S	y_o mm	y_t/D	A m^2	R m	n	λ_c	τ_o N/m^2	Temp C°	R_e	k_s mm	Fr
1	0.00943	0.00225	64.5	0.37	0.01706	0.04602	0.011	0.027	1.02	18.6	96753.2	0.48	0.73
2	0.01997	0.00225	101.7	0.49	0.02827	0.06335	0.011	0.022	1.40	18.6	170333.0	0.34	0.74
3	0.00979	0.00303	62.7	0.36	0.01654	0.04506	0.012	0.031	1.34	19.0	102512.4	0.82	0.80
4	0.02193	0.00316	102.2	0.49	0.02843	0.06356	0.012	0.027	1.97	19.1	188887.4	0.72	0.81
5	0.01728	0.00171	99.7	0.48	0.02765	0.06253	0.010	0.021	1.05	19.6	152410.6	0.25	0.66
6	0.00979	0.00315	63.0	0.36	0.01663	0.04522	0.012	0.032	1.40	17.2	97873.7	1.00	0.79
7	0.02223	0.00312	100.7	0.49	0.02796	0.06295	0.011	0.024	1.93	17.3	184396.2	0.50	0.84
8	0.00844	0.00275	60.4	0.36	0.01586	0.04379	0.012	0.033	1.18	18.0	87369.6	1.09	0.73
9	0.02036	0.00276	98.7	0.48	0.02734	0.06212	0.011	0.024	1.68	18.1	173835.4	0.48	0.79
10	0.00765	0.00182	61.3	0.36	0.01614	0.04431	0.011	0.028	0.79	18.5	79721.3	0.56	0.64
11	0.01714	0.00178	101.5	0.49	0.02822	0.06329	0.011	0.024	1.10	18.5	145951.1	0.45	0.64
12	0.01704	0.00144	105.1	0.50	0.02929	0.06467	0.011	0.022	0.91	19.2	145297.3	0.27	0.60
13	0.01884	0.00209	104.9	0.50	0.02923	0.06460	0.011	0.025	1.32	19.5	161958.6	0.61	0.66
14	0.02072	0.00286	102.3	0.49	0.02845	0.06359	0.012	0.027	1.78	19.5	180170.9	0.76	0.76
15	0.00979	0.00289	63.8	0.37	0.01684	0.04561	0.012	0.031	1.29	19.4	102920.2	0.84	0.78
16	0.00817	0.00237	63.2	0.36	0.01669	0.04534	0.013	0.035	1.05	18.8	84901.2	1.34	0.66
17	0.01013	0.00263	63.0	0.36	0.01662	0.04520	0.011	0.025	1.16	18.9	105670.8	0.36	0.82
18	0.01759	0.00192	100.9	0.49	0.02802	0.06303	0.011	0.024	1.18	18.1	148729.9	0.46	0.66
19	0.00752	0.00198	60.0	0.35	0.01575	0.04358	0.012	0.030	0.85	18.9	79750.7	0.69	0.66
20	0.01940	0.00243	104.1	0.50	0.02901	0.06431	0.012	0.027	1.54	17.0	157241.1	0.82	0.69
21	0.00988	0.00248	65.9	0.37	0.01748	0.04677	0.011	0.028	1.14	17.1	96889.9	0.65	0.74
22	0.02052	0.00306	99.1	0.48	0.02748	0.06231	0.012	0.027	1.87	17.7	173152.7	0.73	0.79
23	0.00926	0.00308	61.0	0.36	0.01606	0.04415	0.012	0.032	1.34	17.9	95245.7	0.96	0.79
24	0.02893	0.00215	155.1	0.67	0.04429	0.07980	0.013	0.032	1.68	19.2	201269.1	1.72	0.53
25	0.03220	0.00262	155.5	0.67	0.04439	0.07987	0.013	0.031	2.05	18.0	217251.4	1.68	0.59
26	0.03207	0.00195	161.7	0.69	0.04615	0.08112	0.012	0.026	1.55	19.0	216645.5	0.82	0.55
27	0.03507	0.00172	161.6	0.69	0.04612	0.08110	0.010	0.019	1.37	19.8	241637.2	0.19	0.60
28	0.02872	0.00238	163.1	0.69	0.04655	0.08138	0.015	0.040	1.90	18.0	188266.4	3.71	0.48
29	0.03222	0.00265	157.8	0.67	0.04505	0.08035	0.013	0.033	2.09	18.2	216571.7	1.96	0.57
30	0.02612	0.00192	151.8	0.65	0.04331	0.07905	0.013	0.033	1.49	18.6	181400.6	1.92	0.50
31	0.03507	0.00288	163.9	0.69	0.04678	0.08153	0.013	0.033	2.30	19.2	236063.5	2.01	0.59
32	0.03375	0.00223	160.1	0.68	0.04571	0.08080	0.012	0.026	1.77	19.1	229856.3	0.86	0.59
33	0.02182	0.00105	157.1	0.67	0.04484	0.08021	0.012	0.028	0.83	19.0	149959.2	1.10	0.39

TABLE 13 CLEAR WATER EXPERIMENTS IN CIRCULAR CHANNEL WITH 47 mm THICK BED (ROUGHNESS II (ks=1.4 mm))

	Q m^3/s	S	y_0 mm	y_t/D	A m^2	R m	n	λ_c	τ_0 N/m^2	T C^o	R_e	ks mm	Fr
1	0.00926	0.00340	62.4	0.36	0.01660	0.04520	0.013	0.038	1.49	15.5	88671.8	1.79	0.75
2	0.00901	0.00370	59.9	0.35	0.01588	0.04382	0.013	0.040	1.60	15.4	87309.4	1.93	0.78
3	0.01068	0.00410	64.7	0.37	0.01727	0.04640	0.013	0.039	1.86	15.5	101015.4	1.93	0.82
4	0.02107	0.00410	96.5	0.47	0.02684	0.06140	0.013	0.032	2.49	15.6	170226.6	1.43	0.84
5	0.02126	0.00320	102.8	0.49	0.02876	0.06399	0.012	0.030	2.02	15.9	168214.5	1.08	0.77
6	0.02023	0.00280	103.5	0.50	0.02897	0.06426	0.012	0.029	1.79	15.9	159563.3	1.07	0.72
7	0.01675	0.00206	99.3	0.48	0.02757	0.06238	0.012	0.027	11.26	16.4	136513.0	0.76	0.64
8	0.00888	0.00195	68.9	0.38	0.01840	0.04835	0.012	0.032	0.93	16.4	84015.0	1.01	0.62
9	0.00828	0.00310	63.7	0.37	0.01686	0.04559	0.014	0.046	1.39	17.1	82119.2	3.04	0.65
10	0.01843	0.00311	94.9	0.47	0.02625	0.06058	0.012	0.030	1.85	17.4	157166.5	1.08	0.76
11	0.00863	0.00321	60.2	0.35	0.01584	0.04370	0.013	0.037	1.38	17.5	88166.1	1.54	0.75
12	0.0196	0.0031	98.7	0.48	0.0275	0.0623	0.012	0.030	1.91	17.0	162539.4	1.13	0.76
13	0.0118	0.0034	71.9	0.39	0.0194	0.0501	0.013	0.036	1.68	17.0	111592.0	1.68	0.76
14	0.01858	0.00289	97.8	0.48	0.02724	0.06199	0.012	0.030	1.76	16.7	153387.9	1.13	0.73
15	0.01077	0.00295	70.4	0.39	0.01897	0.04939	0.013	0.035	1.43	17.0	102543.7	1.53	0.72
16	0.00841	0.00189	66.4	0.38	0.01778	0.04730	0.012	0.031	0.88	17.0	81879.6	0.92	0.62
17	0.01684	0.00211	98.6	0.48	0.02746	0.06230	0.012	0.027	1.29	17.2	140325.8	0.78	0.65
18	0.02030	0.00348	99.2	0.48	0.02770	0.06260	0.013	0.032	2.14	15.9	162931.1	1.39	0.78
19	0.01000	0.00210	71.3	0.39	0.01920	0.04980	0.012	0.031	1.04	17.2	95455.4	0.90	0.66
20	0.00920	0.00280	65.1	0.37	0.01740	0.04660	0.013	0.037	1.28	15.8	87518.2	1.57	0.70
21	0.01020	0.00340	64.5	0.37	0.01720	0.04630	0.013	0.035	1.55	15.9	97720.4	1.38	0.78
22	0.01812	0.00212	104.3	0.50	0.02920	0.06456	0.012	0.028	1.34	16.1	143159.4	0.87	0.64
23	0.03327	0.00290	150.7	0.65	0.04314	0.07892	0.013	0.030	2.23	15.0	211446.3	1.44	0.64
24	0.03366	0.00200	158.2	0.68	0.04530	0.08053	0.011	0.023	1.60	15.1	208447.0	0.53	0.60
25	0.03370	0.00330	146.2	0.64	0.04180	0.07790	0.013	0.031	2.52	15.1	218516.8	1.60	0.68
26	0.02884	0.00174	158.1	0.68	0.04517	0.08038	0.012	0.027	1.37	17.0	187700.4	0.96	0.51
27	0.02111	0.00265	107.4	0.51	0.03003	0.06556	0.012	0.028	1.70	17.0	168518.3	0.86	0.72
28	0.03359	0.00165	156.9	0.67	0.04482	0.08013	0.010	0.019	1.30	17.2	220736.5	0.15	0.60
29	0.03664	0.00301	161.0	0.69	0.04600	0.08096	0.013	0.030	2.39	17.2	236987.1	1.51	0.63
30	0.0337	0.0032	157.4	0.67	0.0451	0.0804	0.014	0.036	2.53	17.0	219471.8	2.75	0.60
31	0.03397	0.00260	168.0	0.71	0.04807	0.08230	0.014	0.033	2.06	16.8	211679.8	2.08	0.54
32	0.03574	0.00214	161.8	0.69	0.04633	0.08120	0.011	0.023	1.71	17.1	229740.6	0.51	0.61
33	0.03018	0.00181	165.6	0.70	0.04739	0.08192	0.013	0.029	1.46	17.2	191733.1	1.27	0.49
34	0.02150	0.00260	109.2	0.52	0.03071	0.06644	0.012	0.027	1.68	17.2	171104.0	0.85	0.70
35	0.03360	0.00240	160.4	0.68	0.04594	0.08098	0.013	0.029	1.92	15.8	210160.8	1.27	0.58
36	0.03630	0.00300	161.4	0.69	0.04622	0.08120	0.013	0.031	2.41	15.8	226096.0	1.72	0.20

TABLE D4 CLEAR WATER EXPERIMENTS IN CHANNEL WITH 77 mm THICK BED (SMOOTH BOUNDARY)

	Q m^3/s	S	y_o mm	y_t/D	A m^2	R m	n	λ_c	τ_o N/m^2	T C^o	R_e	Ks(mm)	Fr
1	0.0215	0.0037	75.1	0.50	0.0220	0.0519	0.009	0.016	1.88	18.5	192778.7	0.00	1.16
2	0.0076	0.0011	60.4	0.45	0.0174	0.0440	0.010	0.021	0.50	19.0	73852.3	0.09	0.58
3	0.0052	0.0022	38.1	0.38	0.0108	0.0310	0.010	0.023	0.68	19.0	57394.3	0.11	0.81
4	0.0066	0.0019	44.6	0.40	0.0127	0.0350	0.009	0.020	0.67	18.5	69550.7	0.01	0.81
5	0.0060	0.0008	54.0	0.43	0.0155	0.0410	0.009	0.017	0.32	18.0	59027.1	-0.11	0.54
6	0.0089	0.0014	60.2	0.45	0.0174	0.0440	0.009	0.019	0.62	19.0	84824.8	0.01	0.68
7	0.0057	0.0020	42.0	0.39	0.0119	0.0335	0.010	0.023	0.65	17.5	59349.7	0.10	0.76
8	0.0073	0.0010	58.6	0.44	0.0169	0.0434	0.009	0.019	0.44	16.0	66792.3	-0.03	0.58
9	0.0057	0.0020	38.4	0.38	0.0109	0.0312	0.008	0.018	0.61	15.0	56868.7	-0.07	0.88
10	0.0062	0.0009	53.5	0.43	0.0154	0.0406	0.009	0.018	0.36	15.2	57558.1	-0.10	0.58
11	0.0056	0.0020	43.5	0.40	0.0124	0.0345	0.010	0.026	0.67	16.0	55477.9	0.28	0.71
12	0.0109	0.0017	65.6	0.47	0.0190	0.0472	0.010	0.020	0.80	15.0	93828.8	0.06	0.73
13	0.0127	0.0021	67.1	0.47	0.0195	0.0480	0.009	0.019	1.01	15.0	108382.3	0.05	0.82
14	0.0152	0.0020	80.7	0.52	0.0236	0.0545	0.010	0.021	1.09	19.0	135003.1	0.19	0.74
15	0.0148	0.0017	84.6	0.53	0.0248	0.0563	0.010	0.021	0.94	20.0	132931.9	0.18	0.67
16	0.0258	0.0013	126.5	0.67	0.0374	0.0708	0.009	0.015	0.91	18.3	184888.1	-0.02	0.61
17	0.0246	0.0009	135.9	0.70	0.0400	0.0730	0.009	0.014	0.64	18.3	169898.5	-0.08	0.52
18	0.0231	0.0015	116.7	0.64	0.0340	0.0670	0.010	0.018	0.99	18.3	172317.0	0.06	0.63
19	0.0233	0.0026	94.4	0.56	0.0278	0.0603	0.009	0.018	1.55	19.0	193924.4	0.07	0.88
20	0.0174	0.0021	84.6	0.53	0.0248	0.0562	0.010	0.018	1.14	19.0	151768.5	0.07	0.79
21	0.0152	0.0013	85.2	0.53	0.0250	0.0565	0.009	0.016	0.71	19.0	131936.6	-0.05	0.68
22	0.0230	0.0008	126.0	0.67	0.0372	0.0707	0.008	0.011	0.56	18.0	163662.6	-0.13	0.55
23	0.0351	0.0022	118.8	0.64	0.0351	0.0687	0.008	0.012	1.50	18.0	257400.9	-0.06	0.92
24	0.0215	0.0026	89.7	0.55	0.0264	0.0584	0.009	0.018	1.50	16.7	172679.8	0.07	0.88
25	0.0174	0.0023	82.1	0.52	0.0241	0.0552	0.010	0.019	1.24	17.0	145469.9	0.09	0.82
26	0.0278	0.0013	126.2	0.67	0.0372	0.0707	0.008	0.013	0.92	15.0	183647.3	-0.08	0.66
27	0.0228	0.0010	125.6	0.66	0.0371	0.0706	0.009	0.014	0.68	15.0	151126.0	-0.08	0.55
28	0.0337	0.0024	129.3	0.68	0.0381	0.0715	0.009	0.017	1.66	15.0	220003.9	0.06	0.77
29	0.0161	0.0017	86.1	0.53	0.0253	0.0569	0.010	0.019	0.95	15.5	127260.7	0.07	0.70
30	0.0206	0.0028	86.3	0.54	0.0254	0.0570	0.010	0.019	1.58	15.8	163990.0	0.11	0.90
31	0.0183	0.0024	83.6	0.53	0.0245	0.0558	0.010	0.019	1.29	16.0	148513.2	0.07	0.84
32	0.0316	0.0025	122.9	0.66	0.0363	0.0698	0.010	0.018	1.71	15.5	214040.9	0.11	0.79
33	0.0246	0.0013	127.2	0.67	0.0375	0.0710	0.009	0.016	0.87	16.0	166087.6	-0.01	0.58
34	0.0219	0.0010	124.4	0.66	0.0367	0.0702	0.009	0.016	0.69	15.5	147750.2	-0.04	0.54
35	0.0144	0.0017	84.6	0.53	0.0248	0.0563	0.015	0.022	0.95	16.0	116683.2	0.26	0.65
36	0.0214	0.0027	91.9	0.55	0.0270	0.0593	0.010	0.020	1.55	15.7	165854.9	0.15	0.85
37	0.0170	0.0023	82.3	0.52	0.0241	0.0553	0.010	0.020	1.23	16.0	138864.9	0.12	0.80
38	0.0327	0.0025	125.4	0.66	0.0370	0.0705	0.010	0.018	1.73	16.0	221907.6	0.10	0.79
39	0.0258	0.0013	130.0	0.68	0.0383	0.0717	0.009	0.016	0.91	16.0	172089.4	-0.00	0.59
40	0.0231	0.0010	126.3	0.67	0.0373	0.0707	0.009	0.014	0.67	16.0	156188.9	-0.08	0.55
41	0.0164	0.0017	86.6	0.54	0.0254	0.0571	0.009	0.018	0.93	16.0	130994.4	0.04	0.71
42	0.0213	0.0028	90.3	0.55	0.0265	0.0587	0.010	0.020	1.60	15.0	163808.3	0.15	0.87
43	0.0172	0.0023	83.6	0.53	0.0245	0.0558	0.010	0.020	1.25	15.0	136475.8	0.15	0.79
44	0.0332	0.0025	125.9	0.67	0.0371	0.0707	0.009	0.017	1.71	16.0	225276.2	0.07	0.80
45	0.0250	0.0012	126.0	0.67	0.0372	0.0707	0.009	0.015	0.84	16.0	169497.6	-0.04	0.60

TABLE D5 CLEAR WATER EXPERIMENTS IN CHANNEL WITH 77 mm THICK BED
(ROUGHNESS I; ks = 0.8 mm)

	Q m^3/s	S	y_0 mm	y_t/D	A m^2	R m	n	λ_c	τ_o N/m^2	Temp. C°	R_e	k_s mm	Fr
1	0.0146	0.0027	76.3	0.50	0.0224	0.0527	0.0113	0.027	1.40	17.8	127548.7	0.56	0.76
2	0.0100	0.0025	61.0	0.45	0.0178	0.0450	0.0110	0.027	1.09	17.5	93824.8	0.53	0.74
3	0.0067	0.0020	51.8	0.42	0.0150	0.0400	0.0120	0.031	0.77	17.8	66150.9	0.75	0.64
4	0.0088	0.0024	58.9	0.45	0.0170	0.0430	0.0120	0.031	1.04	17.8	83576.9	0.86	0.69
5	0.0127	0.0031	68.6	0.48	0.0200	0.0490	0.0120	0.030	1.49	15.0	107130.4	0.80	0.79
6	0.0124	0.0019	75.9	0.50	0.0222	0.0523	0.0111	0.026	0.99	15.2	101861.8	0.46	0.66
7	0.0084	0.0025	60.3	0.45	0.0174	0.0440	0.0130	0.038	1.08	17.0	77585.0	1.63	0.64
8	0.0083	0.0020	63.4	0.46	0.0184	0.0460	0.0130	0.035	0.91	16.5	75191.3	1.37	0.59
9	0.0134	0.0019	81.5	0.52	0.0239	0.0549	0.0111	0.026	1.01	15.0	107168.8	0.48	0.64
10	0.0090	0.0021	61.2	0.45	0.0178	0.0451	0.0110	0.029	0.92	15.1	79311.0	0.63	0.67
11	0.0101	0.0030	60.8	0.45	0.0177	0.0448	0.0120	0.032	1.30	14.0	86352.9	0.98	0.75
12	0.0101	0.0023	64.8	0.47	0.0189	0.0470	0.0120	0.030	1.07	15.1	87084.0	0.80	0.68
13	0.0124	0.0031	66.8	0.47	0.0195	0.0480	0.0120	0.029	1.44	15.1	105755.3	0.70	0.80
14	0.0207	0.0016	122.3	0.66	0.0361	0.0697	0.0116	0.026	1.06	17.3	147208.7	0.68	0.52
15	0.0194	0.0019	110.1	0.62	0.0325	0.0659	0.0119	0.027	1.22	17.5	145745.0	0.86	0.57
16	0.0124	0.0017	77.4	0.51	0.0228	0.0532	0.0107	0.024	0.89	17.8	108012.4	0.35	0.63
17	0.0130	0.0018	79.5	0.51	0.0234	0.0541	0.0110	0.025	0.95	17.8	111927.9	0.42	0.64
18	0.0223	0.0017	120.2	0.65	0.0355	0.0691	0.0111	0.024	1.17	16.0	154845.9	0.47	0.58
19	0.0222	0.0018	116.3	0.64	0.0343	0.0679	0.0110	0.023	1.20	16.2	157033.3	0.41	0.60
20	0.0170	0.0029	83.5	0.53	0.0245	0.0558	0.0114	0.027	1.60	16.0	138152.2	0.60	0.78
21	0.0142	0.0018	84.9	0.53	0.0249	0.0564	0.0110	0.025	1.01	16.0	114939.3	0.43	0.64
22	0.0164	0.0033	78.9	0.51	0.0231	0.0537	0.0116	0.028	1.74	15.0	132266.8	0.70	0.82
23	0.0204	0.0016	118.7	0.64	0.0350	0.0686	0.0116	0.026	1.10	15.0	139150.7	0.67	0.54
24	0.0218	0.0014	130.2	0.68	0.0384	0.0717	0.0114	0.024	0.98	15.0	141718.0	0.54	0.49
25	0.0254	0.0024	125.7	0.67	0.0371	0.0706	0.0123	0.029	1.68	14.2	164580.8	1.07	0.61
26	0.0174	0.0031	85.3	0.53	0.0250	0.0566	0.0118	0.028	1.71	15.0	136741.0	0.79	0.77
27	0.0310	0.0023	77.2	0.51	0.0226	0.0529	0.0116	0.028	1.18	15.0	106759.8	0.70	0.68
28	0.0124	0.0018	80.4	0.52	0.0235	0.0544	0.0116	0.028	0.96	15.0	99227.9	0.69	0.60
29	0.0163	0.0033	79.9	0.52	0.0234	0.0542	0.0118	0.029	1.75	15.0	131402.0	0.80	0.81
30	0.0206	0.0017	119.6	0.65	0.0353	0.0689	0.0120	0.027	1.16	15.0	139654.9	0.85	0.54
31	0.0222	0.0020	120.1	0.65	0.0355	0.0690	0.0122	0.028	1.39	15.0	149927.9	1.00	0.57
32	0.0278	0.0031	115.8	0.63	0.0342	0.0678	0.0115	0.025	2.08	15.0	191107.8	0.63	0.76
33	0.0146	0.0020	83.7	0.53	0.0245	0.0559	0.0110	0.025	1.09	14.8	114896.8	0.42	0.67
34	0.0142	0.0020	83.0	0.53	0.0243	0.0555	0.0111	0.025	1.07	15.2	113620.6	0.45	0.66
35	0.0179	0.0037	82.1	0.52	0.0241	0.0552	0.0118	0.029	2.00	15.2	143673.3	0.84	0.85
36	0.0257	0.0023	124.3	0.66	0.0367	0.0702	0.0117	0.026	1.59	15.2	171713.3	0.72	0.63
37	0.0256	0.0078	129.8	0.68	0.0383	0.0715	0.0114	0.025	1.37	15.2	167332.5	0.57	0.58

TABLE 06 CLEAR WATER EXPERIMENTS IN CHANNEL WITH 77 mm THICK BED
(ROUGHNESS I; ks= 1.4 mm)

	Q m^3/s	S	y_0 mm	y_t/D	A m^2	R m	n	λ_c	τ_o N/m^2	Temp. C°	R_e	k_s mm	Fr
1	0.0112	0.0028	71.2	0.49	0.0208	0.0500	0.0130	0.034	1.35	18.0	105123.1	1.36	0.69
2	0.0127	0.0025	75.7	0.50	0.0221	0.0520	0.0122	0.030	1.28	17.0	109271.6	1.01	0.68
3	0.0099	0.0025	66.0	0.47	0.0192	0.0470	0.0130	0.035	1.16	18.0	91354.8	1.40	0.66
4	0.0101	0.0032	61.9	0.46	0.0179	0.0450	0.0130	0.036	1.41	17.5	93437.3	1.44	0.74
5	0.0122	0.0027	73.9	0.50	0.0216	0.0510	0.0130	0.034	1.35	16.0	103032.0	1.34	0.68
6	0.0127	0.0021	78.9	0.51	0.0231	0.0536	0.0118	0.029	1.08	17.0	107254.9	0.80	0.64
7	0.0140	0.0031	77.1	0.51	0.0226	0.0527	0.0127	0.033	1.60	17.0	119170.1	1.45	0.73
8	0.0146	0.0034	80.6	0.52	0.0236	0.0543	0.0136	0.038	1.82	17.0	122422.2	2.16	0.71
9	0.0279	0.0039	125.1	0.67	0.0369	0.0702	0.0140	0.037	2.67	17.0	194217.6	2.62	0.68
10	0.0311	0.0040	125.1	0.67	0.0369	0.0702	0.0128	0.031	2.77	17.0	216308.2	1.46	0.75
11	0.0263	0.0029	120.2	0.65	0.0355	0.0688	0.0122	0.028	1.93	18.0	191017.9	0.99	0.68
12	0.0144	0.0028	81.6	0.52	0.0239	0.0548	0.0127	0.033	1.50	17.0	120235.0	1.38	0.68
13	0.0144	0.0029	79.3	0.52	0.0232	0.0537	0.0124	0.032	1.53	18.0	124601.4	1.17	0.72
14	0.0158	0.0039	79.5	0.52	0.0233	0.0538	0.0132	0.036	2.07	18.1	137378.4	1.74	0.79
15	0.0297	0.0036	120.6	0.65	0.0356	0.0690	0.0122	0.028	2.45	17.6	213502.0	1.01	0.76
16	0.0268	0.0029	121.2	0.65	0.0358	0.0691	0.0120	0.027	1.93	17.6	192222.2	0.92	0.68
17	0.0267	0.0025	126.2	0.67	0.0372	0.0705	0.0119	0.026	1.71	17.6	187709.0	0.81	0.64
18	0.0143	0.0031	79.1	0.52	0.0232	0.0536	0.0128	0.034	1.65	16.2	118384.9	1.57	0.71
19	0.0146	0.0033	77.9	0.51	0.0228	0.0531	0.0126	0.033	1.71	16.7	123320.1	1.35	0.75
20	0.0258	0.0032	115.6	0.63	0.0342	0.0675	0.0125	0.030	2.13	15.2	177714.9	1.22	0.71

TABLE D7 CLEAR WATER EXPERIMENTS IN CHANNEL WITH 120mm THICK BED (SMOOTH BOUNDARY)

	Q m^3/s	S	y_o mm	y_t/D	A m^2	R m	n	λ_c	τ_o N/m^2	Temp. C°	R_e	k_s mm	Fr
1	0.019	0.001	120.9	0.79	0.035	0.064	0.009	0.015	0.54	15.2	121192.4	-0.10	0.46
2	0.006	0.001	54.2	0.57	0.016	0.04	0.010	0.021	0.40	15.4	55116.7	0.03	0.53
3	0.008	0.001	67.7	0.62	0.021	0.047	0.011	0.025	0.52	16.0	68605.1	0.30	0.50
4	0.007	0.002	48.2	0.55	0.015	0.037	0.010	0.024	0.75	16.0	65571.2	0.20	0.72
5	0.011	0.002	70.2	0.62	0.021	0.048	0.010	0.022	0.76	16.2	90887.5	0.17	0.63
6	0.016	0.001	100.1	0.72	0.03	0.059	0.010	0.021	0.79	16.8	118428.3	0.16	0.53
7	0.019	0.001	119.1	0.78	0.035	0.064	0.010	0.018	0.70	15.8	123997.4	0.05	0.47
8	0.007	0.002	50.3	0.56	0.015	0.038	0.010	0.023	0.61	15.0	61450.2	0.12	0.66
9	0.019	0.003	87.1	0.68	0.026	0.055	0.010	0.022	1.45	16.0	142552.1	0.25	0.77
10	0.022	0.003	88.9	0.69	0.027	0.056	0.010	0.021	1.73	16.3	163318.9	0.19	0.85
11	0.006	0.003	40.5	0.53	0.012	0.032	0.010	0.026	0.87	16.7	61118.8	0.24	0.83
12	0.019	0.001	120.4	0.79	0.035	0.064	0.009	0.016	0.61	16.2	125965.8	-0.04	0.47
13	0.019	0.001	119.5	0.79	0.035	0.064	0.009	0.017	0.61	16.8	124913.1	-0.02	0.46
14	0.008	0.001	55.9	0.58	0.017	0.041	0.009	0.018	0.45	17.0	67436.6	-0.06	0.60
15	0.023	0.003	90.1	0.69	0.027	0.056	0.010	0.020	1.81	17.0	172573.5	0.18	0.87
16	0.006	0.002	40.7	0.53	0.012	0.033	0.010	0.023	0.68	16.7	57798.2	0.09	0.78
17	0.013	0.002	71.7	0.63	0.022	0.049	0.009	0.018	0.77	16.6	104571.8	-0.01	0.70
18	0.022	0.003	91.0	0.69	0.027	0.056	0.010	0.021	1.77	16.0	164757.7	0.21	0.84
19	0.007	0.002	45.2	0.54	0.014	0.035	0.009	0.021	0.69	16.0	63801.3	0.06	0.76
20	0.014	0.002	76.3	0.64	0.023	0.051	0.009	0.018	0.80	15.6	106404.1	0.01	0.68
21	0.008	0.001	58.2	0.58	0.018	0.043	0.009	0.019	0.53	15.5	71344.3	-0.03	0.63
22	0.019	0.001	119.6	0.79	0.035	0.064	0.010	0.018	0.65	15.4	120612.3	0.02	0.46
23	0.019	0.002	110.7	0.76	0.033	0.062	0.011	0.022	0.91	15.8	126521.6	0.26	0.52
24	0.01	0.002	58.9	0.59	0.018	0.043	0.009	0.020	0.71	17.0	84002.7	0.04	0.70
25	0.016	0.002	79.0	0.65	0.024	0.052	0.009	0.018	1.01	14.2	118318.6	0.03	0.75
26	0.007	0.002	45.6	0.54	0.014	0.036	0.010	0.023	0.73	15.0	61823.1	0.14	0.75

TABLE 08 CLEAR WATER EXPERIMENTS IN CHANNEL WITH 120mm THICK BED (ROUGHNESS I;ks=0.8 mm)

	Q m^3/s	S	y_0 mm	y_t/D	A m^2	R m	n	λ_c	τ_0 N/m^2	Temp. C^o	R_e	k_s mm	Fr
1	0.022	0.003	89.2	0.69	0.027	0.0557	0.010	0.021	1.75	16.3	163159.0	0.21	0.85
2	0.007	0.002	50.3	0.56	0.015	0.0385	0.010	0.024	0.62	15.0	61313.0	0.17	0.65
3	0.019	0.001	125.3	0.81	0.036	0.0645	0.012	0.027	0.92	15.7	118266.0	0.77	0.43
4	0.015	0.002	86.6	0.68	0.026	0.0548	0.011	0.026	1.00	15.1	106576.0	0.50	0.59
5	0.008	0.003	51.9	0.57	0.016	0.0390	0.011	0.027	0.98	15.2	73500.1	0.42	0.75
6	0.022	0.004	93.1	0.70	0.028	0.0569	0.011	0.025	1.96	14.9	154884.1	0.54	0.79
7	0.022	0.003	96.2	0.71	0.029	0.0580	0.011	0.026	1.96	14.9	154926.4	0.63	0.77
8	0.015	0.002	87.4	0.68	0.026	0.0551	0.012	0.027	1.05	14.9	106141.8	0.64	0.58
9	0.018	0.002	120.5	0.79	0.035	0.0637	0.012	0.028	0.96	14.1	113111.5	0.86	0.46
10	0.022	0.004	93.1	0.70	0.028	0.0570	0.011	0.025	2.00	14.1	153541.1	0.53	0.80
11	0.006	0.003	43.8	0.54	0.013	0.0344	0.011	0.031	0.85	14.2	55382.7	0.56	0.72
12	0.015	0.002	83.2	0.67	0.025	0.0535	0.011	0.025	1.08	16.0	111966.1	0.45	0.63
13	0.022	0.003	90.7	0.69	0.027	0.0563	0.010	0.021	1.77	16.0	164939.6	0.20	0.85
14	0.023	0.003	99.5	0.72	0.03	0.0589	0.011	0.024	1.84	16.0	163726.8	0.46	0.76
15	0.008	0.003	50.2	0.56	0.015	0.0381	0.011	0.028	0.99	17.0	74209.1	0.48	0.76
16	0.015	0.002	84.7	0.67	0.025	0.0540	0.011	0.027	1.11	17.2	114409.0	0.61	0.62
17	0.022	0.002	115.8	0.77	0.034	0.0628	0.011	0.024	1.30	17.2	153193.5	0.43	0.58
18	0.019	0.002	110.8	0.76	0.033	0.0618	0.011	0.025	1.02	15.8	126475.7	0.50	0.52

TABLE 09 CLEAR WATER EXPERIMENTS IN CHANNEL WITH 120mm THICK BED
(ROUGHNESS II;ks=1.4 mm)

	$Q(m^3/s)$	S	y_0 mm	y_t/D	$A(m^2)$	R(m)	n	λ_c	τ_o N/m^2	Temp. C°	R_e	k_s mm	Fr
1	0.014	0.003	79.6	0.65	0.0240	0.0522	0.013	0.037	1.65	14.8	107697.8	1.87	0.66
2	0.015	0.004	78.9	0.65	0.0238	0.0519	0.013	0.038	1.92	14.9	114978.7	1.95	0.71
3	0.019	0.004	88.0	0.68	0.0264	0.0553	0.013	0.037	2.30	14.9	135040.3	2.00	0.74
4	0.015	0.004	80.0	0.66	0.0241	0.0524	0.015	0.044	2.26	14.3	114100.1	3.19	0.71
5	0.018	0.003	90.9	0.69	0.0272	0.0563	0.012	0.030	1.67	14.4	129243.8	0.94	0.69
6	0.015	0.003	81.4	0.66	0.0245	0.0529	0.013	0.034	1.65	14.6	112829.0	1.48	0.68
7	0.016	0.004	79.4	0.65	0.0239	0.0521	0.013	0.034	1.84	14.6	117053.1	1.47	0.73
8	0.014	0.003	81.0	0.66	0.0244	0.0527	0.013	0.034	1.46	14.6	106454.9	1.40	0.65
9	0.014	0.003	80.3	0.66	0.0242	0.0525	0.013	0.034	1.36	14.7	101792.5	1.46	0.62
10	0.014	0.002	82.3	0.66	0.0248	0.0532	0.013	0.033	1.30	14.8	103516.4	1.27	0.61
11	0.017	0.003	89.2	0.69	0.0267	0.0557	0.012	0.032	1.52	14.9	119676.2	1.19	0.64
12	0.015	0.003	78.8	0.65	0.0237	0.0519	0.013	0.037	1.75	14.9	110596.4	1.83	0.69
13	0.017	0.004	78.3	0.65	0.0236	0.0517	0.012	0.030	2.04	15.0	132070.6	0.93	0.83
14	0.019	0.004	85.4	0.67	0.0257	0.0544	0.012	0.030	2.11	14.2	138395.4	0.98	0.80
15	0.014	0.003	75.2	0.64	0.0227	0.0504	0.012	0.032	1.60	14.2	108668.9	1.09	0.73
16	0.017	0.003	86.6	0.68	0.0260	0.0548	0.012	0.029	1.51	14.5	120322.3	0.90	0.68
17	0.014	0.002	86.8	0.68	0.0260	0.0549	0.012	0.029	1.08	14.5	102967.1	0.80	0.59

APPENDIX E

VELOCITY MEASUREMENTS DATA

VELOCITY PROFILE – V5

pipe (D=305 mm) with smooth flat bed
bed width B=220 mm

Bed thickness	47 mm	
Bed condition	=smooth bed	
Discharge	0.01205 m3/s	
Slope	0.002287	
Normal Depth	71.25 mm	
Velocity	0.63 m/s	
Current meter	V=0.55822*N+3.06438	cm/s(0<N<48HZ)
=1094=	V=0.53385*N+4.40104	cm/s (48<N<272HZ)
Date:29/9/89		

At the centre

y mm	N HZ	V cm/s
10	87.00	52.54
20	99.75	59.40
30	105.60	62.55
40	108.05	63.87
50	109.43	64.61
60	106.45	63.01
70	101.40	60.29

At 30 mm from the centre

y mm	N HZ	V cm/s
10	103.70	61.53
20	114.33	67.25
30	114.43	67.3
40	118.55	69.52
50	115.35	67.8
60	112.53	66.28
70	101.43	60.3

At 60 mm from the centre

y mm	N HZ	V cm/s
10	106.20	62.87
20	118.45	69.47
30	123.38	72.12
40	123.55	72.21
50	120.25	70.43
60	116.00	68.15
70	108.50	64.11

at 110 mm from the centre

y mm	N HZ	V cm/s
10	94.08	56.35
20	100.85	59.99
30	105.08	62.27
40	112.15	66.08
50	113.30	66.69
60	108.90	64.33
70	99.35	59.19

VELOCITY PROFILE–V6

pipe (D=305 mm) with smooth flat bed
bed width B=220 mm

Bed thickness	47 mm	
Bed Condition	=smooth bed	
Discharge	0.0087 m3/s	
Slope	0.0009	
Normal Depth	67.166 mm	
Velocity	0.49 m/s	
Current meter	V=0.56443662*N+4.16478873	cm/s(0<N<45.8HZ)
=1398=	V=0.538135593*N+5.72881354	cm/s (46<N<267HZ)

At the centre

y mm	N HZ	V cm/s
7.5	74.9	44.39
10	77.23	45.63
15	81.25	47.78
20	82.13	48.25
30	85.5	50.05
40	87.9	51.33
50	87.3	51.01
55	86.8	50.74

30 mm from the centre

y mm	N HZ	V cm/s
7.5	70.1	41.82
10	71.9	42.78
15	75.8	44.87
20	78.9	46.52
30	83.1	48.76
40	84.8	49.67
50	86	50.31
55	86.1	50.37

60 mm from the centre

y mm	N HZ	V cm/s
7.5	70.5	42.04
10	71.95	42.81
15	76.05	45.00
20	78.52	46.32
30	82.8	48.60
40	82	48.18
50	84.6	49.56
55	84.4	49.46

VELOCITY PROFILE — V 7

pipe (D=305 mm) with smooth flat bed
bed width B=220 mm

Bed thickness	47 mm	
Bed Condition	=smooth bed	
Discharge	0.0304 m3/s	
Slope	0.00092	
Normal Depth	157.62 mm	
Velocity	0.68 m/s	
Current meter	V=0.56443662*N+4.16478873	cm/s(0<N<45.8HZ)
=1398=	V=0.538135593*N+5.72881354	cm/s (46<N<267HZ)
Date:24/7/89		

At the centre

y mm	N HZ	V cm/s
7.5	104.425	61.9236228
10	105.65	62.5828389
15	115.1	67.6682203
20	116.575	68.4619703
25	122.125	71.4486228
30	125.55	73.2917372
40	131.3	76.3860169
50	131.75	76.6281779
60	136.225	79.0363347
70	135.45	78.6192796
80	135.075	78.4174788
90	132.325	76.9376059
100	133.25	77.4353813
110	130.3	75.8478813
120	127.75	74.4756355
130	128.925	75.1079449
140	123.55	72.2154661
150	118.6	69.5516949

30mm from the centre

y mm	N HZ	V cm/s
7.5	103.6	61.479661
10	107.625	63.645657
15	115.1	67.86822
20	119.9	70.251271
25	123.3	72.080932
30	129.05	75.175212
40	127.675	74.435275
50	135.1	78.430932
60	134.45	78.081144
70	135.2	78.484746
80	132.2	76.870339
90	134.6	78.161864
100	133.025	77.314301
110	132.125	76.829979
120	131.43	76.455975
130	124.55	72.753602
140	123.125	71.986758
150	117.05	68.717585

60mm from the centre

y mm	N HZ	V cm/s
7.5	107.55	63.6052966
10	108.075	63.8878178
15	116.175	68.2467161
20	122.275	71.5293432
25	126.4	73.7491525
30	127.2	74.179661
40	133.1	77.354661
50	134.1	77.8927966
60	136.125	78.9825211
70	136.075	78.9556144
80	136.575	79.2246822
90	134.875	78.3098516
100	135.325	78.5520127
110	132.75	77.1663135
120	129.075	75.1866652
130	129.05	75.1752118
140	122.325	71.55625
150	117.45	68.9328389

90mm from the centre

y mm	N HZ	V cm/s
7.5	99.55	59.300212
10	97.95	58.4391 95
15	106.8	63.201695
20	110.025	64.937182
25	113.225	66.659216
30	114.575	67.385699
40	121.225	70.964301
50	123.375	72.121292
60	125.1	73.049576
70	129.075	75.188665
80	129.3	75.309746
90	130.875	76.157309
100	125.85	73.453178
110	128.5	74.879237
120	121.45	71.085381
130	122.9	71.865678
140	115.475	67.870021
150	105.875	62.703919

VELOCITY PROFILE — V 11

pipe (D = 305 mm) with smooth flat bed
bed width B = 265 mm

Bed thickness 77 mm
Bed condition = smooth bed
Discharge 0.00418 m3/s
Slope 0.002427
Normal Depth 32.128 mm
Velocity= 0.464 m/s

Current meter V = 0.55822*N + 3.06438 cm/s (0 < N < 48HZ)
=1094= V = 0.53385*N + 4.40104 cm/s (48 < N < 272HZ)
Date:23/10/89

At the centre

y mm	N HZ	V cm/s
7.5	64.88	39.04
10	66.50	39.90
15	71.42	42.53
20	75.10	44.49
25	76.90	45.45
30	78.70	46.42

40 mm from centre

y mm	N HZ	V cm/s
7.5	67.24	40.30
10	68.16	40.79
15	74.06	43.94
20	76.58	45.28
25	78.82	46.47
30	78.54	46.30

70 mm from centre

y mm	N HZ	V cm/s
7.5	64.66	38.92
10	66.96	40.15
15	71.58	42.61
20	73.66	43.72
25	76.78	45.39
30	76.48	45.23

100 mm from centre

y mm	N HZ	V cm/s
7.5	63.96	38.55
10	67.22	40.29
15	69.88	41.71
20	73.60	43.69
25	72.76	43.24
30	70.24	41.90

VELOCITY PROFILE —V12

pipe (D=305 mm) with smooth flat bed
bed width B=265 mm

Bed thickness	77 mm
Bed condition	=smooth bed
Discharge	0.0219 m3/s
Slope	0.001
Normal Depth	124.4 mm
Velocity=	0.598 m/s

CURRENT METER =1399= Date:23/11/89

V=0.565625*N+3.48625 cm/s(0<N<46.4HZ)

V=0.543103448*N+4.48275861 cm/s (46.4<N<267HZ)

At the centre

y mm	N HZ	V cm/s
7.5	79.72	47.78
10	79.70	47.77
15	86.64	51.54
20	91.06	53.94
40	100.98	59.33
60	102.62	60.22
80	100.06	58.83
100	90.88	53.84
120	85.34	50.83

At 60 mm from the centre

y mm	N HZ	V cm/s
7.5	85.44	50.89
15	93.02	55.00
20	97.92	57.66
40	101.08	59.38
60	101.64	59.68
80	102.34	60.06
100	91.44	54.14
120	86.16	51.28

At 100 mm from the centre

Y mm	N HZ	V cm/s
7.5	80.50	48.20
10	80.00	47.93
15	87.00	51.73
20	92.86	54.92
40	103.80	60.86
60	105.00	61.51
80	102.16	59.97
100	96.00	56.62
120	90.38	53.57

VELOCITY PROFILE — V 13

pipe (D=305 mm) with smooth flat bed
bed width B=265 mm

Bed thickness	77 mm
Bed condition	=smooth bed
Discharge	0.0174 m3/s
Slope	0.00229
Normal Depth	82.1 mm
Velocity=	0.721 m/s

CURRENT METER V=0.565625*N+3.48625 cm/s(0<N<46.4HZ)
=1399= V=0.543103448*N+4.48275861 cm/s (46.4<N<267HZ)
Date:23/11/89

At the centre

y mm	N HZ	V cm/s
10	107.48	62.8555172
15	114.98	66.92879306
20	121.92	70.69793099
30	128.18	74.09775857
40	133.8	77.14999995
50	136.14	78.42086202
60	135.82	78.24706892
75	129.48	74.80379306

50mm from the centre

y mm	N HZ	V cm/s
10	91.525	54.19
15	95.875	56.552
20	98.425	57.94
30	113.35	66.04
40	119.225	69.234
50	122.475	70.999
60	129.4	74.8
75	128.975	74.53

100mm from the centre

y mm	N HZ	V cm/s
10	94.6	55.86034479
15	100.275	58.94245686
20	101.4	59.55344824
30	111.3	64.93017237
40	118.2	68.67758616
50	124.625	72.16702582
60	125.775	72.79159478
75	122.25	70.87715513

VELOCITY PROFILE —V 14

pipe (D=305 mm) with smooth flat bed
bed width B=265 mm

Bed thickness	77 mm	
Bed condition	=smooth bed	
Discharge	0.02219 m3/s	
Slope	0.001198	
Normal Depth	124.7 mm	
Velocity=	0.603 m/s	
Current meter	V=0.55822*N+3.06438	cm/s(0<N<48HZ)
=1094=	V=0.53385*N+4.40104	cm/s (48<N<272HZ)
Date:24/10/89		

At the centre

y mm	N HZ	V cm/s
7.5	82.26	48.315541
10	84.42	49.468657
15	89	51.91369
20	95.02	55.127467
30	99.44	57.487084
40	105.48	60.711538
60	110.32	63.295372
80	112.54	64.480519
100	111.64	64.000054
115	110.64	63.466204

VELOCITY PROFILE — V 15
pipe (D=305 mm) with smooth bed
bed width B=265 mm

Bed thickness 77 mm
Bed condition =smooth bed
Discharge (Q) =0.018645 m3/s
Channel slope (S) =0.00282
Normal depth (yo) =78.95 mm
Velocity (V) =0.446 m/s

At the centrte		
y mm	N	V m/s
7.5	127.1	72.25336
10	128.46	72.9794
15	136.4	77.21818
20	142.8	80.634
25	147.22	82.99443
30	152.44	85.78113
40	155.46	87.39336
50	156.92	88.17278
60	154.28	86.76
70	152.68	85.909
75	148.16	83.496

VELOCITY PROFILE — V16
pipe (D=305 mm) with rough bed (ks=0.8 mm)
bed width B=265 mm

Bed thickness	77 mm
Bed condition	=rough bed (ks=0.88 mm)
Discharge	0.0117 m3/s
Slope	0.00149
Normal Depth	82.02 mm
Velocity=	0.486 m/s

Current meter =1399= Date:28/3/90 V=0.565625*N+3.48625 cm/s

At the centre

y mm	N HZ	V cm/s
10	73.16	44.87
12	81.92	49.82
15	84.22	51.12
20	88.82	53.73
30	96.22	57.91
50	98.38	59.13
60	93.48	56.36
70	93.3	56.26
75	91.3	55.13

At 40 mm from the centre

y mm	N HZ	V cm/s
10	70.44	43.33
12	71.58	43.97
15	76.18	46.58
20	81.4	49.53
30	87.22	52.82
50	92.04	55.55
60	89.84	54.30
70	87.78	53.14
75	87.04	52.72

At 70 mm from the centre

y mm	N HZ	V cm/s
10	63.32	39.30
12	64.66	40.06
15	68.56	42.27
20	72.04	44.23
30	79.98	48.72
50	86.52	52.42
60	82.72	50.27
70	85.5	51.85
75	83	50.43

At 110 mm from the centre

y mm	N HZ	V cm/s
10	59.32	37.04
12	60.68	37.81
15	63.98	39.67
20	67.64	41.75
30	72.98	44.77
50	80.18	48.84
60	79.84	48.65
70	78.04	47.63
75	75.66	46.28

VELOCITY PROFILE－V 17
pipe (D=305 mm) with rough bed (ks=0.8 mm)
bed width B=265 mm

Bed thickness	77 mm
Bed condition	Rough I(ks=0.8
Discharge	0.0219 m3/s
Slope	0.00169
Normal Depth	116.53 mm
Velocity=	0.637 m/s

Current meter =1399=
Date:22/3/90
V=0.565625*N+3.48625

At the centre

y mm	N HZ	V cm/s
10	90.340	54.585
12	94.760	57.085
15	96.560	58.103
20	102.920	61.700
30	108.420	64.811
40	113.080	67.447
60	124.260	73.771
80	125.760	74.619
100	123.680	73.443
110	120.960	71.904

At 30 mm from the centre

y mm	N HZ	V cm/s
10	95.30	57.39
12	94.68	57.04
15	98.12	58.99
20	101.58	60.94
30	111.30	66.44
40	120.56	71.68
60	123.76	73.49
80	128.38	76.10
100	124.56	73.94
110	121.14	72.01

At 80 mm from the centre

y mm	N HZ	V cm/s
10	94.12	56.72
12	95.64	57.58
15	102.44	61.43
20	110.82	66.17
30	118.90	70.74
40	125.80	74.64
60	130.40	77.24
80	125.48	74.46
100	121.30	72.10
110	100.34	60.24

VELOCITY PROFILE — V18
pipe (D=305 mm) with rough bed (ks=0.8 mm)
bed width B=265 mm

Bed thickness	77 mm
Bed condition	=rough I (ks=0.8 mm)
Discharge	0.00783 m3/s
Slope	0.00286
Normal Depth	53.88 mm
Velocity=	0.501 m/s

Current meter V=0.455819693*N+5.1202096869 cm/s
=43=
Date:26/4/90

At the centre

y mm	N HZ	V cm/s
10	92.38	47.23
12	97.06	49.36
15	100.42	50.89
20	102.64	51.91
30	108.80	54.71
40	112.04	56.19
50	110.38	55.43

At 30mm from the centre

y mm	N HZ	V cm/s
10	78.20	40.77
12	86.00	44.32
15	88.66	45.53
20	91.68	46.91
30	99.10	50.29
40	105.28	53.11
50	104.80	52.89

At 60mm from the centre

y mm	N HZ	V cm/s
10	94.00	47.97
12	98.16	49.86
15	103.00	52.07
20	108.52	54.59
30	111.36	55.88
40	114.62	57.37
50	106.66	53.74

VELOCITY PROFILE — V 19

pipe (D=305 mm) with rough bed (ks=1.4 mm)

bed width B=265 mm

Bed thickness	77 mm
Bed condition	=rough II
Discharge	0.00802 m3/s
Slope	0.00229
Normal Depth	60.84 mm
Velocity=	0.455 m/s

Current meter V=0.3648743142*N+6.4678 cm/s

=2=(D=4mm:

Date:4/5/90

At the centre

y mm	N HZ	V cm/s
4	69.52	31.83
5	76.20	34.27
7.5	93.16	40.46
10	96.54	41.69
12	99.00	42.59
15	103.96	44.40
20	109.38	46.38
30	118.24	49.61
40	117.56	49.36
50	118.12	49.57
55	118.34	49.65

At 30 mm from the centre

y mm	N HZ	V cm/s
4	64.78	30.10
5	71.60	32.59
7.5	77.24	34.65
10	82.60	36.61
12	89.54	39.14
15	91.02	39.68
20	96.90	41.82
30	107.06	45.53
40	107.42	45.66
50	112.06	47.36
55	112.96	47.68

At 55mm from the centre

y mm	N HZ	V cm/s
10	69.52	42.81
12	71.40	43.87
15	73.54	45.08
20	81.54	49.61
30	87.20	52.81
40	87.52	52.99
50	87.40	52.92
55	82.02	49.88

At 95 mm from the centre

y mm	N HZ	V cm/s
10	67.96	41.93
12	71.14	43.72
15	71.54	43.95
20	80.74	49.15
30	89.10	53.88
40	90.64	54.75
50	88.00	53.26
55	82.90	50.38

VELOCITY PROFILE-V 20

pipe (D=305 mm) with smooth flat bed
bed width= 298 mm

Bed thickness	=120	mm
Discharge (Q)	=0.007571	m3/s
Channel Slope (S)	=0.0011	
Normal Depth (yo)	=55.94	mm
Velocity (V)	=0.446	m/s

CURRENT METER: V=0.455819631*N+5.1202096869 cm/s

At centre		
y mm	N HZ	V cm/s
7.5	89.3	45.8
10	91.72	46.9
12	93.16	47.6
15	95.9	48.8
20	97.12	49.4
30	104.96	53.0
40	106.56	53.7
50	104.84	52.9

At 30 mm from the centre		
y mm	N HZ	V cm/s
7.5	87.3	44.9
10	89.94	46.1
12	92.02	47.1
15	94.34	48.1
20	98.54	50.0
30	101.82	51.5
40	102.48	51.8
50	102.94	52.0

At 90 mm from the centre		
y mm	N HZ	V cm/s
7.5	68.62	36.4
10	71.5	37.7
12	72.84	38.3
15	76.48	40.0
20	79.48	41.3
30	85.04	43.9
40	87.76	45.1
50	81.8	42.4

VELOCITY PROFILE — V 21

pipe (D = 305 mm) with smooth flat bed
bed width B = 298 mm

Bed thickness 120 mm
Bed condition smooth
Discharge 0.019144 m3/s
Slope 0.00112
Normal Depth 119.08 mm
Velocity= 0.551 m/s

Current meter V=0.455819631*N+5.1202096869 cm/s
No. 43 D=10 mm
Date:23/10/89

at the centre

Y mm	N HZ	V cm/s
7.5	86.80	44.69
10	95.24	48.53
12	98.10	49.84
15	100.92	51.12
20	107.14	53.96
25	107.90	54.30
40	118.10	58.95
60	118.24	59.02
80	115.58	57.80
100	111.28	55.84
110	110.18	55.34

At 40mm from the centre

y mm	N HZ	V cm/s
7.5	88.66	45.53
10	88.18	45.31
12	91.32	46.75
15	95.12	48.48
20	96.66	49.18
25	102.68	51.92
40	106.56	53.69
60	113.90	57.04
80	115.44	57.74
100	112.14	56.24
110	112.78	56.53

At 75mm from the centre

y mm	N HZ	V cm/s
7.5	93.26	47.62
10	98.20	49.88
12	101.80	51.52
15	106.24	53.55
20	106.28	53.56
25	109.58	55.07
40	116.48	58.21
60	112.30	56.30
80	119.18	59.45
100	113.40	56.81

At 110 from the centre

y mm	N HZ	V cm/s
7.5	97.26	49.45
10	96.12	48.93
12	94.16	48.04
15	103.36	52.23
20	107.86	54.28
25	112.66	56.47
40	112.54	56.42
60	117.88	58.85
80	113.04	56.65
100	112.66	56.47

VELOCITY PROFILE — V 22

PIPE (D=305 mm) WITH ROUGH (ks=0.8 mm) FLAT BED
bed width B=298 mm

Bed thickness	120 mm
Bed condition	rough I (ks=0.8mm)
Discharge	0.0147 m3/s
Slope	0.0021
Normal Depth	83.24 mm
Velocity=	0.586 m/s

Current meter V=0.543103448*N+4.48275861 cm/s
1399 46.4 <N<267 HZ
Date:23/10/89

at centre

y mm	N HZ	V cm/s
10	88.68	52.65
12	94.76	55.95
15	97.94	57.67
20	102.60	60.21
30	108.04	63.16
40	116.50	67.75
50	118.76	68.98
60	117.30	68.19
70	111.60	65.09
80	105.20	61.62

at 30 mm from the centre

y mm	N HZ	V cm/s
10	73.50	44.40
12	78.10	46.90
15	83.36	49.76
20	93.60	55.32
30	98.40	57.92
40	107.00	62.59
50	109.80	64.12
60	110.82	64.67
70	115.36	67.14
80	106.98	62.58

at 60 mm from the centre

y mm	N HZ	V cm/s
10	74.46	44.92
12	76.54	46.05
15	82.52	49.30
20	89.60	53.14
30	95.40	56.29
40	103.50	60.69
50	109.40	63.90
60	107.86	63.06
70	103.12	60.49
80	93.30	55.15

at 110 mm from the centre

y mm	N HZ	V cm/s
10	71.40	43.26
12	74.90	45.16
15	78.40	47.06
20	87.90	52.22
30	96.12	56.69
40	102.70	60.26
50	102.30	60.04
60	99.52	58.53
70	93.10	55.05
80	79.10	47.44

VELOCITY PROFILE – V 23

pipe (D = 305 mm) with smooth flat bed
bed width B = 298 mm

Bed thickness	120 mm
Bed condition	smoooth
Discharge	0.018752 m3/s
Slope	0.00144
Normal Depth	125.69 mm
Velocity =	0.515 m/s

Current meter V = 0.455819631 * N + 5.1202096869 cm/s
No. 43 D = 10 mm
Date: 23/10/89

At the centre

y mm	N HZ	V cm/s
8	92.58	47.32
10	93.82	47.89
12	96.58	49.14
15	103.32	52.22
20	108.42	54.54
30	114.50	57.31
40	122.42	60.92
60	128.26	63.58
80	123.78	61.54
100	116.62	58.28
110	111.64	56.01
120	103.10	52.12

VELOCITY PROFILE – V 24

PIPE (D = 305 mm) WITH ROUGH BED (ks = 0.8 mm)
bed width B = 298 mm

Flume Diameter	305 mm
Bed condition	smooth bed
Bed thickness	120 mm
Discharge	0.0065 m3/s
Slope	0.0026
Normal Depth	45.84 mm
Velocity =	0.468 m/s

Current meter V = 0.455819631 * N + 5.1202096869 cm/s
No. 43 D = 10 mm
Date: 23/10/89

At the centre

y mm	N HZ	V cm/s
8	89.25	45.80
10	92.78	47.41
12	94.05	47.99
15	96.08	48.91
20	102.55	51.86
30	106.58	53.70
40	105.00	52.98

At 55 mm from the centre

y. mm	N HZ	V cm/s
8	86.40	44.50
10	86.60	44.59
12	90.63	46.43
15	91.93	47.02
20	97.03	49.35
30	101.85	51.55
40	104.70	52.84

At 110 mm from the centre

y mm	N HZ	V cm/s
8	72.83	38.32
10	78.53	40.91
12	80.48	41.80
15	83.35	43.11
20	88.73	45.56
30	90.80	46.51
40	88.05	45.26

APPENDIX F

TURBULENCE MEASUREMENTS DATA

TURBULENCE INTENSITY PROFILES – T 1
CHANNEL OF CIRCULAR CROSS SECTION (D=305 mm)

Bed Thickness	47 mm
Discharge	0 00898 m3/s
Slope	0 002679
Mean Shear S .	1 0796 N/m2
Mean Velocity	0 62 m/s
Normal Depth	55 7 mm
yt/D	0 337
Temperature	19 C
Bed condition	=smooth

AT CENTRE:

y (mm)	u(m/s)	RMS	u/V	TI (RMS/u) %	RMS/V	y/y_o	yt/D
2	0 369	0.040	0.60	10.84	0.065	0.036	0.16
3	0.391	0.048	0.63	12.28	0.077	0.054	0.16
4	0 404	0.048	0.65	11.88	0.077	0.072	0.17
5	0 437	0.048	0.71	10.98	0.077	0.090	0.17
6	0 448	0.047	0.72	10.49	0.076	0.108	0.17
10	0 480	0.043	0.77	8.96	0.069	0.180	0.19
20	0 547	0.044	0.88	8.04	0.071	0.359	0.22
23	0 586	0.040	0.95	6.83	0.065	0.413	0.23
45	0 605	0.028	0.98	4.63	0.045	0.808	0.30
54	0 615	0.030	0.99	4.88	0.048	0.969	0.33

At 35 mm from the centre

y (mm)	u(m/s)	RMS	u/V	TI (RMS/u) %	RMS/V	y/y_o	yt/D
2	0 394	0 044	0.636	11.17	0.071	0.036	0.16
3	0 429	0 046	0.692	10.72	0.074	0.054	0.16
4	0 443	0 045	0.715	10.16	0.073	0.072	0.17
5	0 459	0.046	0.741	10.02	0.074	0.090	0.17
6	0 483	0.047	0.779	9.73	0.076	0.108	0.17
10	0 516	0.042	0.832	8.14	0.068	0.180	0.19
20	0 566	0.043	0.913	7.60	0.069	0.359	0.22
35	0 612	0.031	0.987	5.07	0.050	0.628	0.27
45	0 617	0.030	0.995	4.86	0.048	0.808	0.30
54	0 625	0.027	1.008	4.32	0.044	0.969	0.33
55	0 606	0.090	0.978	14.85	0.145	0.987	0.33

AT 65 mm from the centre

y (mm)	u(m/s)	RMS	u/V	TI (RMS/u) %	RMS/V	y/y_o	yt/D
2	0 403	0.059	0.650	14.64	0.095	0.036	0.16
3	0 431	0.052	0.695	12.06	0.084	0.054	0.16
4	0 445	0.055	0.718	12.36	0.089	0.072	0.17
5	0 464	0.046	0.749	9.91	0.074	0.090	0.17
6	0 481	0.050	0.776	10.40	0.081	0.108	0.17
10	0 519	0.043	0.837	8.29	0.069	0.180	0.19
20	0 572	0.040	0.923	6.99	0.065	0.359	0.22
35	0 616	0.033	0.994	5.36	0.053	0.628	0.27
45	0 621	0.029	1.002	4.67	0.047	0.808	0.30
55	0 604	0.038	0.974	6.29	0.061	0.987	0.33

At 100 mm from the centre

y (mm)	u(m/s)	RMS	u/V	TI (RMS/u) %	RMS/V	y/y_o	yt/D
2	0 338	0.060	0.545	17.751	0.097	0.036	0.161
3	0 347	0 061	0.560	17.579	0.098	0.054	0.164
4	0 369	0 062	0.595	16.802	0.100	0.072	0.167
5	0 408	0.061	0.658	14.951	0.098	0.090	0.170
6	0.418	0.060	0.674	14.354	0.097	0.108	0.174
10	0.474	0.061	0.765	12.869	0.098	0.180	0.187
20	0.531	0.060	0.857	11.299	0.097	0.359	0.220
35	0.559	0.051	0.902	9.123	0.082	0.628	0.269
45	0 569	0.048	0.918	8.436	0.077	0.808	0.302
55	0 488	0.055	0.787	11.270	0.089	0.987	0.334

TURBULENCE INTENSITY PROFILES–T2
CHANNEL OF CIRCULAR CROSS SECTION (D=305 mm)

Bed Thickness	=47	mm
Discharge	=0.00681	m3/s
Slope	=0.00145	
Mean Shear Stress	=0.597	N/m2
Mean Velocity	=0.458	m/s
Normal Depth	=57.2	mm
yt/D	0.341475	
Temperature	19 C	
Bed condition	smooth	

AT CENTRE:

y (mm)	u(m/s)	RMS	u/V	TI (RMS/u)%	RMS/V	y/y_o	yt/D
2	0.285	0.047	0.62	16.49	0.103	0.035	0.161
3	0.320	0.050	0.70	15.63	0.109	0.052	0.164
4	0.333	0.037	0.73	11.11	0.081	0.070	0.167
6	0.363	0.037	0.79	10.19	0.081	0.105	0.174
10	0.392	0.040	0.86	10.20	0.087	0.175	0.187
15	0.407	0.037	0.89	9.09	0.081	0.262	0.203
25	0.434	0.029	0.95	6.68	0.063	0.437	0.236
35	0.453	0.034	0.99	7.51	0.074	0.612	0.269
45	0.473	0.027	1.03	5.71	0.059	0.787	0.302
54	0.493	0.030	1.08	6.09	0.066	0.945	0.331

At 40 mm from the centre

y (mm)	u(m/s)	RMS	u/V	TI (RMS/u)%	RMS/V	y/y_o	yt/D
2	0.293	0.032	0.640	10.92	0.070	0.035	0.161
3	0.324	0.036	0.708	11.11	0.079	0.052	0.164
4	0.327	0.032	0.714	9.79	0.070	0.070	0.167
5	0.349	0.033	0.762	9.46	0.072	0.087	0.170
10	0.369	0.031	0.806	8.40	0.068	0.175	0.187
25	0.422	0.028	0.922	6.64	0.061	0.437	0.236
40	0.447	0.024	0.976	5.37	0.052	0.700	0.285
50	0.460	0.020	1.005	4.35	0.044	0.875	0.318

AT 85 mm from the centre

y (mm)	u(m/s)	RMS	u/V	TI (RMS/u)%	RMS/V	y/y_o	yt/D
2	0.253	0.046	0.552	18.18	0.100	0.035	0.161
3	0.263	0.055	0.574	20.91	0.120	0.052	0.164
4	0.281	0.045	0.614	16.01	0.098	0.070	0.167
5	0.268	0.044	0.585	16.42	0.096	0.087	0.170
10	0.348	0.048	0.760	13.79	0.105	0.175	0.187
25	0.428	0.032	0.935	7.48	0.070	0.437	0.236
45	0.458	0.029	1.000	6.33	0.063	0.787	0.302
54	0.460	0.026	1.005	5.65	0.057	0.945	0.331

TURBULENCE INTENSITY PROFILES –T 3
CHANNEL OF CIRCULAR CROSS SECTION (D=305 mm)

Bed Thickness =47 mm
Discharge 0.0067 m3/s
Slope 0.0015
Mean Shear Stress 0.6530 N/m2
Mean Velocity 0.4270 m/s
Normal Depth 59.5 mm
yt/D 0.589
Temperature 20 C
Bed condition: Rough. I (ks=0.8 mm)

AT CENTRE:

y (mm)	u(m/s)	RMS	u/V	TI RMS/u%	RMS/V	y/y_o	yt/D
2	0.244	0.040	0.571	0.164	0.094	0.034	0.161
3	0.273	0.037	0.639	0.136	0.087	0.050	0.164
4	0.286	0.037	0.670	0.129	0.087	0.067	0.167
5	0.280	0.038	0.656	0.136	0.089	0.084	0.170
6	0.270	0.038	0.632	0.141	0.089	0.101	0.174
10	0.305	0.042	0.714	0.138	0.098	0.168	0.187
20	0.379	0.043	0.888	0.113	0.101	0.336	0.220
35	0.443	0.028	1.037	0.063	0.066	0.588	0.269
45	0.434	0.025	1.016	0.058	0.059	0.756	0.302
55	0.419	0.032	0.981	0.076	0.075	0.924	0.334

At 45 mm from the centre:

y (mm)	u(m/s)	RMS	u/V	TI (RMS/u)%	RMS/V	y/y_o	yt/D
2	0.257	0.037	0.602	0.144	0.087	0.034	0.161
3	0.280	0.033	0.656	0.118	0.077	0.050	0.164
4	0.291	0.038	0.681	0.131	0.089	0.067	0.167
5	0.309	0.040	0.724	0.129	0.094	0.084	0.170
6	0.300	0.043	0.703	0.143	0.101	0.101	0.174
10	0.308	0.038	0.721	0.123	0.089	0.168	0.187
20	0.357	0.041	0.836	0.115	0.096	0.336	0.220
35	0.449	0.034	1.052	0.076	0.080	0.588	0.269
45	0.481	0.028	1.126	0.058	0.066	0.756	0.302
55	0.483	0.033	1.131	0.068	0.077	0.924	0.334

At 95 mm from the centre:

y (mm)	u(m/s)	RMS	u/V	TI (RMS/u)%	RMS/V	y/y_o	yt/D
2	0.200	0.047	0.468	0.235	0.110	0.034	0.161
3	0.205	0.043	0.480	0.210	0.101	0.050	0.164
4	0.227	0.034	0.532	0.150	0.080	0.067	0.167
5	0.223	0.043	0.522	0.193	0.101	0.084	0.170
6	0.230	0.046	0.539	0.200	0.108	0.101	0.174
10	0.256	0.039	0.600	0.152	0.091	0.168	0.187
15	0.302	0.050	0.707	0.166	0.117	0.252	0.203
20	0.394	0.055	0.923	0.140	0.129	0.336	0.220
35	0.432	0.060	1.012	0.139	0.141	0.588	0.269
45	0.446	0.058	1.044	0.130	0.136	0.756	0.302
55	0.420	0.058	0.984	0.138	0.136	0.924	0.334

TURBULENCE INTENSITY PROFILES–T4
CHANNEL OF CIRCULAR CROSS SECTION (D=305 mm)

Bed Thickness	=47	mm
Discharge	=0.0064	m3/s
Slope	=0.00128	
Mean Shear Stress	=0.554	N/m2
Mean Velocity	=0.4	m/s
Normal Depth	=60.5	mm
yt/D	=0.35	
Bed condition	= k_s= 0. 8 mm	

AT CENTRE:

y (mm)	u(m/s)	RMS	u/V	TI (RMS/u)%	RMS/V	y/y_o	yt/D
2	0.223	0.04	0.558	17.94	0.100	0.033	0.161
3	0.233	0.029	0.583	12.45	0.073	0.050	0.164
4	0.244	0.031	0.611	12.70	0.078	0.066	0.167
5	0.261	0.031	0.653	11.88	0.078	0.083	0.170
6	0.259	0.028	0.648	10.81	0.070	0.099	0.174
10	0.307	0.028	0.768	9.12	0.070	0.165	0.187
20	0.347	0.03	0.868	8.65	0.075	0.331	0.220
35	0.387	0.027	0.968	6.98	0.068	0.579	0.269
45	0.401	0.022	1.003	5.49	0.055	0.744	0.302
55	0.421	0.026	1.053	6.18	0.065	0.909	0.334

At 45 mm from the centre

y (mm)	u(m/s)	RMS	u/V	TI (RMS/u)%	RMS/V	y/y_o	yt/D
2	0.289	0.037	0.723	12.80	0.093	0.033	0.164
3	0.295	0.033	0.738	11.19	0.083	0.050	0.167
4	0.292	0.038	0.731	13.01	0.095	0.066	0.170
5	0.328	0.04	0.821	12.20	0.100	0.083	0.174
6	0.324	0.043	0.811	13.27	0.108	0.099	0.187
10	0.352	0.038	0.881	10.80	0.095	0.165	0.220
20	0.402	0.041	1.006	10.20	0.103	0.331	0.269
35	0.445	0.034	1.113	7.64	0.085	0.579	0.302
45	0.387	0.028	0.968	7.24	0.070	0.744	0.334
55	0.374	0.033	0.936	8.82	0.083	0.909	0.334426

At 90 mm from the centre

y (mm)	u(m/s)	RMS	u/V	TI (RMS/u)%	RMS/V	y/y_o	yt/D
2	0.140	0.049	0.350	35.00	0.123	0.033	0.161
3	0.178	0.048	0.445	26.97	0.120	0.050	0.164
4	0.184	0.043	0.460	23.37	0.108	0.066	0.167
5	0.192	0.042	0.480	21.88	0.105	0.083	0.170
10	0.242	0.039	0.606	16.12	0.098	0.165	0.187
20	0.376	0.047	0.941	12.50	0.118	0.331	0.220
35	0.391	0.041	0.978	10.49	0.103	0.579	0.269
45	0.437	0.029	1.093	6.64	0.073	0.744	0.302
55	0.410	0.025	1.026	6.10	0.063	0.909	0.334

TURBULENCE INTENSITY PROFILES–T 5
CHANNEL OF CIRCULAR CROSS SECTION (D=305 mm)

Bed Thickness	=47	mm
Discharge	=0.0173	m3/s
Slope	=0.0016	
Mean Shear Stress	=1.01	N/m2
Mean Velocity	=0.59	m/s
Normal Depth	=104.7	mm
yt/D	=0.50	
Temperature	=20.1	C
Bed condition	=rough. I	(ks=0.8 mm)

AT CENTRE:

y (mm)	u(m/s)	RMS	u/V	TI (RMS/u)%	RMS/V	y/y_o	yt/D
2	0.316	0.046	0.534	14.557	0.078	0.019	0.161
3	0.370	0.051	0.625	13.784	0.086	0.029	0.164
4	0.377	0.047	0.637	12.467	0.079	0.038	0.167
5	0.381	0.045	0.644	11.811	0.076	0.048	0.170
10	0.444	0.049	0.750	11.036	0.083	0.096	0.187
30	0.549	0.046	0.928	8.379	0.078	0.287	0.252
50	0.591	0.052	0.999	8.799	0.088	0.478	0.318
70	0.620	0.029	1.048	4.677	0.049	0.669	0.384
90	0.635	0.033	1.073	5.197	0.056	0.860	0.449
98	0.667	0.029	1.127	4.348	0.049	0.936	0.475

At 40 mm from the centre

y (mm)	u(m/s)	RMS	u/V	TI (RMS/u)%	RMS/V	y/y_o	yt/D
2	0.372	0.042	0.629	11.290	0.071	0.019	0.161
3	0.342	0.048	0.578	14.035	0.081	0.029	0.164
4	0.376	0.047	0.635	12.500	0.079	0.038	0.167
5	0.442	0.050	0.747	11.312	0.085	0.048	0.170
10	0.507	0.052	0.857	10.256	0.088	0.096	0.187
30	0.616	0.037	1.041	6.006	0.063	0.096	0.252
50	0.654	0.032	1.105	4.893	0.054	0.287	0.318
70	0.648	0.032	1.095	4.938	0.054	0.478	0.384
90	0.662	0.029	1.119	4.381	0.049	0.669	0.449
98	0.640	0.034	1.082	5.313	0.057	0.860	0.475

TURBULENCE INTENSITY PROFILES — T6
CHANNEL OF CIRCULAR CROSS SECTION (D=305 mm)

Bed Thick	47 mm
Discharge	0.0181 m3/s
Slope	0.0013
Mean Shear Stress	0.8417 N/m2
Mean Velocity	0.6043 m/s
Normal Depth	107.52 mm
yt/D	0.507
Temperature	20 C
Bed Condition	smooth

AT CENTRE:

y (mm)	u(m/s)	r.m.s	u/V	TI rms/u%	r.m.s/V	y/Yo	yt/D
2	0.408	0.044	0.675	10.784	0.073	0.019	0.161
3	0.424	0.048	0.702	11.321	0.079	0.028	0.164
4	0.432	0.045	0.715	10.417	0.074	0.037	0.167
5	0.467	0.053	0.773	11.349	0.088	0.047	0.170
6	0.484	0.045	0.801	9.296	0.074	0.056	0.174
10	0.515	0.044	0.852	8.544	0.073	0.093	0.187
20	0.556	0.050	0.920	8.993	0.083	0.186	0.220
30	0.589	0.045	0.975	7.640	0.074	0.279	0.252
50	0.618	0.040	1.023	6.472	0.066	0.465	0.318
65	0.664	0.034	1.099	5.120	0.056	0.605	0.367
80	0.670	0.034	1.109	5.075	0.056	0.744	0.416
100	0.675	0.039	1.117	5.778	0.065	0.930	0.482
105	0.682	0.039	1.129	5.718	0.065	0.977	0.498

At 45 mm right of centre:

y (mm)	u(m/s)	RMS	u/V	TI (RMS/u)%	RMS/V	y/y_o	yt/D
2	0.402	0.046	0.665	11.443	0.076	0.019	0.161
3	0.431	0.049	0.713	11.369	0.081	0.028	0.164
4	0.438	0.050	0.725	11.416	0.083	0.037	0.167
5	0.441	0.045	0.730	10.204	0.074	0.047	0.170
6	0.478	0.047	0.791	9.833	0.078	0.056	0.174
10	0.502	0.059	0.831	11.753	0.098	0.093	0.187
20	0.536	0.052	0.887	9.701	0.086	0.186	0.220
30	0.575	0.046	0.952	8.000	0.076	0.279	0.252
50	0.605	0.039	1.001	6.446	0.065	0.465	0.318
65	0.628	0.026	1.039	4.140	0.043	0.605	0.367
80	0.636	0.026	1.052	4.088	0.043	0.744	0.416
100	0.645	0.043	1.067	6.667	0.071	0.930	0.482

AT 90 mm right of centre:

y (mm)	u(m/s)	RMS	u/V	TI (RMS/u)%	RMS/V	y/y_o	yt/D
2	0.318	0.070	0.526	22.013	0.116	0.019	0.161
3	0.368	0.067	0.609	18.207	0.111	0.028	0.164
4	0.416	0.065	0.688	15.625	0.108	0.037	0.167
5	0.408	0.055	0.675	13.480	0.091	0.047	0.170
6	0.430	0.054	0.712	12.558	0.089	0.056	0.174
10	0.461	0.054	0.763	11.714	0.089	0.093	0.187
20	0.521	0.044	0.862	8.445	0.073	0.186	0.220
30	0.565	0.042	0.935	7.434	0.070	0.279	0.252
50	0.636	0.046	1.052	7.233	0.076	0.465	0.318
65	0.645	0.040	1.067	6.202	0.066	0.605	0.367
80	0.621	0.038	1.028	6.119	0.063	0.744	0.416
100	0.620	0.036	1.026	5.806	0.060	0.930	0.482

TURBULENCE INTENSITY PROFILES–T 7
CHANNEL OF CIRCULAR CROSS SECTION (D=305 mm)

Bed Thickness	=120	mm
Discharge	0.0097	m3/s
Slope	0.0011	
Mean Shear Stress	0.4993	N/m2
Mean Velocity	0.4793	m/s
Normal Depth	66.7	mm
yt/D	0.612	
Temperature	14	C
Bed condition	smooth	

AT CENTRE:

y (mm)	u(m/s)	RMS	u/V	TI RMS/u%	RMS/V	y/y_o	yt/D
4	0.366	0.050	0.764	13.661	0.104	0.060	0.407
6	0.410	0.045	0.855	10.976	0.094	0.090	0.413
8	0.420	0.045	0.876	10.714	0.094	0.120	0.420
10	0.432	0.046	0.901	10.648	0.096	0.150	0.426
20	0.470	0.047	0.981	10.000	0.098	0.300	0.459
30	0.503	0.038	1.049	7.555	0.079	0.450	0.492
40	0.568	0.024	1.185	4.225	0.050	0.599	0.525
50	0.543	0.030	1.133	5.525	0.063	0.749	0.557
60	0.549	0.025	1.145	4.554	0.052	0.899	0.590
66	0.543	0.034	1.133	6.262	0.071	0.989	0.610

At 45 mm right of centre:

y (mm)	u(m/s)	RMS	u/V	TI (RMS/u)%	RMS/V	y/y_o	yt/D
4	0.288	0.039	0.601	13.542	0.081	0.060	0.407
6	0.298	0.036	0.622	12.081	0.075	0.090	0.413
8	0.309	0.035	0.645	11.327	0.073	0.120	0.420
10	0.353	0.034	0.736	9.632	0.071	0.150	0.426
20	0.454	0.028	0.947	6.167	0.058	0.300	0.459
30	0.504	0.024	1.051	4.762	0.050	0.450	0.492
40	0.517	0.021	1.079	4.062	0.044	0.599	0.525
50	0.535	0.022	1.116	4.112	0.046	0.749	0.557
60	0.532	0.021	1.110	3.947	0.044	0.899	0.590
66	0.516	0.031	1.077	6.008	0.065	0.989	0.610

At 80 mm right of centre:

y (mm)	u(m/s)	RMS	u/V	TI (RMS/u)%	RMS/V	y/y_o	yt/D
4	0.281	0.035	0.586	12.456	0.073	0.060	0.407
6	0.280	0.034	0.584	12.143	0.071	0.090	0.413
8	0.286	0.036	0.597	12.587	0.075	0.120	0.420
10	0.298	0.037	0.622	12.416	0.077	0.150	0.426
20	0.383	0.034	0.799	8.877	0.071	0.300	0.459
30	0.437	0.037	0.912	8.467	0.077	0.300	0.492
40	0.487	0.027	1.016	5.544	0.056	0.450	0.525
50	0.488	0.022	1.018	4.508	0.046	0.599	0.557
60	0.474	0.026	0.989	5.485	0.054	0.749	0.590
66	0.434	0.029	0.905	6.682	0.061	0.899	0.610

TURBULENCE INTENSITY PROFILES – T 8
CHANNEL OF CIRCULAR CROSS SECTION (D=305 mm)

Bed Thickness	=47	mm
Discharge	0.0271	m3/s
Slope	0.0010	
Mean Shear Stress	0.7563	N/m2
Mean Velocity	0.6134	m/s
Normal Depth	155.1	mm
yt/D	0.663	
Temperature	21.5	C
Bed Condition	smooth	

AT CENTRE:

y (mm)	u(m/s)	r.m.s	u/V	TI rms/u	r.m.s/V	y/y_o	yt/D
2	0.420	0.059	0.685	14.048	0.096	0.013	0.161
3	0.436	0.052	0.711	11.927	0.085	0.019	0.164
4	0.479	0.049	0.781	10.230	0.080	0.026	0.167
5	0.491	0.059	0.800	12.016	0.096	0.032	0.170
6	0.515	0.060	0.840	11.650	0.098	0.039	0.174
10	0.528	0.051	0.861	9.659	0.083	0.064	0.187
20	0.608	0.048	0.991	7.895	0.078	0.129	0.220
30	0.644	0.047	1.050	7.298	0.077	0.193	0.252
50	0.622	0.034	1.014	5.466	0.055	0.322	0.318
70	0.627	0.033	1.022	5.263	0.054	0.451	0.384
90	0.629	0.038	1.025	6.041	0.062	0.580	0.449
110	0.642	0.041	1.047	6.386	0.067	0.709	0.515
130	0.642	0.038	1.047	5.919	0.062	0.838	0.580
140	0.618	0.038	1.008	6.149	0.062	0.903	0.613
150	0.629	0.056	1.025	8.903	0.091	0.967	0.646

At 45 mm right of centre:

y (mm)	u(m/s)	RMS	u/V	TI (RMS/u)%	RMS/V	y/y_o	yt/D
2	0.334	0.041	0.545	12.275	0.067	0.013	0.161
3	0.350	0.040	0.571	11.429	0.065	0.019	0.164
4	0.370	0.039	0.603	10.541	0.064	0.026	0.167
5	0.385	0.045	0.628	11.688	0.073	0.032	0.170
6	0.393	0.041	0.641	10.433	0.067	0.039	0.174
10	0.461	0.046	0.752	9.978	0.075	0.064	0.187
20	0.503	0.039	0.820	7.753	0.064	0.129	0.220
30	0.565	0.043	0.921	7.611	0.070	0.193	0.252
50	0.580	0.046	0.946	7.931	0.075	0.322	0.318
70	0.600	0.042	0.978	7.000	0.068	0.451	0.384
90	0.597	0.038	0.973	6.365	0.062	0.580	0.449
110	0.593	0.050	0.967	8.432	0.082	0.709	0.515
130	0.596	0.026	0.972	4.362	0.042	0.838	0.580
140	0.563	0.043	0.918	7.638	0.070	0.903	0.613
150	0.561	0.043	0.915	7.665	0.070	0.967	0.646

AT 90 mm right of centre:

y (mm)	u(m/s)	RMS	u/V	TI (RMS/u)%	RMS/V	y/y_o	yt/D
2	0.169	0.039	0.276	23.077	0.064	0.013	0.161
3	0.180	0.034	0.293	18.889	0.055	0.019	0.164
4	0.203	0.039	0.331	19.212	0.064	0.026	0.167
5	0.207	0.042	0.337	20.290	0.068	0.032	0.170
6	0.213	0.039	0.347	18.310	0.064	0.039	0.174
10	0.264	0.042	0.430	15.909	0.068	0.064	0.187
20	0.308	0.031	0.502	10.065	0.051	0.129	0.220
30	0.390	0.038	0.636	9.744	0.062	0.193	0.252
50	0.523	0.045	0.853	8.604	0.073	0.322	0.318
70	0.569	0.054	0.928	9.490	0.088	0.451	0.384
90	0.550	0.045	0.897	8.182	0.073	0.580	0.449
110	0.584	0.048	0.952	8.219	0.078	0.709	0.515
130	0.607	0.035	0.990	5.766	0.057	0.838	0.580
140	0.595	0.032	0.970	5.378	0.052	0.903	0.613
150	0.526	0.052	0.858	9.886	0.085	0.967	0.646

TURBULENCE INTENSITY PROFILES-T9
CHANNEL OF CIRCULAR CROSS SECTION (D=305 mm)

Bed Thickness	=120	mm
Discharge	0.0183	m3/s
Slope	0.0011	
Mean Shear Stress	0.6600	N/m2
Mean Velocity	0.5924	m/s
Normal Depth	104.4	mm
yt/D	0.736	
Temperature	13	C
Bed condition	smooth	

AT CENTRE:

y (mm)	u(m/s)	r.m.s	u/V	TI rms/u%	r.m.s/V	y/y_o	yt/D
2	0.379	0.047	0.640	12.401	0.079	0.019	0.400
3	0.382	0.044	0.645	11.518	0.074	0.029	0.403
5	0.386	0.042	0.652	10.881	0.071	0.048	0.410
10	0.458	0.048	0.773	10.480	0.081	0.096	0.426
20	0.512	0.049	0.864	9.570	0.083	0.192	0.459
40	0.538	0.053	0.908	9.851	0.089	0.383	0.525
60	0.536	0.044	0.905	8.209	0.074	0.575	0.590
70	0.632	0.036	1.067	5.696	0.061	0.670	0.623
80	0.631	0.040	1.065	6.339	0.068	0.766	0.656
90	0.651	0.039	1.099	5.991	0.066	0.862	0.689
100	0.655	0.037	1.106	5.649	0.062	0.958	0.721

At 50 mm right of centre:

y (mm)	u(m/s)	RMS	u/V	TI (RMS/u)%	RMS/V	y/y_o	yt/D
2	0.449	0.044	0.758	9.800	0.074	0.019	0.400
3	0.460	0.049	0.777	10.652	0.083	0.029	0.403
5	0.508	0.060	0.858	11.811	0.101	0.048	0.410
10	0.517	0.063	0.873	12.186	0.106	0.096	0.426
20	0.610	0.044	1.030	7.213	0.074	0.192	0.459
30	0.647	0.049	1.092	7.573	0.083	0.287	0.492
40	0.607	0.038	1.025	6.260	0.064	0.383	0.525
50	0.680	0.025	1.148	3.676	0.042	0.479	0.557
60	0.688	0.036	1.161	5.233	0.061	0.575	0.590
80	0.676	0.033	1.141	4.882	0.056	0.766	0.656
90	0.653	0.030	1.102	4.594	0.051	0.862	0.689
100	0.625	0.042	1.055	6.720	0.071	0.958	0.721

AT 90 mm right of centre:

y (mm)	u(m/s)	RMS	u/V	TI (RMS/u)%	RMS/V	y/y_o	yt/D
2	0.410	0.057	0.692	13.902	0.096	0.019	0.400
3	0.423	0.056	0.714	13.239	0.095	0.029	0.403
5	0.446	0.056	0.753	12.556	0.095	0.048	0.410
10	0.491	0.050	0.829	10.183	0.084	0.096	0.426
20	0.549	0.046	0.927	8.379	0.078	0.192	0.459
30	0.562	0.054	0.949	9.609	0.091	0.287	0.492
40	0.625	0.049	1.055	7.840	0.083	0.383	0.525
50	0.602	0.045	1.016	7.475	0.076	0.479	0.557
60	0.594	0.050	1.003	8.418	0.084	0.575	0.590
80	0.526	0.060	0.888	11.407	0.101	0.766	0.656
90	0.491	0.075	0.829	15.275	0.127	0.862	0.689
100	0.249	0.054	0.420	21.687	0.091	0.958	0.721

TURBULENCE INTENSITY PROFILES—T 10
CHANNEL OF CIRCULAR CROSS SECTION (D=305 mm)

Bed Thickness	=120	mm
Discharge	0.0103	m3/s
Slope	0.0032	
Mean Shear Stress	1.3926	N/m2
Mean Velocity	0.5547	m/s
Normal Depth	61.5	mm
yt/D	0.595	
Temperature	14.3	C
Bed condition	k_s=1.4	mm

AT CENTRE:

y (mm)	u(m/s)	RMS	u/V	TI RMS/u%	r.m.s/V	y/y_o	yt/D
2	0.299	0.056	0.539	18.729	0.101	0.033	0.400
3	0.328	0.053	0.591	16.159	0.096	0.049	0.403
5	0.335	0.057	0.604	17.015	0.103	0.081	0.410
7	0.376	0.054	0.678	14.362	0.097	0.114	0.416
10	0.448	0.055	0.808	12.277	0.099	0.163	0.426
20	0.572	0.049	1.031	8.566	0.088	0.325	0.459
30	0.615	0.044	1.109	7.154	0.079	0.488	0.492
40	0.656	0.051	1.183	7.774	0.092	0.650	0.525
50	0.697	0.033	1.257	4.735	0.059	0.813	0.557
60	0.693	0.029	1.249	4.185	0.052	0.976	0.590

At 50 mm right of centre:

y (mm)	u(m/s)	RMS	u/V	TI (RMS/u)%	RMS/V	y/y_o	yt/D
2	0.204	0.040	0.368	19.608	0.072	0.033	0.400
3	0.261	0.046	0.471	17.625	0.083	0.049	0.403
5	0.361	0.062	0.651	17.175	0.112	0.081	0.410
7	0.379	0.046	0.683	12.137	0.083	0.114	0.416
10	0.393	0.039	0.708	9.924	0.070	0.163	0.426
20	0.511	0.040	0.921	7.828	0.072	0.325	0.459
30	0.583	0.043	1.051	7.376	0.078	0.488	0.492
40	0.639	0.044	1.152	6.886	0.079	0.650	0.525
50	0.582	0.057	1.049	9.794	0.103	0.813	0.557
60	0.638	0.031	1.150	4.859	0.056	0.976	0.590

AT 90 mm right of centre:

y (mm)	u(m/s)	RMS	u/V	TI (RMS/u)%	RMS/V	y/y_o	yt/D
2	0.194	0.052	0.350	26.804	0.094	0.033	0.400
3	0.197	0.042	0.355	21.320	0.076	0.049	0.403
5	0.252	0.052	0.454	20.635	0.094	0.081	0.410
10	0.203	0.046	0.366	22.660	0.083	0.163	0.426
20	0.27	0.050	0.487	18.519	0.090	0.163	0.459
30	0.272	0.039	0.490	14.338	0.070	0.325	0.492
40	0.49	0.047	0.883	9.592	0.085	0.488	0.525
50	0.475	0.058	0.856	12.211	0.105	0.650	0.557
60	0.454	0.053	0.818	11.674	0.096	0.813	0.590

TURBULENCE INTENSITY PROFILES — T 11
CHANNEL OF CIRCULAR CROSS SECTION (D=305 mm)

Bed Thickness	=120	mm
Discharge	0.0198	m3/s
Slope	0.0026	
Mean Shear Stress	1.5746	N/m2
Mean Velocity	0.6307	m/s
Normal Depth	105.9	mm
yt/D	0.741	
Temperature	13	C
Bed condition	Rough. II	(ks=1.4mm)

AT CENTRE:

y (mm)	u(m/s)	r.m.s	u/V	TI RMS/u%	r.m.s/V	y/y_o	yt/D
2	0.374	0.045	0.593	12.032	0.071	0.019	0.400
3	0.375	0.045	0.595	12.000	0.071	0.028	0.403
5	0.389	0.052	0.617	13.368	0.082	0.047	0.410
7	0.439	0.045	0.696	10.251	0.071	0.066	0.416
10	0.489	0.047	0.775	9.611	0.075	0.094	0.426
20	0.498	0.055	0.790	11.044	0.087	0.189	0.459
30	0.658	0.039	1.043	5.927	0.062	0.283	0.492
50	0.672	0.053	1.065	7.887	0.084	0.472	0.557
70	0.689	0.043	1.092	6.241	0.068	0.661	0.623
90	0.721	0.033	1.143	4.577	0.052	0.850	0.689
100	0.721	0.033	1.143	4.577	0.052	0.945	0.721

At 45 mm right of centre:

y (mm)	u(m/s)	RMS	u/V	TI (RMS/u)%	RMS/V	y/y_o	yt/D
2	0.295	0.059	0.468	20.000	0.094	0.019	0.400
3	0.335	0.059	0.531	17.612	0.094	0.028	0.403
5	0.467	0.078	0.740	16.702	0.124	0.047	0.410
7	0.479	0.076	0.759	15.866	0.120	0.066	0.416
10	0.529	0.060	0.839	11.342	0.095	0.094	0.426
20	0.680	0.050	1.078	7.353	0.079	0.189	0.459
30	0.733	0.046	1.162	6.276	0.073	0.283	0.492
50	0.766	0.031	1.214	4.047	0.049	0.472	0.557
70	0.741	0.024	1.175	3.239	0.038	0.661	0.623
90	0.729	0.032	1.156	4.390	0.051	0.850	0.689
100	0.703	0.036	1.115	5.121	0.057	0.945	0.721

AT 95 mm right of centre:

y (mm)	u(m/s)	RMS	u/V	TI (RMS/u)%	RMS/V	y/y_o	yt/D
2	0.175	0.039	0.277	22.286	0.062	0.019	0.400
3	0.191	0.040	0.303	20.942	0.063	0.028	0.403
5	0.258	0.044	0.409	17.054	0.070	0.047	0.410
10	0.500	0.043	0.000	8.600	0.068	0.094	0.426
20	0.617	0.047	0.978	7.618	0.075	0.189	0.459
30	0.586	0.057	0.929	9.727	0.090	0.283	0.492
50	0.647	0.055	1.026	8.501	0.087	0.472	0.557
70	0.461	0.056	0.731	12.148	0.089	0.661	0.623

APPENDIX G

EINSTEIN-VANONI SEPARATION METHOD

APPENDIX G

EINSTEIN-VANONI SEPARATION METHOD

Since some of the present experiments were carried out in a flume with rough bed and smooth glass walls, the resistance to flow caused by the roughness of the boundary was not uniform through out the wetted perimeter. Therefore, hydraulic parameters such as hydraulic radius and friction factor due to bed only, were considered for analysis by splitting the overall parameters into their constituent parts corresponding to bed and glass side walls.

In order to eliminate the effect of side wall friction, Einstein (1942) technique was adopted. it divides the cross sectional area of flow into three sub sections as shown in Figure G.1 , each representing a separate channel in which the flow is affected by only one boundary. By eliminating the side wall effect, the channel can be considered as a wide channel were only the bed roughness is affecting the flow.

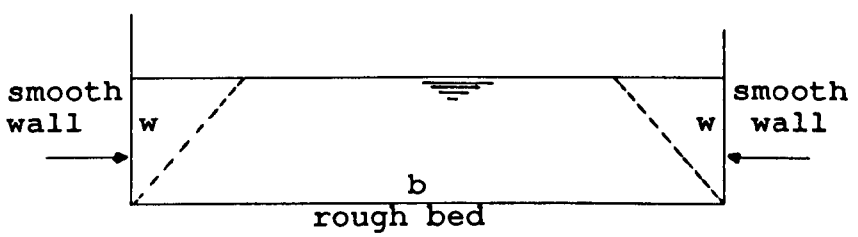

FIGURE G.1 SUBSECTIONS OF FLOW IN EINSTEIN'S THEORY

The friction factor of a uniform flow λ is related to flow velocity V, hydraulic radius R and the bed slope S in the Darcy-Weisbach's equation as:

$$\lambda = \frac{8gRS}{V^2} \qquad (G.1)$$

By applying the Darcy-Weisbach's equation for each sub section of the flow, it could be shown that:

$$\frac{\lambda}{R} = \frac{\lambda_w}{R_w} = \frac{\lambda_b}{R_b} = \frac{8gS}{V^2} \qquad (G.2)$$

where subscripts $_w$ and $_b$ represent the side walls and the bed of the channel respectively.

Assuming the pipe wall to be smooth expression for smooth pipes,

$$\frac{1}{\sqrt{\lambda_w}} = 2 \text{ Log } \left[\frac{R_{ew}\sqrt{\lambda_w}}{2.51}\right] \qquad (G.3)$$

can be used.

Overall Reynolds' number of the flow can be calculated as

$$R_e = \frac{4\ R\ V}{\upsilon} \qquad (G.4)$$

Similarly the wall Reynolds' number is given by

$$R_{ew} = \frac{4\ R_w\ V}{\upsilon} \qquad (G.5)$$

By solving equation G2 for R_w results in:

$$R_w = \frac{\lambda_w\ V^2}{8\ g\ S} \qquad (G.6)$$

and by solving equation G3 using iterative procedure the

friction coefficient of the side wall is determined.

According to the composite roughness equation proposed by Vanoni and Brook (1957)

$$p\,\lambda_0 = P_w\,\lambda_w + P_b\,\lambda_b \qquad (G.7)$$

where P_b is the wetted perimeter of the bed which is equal to the flat bed width (b), P_w is the wetted perimeter of side wall , $(P-P_b)$, and P is the total wetted perimeter.

By solving equation G.7 for λ_b results in

$$\lambda_b = \lambda_o + \frac{R_w}{R_b}\,(\lambda_o - \lambda_w) \qquad (G.8)$$

where R_b is the hydraulic radius of the bed

$$R_b = \frac{A_b}{P_b} = \frac{A - R_w P_w}{P_b} \qquad (G.9)$$

Equivalent roughness of the bed ,k_{sb}, according to the Colebrook-White equation

$$k_{sb} = 14.8\,R_b\,\left(10^{-1/2\sqrt{\lambda_b}} - \frac{2.51}{R_{*b}\sqrt{\lambda_b}}\right) \qquad (G.10)$$

The shear stress exerted on the bed can be expressed as

$$\tau_b = \rho\,g\,R_b\,S \qquad (G.11)$$

in which ρ is density of water.

APPENDIX H

BED LOAD TRANSPORT EXPERIMENTAL DATA

TABLE H1 BED LOAD EXPERIMENTAL DATA IN CHANNEL WITH 47 mm THICK SMOOTH BED

a) flows up to half full depths

Ex. No.	Q (m^3/s)	y_o (mm)	R (m)	V (m/s)	S	T (C^o)	R_e	λ_s	Ks mm	Fr	C_v	d_{50} mm
1	0.0087	66.10	0.0468	0.498	0.0012	20	91711.46	0.018	-0.01	0.65	0.0000726	0.53
2	0.0070	66.28	0.0469	0.399	0.0006	20	77313.3	0.013	-0.17	0.55	0.0000186	0.53
3	0.0119	58.60	0.0428	0.773	0.0041	20	130246.5	0.023	0.23	1.07	0.0004603	0.53
4	0.0106	62.90	0.0451	0.641	0.0026	21	116555.5	0.022	0.20	0.86	0.0000904	0.53
5	0.0258	106.20	0.0651	0.866	0.0028	20	222029.0	0.019	0.14	0.88	0.0001512	0.53
6	0.0177	101.20	0.0631	0.630	0.0011	21	160196.0	0.014	-0.07	0.66	0.0000439	0.53
7	0.0212	102.20	0.0635	0.749	0.0021	21	191628.5	0.019	0.11	0.78	0.0000387	0.53
8	0.0089	64.64	0.0460	0.520	0.0011	20	94327.3	0.015	-0.09	0.69	0.0000591	1
9	0.0073	65.70	0.0466	0.421	0.0007	20	77282.6	0.015	-0.13	0.55	0.0000427	1
10	0.0120	58.00	0.0424	0.794	0.0042	20	132523.5	0.022	0.19	1.11	0.0003943	1
11	0.0106	62.50	0.0449	0.646	0.0027	20	114031.8	0.019	0.20	0.87	0.0001282	1
12	0.0255	106.40	0.0652	0.856	0.0027	20	219619.4	0.019	0.14	0.87	0.0002021	1
13	0.0177	104.70	0.0640	0.607	0.0012	20	152924.1	0.017	0.00	0.63	0.0000330	1
14	0.0201	104.00	0.0642	0.696	0.0018	20	175793.0	0.019	0.11	0.72	0.0000313	1
15	0.0089	66.00	0.0467	0.509	0.0012	20	93661.5	0.017	-0.04	0.67	0.0000625	2
16	0.0073	67.00	0.0473	0.411	0.0007	20	76571.4	0.015	-0.12	0.54	0.0000409	2
17	0.0119	58.00	0.0424	0.788	0.0039	20	131393.5	0.021	0.14	1.10	0.0003917	2
18	0.0106	62.50	0.0449	0.646	0.0025	20	114031.8	0.019	0.14	0.87	0.0002084	2
19	0.0254	106.70	0.0653	0.855	0.0027	20	219481.2	0.019	0.14	0.87	0.0003115	2
20	0.0176	104.50	0.0644	0.606	0.0012	20	153588.6	0.017	0.00	0.63	0.0000872	2
21	0.0201	102.00	0.0634	0.710	0.0017	20	177365.9	0.017	0.03	0.74	0.0000886	2
22	0.0086	66.20	0.0469	0.492	0.0011	18	86286.8	0.017	-0.06	0.64	0.0000730	2.9
23	0.0075	67.00	0.0473	0.423	0.0008	18	74919.3	0.016	-0.12	0.55	0.0000329	2.9
24	0.0120	58.00	0.0424	0.794	0.0040	19	129316.9	0.021	0.14	1.10	0.0006496	2.9
25	0.0106	62.50	0.0449	0.645	0.0025	18	108585.5	0.021	0.14	0.87	0.0002818	2.9
26	0.0179	104.70	0.0645	0.616	0.0013	19	150459.7	0.017	0.03	0.64	0.0001296	2.9
27	0.0202	103.36	0.0639	0.705	0.0019	19	173154.9	0.019	0.12	0.73	0.0001258	2.9
28	0.0089	65.30	0.0464	0.515	0.0012	18	89454.5	0.017	-0.06	0.68	0.0000753	5.6
29	0.0120	58.00	0.0424	0.793	0.0043	19	127643.7	0.023	0.22	1.10	0.0008640	5.6
30	0.0106	62.10	0.0447	0.650	0.0025	19	110187.9	0.021	0.12	0.88	0.0003286	5.6
31	0.0177	105.20	0.0647	0.605	0.0013	18	146625.5	0.017	0.03	0.62	0.0002142	5.6
32	0.0201	104.50	0.0644	0.692	0.0019	18	167027.5	0.020	0.18	0.70	0.0003258	5.6
33	0.0094	66.00	0.0468	0.539	0.0012	18	94407.6	0.015	-0.09	0.70	0.0000713	8.4
34	0.0121	59.50	0.0432	0.780	0.0039	18	125856.9	0.022	0.17	1.08	0.0008375	8.4
35	0.0106	62.50	0.0449	0.645	0.0025	18	108577.6	0.021	0.13	0.87	0.0004072	8.4
36	0.0177	104.90	0.0645	0.612	0.0012	18	147685.1	0.017	-0.00	0.63	0.0001325	8.4
37	0.0205	105.00	0.0646	0.702	0.0019	18	169990.5	0.020	0.15	0.72	0.0002957	8.4

TABLE H1 BED LOAD EXPERIMENTAL DATA IN CHANNEL WITH 47 mm THICK SMOOTH BED

b) flows more than half full depth

Ex. No.	Q (m^3/s)	y_o (mm)	R (m)	V (m/s)	S	T (C^o)	R_e	λ_s	Ks mm	Fr	C_v	d_{50} mm
1	0.0222	154.98	0.0797	0.503	0.0005	20	157750.0	0.012	−0.13	0.40	0.0000104	0.53
2	0.0312	158.50	0.0805	0.689	0.0010	20	221062.0	0.013	−0.07	0.55	0.0000328	0.53
3	0.0257	200.77	0.0856	0.456	0.0006	20	153667.1	0.018	0.09	0.30	0.0000066	0.53
4	0.0227	155.20	0.0797	0.514	0.0005	20	161197.5	0.011	−0.16	0.42	0.0000172	1
5	0.0303	157.50	0.0803	0.675	0.0010	20	213291.0	0.014	−0.05	0.54	0.0000348	1
6	0.0257	202.50	0.0856	0.452	0.0005	20	153134.2	0.018	−0.00	0.30	0.0000129	1
7	0.0216	154.20	0.0796	0.492	0.0005	20	153973.0	0.012	−0.14	0.40	0.0000284	2
8	0.0306	157.70	0.0803	0.681	0.0011	20	215232.7	0.015	−0.15	0.55	0.0000968	2
9	0.0254	201.20	0.0856	0.450	0.0005	20	151500.7	0.017	0.04	0.29	0.0000114	2
10	0.0220	155.80	0.0799	0.495	0.0005	19	150270.9	0.012	−0.16	0.40	0.0000285	2.9
11	0.0300	158.20	0.0804	0.665	0.0011	19	204055.3	0.016	0.00	0.53	0.0002151	2.9
12	0.0258	201.90	0.0856	0.455	0.0005	19	147954.0	0.018	0.06	0.30	0.0000228	2.9
13	0.0218	145.70	0.0776	0.525	0.0005	19	156687.5	0.010	−0.16	0.45	0.0000278	5.6
14	0.0303	158.30	0.0805	0.671	0.0010	19	205000.4	0.014	−0.05	0.54	0.0001938	5.6
15	0.0295	158.50	0.0805	0.653	0.0010	18	196989.6	0.015	−0.03	0.52	0.0001362	8.4
16	0.0240	156.20	0.0800	0.539	0.0006	18	161672.9	0.013	−0.11	0.44	0.0000387	8.4

TABLE H2 BED LOAD EXPERIMENTAL DATA IN CHANNEL WITH 47 mm THICK ROUGH BED

a) flows up to half full depths (ks = 0.8 mm)

Ex. No.	Q m^3/s	y_o mm	R m	R_b m	V m/s	S	T C^o	R_e	λ_s	Ks mm	Fr	C_v	d_{50} mm
1	0.00979	64.88	0.0462	0.0584	0.570	0.0029	19.4	102259.2	0.033	1.10	0.75	0.0001766	2
2	0.00817	63.90	0.0457	0.0586	0.484	0.0024	18.8	84578.9	0.037	1.56	0.64	0.0000945	2
3	0.01013	63.66	0.0456	0.0544	0.602	0.0027	18.9	105254.1	0.027	0.52	0.80	0.0002420	2
4	0.00752	60.60	0.0439	0.0529	0.472	0.0020	18.9	79474.7	0.031	0.81	0.65	0.0001174	2.90
5	0.00988	66.46	0.0471	0.0583	0.560	0.0026	17.1	96590.6	0.030	0.84	0.73	0.0001746	2.90
6	0.00926	62.33	0.0449	0.0565	0.564	0.0031	17.9	94548.8	0.034	1.24	0.76	0.0002465	2.90
7	0.00979	63.60	0.0455	0.0569	0.583	0.0031	17.2	97542.8	0.033	1.07	0.78	0.0002968	5.60
8	0.00844	60.96	0.0441	0.0549	0.527	0.0027	18	87078.2	0.034	1.18	0.72	0.0002011	5.60
9	0.00765	61.76	0.0445	0.0531	0.470	0.0019	18.5	79520.9	0.029	0.67	0.64	0.0001352	5.60
10	0.00943	65.43	0.0465	0.0558	0.544	0.0023	18.6	96242.1	0.028	0.63	0.72	0.0001305	8.4
11	0.00979	63.63	0.0456	0.0572	0.582	0.0031	19	101977.9	0.033	1.09	0.78	0.0003036	8.4

TABLE H2 BED LOAD EXPERIMENTAL DATA IN CHANNEL WITH 47 mm THICK ROUGH BED

b) flows more than half full depth (ks = 0.8 mm)

Ex. No.	Q (m^3/s)	y_o (mm)	R (m)	R_b m	V (m/s)	S	T (C^o)	R_e	λ_s	Ks mm	Fr	C_v	d_{50} mm
1	0.01704	105.46	0.0648	0.0817	0.579	0.0016	17	136031.2	0.024	0.45	0.60	0.0001224	2
2	0.01884	105.42	0.0648	0.0881	0.644	0.0022	20	162159.2	0.028	0.84	0.66	0.0000820	2
3	0.02072	103.38	0.0640	0.0877	0.720	0.0029	20	179305.2	0.028	0.85	0.75	0.0001470	2
4	0.03375	160.90	0.0810	0.1260	0.735	0.0022	17	218627.6	0.026	0.91	0.58	0.0000537	2
5	0.02182	157.08	0.0802	0.1219	0.487	0.0011	17	143417.0	0.028	1.09	0.39	0.0000177	2
6	0.01759	101.26	0.0632	0.0814	0.625	0.0020	18	148489.3	0.025	0.57	0.66	0.0001057	2.90
7	0.01940	104.66	0.0645	0.0889	0.665	0.0025	17	156865.5	0.029	0.97	0.69	0.0001138	2.90
8	0.02052	99.53	0.0625	0.0854	0.743	0.0032	18	172829.2	0.028	0.92	0.79	0.0001271	2.90
9	0.02893	155.14	0.0798	0.1317	0.653	0.0022	17	191550.1	0.032	1.74	0.53	0.0000328	2.90
10	0.03220	156.20	0.0800	0.1367	0.722	0.0028	17	212389.3	0.034	2.15	0.59	0.0002947	2.90
11	0.02223	101.77	0.0634	0.0829	0.786	0.0031	17	183511.8	0.025	0.55	0.82	0.0004907	5.60
12	0.02036	99.44	0.0624	0.0822	0.738	0.0029	18	173221.0	0.026	0.62	0.78	0.0002032	5.60
13	0.01714	102.10	0.0635	0.0819	0.604	0.0019	19	145585.3	0.025	0.58	0.63	0.0000933	5.60
14	0.03222	158.70	0.0805	0.1374	0.711	0.0026	17	210519.7	0.033	2.02	0.57	0.0000630	5.60
15	0.02612	152.10	0.0791	0.1342	0.602	0.0020	19	181164.3	0.035	2.43	0.50	0.0000406	5.60
16	0.01997	102.80	0.0638	0.0805	0.698	0.0023	19	169496.7	0.023	0.42	0.73	0.0002532	8.4
17	0.02193	103.23	0.0640	0.0874	0.763	0.0032	19	188046.4	0.028	0.84	0.79	0.0003057	8.4
18	0.01728	100.18	0.0627	0.0761	0.622	0.0018	20	152066.5	0.023	0.34	0.66	0.0000973	8.4
19	0.03207	162.03	0.0812	0.1276	0.693	0.0020	17	206909.9	0.027	1.01	0.55	0.0000833	8.4
20	0.03507	162.88	0.0813	0.1070	0.754	0.0018	20	240437.6	0.020	0.28	0.59	0.0003949	8.4

TABLE H3 BED LOAD EXPERIMENTAL DATA IN CHANNEL WITH 47 mm THICK ROUGH BED

a) flows up to half full depth (ks=1.4 mm)

Ex. No.	Q m3/s	y_0 mm	R m	R_b m	V m/s	S	T C^o	R_e	λ_s	Ks mm	Fr	C_v	d_{50} mm
1	0.0089	69.28	0.0486	0.0162	0.479	0.0020	16.4	83833.7	0.033	1.19	0.61	0.0000783	2.0
2	0.0083	64.15	0.0459	0.0619	0.487	0.0031	17.1	81889.4	0.050	3.90	0.65	0.0000559	2.0
3	0.0086	60.83	0.0441	0.0569	0.538	0.0032	17.5	87843.4	0.039	1.78	0.73	0.0001342	2.0
4	0.0118	72.45	0.0504	0.0679	0.603	0.0034	17	111239.1	0.037	1.84	0.75	0.0001142	2.9
5	0.0108	70.94	0.0496	0.0660	0.563	0.0030	17	102259.7	0.037	1.74	0.71	0.0001289	2.9
6	0.0084	66.40	0.0473	0.0586	0.473	0.0019	17	81879.6	0.031	0.92	0.62	0.0001650	2.9
7	0.0100	71.25	0.0498	0.0623	0.521	0.0021	17.2	95455.4	0.031	0.90	0.66	0.0000444	5.60
8	0.0092	65.82	0.0470	0.0618	0.523	0.0029	15.8	87160.5	0.039	1.94	0.69	0.0001288	5.60
9	0.0102	64.98	0.0466	0.0607	0.586	0.0035	15.9	97470.7	0.036	1.55	0.77	0.0002567	5.60
10	0.0093	62.88	0.0454	0.0594	0.553	0.0034	15.5	88451.6	0.040	1.97	0.74	0.0001071	8.4
11	0.0090	60.76	0.0443	0.0578	0.559	0.0037	15.4	86898.6	0.042	2.24	0.76	0.0002491	8.4
12	0.0107	65.63	0.0469	0.0626	0.609	0.0041	15.5	100484.5	0.041	2.30	0.80	0.0004605	8.4

TABLE H3 BED LOAD EXPERIMENTAL DATA IN CHANNEL WITH 47 mm THICK ROUGH BED

b) flows more than half full depth (ks=1.4 mm)

Ex. No.	Q m^3/s	y_0 mm	R m	R_b m	V m/s	S	T C^o	R_e	λ_s	Ks mm	Fr	C_v	d_{50} mm
1	0.0288	158.78	0.0805	0.1314	0.636	0.0019	17	188163.1	0.030	1.45	0.51	0.0000149	2.0
2	0.0211	107.98	0.0658	0.0925	0.698	0.0027	17	168906.6	0.029	1.00	0.71	0.0000841	2.0
3	0.0336	158.38	0.0804	0.1000	0.742	0.0017	17	219480.6	0.019	0.18	0.59	0.0000373	2.0
4	0.0184	96.03	0.0610	0.0848	0.693	0.0031	17	156371.0	0.031	1.17	0.75	0.0000888	2.0
5	0.0337	158.75	0.0806	0.1465	0.740	0.0033	17	218328.4	0.038	3.16	0.59	0.0000576	2.9
6	0.0196	99.30	0.0626	0.0877	0.708	0.0031	17	162098.3	0.030	1.17	0.75	0.0000986	2.9
7	0.0186	98.32	0.0622	0.0874	0.678	0.0030	17	153053.3	0.031	1.30	0.72	0.0000926	2.9
8	0.0340	168.00	0.0823	0.1465	0.707	0.0026	17	211679.8	0.033	2.08	0.54	0.0000296	2.9
9	0.0357	161.80	0.0812	0.1180	0.771	0.0021	17	229740.6	0.023	0.51	0.61	0.0000408	2.9
10	0.0168	99.00	0.0625	0.0849	0.610	0.0022	17	140046.1	0.029	0.95	0.65	0.0000619	2.9
11	0.0203	99.76	0.0628	0.0905	0.730	0.0036	16	162548.7	0.033	1.59	0.77	0.0001826	5.60
12	0.0181	104.26	0.0646	0.0878	0.620	0.0021	16	143159.4	0.028	0.87	0.64	0.0000555	5.60
13	0.0302	165.58	0.0819	0.1336	0.637	0.0018	17	191733.1	0.029	1.27	0.49	0.0000120	5.60
14	0.0215	109.50	0.0665	0.0945	0.698	0.0027	17	170882.1	0.029	1.00	0.70	0.0000736	5.60
15	0.0336	160.43	0.0810	0.1312	0.731	0.0024	16	210160.8	0.029	1.26	0.58	0.0000340	5.60
16	0.0363	161.65	0.0812	0.1401	0.784	0.0031	16	225903.5	0.032	1.86	0.62	0.0000717	5.60
17	0.0211	97.58	0.0619	0.0896	0.776	0.0042	16	169411.3	0.034	1.69	0.83	0.0004330	8.4
18	0.0213	103.68	0.0643	0.0920	0.733	0.0033	16	167562.1	0.031	1.26	0.76	0.0002085	8.4
19	0.0202	104.20	0.0645	0.0917	0.693	0.0029	16	159069.4	0.030	1.21	0.72	0.0001819	8.4
20	0.0333	151.23	0.0790	0.1290	0.768	0.0029	15	211000.5	0.031	1.53	0.64	0.0000950	8.4
21	0.0337	158.18	0.0805	0.1148	0.743	0.0020	15	208447.0	0.023	0.53	0.60	0.0000501	8.4
22	0.0337	146.53	0.0779	0.1285	0.804	0.0034	15	218242.2	0.033	1.89	0.68	0.0001966	8.4

TABLE H4 BED LOAD EXPERIMENTAL DATA IN CHANNEL WITH 77 mm THICK SMOOTH BED

a) flows up to half full depth

EX. No.	Q m^3/s	y_o mm	R m	V m/s	S	T C^o	R_e	λ_s	Ks mm	Fr	C_v	d_{50} mm
1	0.0215	76.53	0.0530	0.962	0.00364	19	192189.0	0.016	0.01	1.13	0.0004487	0.53
2	0.0174	81.63	0.0550	0.727	0.00235	19	153511.5	0.019	0.09	0.83	0.0003160	0.53
3	0.0152	80.68	0.0545	0.644	0.00204	19	135003.1	0.021	0.19	0.74	0.0000950	0.53
4	0.0148	84.60	0.0553	0.596	0.00170	20	132931.9	0.021	0.18	0.67	0.0000817	0.53
5	0.0076	60.43	0.0440	0.432	0.00114	19	73823.5	0.021	0.10	0.58	0.0000490	0.53
6	0.0052	38.70	0.0310	0.474	0.00227	19	57184.9	0.025	0.18	0.79	0.0001688	0.53
7	0.0066	45.58	0.0360	0.509	0.00206	19	69182.2	0.022	0.11	0.78	0.0001966	1.00
8	0.0060	54.00	0.0410	0.385	0.00079	18	59027.1	0.017	−0.01	0.54	0.0000235	1.00
9	0.0089	61.15	0.0450	0.502	0.00145	19	86513.6	0.020	0.07	0.66	0.0000888	1.00
10	0.0057	42.80	0.0240	0.469	0.00196	18	59070.4	0.024	0.16	0.74	0.0003480	2.00
11	0.0073	58.74	0.0435	0.427	0.00107	16	66737.0	0.020	0.00	0.58	0.0001344	2.00
12	0.0057	39.38	0.0318	0.512	0.00204	16	58016.2	0.020	−0.02	0.84	0.0003107	2.9
13	0.0062	54.33	0.0410	0.400	0.00103	15	57318.2	0.021	0.02	0.56	0.0000524	2.9
14	0.0056	45.35	0.0357	0.432	0.00206	16	54905.4	0.031	0.61	0.66	0.0003580	5.6
15	0.0074	53.63	0.0406	0.480	0.00223	16	69515.6	0.031	0.73	0.68	0.0003518	5.6
16	0.0109	66.98	0.0479	0.560	0.00185	15	93199.7	0.022	0.19	0.71	0.0003616	8.4
17	0.0127	68.63	0.0488	0.635	0.00212	15	107547.0	0.020	0.10	0.79	0.0007472	8.4

TABLE H4 BED LOAD EXPERIMENTAL DATA IN CHANNEL WITH 77 mm THICK SMOOTH BED
b) flows more than half full depth

EX. No.	Q m^3/s	y_o mm	R m	V m/s	S	T C^o	R_e	λ_s	Ks mm	Fr	C_v	d_{50} mm
1	0.0258	127.10	0.0710	0.688	0.0014	18	184473.0	0.017	0.03	0.61	0.0000734	0.53
2	0.0246	136.73	0.0730	0.611	0.0009	18	169358.0	0.015	−0.06	0.52	0.0000410	0.53
3	0.0231	117.60	0.0680	0.665	0.0014	19	171711.9	0.017	0.05	0.62	0.0000426	0.53
4	0.0233	95.60	0.0608	0.826	0.0026	19	190574.2	0.018	0.08	0.86	0.0001721	1.00
5	0.0174	86.06	0.0569	0.688	0.0021	19	148896.2	0.019	0.12	0.76	0.0001952	1.00
6	0.0152	86.70	0.0572	0.597	0.0014	19	131065.6	0.017	0.00	0.66	0.0000820	1.00
7	0.0230	126.84	0.0709	0.614	0.0009	18	163083.6	0.012	−0.13	0.54	0.0000560	1.00
8	0.0215	91.00	0.0590	0.803	0.0027	17	171716.8	0.020	0.14	0.86	0.0002687	2.00
9	0.0174	83.33	0.0557	0.713	0.0023	17	143560.4	0.020	0.14	0.80	0.0003971	2.00
10	0.0278	127.46	0.0710	0.739	0.0016	17	190815.2	0.016	0.01	0.65	0.0001559	2.00
11	0.0228	126.63	0.0708	0.611	0.0011	15	150508.1	0.017	0.02	0.54	0.0001554	2.00
12	0.0337	130.83	0.0719	0.875	0.0025	15	218674.0	0.018	0.12	0.76	0.0002334	2.00
13	0.0161	87.40	0.0575	0.625	0.0017	17	130420.9	0.020	0.01	0.69	0.0001734	2.9
14	0.0206	88.45	0.0579	0.791	0.0029	16	166202.3	0.021	0.24	0.86	0.0007138	2.9
15	0.0183	84.73	0.0563	0.736	0.0024	16	147738.2	0.019	0.01	0.82	0.0004407	2.9
16	0.0316	124.05	0.0701	0.863	0.0026	16	213032.6	0.019	0.15	0.77	0.0002586	2.9
17	0.0246	128.43	0.0713	0.650	0.0013	16	165239.8	0.017	0.02	0.57	0.0000952	2.9
18	0.0219	125.16	0.0704	0.594	0.0011	16	147277.6	0.017	0.01	0.53	0.0000704	2.9
19	0.0144	86.20	0.0570	0.570	0.0018	17	117920.3	0.025	0.45	0.63	0.0004324	5.6
20	0.0214	93.07	0.0598	0.780	0.0028	16	165017.1	0.021	0.24	0.83	0.0006500	5.6
21	0.0170	83.45	0.0558	0.695	0.0023	16	138157.4	0.021	0.19	0.78	0.0005896	5.6
22	0.0327	127.86	0.0712	0.866	0.0026	16	219729.3	0.020	0.19	0.76	0.0004599	5.6
23	0.0258	131.93	0.0722	0.664	0.0013	16	170774.5	0.017	0.02	0.57	0.0001799	5.6
24	0.0231	127.76	0.0711	0.612	0.0011	16	155269.9	0.016	0.00	0.54	0.0001336	5.6
25	0.0164	87.73	0.0576	0.635	0.0018	16	130348.5	0.020	0.15	0.70	0.0003327	8.4
26	0.0213	92.25	0.0595	0.786	0.0029	15	162365.3	0.022	0.29	0.84	0.0004676	8.4
27	0.0172	83.58	0.0558	0.704	0.0023	15	136475.8	0.020	0.15	0.79	0.0006394	8.4
28	0.0332	128.15	0.0712	0.879	0.0025	15	217603.7	0.018	0.10	0.77	0.0009053	8.4
29	0.0250	126.75	0.0709	0.669	0.0013	15	164720.0	0.016	0.00	0.59	0.0001256	8.4

TABLE H5 BED LOAD EXPERIMENTAL DATA IN CHANNEL WITH 77 mm THICK ROUGH BED
a) flows up to half full depth; (ks=0.8mm)

EX. No.	Q m^3/s	y_0 mm	R m	R_b m	V m/s	S	T C^o	R_e	λ_s	Ks mm	Fr	C_v	d_{50} mm
1	0.0124	77.33	0.0532	0.0626	0.544	0.0019	18	107944.0	0.027	0.59	0.64	0.0000364	1
2	0.0146	77.00	0.0530	0.0641	0.643	0.0028	18	127175.3	0.028	0.74	0.75	0.0000783	1
3	0.0100	61.48	0.0450	0.0518	0.564	0.0026	18	93907.3	0.028	0.62	0.74	0.0001367	1
4	0.0130	79.68	0.0542	0.0632	0.553	0.0018	18	111860.0	0.025	0.50	0.64	0.0000497	1
5	0.0067	51.83	0.0400	0.0454	0.450	0.0021	18	67083.8	0.032	0.81	0.65	0.0000441	1
6	0.0164	79.46	0.0540	0.0671	0.704	0.0036	15	132068.1	0.031	1.06	0.81	0.0002136	2
7	0.0088	59.48	0.0440	0.0524	0.510	0.0026	18	83748.4	0.035	1.28	0.68	0.0001361	2
8	0.0127	69.52	0.0490	0.0591	0.626	0.0032	15	106580.7	0.031	1.00	0.78	0.0001878	2
9	0.0131	77.68	0.0532	0.0640	0.577	0.0023	15	106677.7	0.029	0.81	0.68	0.0000948	2.9
10	0.0124	76.95	0.0528	0.0626	0.551	0.0021	15	101633.7	0.028	0.71	0.65	0.0000965	2.9
11	0.0084	60.76	0.0450	0.0595	0.476	0.0026	17	78253.5	0.041	2.06	0.63	0.0001426	2.9
12	0.0083	63.70	0.0460	0.0565	0.451	0.0022	17	74912.4	0.039	1.93	0.58	0.0001084	2.9
13	0.0134	82.14	0.0552	0.0656	0.556	0.0019	15	106645.7	0.027	0.62	0.63	0.0001422	5.6
14	0.0090	61.70	0.0451	0.0527	0.505	0.0023	15	79376.1	0.031	0.88	0.66	0.0001296	5.6
15	0.0101	61.60	0.0451	0.0534	0.566	0.0030	14	86338.7	0.033	1.08	0.75	0.0001911	5.6
16	0.0124	80.64	0.0545	0.0647	0.525	0.0018	15	99499.9	0.028	0.69	0.60	0.0000556	5.6
17	0.0163	80.80	0.0546	0.0676	0.688	0.0033	15	130481.3	0.030	0.93	0.79	0.0002426	5.6
18	0.0101	65.78	0.0473	0.0571	0.528	0.0026	15	87053.2	0.034	1.28	0.67	0.0002928	8.4
19	0.0124	68.06	0.0485	0.0576	0.625	0.0031	15	105513.2	0.030	0.84	0.78	0.0003652	8.4
20	0.0142	83.64	0.0558	0.0659	0.580	0.0020	15	112959.1	0.026	0.53	0.65	0.0001307	8.4
21	0.0179	83.28	0.0557	0.0700	0.734	0.0038	15	142719.5	0.031	1.06	0.83	0.0005125	8.4

TABLE H5 BED LOAD EXPERIMENTAL DATA IN CHANNEL WITH 77 mm THICK ROUGH BED
b) flows more than half full depth; (ks=0.8mm)

EX. No.	Q m^3/s	y_0 mm	R m	R_b m	V m/s	S	T C^o	R_e	λ_s	Ks mm	Fr	C_v	d_{50} mm
1	0.0207	122.32	0.0697	0.0900	0.573	0.0016	17	147255.9	0.026	0.68	0.52	0.0000245	1
2	0.0194	111.00	0.0663	0.0886	0.591	0.0020	18	145208.5	0.030	1.21	0.57	0.0000272	1
3	0.0223	120.87	0.0693	0.0889	0.625	0.0018	16	154334.0	0.025	0.63	0.57	0.0000523	2
4	0.0222	117.06	0.0682	0.0859	0.642	0.0019	16	156808.1	0.025	0.56	0.60	0.0000578	2
5	0.0170	84.70	0.0563	0.0689	0.683	0.0029	16	137040.8	0.028	0.72	0.76	0.0002630	2
6	0.0142	85.22	0.0565	0.0665	0.568	0.0019	16	114416.5	0.025	0.48	0.63	0.0001176	2
7	0.0204	119.08	0.0688	0.0898	0.580	0.0017	15	138545.5	0.027	0.82	0.53	0.0000526	2.9
8	0.0218	130.72	0.0719	0.0946	0.566	0.0015	15	141462.4	0.026	0.74	0.49	0.0000326	2.9
9	0.0254	126.27	0.0707	0.0994	0.683	0.0026	14	164272.7	0.031	1.43	0.61	0.0000692	2.9
10	0.0174	85.68	0.0567	0.0708	0.690	0.0031	15	136034.2	0.029	0.90	0.77	0.0001040	2.9
11	0.0206	120.12	0.0691	0.0949	0.580	0.0019	15	139326.4	0.031	1.39	0.53	0.0000773	5.6
12	0.0222	120.34	0.0691	0.0959	0.625	0.0023	15	150147.8	0.032	1.51	0.57	0.0000768	5.6
13	0.0278	117.04	0.0682	0.0908	0.803	0.0033	15	190401.1	0.027	0.85	0.75	0.0001856	5.6
14	0.0146	84.44	0.0562	0.0663	0.589	0.0020	15	114366.5	0.026	0.51	0.66	0.0001392	8.4
15	0.0256	130.10	0.0716	0.0937	0.668	0.0020	15	167154.9	0.025	0.63	0.58	0.0003587	8.4
16	0.0257	124.64	0.0703	0.0968	0.698	0.0026	15	171476.8	0.029	1.13	0.62	0.0000985	8.4

TABLE H6 BED LOAD EXPERIMENTAL DATA IN CHANNEL WITH 77 mm THICK ROUGH BED

a) flows up to half full depth; (ks=1.4mm)

EX. No.	Q m^3/s	y_0 mm	R m	R_b m	V m/s	S	T C^o	R_e	λ_s	Ks mm	Fr	C_v	d_{50} mm
1	0.0127	78.93	0.0536	0.065	0.547	0.0021	17	107254.9	0.029	0.80	0.63	0.0000782	2.0
2	0.0127	76.36	0.0524	0.065	0.568	0.0025	17	108814.0	0.032	1.15	0.67	0.0001673	2.0
3	0.0140	77.94	0.0531	0.067	0.611	0.0031	17	118726.4	0.034	1.48	0.71	0.0001636	2.0
4	0.0146	81.07	0.0545	0.072	0.612	0.0035	17	122158.1	0.040	2.39	0.70	0.0001098	2.0
5	0.0099	66.30	0.0470	0.059	0.514	0.0028	18	91354.6	0.039	1.98	0.65	0.0000702	2.0
6	0.0101	62.26	0.0450	0.055	0.557	0.0033	18	93380.3	0.038	1.68	0.73	0.0001912	2.0
7	0.0144	82.83	0.0553	0.071	0.591	0.0029	17	119559.6	0.035	1.72	0.67	0.0001595	2.9
8	0.0144	80.58	0.0543	0.069	0.608	0.0029	18	123856.4	0.034	1.40	0.70	0.0001996	2.9
9	0.0158	80.78	0.0544	0.071	0.668	0.0039	18	136541.9	0.037	1.99	0.76	0.0001811	2.9
10	0.0122	74.36	0.0510	0.064	0.561	0.0028	16	102944.3	0.035	1.56	0.67	0.0000629	5.6
11	0.0143	79.80	0.0540	0.069	0.610	0.0031	16	118002.4	0.035	1.59	0.70	0.0000984	5.6
12	0.0146	79.18	0.0537	0.068	0.629	0.0033	17	122570.6	0.035	1.56	0.73	0.0001356	5.6
13	0.0146	73.84	0.0510	0.064	0.677	0.0040	16	123459.8	0.035	1.55	0.81	0.0003230	5.6
14	0.0132	81.42	0.0547	0.068	0.554	0.0023	16	107957.0	0.032	1.13	0.63	0.0000313	8.4
15	0.0135	78.10	0.0532	0.066	0.590	0.0027	16	111975.6	0.032	1.21	0.69	0.0000700	8.4
16	0.0156	82.88	0.0553	0.07	0.639	0.0031	16	126759.5	0.033	1.33	0.72	0.0001681	8.4
17	0.0156	80.26	0.0542	0.069	0.662	0.0036	17	129873.7	0.035	1.55	0.76	0.0002285	8.4

TABLE H6 BED LOAD EXPERIMENTAL DATA IN CHANNEL WITH 77 mm THICK ROUGH BED

b) flows more than half full depth; (ks=1.40mm)

EX. No.	Q m^3/s	y_0 mm	R m	R_b m	V m/s	S	T C^o	R_e	λ_s	Ks mm	Fr	C_v	d_{50} mm
1	0.0279	125.72	0.0704	0.107	0.753	0.0040	17	193694.2	0.039	2.90	0.67	0.0000608	2.0
2	0.0311	126.34	0.0705	0.103	0.834	0.0041	17	215158.8	0.032	1.68	0.74	0.0001009	2.0
3	0.0263	120.74	0.0690	0.095	0.737	0.0029	18	190591.6	0.029	1.14	0.67	0.0000514	2.0
4	0.0297	122.12	0.0694	0.097	0.824	0.0037	18	212217.9	0.029	1.17	0.75	0.0001273	2.9
5	0.0268	121.95	0.0693	0.095	0.745	0.0029	18	191658.0	0.028	1.02	0.67	0.0000887	2.9
6	0.0267	127.46	0.0708	0.096	0.711	0.0025	18	186742.0	0.027	0.88	0.63	0.0000836	2.9
7	0.0258	117.50	0.0681	0.096	0.742	0.0033	15	176352.2	0.032	2.21	0.69	0.0002057	5.6
8	0.0245	117.88	0.0682	0.093	0.703	0.0027	16	172110.1	0.029	1.14	0.65	0.0001474	5.6
9	0.0248	124.80	0.0701	0.096	0.674	0.0024	16	169673.2	0.029	1.10	0.60	0.0000858	5.6
10	0.0228	121.56	0.0692	0.084	0.635	0.0017	16	158336.6	0.023	0.40	0.58	0.0000349	5.6
11	0.0278	120.28	0.0689	0.097	0.783	0.0036	16	192196.9	0.032	1.51	0.72	0.0003618	8.4
12	0.0275	124.86	0.0701	0.098	0.746	0.0030	16	186930.4	0.030	1.23	0.67	0.0002068	8.4
13	0.0238	127.40	0.0708	0.099	0.634	0.0022	16	160447.5	0.030	1.32	0.56	0.0000645	8.4

TABLE H7 BED LOAD EXPERIMENTAL DATA IN CHANNEL WITH 120 mm THICK SMOOTH BED

Ex. No.	Q m^3/s	y_o mm	R m	V m/s	S	T C^o	R_e	λ_s	ks mm	Fr	C_v	d_{50} mm
1	0.0071	50.32	0.0382	0.463	0.0016	15	61450.24	0.023	0.12	0.66	0.0001248	1
2	0.0190	88.33	0.0554	0.718	0.0028	16	141778.7	0.023	0.33	0.75	0.0001171	1
3	0.0218	90.63	0.0563	0.801	0.0032	16	161935.7	0.022	0.27	0.82	0.0001820	1
4	0.0064	41.33	0.0329	0.510	0.0027	17	60838.3	0.027	0.32	0.80	0.0003161	1
5	0.0194	121.93	0.0639	0.546	0.0010	16	125082.0	0.016	0.00	0.46	0.0000574	1
6	0.0189	122.00	0.0639	0.532	0.0011	17	123523.6	0.019	0.09	0.45	0.0001254	2.9
7	0.0076	58.07	0.0424	0.430	0.0012	17	66736.2	0.022	0.12	0.57	0.0002072	2.9
8	0.0227	92.10	0.0567	0.825	0.0035	17	170996.5	0.023	0.32	0.84	0.0004587	2.9
9	0.0061	41.93	0.0333	0.476	0.0020	17	57434.8	0.023	0.12	0.74	0.0004513	2.9
10	0.0128	73.27	0.0496	0.578	0.0018	17	103802.5	0.021	0.14	0.67	0.0003230	2.9
11	0.0223	92.50	0.0568	0.808	0.0034	16	163641.2	0.023	0.34	0.82	0.0004614	5.6
12	0.0070	47.15	0.0364	0.487	0.0022	16	63159.9	0.027	0.33	0.72	0.0003706	5.6
13	0.0136	77.88	0.0515	0.581	0.0017	16	105618.6	0.021	0.14	0.65	0.0003285	5.6
14	0.0084	59.10	0.0430	0.470	0.0015	16	71031.7	0.023	0.15	0.61	0.0002204	5.6
15	0.0189	121.15	0.0638	0.535	0.0011	15	119793.4	0.020	0.12	0.45	0.0001052	5.6
16	0.0188	113.07	0.0623	0.567	0.0017	16	125206.3	0.026	0.59	0.51	0.0000991	8.4
17	0.0096	60.50	0.0437	0.522	0.0019	17	83335.7	0.024	0.26	0.67	0.0002384	8.4
18	0.0159	81.03	0.0528	0.653	0.0023	14	117201.7	0.022	0.23	0.72	0.0004238	8.4
19	0.0069	47.07	0.0364	0.486	0.0022	15	61359.4	0.026	0.14	0.72	0.0002396	8.4
20	0.0052	40.40	0.0323	0.422	0.0020	15	47316.5	0.029	0.41	0.67	0.0002407	2
21	0.0223	116.30	0.0629	0.655	0.0018	14	139594.8	0.020	0.17	0.57	0.0001437	2
22	0.0191	89.03	0.0557	0.716	0.0024	13	132119.5	0.020	0.15	0.75	0.0002941	2
23	0.0076	52.80	0.0396	0.473	0.0016	14	64074.8	0.022	0.10	0.66	0.0002419	2
24	0.0152	77.18	0.0512	0.651	0.0023	14	112971.5	0.022	0.21	0.74	0.0001264	0.5
25	0.0092	52.67	0.0395	0.578	0.0026	14	77982.2	0.024	0.23	0.80	0.0001616	0.5
26	0.0220	95.88	0.0579	0.769	0.0024	16	156724.7	0.019	0.09	0.77	0.0009169	8.4
27	0.0067	47.70	0.0367	0.460	0.0019	15	59048.0	0.026	0.28	0.67	0.0001395	8.4

TABLE H8 BED LOAD EXPERIMENTAL DATA IN CHANNEL WITH 120 mm THICK ROUGH BED
(ks=0.8 mm)

Ex. No.	Q m^3/s	y_0 mm	R m	R_b m	V m/s	S	T C^o	R_e	λ_s	ks mm	Fr	C_v	d_{50} mm
1	0.0188	125.40	0.0645	0.0856	0.518	0.0016	16	118230.2	0.030	1.08	0.43	0.0000398	2
2	0.0145	87.17	0.0550	0.0657	0.555	0.0020	15	106299.3	0.028	0.67	0.58	0.0001220	2
3	0.0085	52.43	0.0394	0.0432	0.533	0.0026	15	73306.3	0.029	0.54	0.74	0.0001919	2
4	0.0218	93.67	0.0572	0.0686	0.780	0.0035	15	154513.2	0.026	0.60	0.79	0.0002110	2
5	0.0221	96.77	0.0581	0.0712	0.767	0.0035	15	154494.1	0.027	0.71	0.76	0.0002742	2.9
6	0.0146	87.87	0.0553	0.0667	0.553	0.0021	15	105888.5	0.030	0.98	0.58	0.0001249	2.9
7	0.0184	120.93	0.0638	0.0844	0.521	0.0017	14	112872.7	0.032	1.32	0.44	0.0000376	2.9
8	0.0221	94.47	0.0574	0.0700	0.783	0.0037	14	152595.8	0.027	0.68	0.79	0.0008535	5.6
9	0.0063	44.37	0.0347	0.0382	0.468	0.0027	14	55148.6	0.034	0.88	0.71	0.0001931	5.6
10	0.0147	84.00	0.0539	0.0634	0.581	0.0022	16	111592.9	0.027	0.66	0.63	0.0001932	5.6
11	0.0223	92.50	0.0568	0.0653	0.808	0.0033	16	163641.2	0.022	0.30	0.82	0.0004175	5.6
12	0.0231	99.82	0.0590	0.0715	0.777	0.0033	16	163520.1	0.025	0.53	0.75	0.0006347	8.4
13	0.0081	50.67	0.0384	0.0423	0.527	0.0027	17	74018.2	0.030	0.60	0.75	0.0002008	8.4
14	0.0146	84.80	0.0542	0.0653	0.574	0.0023	17	114364.9	0.030	0.93	0.61	0.0000827	8.4
15	0.0225	116.70	0.0630	0.0807	0.659	0.0024	17	152574.5	0.027	0.74	0.57	0.0002594	8.4
16	0.0188	112.13	0.0621	0.0771	0.571	0.0018	16	125723.5	0.028	0.78	0.51	0.0000712	8.4

TABLE H9 BED LOAD EXPERIMENTAL DATA IN CHANNEL WITH 120 mm TH
(ks=1.4 mm)

Ex. No.	Q m^3/s	y_0 mm	R m	R_b m	V m/s	S	T C^o	R_e	λ_s	ks mm	Fr	C_v	d_{50} mm
1	0.0143	80.00	0.0524	0.0659	0.594	0.00331	15	107504.3	0.039	2.10	0.66	0.0000613	8.4
2	0.0152	79.30	0.0521	0.0659	0.636	0.00394	15	114786.2	0.040	2.32	0.71	0.0001377	8.4
3	0.0186	88.60	0.0555	0.0719	0.699	0.00425	15	134692.9	0.038	2.12	0.73	0.0002864	8.4
4	0.0154	80.50	0.0526	0.0682	0.636	0.00443	14	113852.0	0.045	3.40	0.70	0.0002644	8.4
5	0.0183	91.35	0.0564	0.0698	0.669	0.00306	14	128951.3	0.030	1.04	0.68	0.0001835	8.4
6	0.0152	81.90	0.0531	0.0660	0.617	0.00321	15	112548.9	0.035	1.61	0.67	0.0001599	5.6
7	0.0156	79.93	0.0523	0.0795	0.648	0.00361	15	116788.0	0.035	1.59	0.72	0.0002502	5.6
8	0.0143	81.38	0.0529	0.0653	0.584	0.00282	15	106276.3	0.034	1.46	0.64	0.0001009	5.6
9	0.0136	80.60	0.0526	0.0650	0.560	0.00268	15	101670.6	0.035	1.57	0.62	0.0000510	5.6
10	0.0139	82.30	0.0532	0.0651	0.561	0.00249	15	103515.9	0.033	1.28	0.61	0.0000444	2.9
11	0.0166	89.23	0.0557	0.0697	0.620	0.00290	15	119651.4	0.033	1.37	0.64	0.0000578	2.9
12	0.0146	79.30	0.0521	0.0657	0.611	0.00360	15	110333.2	0.039	2.24	0.68	0.0001102	2.9
13	0.0174	79.25	0.0521	0.0631	0.726	0.00400	15	131484.8	0.031	1.06	0.81	0.0003281	2.9
14	0.0144	75.73	0.0506	0.0608	0.630	0.00323	14	108420.9	0.032	1.16	0.72	0.0001253	2
15	0.0166	87.00	0.0550	0.0668	0.637	0.00280	15	120094.2	0.030	0.93	0.67	0.0000847	2
16	0.0142	86.78	0.0549	0.0585	0.636	0.00200	15	102969.0	0.029	0.81	0.58	0.0000654	2

APPENDIX I

ACKERS-WHITE EQUATIONS

APPENDIX I

THE ACKERS-WHITE EQUATIONS FOR SEWERS

This Appendix presents in outline the Ackers-White equations modified foe determination of the rate of sediment transport in full and part-full sewers. The Ackers-White equations may be used in combination with the Colebrook-White equation for computing the equilibrium depth of sediment deposit that may occur in sewer, as well as determining the rates of sediment deposition and erosion. The methodology described applies only to non-cohesive sediments.

The Ackers-White Equations were originally derived for determining sediment transport rates in alluvial channels, and the equations have been modified subsequently to apply to sediment transport in full and part-full sewers.

Sediment transport is described by the ratio of the appropriate shear force on the sediment bed to the immersed weight of a layer of sediment particles. A general mobility number is defined:

$$F_{gr} = \frac{u_*^n}{\sqrt{g(S_s-1)d}} \quad \frac{V^{1-n}}{\left[\sqrt{32}\,\mathrm{Log}\ (12R/d)\right]^{1-n}} \qquad (I.1)$$

For coarse sediment (n=0) the expression reduces to the form:

$$F_{gr} = \frac{V}{\sqrt{g(S_s-1)d}} \quad \frac{1}{(\sqrt{32}\ \mathrm{Log}\ (12R/d)} \qquad (I.2)$$

For fine sediments (n=1), Equation (I.1) may be written:

$$F_{gr} = \frac{u_*}{\sqrt{g(S_s-1)d}} \qquad (I.3)$$

For transitional sizes of sediment, n may take a value between 0 and 1, depending on the dimensionless expression for grain diameter:

$$D_{gr} = d \left[\frac{g\ (S_s - 1)}{\upsilon^2} \right]^{1/3} \qquad (I.4)$$

The efficiency of sediment transport is dependent on the mobility number F_{gr}, and there is a critical value of F_{gr}, denoted A_{gr}, below which no sediment will be moved, and the transport efficiency is zero. A general transport parameter may be defined:

$$G_{gr} = c \left[\frac{F_{gr}}{A_{gr}} - 1 \right]^m \qquad (I.5)$$

The non-dimensional transport parameter is related to the primary variables:

$$G_{gr} = C_v \ (R/d) \left[\frac{A}{W_* R} \right]^{1-n} \left[\frac{u_*}{V} \right]^n \qquad (I.6)$$

Thus, for coarse sediment (n=0):

$$G_{gr} = C_v \ \frac{A}{W_* d} \qquad (I.7)$$

For fine sediment (n=1)

$$G_{gr} = C_v \ (R/d) \left[\frac{u_*}{V} \right] \qquad (I.8)$$

The exponents n and m and coefficient A_{gr} and c are related to the dimensionless grain diameter for $1.0 < D_{gr} < 60$.

$$n = 1.00 - 0.56 \ \text{Log}\ D_{gr} \qquad (I.9)$$

$$A_{gr} = 0.14 + \frac{0.23}{\sqrt{D_{gr}}} \qquad (I.10)$$

$$m = 1.34 + \frac{9.66}{D_{gr}} \qquad (I.11)$$

$$\text{Log } c = 2.86 \text{ Log } D_{gr} - (\log D_{gr})^2 - 3.53 \qquad (I.12)$$

For coarse sediments, i.e $D_{gr} > 60$:

$n = 0.00$

$A_{gr} = 0.17$

$m = 1.5$

$c = 0.25$

Colebrook-White Equation

The Colebrook-White Equation is the friction equation most commonly used in the UK for calculating hydraulic conditions in sewers.

For part-full sewers the equation may be expressed in terms of the hydraulic mean depth:

$$V = -\sqrt{32gRS}\ \text{Log}\left[\frac{k_s}{14.8R} + \frac{1.255\upsilon}{R\sqrt{32gRS}}\right] \qquad (I.13)$$

For sewer flowing full, the hydraulic mean depth may be replaced by the pipe diameter/4 for circular pipe:

$$V = -2\sqrt{2gDS}\ \text{Log}\left[\frac{k_s}{3.7\ D} + \frac{2.51\ \upsilon}{R\sqrt{32gRS}}\right] \qquad (I.14)$$

The linear measure of effective roughness k_s may be a composite value if part of the invert is covered by a sediment deposit. A simple method of combining the sediment roughness k_{ss} and the clean pipe roughness k_{sp} is by straightforward perimeter weighting:

$$k_s = \frac{P_1 k_{ss} + P_2 k_{sp}}{P_1 + P_2} \qquad \text{(I.15)}$$

In Equation I.15, P_1 is the wetted perimeter of the sediment deposit (W_s) and P_2 is the "clean pipe" wetted perimeter. Assessment of the value of sediment roughness should account for any bed forms that may occur. In general, the value of k_{ss} may be considerably greater than the sediment diameter d.

Equivalent Width of Sediment Deposit:

Referring to Equation (I.6) it may be seen that the sediment concentration (C_v) is related to the value taken for the sediment width W_s. In the case of coarse sediment, the sediment concentration is directly proportional to the sediment width Equation (I.7). For sediment transport when a finite sediment deposit exists in the sewer, the equivalent width may be taken as the actual sediment width. For "clean pipe" transport calculations, it is necessary to select a suitable value of W_s. Research has shown that a suitable value may be obtained from:

$$W_s = 10 \times d \qquad \text{(I.16)}$$